University of Southampton

Faculty of Medicine

Cancer Sciences

Inhibition of mRNA Translation Initiation Factors as a Novel Therapeutic Approach in Chronic Lymphocytic Leukaemia (CLL)

by

Sarah Catherine Wilmore

Thesis for the degree of Doctor of Philosophy

January 2020

University of Southampton

Abstract

Faculty of Medicine

Cancer Sciences

Thesis for the degree of Doctor of Philosophy

Inhibition of mRNA Translation Initiation Factors as a Novel Therapeutic Approach in Chronic Lymphocytic Leukaemia (CLL)

by

Sarah Catherine Wilmore

Signalling via the B-cell receptor (BCR) is a major driver of disease progression in chronic lymphocytic leukaemia (CLL) and an established target for therapeutic attack. Studies have demonstrated that BCR-stimulation of CLL cells leads to a substantial increase in global mRNA translation and enhanced translation of oncoprotein *MYC*. Increased translation is associated with increased expression of eukaryotic initiation factor-4A (eIF4A) in CLL cells, but not in healthy donor B cells, and high expression of eIF4E has been documented in CLL compared to normal B cells. This suggested that it may be possible to selectively inhibit global and/or *MYC* mRNA translation in CLL cells using inhibitors targeted against specific components of the translation machinery. I therefore investigated the effects of inhibitors of eIF4A, silvestrol and rocaglamide, and an eIF4E inhibitor, ribavirin in CLL.

Both eIF4A inhibitors (eIF4Ai) and ribavirin reduced anti-IgM-induced global mRNA translation in primary CLL cells, analysed using *O*-propargy 1-puromycin (OPP)-labelling. Inhibition of eIF4A resulted in reduced translation of *MYC*, as well as *MCL1*, a BCL-2 family protein which, like MYC, is linked to poor outcome. Whilst MYC protein expression was reduced, this was associated with a surprising increase in *MYC* mRNA expression, via increased RNA stabilisation. Although, eIF4Ai inhibited mRNA translation in healthy donor B cells, inhibition of eIF4E had no effect on translation in B cells from healthy donors. eIF4E also has a role in the nuclear export of specific eIF4E-target mRNAs, including *MYC*. Ribavirin reduced the nuclear export of mRNA encoding proliferation promoting *CCND1* and *MYC* in CLL samples. *In vivo* studies utilising ribavirin treatment in mice bearing Eμ-*TCL1* leukaemic cells, showed efficacy by reduced tumour burden.

Overall, these results support the hypothesis that inhibition of the translation initiation machinery is an effective strategy to suppress anti-IgM-induced translation in CLL cells, to deprive malignant cells of the tumour-promoting effects of oncoproteins such as MYC and MCL1.

Table of Contents

Table of Tables

Table of Figures

Research Thesis: Declaration of Authorship

Print name:	SARAH CATHERINE WILMORE
Title of thesis:	Inhibition of mRNA Translation Initiation Factors as a Novel Therapeutic Approach in Chronic Lymphocytic Leukaemia (CLL)

I declare that this thesis and the work presented in it are my own and has been generated by me as the result of my own original research.

I confirm that:

1. This work was done wholly or mainly while in candidature for a research degree at this University;
2. Where any part of this thesis has previously been submitted for a degree or any other qualification at this University or any other institution, this has been clearly stated;
3. Where I have consulted the published work of others, this is always clearly attributed;
4. Where I have quoted from the work of others, the source is always given. With the exception of such quotations, this thesis is entirely my own work;
5. I have acknowledged all main sources of help;
6. Where the thesis is based on work done by myself jointly with others, I have made clear exactly what was done by others and what I have contributed myself;
7. None of this work has been published before submission

Signature: Date:

Acknowledgements

I would firstly like to give thanks to my supervisor Professor Graham Packham, for years of support and guidance, and for the opportunities given to me throughout my time in Southampton. These have allowed me to complete my PhD and develop as a scientist. I would also like to thank my second supervisor, Dr Alison Yeomans, for her constant support and advice throughout my studies. I would next like to thank Dr Mark Coldwell for allowing me to use his polysome profiling equipment, and expertise. Thank you to those who assisted me with some of the experiments performed in this thesis, particularly Dr Karly-Rai Rogers Broadway, Dr Alison Yeomans, Sophie Marriott, Dr Matthew Karter and Dr Laura Karydis.

Next, I would like to give thanks to the CLL group as a whole (members old and new), each one of you have guided me and supported me in one way or another. Without you all work would have never been so enjoyable, and I would have struggled without all your knowledge!

To my family and friends, thank you for accepting my absences during my PhD, and supporting me through the hard times. Particularly, Dr Elizabeth Lemm and Dr Karly-Rai Rogers-Broadway, you have both gone above and beyond in supporting me, and without you I wouldn't have been able to do this.

Most importantly, thank you to my partner Robert and our little dog, Clyde. You have sat by me as I've written my thesis and sacrificed our time together. You have both alleviated my stress with ease, and there's no way I could have done it without you both. I'll be eternally grateful for your love and support.

Finally, I'd like to express my gratitude to the tumour bank staff for preparing samples, Cancer Research UK and the University of Southampton, for their funding and opportunities throughout my PhD, and to the patients who so kindly donated their samples for use in my research.

Definitions and Abbreviations

4E-BP	4E-binding protein
4E-SE	4E-sensitivity element
ABC-DLBCL	Activated B-cell – diffuse large B cell lymphoma
AID	Activation-induced cytyidine deaminase
ATM	Ataxia-telangiectasia mutated
ATP	Adenosine triphosphate
BCL2	B-cell lymphoma 2
BCR	B cell receptor
BH3	BCL2-homology domain 3
BIRC3	Baculoviral IAP repeat-containing protein 3
BM	Bone marrow
BSA	Bovine serum albumin
CBM COMPLEX	CARD11-BCL10-MALT1 complex
CD	Cluster of differentiation
cDNA	Complementary DNA
CDS	Coding sequence
CFSE	Carboxyfluorescein succinimidyl ester
cIAP2	Cellular inhibitor of apoptosis 2
CIT	Chemo-immunotherapy
CLL	Chronic lymphocytic leukaemia
CME	Clathrin-mediated endocytosis
CRAC	Ca^{2+} release-activated Ca^{2+} channels
CRD	Coding region instability determinant
CRD-BP	CRD- binding protein
CSR	Class switch recombination
DAG	Diacylglycerol
DEPTOR	DEP domain-containing mTOR-interacting protein
DLBCL	Diffuse large B cell lymphoma

DMSO	Dimethyl sulphoxide
DNA	Deoxyribonucleic acid
DNTP	Deoxyribonucleotide triphosphate
DTT	Dithiothreitol
eEF-1	Eukaryotic translation elongation factor-1
eIF	Eukaryotic initiation factor
eIF4Ai	eIF4A inhibitor
ER	Endoplasmic reticulum
eRF1	Eukaryotic translation termination factor-1
ERK	Extracellular signal-regulated kinase
EZH2	Enhancer of zeste homolog-2
FACS	Fluorescence-activated cell sorting
FCR	Fludarabine, cyclophosphamide and rituximab
FCS	Foetal calf serum
FDA	Food and drug administration
FDC	Follicular dendritic cells
FOXP1	Forkhead box protein P1
FRET	Fluoresence resonance energy transfer
GC	Germinal centre
GCB-DLBCL	Germinal centre B-cell - diffuse large B cell lymphoma
GTP	Guanosine triphosphate
GWAS	Genome-wide association studies
HEP	Humane end-point
HRP	Horseradish peroxidase
HSC	Haematopoietic stem cell
IG	Immunoglobulin
IGHV	Immunoglobulin heavy chain
IκB	Inhibitor of κB
IκK	IκB kinase complex
IL	Interleukin
IP_3	Inositol (1,4,5)-triphosphate

IP3R	IP_3 receptor
IRES	Internal ribosome entry site
IRF8	Interferon regulatory factor 8
ITAF	IRES trans-activating factor
ITAM	Immunoreceptor tyrosine-activation motif
ITIM	Immunoreceptor tyrosine-inhibitory motif
JNK	c-Jun N-terminal kinases
LN	Lymph node
LRPPRC	Leucine-rich pentatricopeptide repeat protein
MAPK	Mitogen-activated protein kinase
MBL	Monoclonal B-cell lymphocytosis
MCL	Mantle cell lymphoma
MCL1	Myeloid cell leukaemia-1
M-CLL	Mutated *IGHV* CLL
MET-tRNA	Methionine-bound tRNA
MFI	Mean fluorescence intensity
MHC	Major histocompatibility complex
mir/miRNA	Micro RNA
M-MLV	Moloney murine leukaemia virus
mRNA	Messenger RNA
mTOR	Mammalian target of rapamycin
mTORC	mTOR complex
MYD88	Myeloid differentiation primary response 88
NCBI	National centre for biotechnology information
NES	Nuclear export sequence
NFAT	Nuclear factor of activated T cells
NF-κB	Nuclear factor kappa-light-chain enhancer of B cells
NK	Natural killer cells
NLR	NOD-like receptor
NLS	Nuclear localisation sequence
NOD/SCID	Nonobese diabetic/severe combined immunodeficiency

NPC	Nuclear pore complex
NSG	NOD/Sci-scid ILRrg$^{-/-}$ mice
PARP	Poly (ADP-ribose) polymerase
PAX5	Paired box protein 5
PBMC	Peripheral blood mononuclear cells
PBS	Phosphate buffered saline
PC	Proliferation centre
PCR	Polymerase chain reaction
PDCD4	Programmed cell death protein 4
PDX	Patient-derived xenograft
PI	Propidium iodide
PI3K	Phosphoinositide 3-kinase
PIC	Pre-initiation complex
PIP_2	Phosphatidylinositol (4,5)-biphosphate
PIP_3	Phosphatidylinositol (3,4,5)-triphosphate
PLCγ2	Phospholipase γ-2
PM	Plasma membrane
PRE-B CELL	Precursor B cell
PRO-B CELL	Progenitor B cell
PTEN	Phosphatase and tensin homolog
RAG	Recombination-activating gene
RAPTOR	Regulatory associated protein of mTOR
RBC	Red blood cell
RIP	RNA immunoprecipitation
RISC	RNA-induced silencing complex
RNAi	RNA interference
RPMI	Roswell park memorial institute media
rRNA	Ribosomal RNA
RSS	Recombination signal sequences
S6K	Ribosomal protein S6 kinase
SDS	Sodium dodecyl sulphate

SF3B1	Splicing factor 3 subunit 1
SHIP	Src homology 2 domain containing inositol polyphosphate 5-phosphatase
SHM	Somatic hypermutation
SHP1	Src homology region 2 domain-containing phosphatase-1
sIGM	Surface immunoglobulin-M
SINE	Selective inhibitor of nuclear export
SNP	Single nucleotide polymorphism
SYK	Spleen tyrosine kinase
TBS	Tris-buffered saline
TBST	TBS-Tween
TCL1	T cell leukaemia 1
TFH CELLS	Follicular T-helper cells
TLR	Toll-like receptor
TnT	Terminal deoxynucleotidyl transferase
tRNA	Transfer RNA
TSC2	Tuberous sclerosis complex subunit 2
U-CLL	Unmutated *IGHV* CLL
UTR	Untranslated region
VEGF	Vascular endothelial growth factor
XPO1	Exportin 1
ZAP-70	Zeta-chain-associated protein kinase 70

Chapter 1

Introduction

1.1 Overview

The overall aim of this project was to characterise pathways of mRNA translational control in chronic lymphocytic leukaemia (CLL) cells, especially downstream of the B-cell receptor (BCR), and to investigate the potential utility of inhibitors targeted against mRNA translation initiation factors as a new approach to drug therapy. This introduction therefore focuses on (i) B-cell development and the importance of the BCR, (ii) key biological and clinical aspects of CLL, (iii) mechanisms of mRNA translation and its selective inhibition using small chemical compounds, and (iv) the interplay of nuclear export and mRNA translation.

1.2 B-cell development

B cells play a key role in adaptive immunity by recognising antigen and provoking humoral antibody-based responses, alongside cell-mediated immunity induced by T cells. B cells develop from haematopoietic stem cells (HSC) and differentiate into mature naïve B cells expressing both immunoglobulin (Ig)-M and IgD on their surface in the bone marrow (BM) (Rowe et al., 1973). At this stage, naïve B cells have not encountered antigen and circulate around the body in the blood or lymph (LeBien and Tedder, 2008). Upon encounter with cognate antigen, B cells may undergo clonal expansion and differentiate into antibody secreting plasma cells or memory B cells (Figure 1-1). This antigen-dependent phase of B-cell development occurs within secondary lymphoid organs, such as the lymph nodes (LN) or the spleen (LeBien and Tedder, 2008).

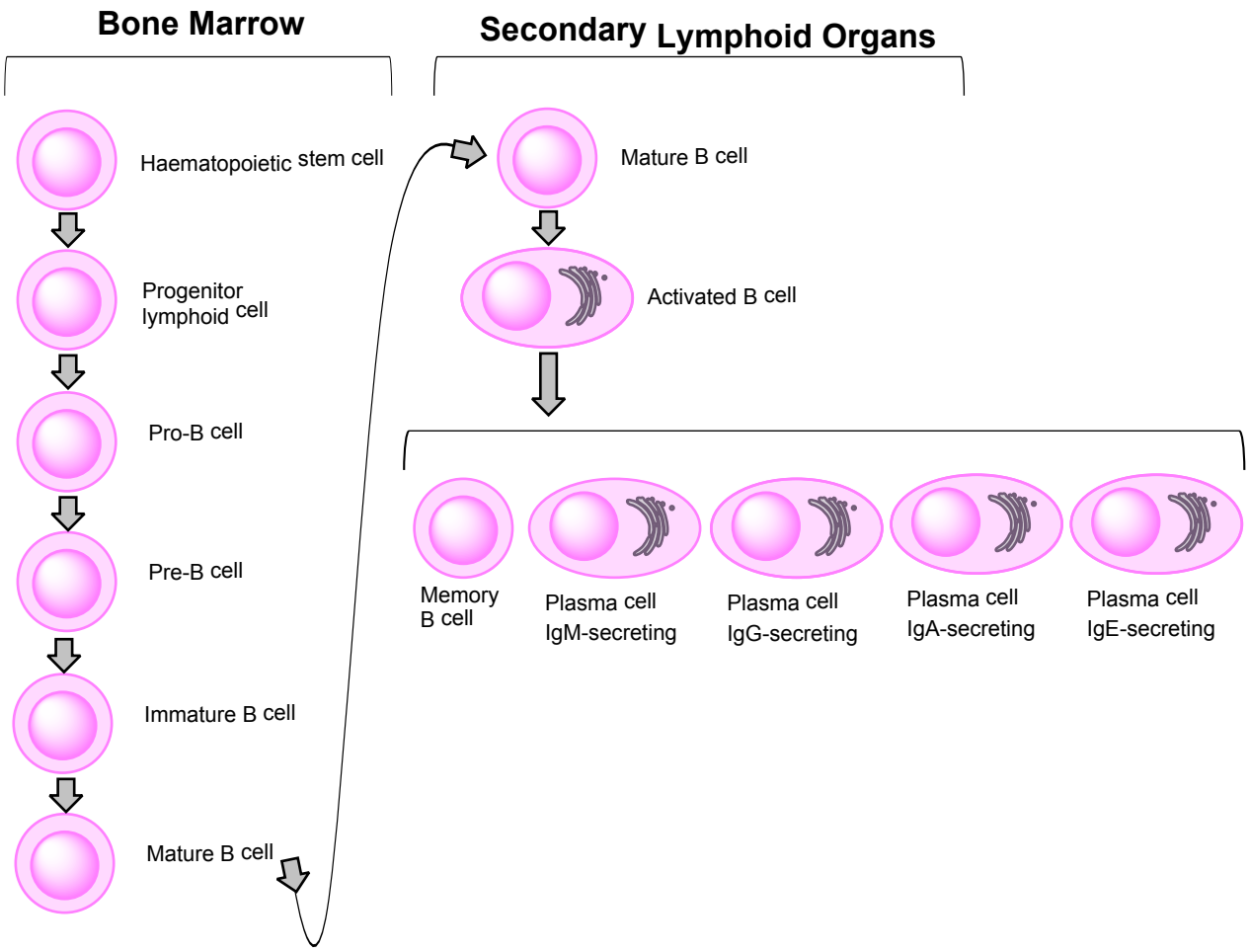

Figure 1-1. Stages of B-cell development.

Multiple stages of B-cell development occur within the bone marrow (BM), beginning with a self-renewing haematopoietic stem cell which differentiates and commits to a cellular lineage thereby giving rise to progenitor lymphoid cells without self-renewing capability. Progenitor lymphoid cells then differentiate into progenitor (pro)-B cells. Pro-B cells then differentiate into precursor (pre)-B cells, supported by stromal cells in the BM. Pre-B cells then proliferate and become immature B cells. The immature B cell then develops into a mature B cell. Mature B cells then leave the BM to peripheral lymphoid organs, such as lymph nodes, where they are activated and differentiate into memory B cells or antibody-secreting plasma cells in response to antigen. Image produced using ChemDraw professional ® v16.0. Image modified from Kuby immunology, 2007 (Kindt, 2007).

1.2.1 Early B-cell development

Between the third and seventh month of foetal development, HSCs migrate from the yolk sac to the foetal liver and the spleen where they then undergo haematopoiesis (LeBien and Tedder, 2008). Following this, HSCs migrate to the BM where they differentiate (Ezine et al., 1984) (Weissman, 2000). Upon birth and onwards, virtually all haematopoiesis occurs within the BM. HSCs self-renew and have huge proliferative capacity and can therefore maintain haematopoietic demands throughout adult life (Wilson and Trumpp, 2006). When HSCs differentiate they lose capacity for self-renewal and become committed to a specific cell lineage by developing into either lymphoid or myeloid progenitors (Weissman, 2000), dependent upon the haematopoietic-inducing microenvironment. It is the lymphoid progenitor cells that give rise to B, T and natural killer (NK) cells.

Within the BM, lymphoid progenitor cells differentiate into the first committed B-cell precursor, progenitor (pro-) B cells with surface expression of a transmembrane tyrosine phosphatase, CD45R, as well as a heterodimer of Ig-α and Ig-β (also known as CD79A/B), the signal transduction unit of the BCR (LeBien and Tedder, 2008). Pro-B cells interact and adhere to stromal cells in the BM which support their development into precursor (pre-) B cells (Jarvis et al., 1997). Adherence of pro-B cells to stromal cells is mediated by cellular adhesion molecules, particularly VLA-4 and its ligand VCAM-1, expressed on the pro-B cell and stromal cells respectively (Miyake et al., 1992).

It is during the development of a pro-B cell into a pre-B cell that rearrangement of the heavy-chain gene locus occurs (Brack et al., 1978, Melchers, 2005, Alt, 1986). Rearrangement of heavy chain V, D and J gene segments represents the first stage of immunoglobulin (Ig) gene diversification (discussed in more detail in section 1.2.2). It affects the variable region of the heavy chain and thus contributes to antigen specificity (Tonegawa, 1983), allowing B cells to recognise a vast range of potential antigens. Lineage commitment in pro-B cells is imposed by PAX5, a transcription factor that activates the expression of various B cell specific genes such as *CD19* and *CD79A*, whilst repressing non B-lineage genes, such as *NOTCH1* (Nutt et al., 1999). This results in the development of a pre-B cell expressing a signalling competent pre-BCR comprising a membrane-bound complex of unique μ heavy chains and surrogate light chains bound to Ig-α and Ig-β (LeBien and Tedder, 2008). Development into a pre-B cell from a pro-B cell is the first stage during which BCR signalling is required for progression (Ehlich et al., 1994, Martensson et al., 2002).

Interleukin-7 (IL-7) is released by stromal cells and binds its receptor (IL-7R), which is expressed by pre-B cells, to downregulate the expression of adhesion molecules on the cell surface (Shriner et al., 2010, Corfe and Paige, 2012). This allows the pre-B cell to detach from the stromal cells and

proliferate (Johnson et al., 2005). Following proliferation, the pre-B cell downregulates expression of IL-7R and becomes unresponsive to IL-7 (Marshall et al., 1998).

Pre-B cells then undergo light-chain gene variable region rearrangements to develop into immature B cells with defined antigen specificity and with unique heavy and light chains expressed on their cell surface, along with Ig-α and Ig-β (Figure 1-2) (Coffman and Weissman, 1983). During light-chain rearrangement, the V, J and C gene segments are re-arranged to result in the expression of either a κ or λ light-chain on the cell surface of an immature B cell, replacing the surrogate light chains (Zou et al., 2003) (see also section 1.2.3). At this stage, BCR signalling is critical, as previously demonstrated in a study where truncation of the cytoplasmic tail of Ig-α resulted in depletion of the majority of immature B cell population compared to truncation in the pre B cell population (Torres et al., 1996). This suggests that differentiation of early B cell progenitors requires increasing signalling capacity throughout the developmental stages.

At this stage, immature B cells are $IgM^+ IgD^-$. The next stage in development is negative selection, where B cells with auto-reactive BCRs are removed from the repertoire via deletion, anergy or receptor editing. Some B cells with BCRs that are reactive to low avidity ligands can enter a state of anergy, where they down-regulate surface IgM (sIgM) and become unresponsive to further antigen stimulation (Goodnow and Basten, 1989, Fulcher et al., 1996). How an immature B cell may respond to antigen, and the consequence of this, is determined in part by the stage of maturation of the cell, as well as ligand avidity. For example, antigen binding to immature B cells with low sIgM expression results in receptor editing (Tze et al., 2003). In contrast, binding of antigen to the BCR of mature B cells with high sIgM can induce apoptosis (Melamed et al., 1998). This is also true depending upon the location of the B cell when its BCR is bound by antigen. For example, activation of the pre-BCR in the BM results in receptor editing, whereas mature B cells in the spleen are deleted following stimulation (Sandel and Monroe, 1999).

Immature B cells in the BM then continue to develop by co-expressing sIgM and sIgD. IgD is produced by alternative splicing of the heavy-chain transcript, producing two distinct mRNAs encoding IgM or IgD with the same antigenic specificity (Moore et al., 1981). Whilst IgM functions as a BCR upon the cell surface, it is currently less clear what role IgD plays in B-cell development or antigen-responsiveness. Maturing B cells then leave the BM and undergo activation, proliferation and further differentiation in peripheral/secondary lymphoid organs, such as the LN (LeBien and Tedder, 2008). Notably, truncation of the cytoplasmic tail of Ig-α (as discussed above) also blocks the migration of immature B cells from the BM to the periphery (Torres et al., 1996), further demonstrating the requirement of BCR-signalling in B-cell development.

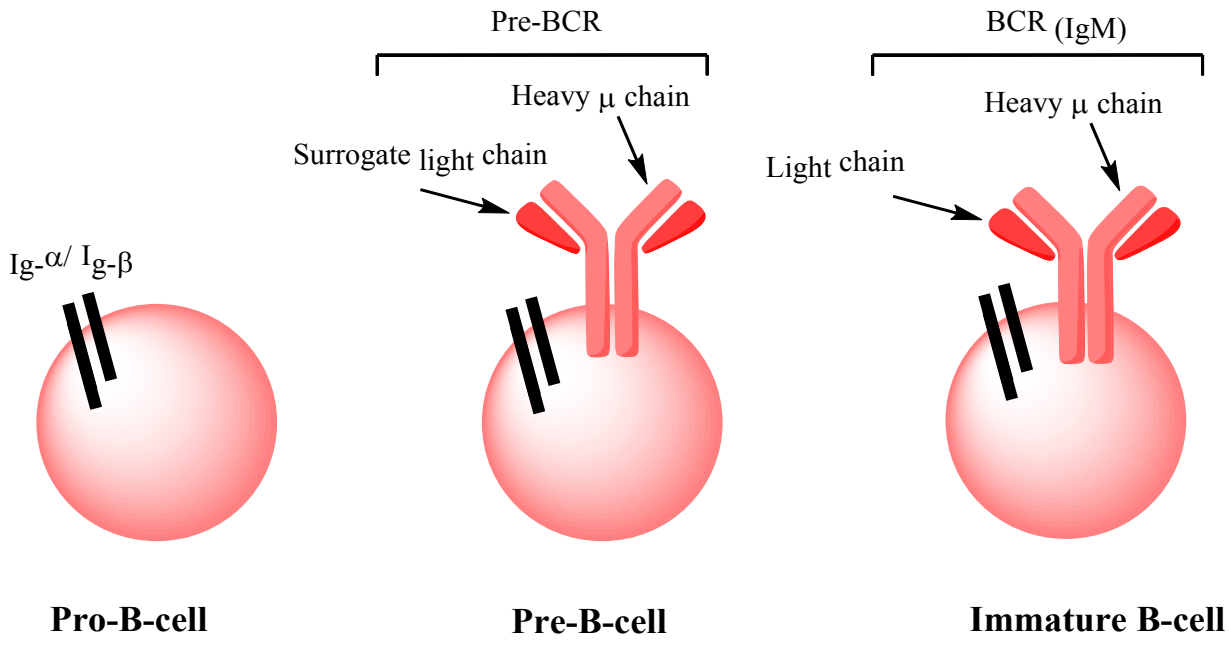

Figure 1-2. Maturation of the BCR during B-cell development.

Pro-B cells express Ig-α and Ig-β on their cell surface. Upon development into a pre-B cell, the cell undergoes heavy chain gene rearrangement, resulting in the expression of a heavy chain and a surrogate light chain on the surface of the pre-B cell, which along with Ig-α and Ig-β, forms the pre-B cell receptor (pre-BCR). Following this, the pre-B cell undergoes light chain gene rearrangements to form an immature B cell with a fully formed BCR, with Ig-α and Ig-β alongside a κ or λ light chain and a μ heavy chain. Image produced using ChemDraw professional ® v16.0. Image modified from Kuby immunology, 2007 (Kindt, 2007).

1.2.2 The germinal centre reaction

The germinal centre (GC) reaction is pivotal for the production of high affinity antibody responses. It occurs following antigen-engagement of the BCR on naïve B cells and the GC reaction is critically dependent on interactions with other immune cells, especially follicular T helper (Tfh) cells (Grewal and Flavell, 1996, Gatto and Brink, 2010). GCs are typically found within secondary lymphoid organs and are characterised by intense B-cell proliferation, selection (apoptosis/rescue from apoptosis) and further Ig diversification (Gatto and Brink, 2010).

Mature B-cells circulate to B-cell follicles of secondary lymphoid organs (Figure 1-3), such as the LN, where they encounter antigen. Once a B cell has encountered antigen it moves to the T-cell – B-cell (T-B) boundary of the follicle for cognate T-cell help to activate the B cell (Gatto and Brink, 2010). Here, Tfh cells present CD40L to the CD40 receptor expressed by B cells for co-stimulation (Grewal and Flavell, 1996). These B cells which have been engaged by cognate antigen proceed to form GCs within these follicles (LeBien and Tedder, 2008).

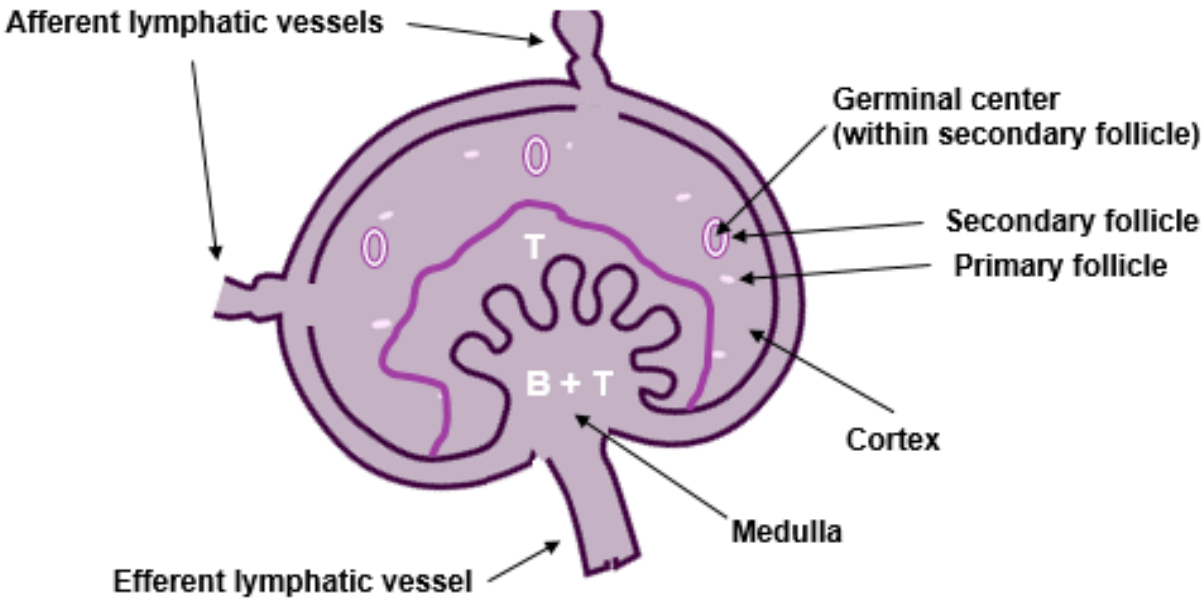

Figure 1-3. Diagram of a lymph node with germinal center sites and the presence of B and T cells.

This diagram demonstrates the presence of T and B cells (in white) within the lymph node and the presence of primary and secondary follicles, of which some contain germinal centers. Mature B cells circulate to secondary lymphoid organs, such as the lymph node, from the peripheral blood, via afferent lymphatic vessels. Here, they encounter antigen and move to the T-B boundary within the follicle. It is here that the B cell, following BCR stimulation by antigen, receives co-stimulatory signals from Tfh cells via the CD40-CD40L interaction. The B cell then forms a germinal centre within the secondary follicle, where they undergo proliferation, class switching and somatic hypermutation. Image produced using ChemDraw professional ® v16.0.

Immune interactions within the GC lead to the formation of humoral antibody-based immunity by B cells and is critically dependent upon the presence of immunological help provided by cognate Tfh cells (Gatto and Brink, 2010, Grewal and Flavell, 1996). Within the GC, antigen-encountered B cells undergo proliferation, class-switch recombination (CSR) and somatic hypermutation (SHM) (Gatto and Brink, 2010). Mature GCs are divided into two distinct zones; the dark-zone and the light-zone (Figure 1-4). During the first stages of GC formation, activated B cells within the dark-zone undergo proliferation, or clonal expansion, and are also known as centroblasts (Gatto and Brink, 2010). In addition to rapid division, centroblasts undergo SHM. During SHM, point-mutations accumulate in the V, D (diversity), J (joining) regions (Dunnick et al., 2009). SHM accounts for the fine-tuning of the antibody specificity for antigen/affinity maturation (Li et al 2004). The mechanisms of SHM and CSR are discussed in more detailed in section 1.2.3.

Following this, these centroblasts become centrocytes and move into the light-zone of the GC, which also contains follicular dendritic cells (FDCs) (Figure 1-4) (Gatto and Brink, 2010). It is here in the light-zone that FDCs present antigen to centrocytes. Centrocytes in the light-zone also encounter Tfh cells (Gatto and Brink, 2010). Centrocytes with high affinity BCRs compete to uptake limited antigen and gain a survival and proliferative advantage following presentation of antigen to cognate Tfh cells, by positive selection. T-cell help by CD40L-CD40 interactions, as well as secretion of cytokines, results in maintained expression of the anti-apoptotic protein BCL2 (Gatto and Brink, 2010). By contrast, centrocytes that fail to effectively engage T-cell help downregulate BCL2 expression and undergo apoptosis, following a process called antigen-mediated selection (Gatto and Brink, 2010). Tfh cells also encourage centrocytes to differentiate further into either memory B cells (for immunological recall) or plasmablasts/plasma B cells (for high level antibody secretion) (Gatto and Brink, 2010) (Figure 1-4).

The maturation of B cells within GCs involves CSR, resulting in the expression of a different class of sIg (Shimizu and Honjo, 1984). Class switching of sIg is determined by cytokines secreted by Tfh cells (Shimizu and Honjo, 1984, Shanmugam et al., 2000). For example, IL-21 encourages class switching to an IgG phenotype, whereas TGF-β can result in an IgA class switch (Shanmugam et al., 2000). This switch of sIg class to other isotypes, such as IgG, IgA or IgE can confer different BCR signalling properties and/or antibody effector functions. Each isotype of Ig has a very short cytoplasmic tail which lacks signalling capacity, except for IgG (Blum et al., 1993). The cytoplasmic tail of IgG is longer, with 28 amino acid residues, and is thought to enhance peripheral immune responses by enhancing Ig-mediated signalling (Wakabayashi et al., 2002).

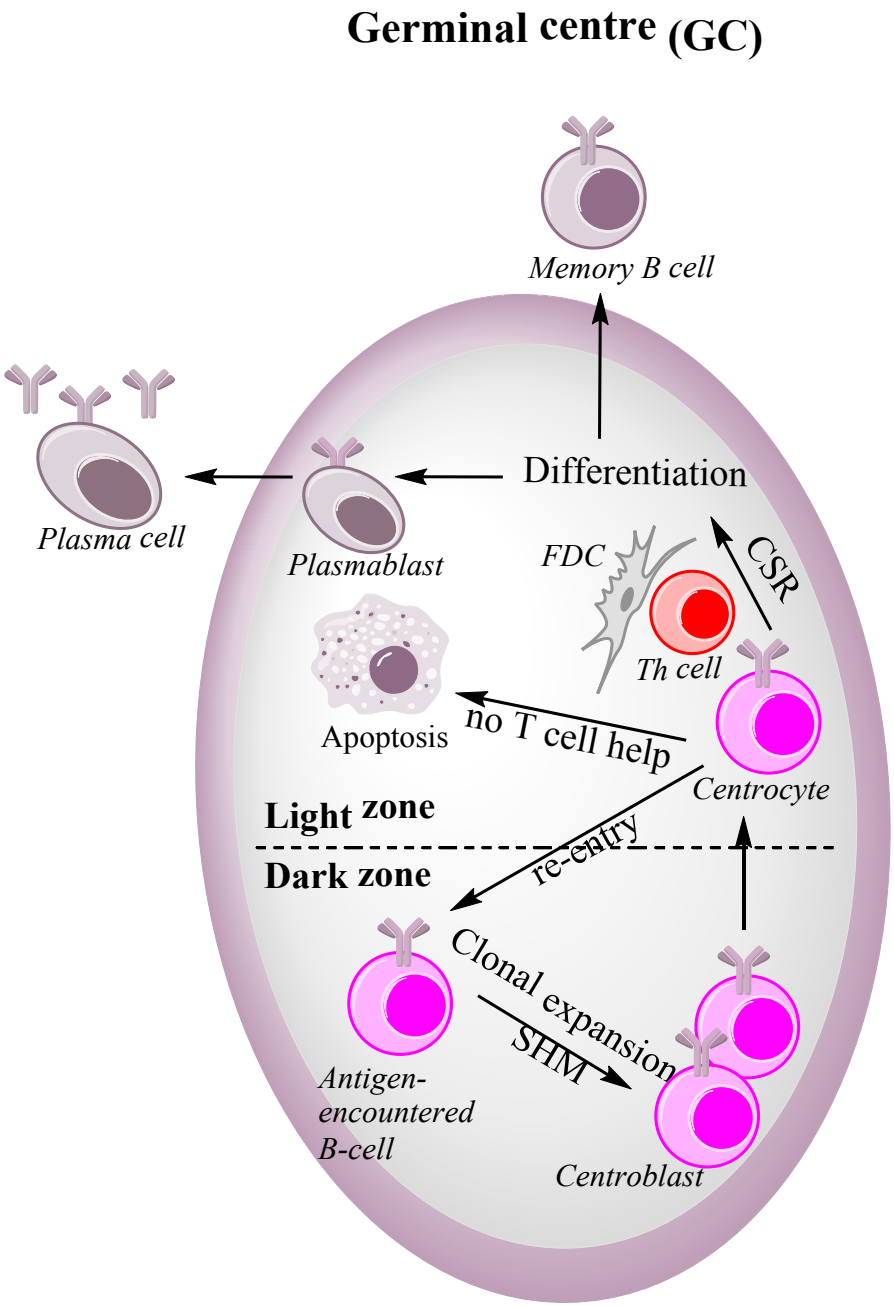

Figure 1-4. The germinal centre reaction.

Antigen-experienced B-cells within a GC undergo proliferation (clonal expansion) and SHM within the dark-zone of the GC to produce centroblasts. Following this expansion, centroblasts move into the light-zone and reduce proliferation rates and become centrocytes (Gatto and Brink, 2010). Centrocytes can also re-enter the dark-zone and undergo further proliferation/rounds of SHM. In the light-zone, centrocytes which encounter follicular dendritic cells (FDCs) and folliclar T-helper (Tfh) cells presenting chemokines and cytokines to facilitate positive selection and class switch recombination (CSR), then undergo differentiation into plasmablasts/plasma cells or into memory B cells (Stavnezer et al., 2008). Centrocytes which do not encounter cognate T-cell help succumb to apoptosis. Plasma cells secrete antibodies as a method of humoral immunity, whereas memory cells express affinity matured Ig genes and are longer surviving, providing faster and more sustained response to re-encountered antigen. Image produced using ChemDraw professional ® v16.0.

1.2.3 The B-cell receptor

The BCR is a transmembrane protein complex, expressed upon the surface of mature B cells, where it recognises antigen and thus promotes signalling and antibody responses. The BCR is comprised of two heavy chain domains, two light chains and an intracellular signal transduction module comprised of Ig-α and Ig-β (Figure 1-5) (Pleiman et al., 1994). The heavy chain spans the cell membrane and is composed of large extracellular domain and a short cytoplasmic region (Pleiman et al., 1994). The heavy chains of the BCR are joined by a disulphide bridge and are comprised of constant regions (C) and variable regions (V). Joined to these heavy chains by disulphide bridges are light chains which also contain C and V regions (Pleiman et al., 1994). The V regions of both heavy and light chains both typically contribute to the antigen-specificity of the BCR and thus this is where antigen binds (Pleiman et al., 1994).

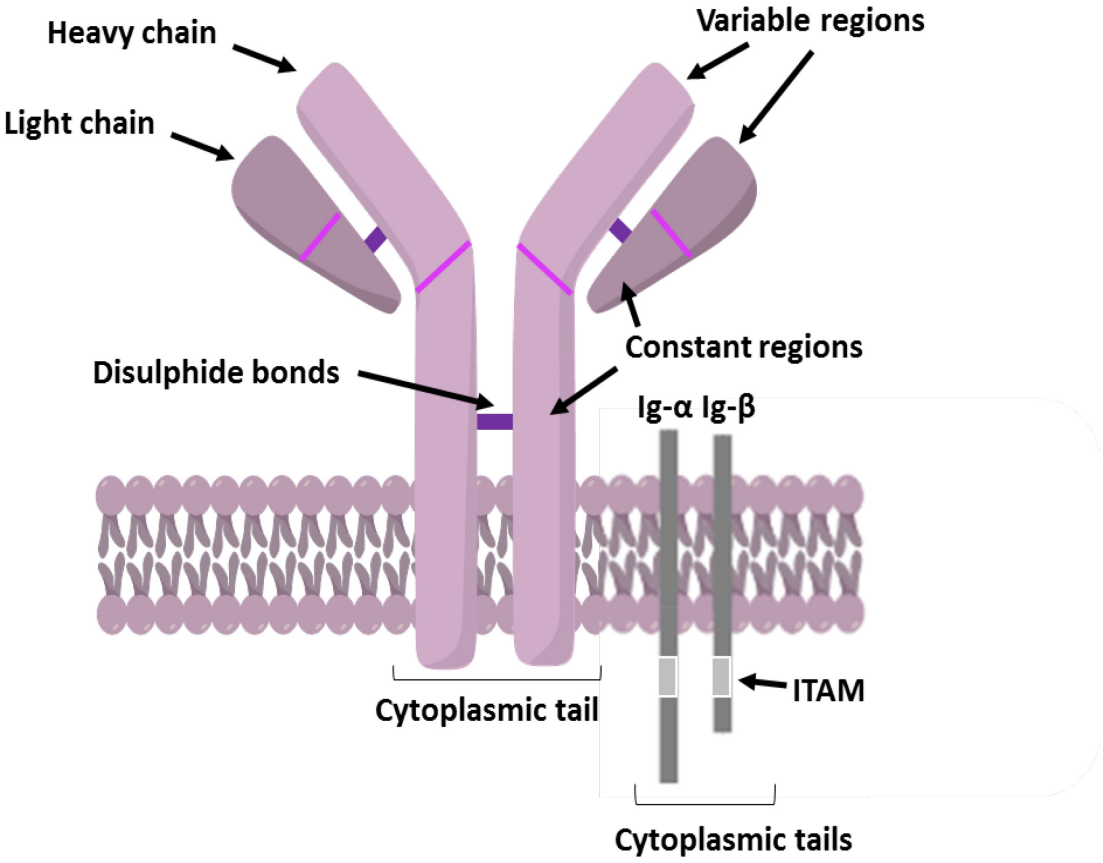

Figure 1-5. Structure of the B-cell receptor (BCR)

The BCR is comprised of two heavy chain domains, two light chains and an intracellular signal transduction module. The heavy chain crosses the cell membrane and is exposed extracellularly and also has a short cytoplasmic region. The heavy chains of the BCR are joined by a disulphide bridge and are comprised of constant regions (C) and variable regions (V). Joined to these heavy chains by disulphide bridges are light chains which also contain constant and variable regions. Following antigen binding, signalling via the BCR occurs through the signal transduction region, comprised of the Ig-α and Ig-β heterodimer, and each contain an immunoreceptor tyrosine activation motif (ITAM) within their intracellular tail. Image produced using ChemDraw professional ® v16.0.

Diversification of the BCR is key to developing a range of varying antigen specificity. It is determined by both the generation of diversity through recombination events, SHM, and the selection of B cells expressing specific BCR based on "fitness". Thus, B cells with auto-reactivity can be negatively-selected through the induction of apoptosis or anergy, whereas high affinity BCRs for foreign antigen can be positively-selected within GCs with help from cognate Tfh cells (Gatto and Brink, 2010, Grewal and Flavell, 1996) .

As discussed in section 1.2.1, initial diversification is generated by the random recombination of individual heavy chain V(D)J gene segments. The first stage is the selection of the D and J gene segments, resulting in an initial D-J rearrangement (Tonegawa, 1983, Brack et al., 1978). This is then followed by choosing of a V segment to join the D-J rearrangement, resulting in a recombined V(D)J exon (Tonegawa, 1983, Melchers, 2005). Light chains lack the D section and only undergo V and J recombination to produce κ or λ chains (van der Burg et al., 2001).

Rearrangement of Ig gene segments involves the recombination activated gene (RAG) enzymes, RAG1 and RAG2, which form a complex with recombination signal sequences (RSS) located adjacent to each of the V,D or J coding segment (van Gent et al., 1996, Fugmann et al., 2000) (Figure 1-6). An RSS consists of heptamer and nonamer elements with 'spacer' sequences of 12 or 23 nucleotides between them (Fugmann et al., 2000). Recombination can only occur with different spacer sequence lengths, such as recombination of an RSS with a 12 nucleotide spacer with an RSS with a 23 nucleotide spacer (Fugmann et al., 2000).

This is followed by cleavage of the DNA strands, as the RAG1/RAG2 complex nicks the DNA at each RSS via hydrolysis (van Gent et al., 1996, Fugmann et al., 2000). A transesterification reaction then occurs to create a double-strand break (DSB) and forms a hairpin intermediate structure, still bound by RAG1/2 (van Gent et al., 1996, Fugmann et al., 2000). Following this cleavage, the four ends of the DNA remain in a complex with RAG1/2 which ensures the ends are stable (Fugmann et al., 2000). The coding ends are then joined by covalent bonds, following slight variations in sequence by deletions and short sequenced insertions. The signalling DNA ends are then joined with minimal processing, with the resulting signal joints being heptamer-heptamer fusions (Fugmann et al., 2000). Opening of the hairpin occurs via an endonuclease, Artemis, which can result in palindromic insertions at the coding joint (Ma et al., 2002). A DNA polymerase, terminal deoxynucleotidyl transferase (TnT) also provides additional nucleotides, by adding GC-rich inserts to the coding joints (Ma et al., 2002). These non-templated alterations at the coding joints during V(D)J recombination contribute a significant amount to the diversity of antigen binding sites of the BCR (Fugmann et al., 2000) with a practically limitless repertoire of antigen recognition.

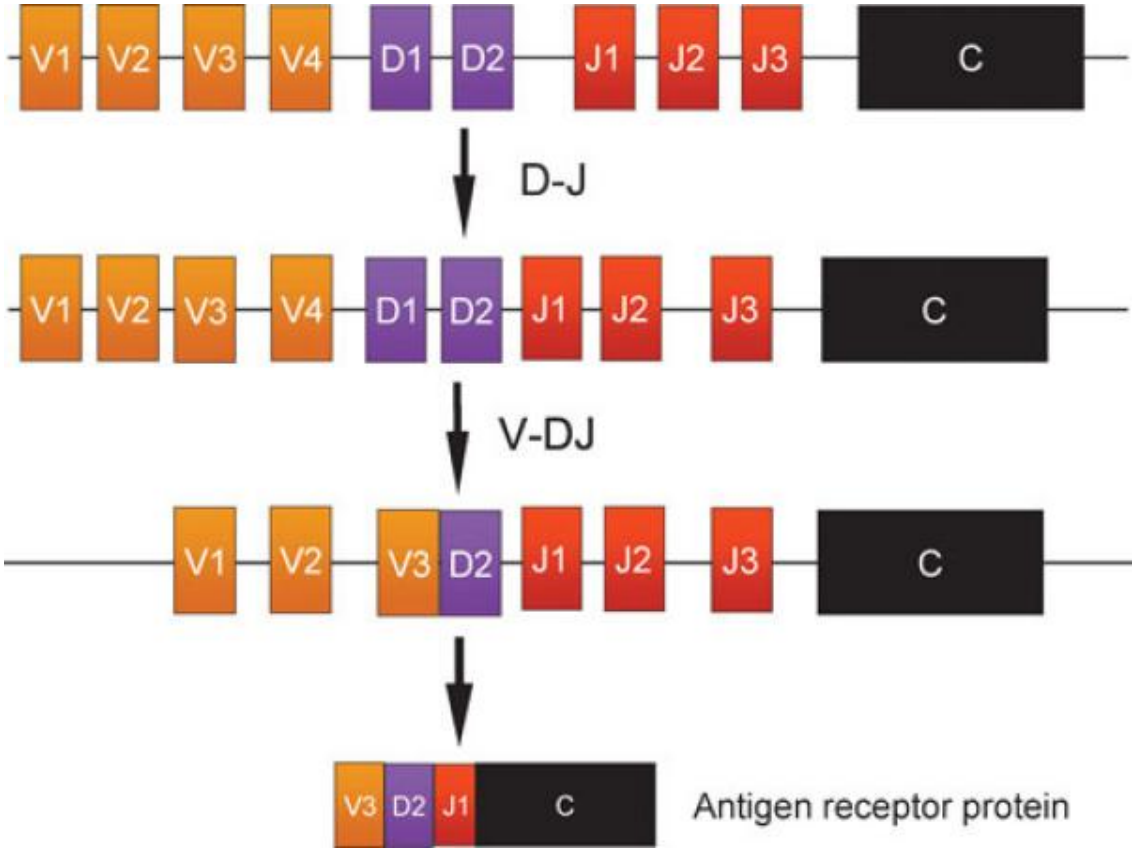

Figure 1-6. V(D)J recombination.

During V(D)J recombination there are two key stages. Firstly, D and J segments are selected and form an initial D-J segment rearrangement. A V (heavy) segment is then chosen and joined with the pre-formed D-J rearrangement to form an V(D)J exon. V(D)J recombination results in a massive increase in the diversity of the antigen binding cleft of the BCR, ultimately resulting in an almost infinite repertoire of antigen specificity. Image taken from (Roth, 2014).

The second wave of Ig diversification occurs during the GC reaction; the processes of SHM and CSR were introduced in section 1.2.3. SHM is initiated by an enzyme called activation-induced cytidine deaminase (AID) (Maul and Gearhart, 2010). AID deaminates cytosine in DNA resulting in uracil in the DNA of the variable region of sIg, further refining the antigen-specificity by the B cell (Maul and Gearhart, 2010). This is followed by CSR to alter the constant region of the BCR, and has no effect on antigen specificity (Maul and Gearhart, 2010). During CSR, there is a further re-arrangement of the heavy-chain Ig gene, whereby the V gene segment combines with a different C segment (Stavnezer et al., 2008). This occurs via a process involving switch regions (also known as DNA flanking sequences), a switch recombinase enzyme, the cytokines produced in the microenvironment and AID (Stavnezer et al., 2008). In CSR, AID is involved in deamination of cytosine in 'switch' regions upstream of the heavy chain constant region locus (Stavnezer et al., 2008). This results in a switch of sIg class from IgM or IgD to other sIg isotypes, such as IgG, IgA or IgE which can possess different signalling properties and antibody effector functions (Stavnezer et al., 2008) (see Table 1).

Table 1. Isotypes of immunoglobulins and their relevant effector functions.

IMMUNOGLOBULIN	FUNCTION
IgM	Primary immune response. Generally pentameric to increase avidity.
IgD	Unknown – secreted IgD only present at very low levels in serum
IgG	Secondary immune response
IgE	Response to parasites and allergies
IgA	Mucosal immunity

1.2.4 Functions of the B-cell receptor

The BCR fulfils two functions essential for B-cell responses, (i) antigen internalisation and (ii) signalling. Both key functions of the BCR are discussed below in sections 1.2.4.1 and 1.2.4.2, and will allow us to further understand the role of the BCR in B cell development and chronic lymphocytic leukaemia (CLL) pathogenesis.

1.2.4.1 Antigen internalisation

Upon binding of the BCR by cognate antigen, the antigen-bound receptor is internalised for processing of the antigen into a peptide for presentation by the B cell to cognate Tfh cells via the major histocompatibility complex (MHC) class II (Cresswell, 1994). Mature B cells constitutively express MHC class II on their surface. Only upon activation do they express co-stimulatory factors, such as CD40, for interaction with Tfh cells (Banchereau et al., 1995). Exogenous antigens are internalised by B cells via receptor-mediated endocytosis (also known as clathrin-mediated endocytosis/CME) (McMahon and Boucrot, 2011). This allows the B cell to process and present the antigen in the form of peptide to Tfh cells. During CME, clathrin is recruited to the plasma membrane, by adaptor and accessory proteins, and forms antigen-filled membrane vesicles (McMahon and Boucrot, 2011). During CME, when the receptor-bound antigen is present in early endosomes, the associated BCR is recycled and moves back to the cell surface, leaving behind the internalised antigen (Forquet et al., 1999). The internalised antigen then moves from this vesicle into increasingly acidic compartments, known as endosomes, before entering the very acidic lysosome. It is within the lysosome, which is around pH 4.5, where hydrolytic enzymes degrade the antigen into oligopeptides of around 13 to 18 amino-acid residues in length for binding to MHC class II (McMahon and Boucrot, 2011, Cresswell, 1994).

MHC class II is produced in the rough endoplasmic reticulum (RER) (Cresswell, 1994). A protein called the invariant chain (or CD74) prevents peptides binding to the cleft of the MHC before it has been transported through the trans-Golgi network into the endosomes containing the relevant antigenic peptides (McMahon and Boucrot, 2011, Cresswell, 1994). When the MHC moves through these acidic compartments, the invariant chain becomes degraded (Cresswell, 1994). When the MHC reaches the lysosome, the antigenic peptide can bind and form a peptide-class II complex (Cresswell, 1994). This complex is then transported to the plasma membrane for antigen presentation to Tfh cells, for CD40-CD40L interactions (Cresswell, 1994), ultimately leading to the activation of the B cell.

1.2.4.2 B-cell receptor signalling

BCR signalling is necessary to determine B cell fate during development, including supporting maturation of pro- to pre B cells and during pre- to immature B cell progression in the BM. Following this, BCR signalling is needed to activate mature B cells in response to binding of cognate antigen, the GC reaction and SHM (Gatto and Brink, 2010). In addition to antigen-induced signalling, the BCR also mediates a low-level antigen-independent (tonic) signal that may be required for the survival of mature B cells (Lam et al., 1997).

Upon stimulation of the BCR following binding of cognate antigen, aggregation of BCRs and the subsequent conformational changes result in signal transduction across the cell membrane via the Ig-α/Ig-β heterodimer by phosphorylation of the dual tyrosine residues present in the ITAMs cytoplasmic tails (Harwood and Batista, 2010a). This occurs by the action of SRC-family kinases, such as LYN (Harwood and Batista, 2010a). This is the initial phase of the BCR signalling cascade (Figure 1-7). The cascade continues as phosphorylation of the ITAMs creates docking sites for SYK and recruits more LYN (Harwood and Batista, 2010a, Kurosaki, 2002, Kurosaki et al., 1994).

LYN also triggers a negative regulatory feedback response that limits BCR activation, mediated by phosphatases (Katagiri et al., 1999). One of these phosphatases is CD45, which is expressed on the cell surface, and can de-phosphorylates LYN to regulate BCR signalling by preventing downstream signalling responses (Katagiri et al., 1999). This balance of LYN phosphorylation and dephosphorylation is controlled by phosphorylation of immunoreceptor tyrosine-based inhibitory motifs (ITIMs) in CD22 and FCγRIIB by LYN (Katagiri et al., 1999, Fujimoto et al., 2006). These factors are docking sites for phosphatases, SHIP1 and 2, which remove the 3' phosphate of the inositol lipid PIP_3 to balance the signalling downstream of PI3K (O'Rourke et al., 1998) (Figure 1-7). This regulatory pathway of BCR signalling inhibition is activated following excessive exposure to (auto)antigen/ chronic BCR stimulation, particularly in the absence of T cell help, and is involved in the B-cell selection process to remove self-reactive B cells from the repertoire (Packham et al., 2014). Phosphorylated ITIMs also recruit and activate SH2-containing tyrosine phosphatase-1 (SHP-1) as well as SHIP-1. SHP-1 controls initial BCR responses via a negative feedback loop (Ono et al., 1997).

The next phase of BCR signalling involves SYK and BTK, which are kinases that couple the initial phase of BCR signalling to further downstream components. SYK is activated following binding to phosphorylated ITAMs and then phosphorylates an adaptor protein, BLNK (Fu et al., 1998). Phosphorylated BLNK then propagates the signal by acting as a scaffold for the assembly of a signalosome complex comprised of BTK, PLCγ2 and GRB2 (Fu et al., 1998, Hashimoto et al., 1998, Weber et al., 2008). Formation of the signalosome means that BTK is in close proximity to PLCγ2 to phosphorylate it (Kurosaki and Tsukada, 2000, Kurosaki et al., 2000). This complex interacts then interacts with BLNK and moves toward the plasma membrane (Fu et al., 1998, Kurosaki and Tsukada, 2000). This BCR signalosome contributes to the further amplification of the BCR signalling cascade. PI3K activation and signalling occurs in parallel, resulting in the phosphorylation of phosphatidylinositol (4,5)-biphosphate (PIP_2), which produces phosphatidylinositol (3,4,5)-triphosphate (PIP_3) (Okkenhaug, 2013). PIP_3 is a docking site which recruits effector proteins like BTK, ATK, PLCγ2 and PKCβ (Okkenhaug, 2013).

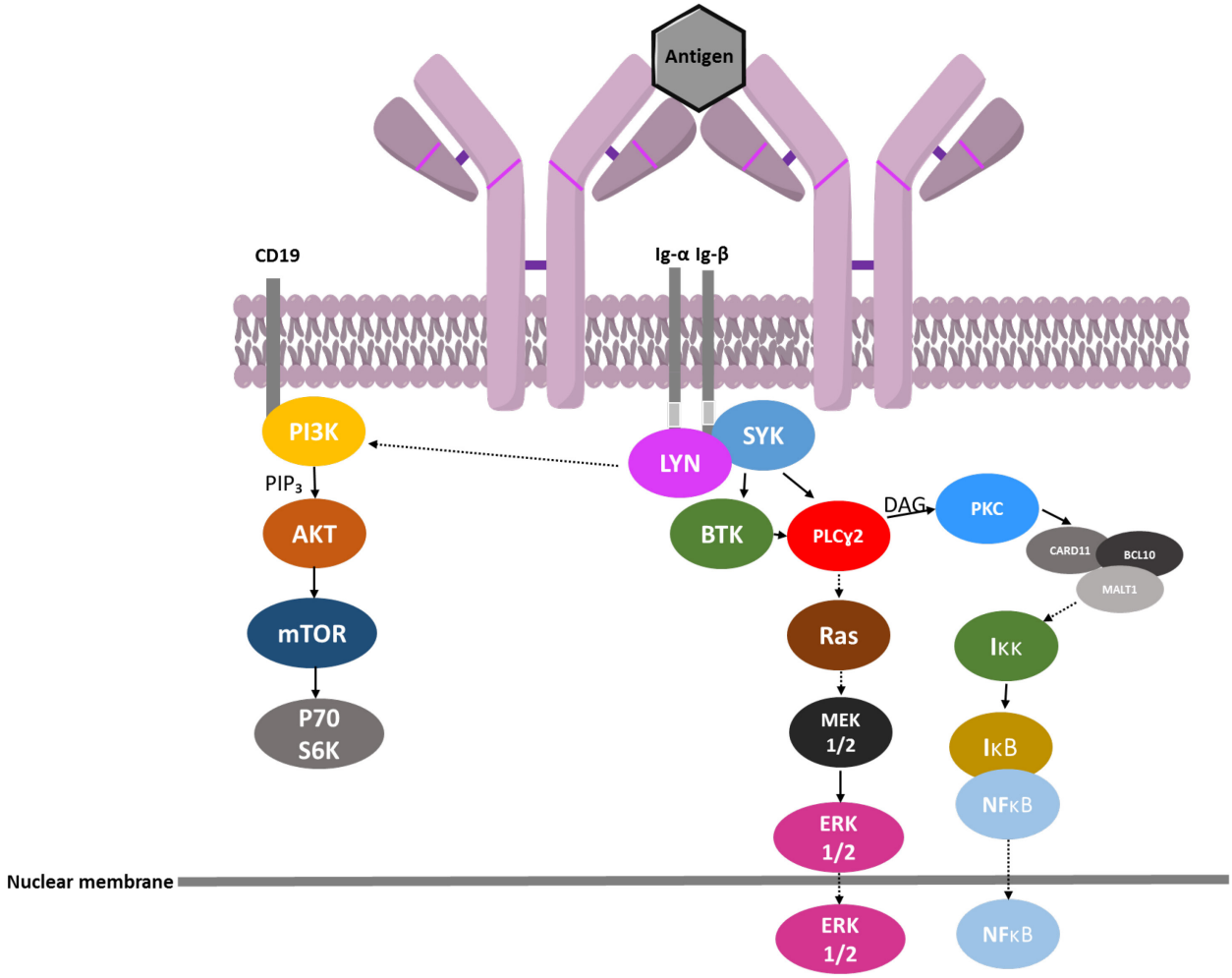

Figure 1-7. Simplified diagram of BCR signalling pathways.

Stimulation of the BCR results in signal transduction via the Ig-α/Ig-β heterodimer across the cell membrane and phosphorylation of the intracellular tyrosine-based activation motifs (ITAMs) within their cytoplasmic tails by LYN. This is the initial phase of the BCR signalling cascade and multiple parallel pathways are activated downstream of this. LYN indirectly activates PI3K which initiates signalling via membrane-bound PIP_2, activating AKT/ERK to stimulate mTOR. mTOR activation results in activation of S6K proteins which drive mRNA translation. Formation of the BCR 'signalosome' containing LYN, SYK and BTK with other adaptor proteins drives activation of PLCγ2. PI3K activation and signalling occurs in parallel, resulting in the phosphorylation of PIP_2, which produces PIP_3. PIP_3 is a docking site which recruits effector proteins like BTK, AKT, PLCγ2 and PKCβ. Downstream of these other pathways are activated. The Ras/MEK/ERK pathway of phosphorylation activates MYC as a transcription factor within the nucleus, amongst others, following increased intracellular calcium via NFAT. PLCγ2 can also activate PKC and downstream of this disable inhibitors of NF-κB, such as IκB, via the 'CBM' complex (CARD11, MALT1 and BCL10). NF-κB is a transcription factor, that when activated in the nucleus, can increase expression of genes associated with cell survival and proliferation. Image produced using ChemDraw professional ® v16.0.

Recruitment of PLCγ2 to the plasma membrane and its activation results in cleavage of PIP_2, which produces diacylglycerol (DAG) and inositol (1,4,5)-triphosphate (IP_3) (Kurosaki et al., 2000). IP_3 binds with its receptor(s) on the membrane of the ER, including the Ca^{2+} ion channel IP3R (Mikoshiba, 2007). Binding of IP_3 to IP3R results in the opening of the ion channel which subsequently results in the release of the ER-stored Ca^{2+} into the cytoplasm (Mikoshiba, 2007). The consequential depletion of ER Ca^{2+} stores induces influx of Ca^{2+} through the plasma membrane via Ca^{2+} release-activated Ca^{2+} channels (CRAC) (Parekh and Putney, 2005). This further phase of Ca^{2+} mobilisation allows extracellular Ca^{2+} to enter the cytoplasm to maintain the increased intracellular Ca^{2+} concentration (Parekh and Putney, 2005) (Figure 1-8).

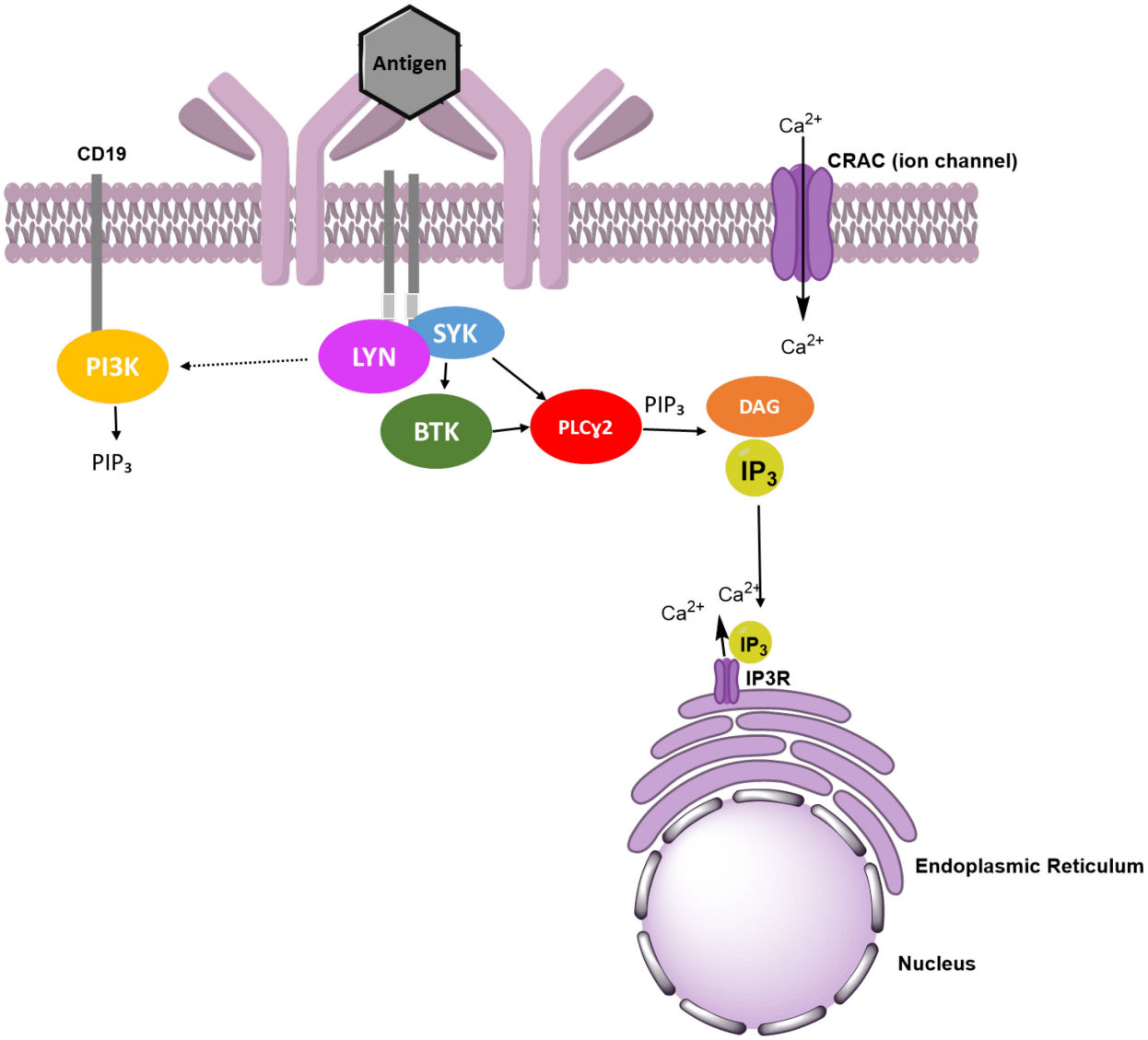

Figure 1-8. Simplified diagram of calcium mobilisation downstream of BCR activation.

Stimulation of the BCR results in signal transduction via the Ig-α/Ig-β heterodimer across the cell membrane and phosphorylation of the intracellular tyrosine-based activation motifs (ITAMs) within their cytoplasmic tails by LYN. This is the initial phase of the BCR signalling cascade and multiple parallel pathways are activated downstream of this. LYN indirectly activates PI3K which initiates signalling via membrane-bound PIP_2, producing PIP_3. Formation of the BCR 'signalosome' containing LYN, SYK and BTK with other adaptor proteins drives activation of PLCγ2. PIP_2 is cleaved by activated PLCγ2 into DAG and IP_3. IP_3 binds to IP3R on the endoplasmic reticulum which results in the subsequent release of calcium ions. This subsequent increase in intracellular calcium concentration activates Ca^{2+} release-activated Ca^{2+} channels (CRAC) which allows extracellular Ca^{2+} to enter the cytoplasm to maintain Ca^{2+} concentration. Image produced using ChemDraw professional ® v16.0.

The biphasic increase in cytoplasmic Ca^{2+} is accompanied by the activation of NFAT, NF-κB and JNK (Dolmetsch et al., 1997). The initial phase of Ca^{2+} release by the ER activates NF-κB and JNK, whereas the second phase with extracellular Ca^{2+} uptake activates NFAT (Dolmetsch et al., 1997). NFAT-family proteins are dephosphorylated by Ca^{2+}-activated calcineurin which results in the translocation and activation of the NFAT proteins into the nucleus, where these proteins can act as transcription factors (Dolmetsch et al., 1997).

Nuclear NFAT activates the transcription of genes encoding cytokines such as *IL-4*, and the NF-κB pathway which drives proliferation and survival by transcription of genes such as *BCL6* and *MYC* (Monticelli and Rao, 2002, Fisher et al., 2006). When cytoplasmic Ca^{2+} concentration decreases, NFAT proteins are translocated into the cytoplasm where they are inactivated (Monticelli and Rao, 2002, Dolmetsch et al., 1997). Overall, these pathways influence B-cell fate in regards to positive signalling or induction of anergy. Antigens can therefore induce either sustained elevated Ca^{2+} signalling responses, or low-level Ca^{2+} which may promote NFAT signalling, but not that of NF-κB (Dolmetsch et al., 1997)

Prior to stimulation, NF-κB-family proteins are retained within the cytoplasm by the inhibitory IκB proteins (Kanarek et al., 2010). IκBs are degraded following the activation of PKC which activates the downstream 'CBM' complex (comprised of CARD11, MALT1 and BCL10) (Kanarek et al., 2010). The CBM complex consequentially phosphorylates IKK leading to the phosphorylation and activation of IκBα, which results in the ubiquitinylation and subsequent degradation of IκB (Kanarek et al., 2010). This leaves NF-κB free to translocate into the nucleus for its role as a transcription factor.

Parallel to the NF-κB signalling pathway, activation of PLCγ2 can result in activation of RAS, which is then bound by GTP (Weber et al., 2008). GTP-bound RAS recruits RAF to the plasma membrane, resulting in the activation of RAF by SRC-family tyrosine kinases. Activated RAF binds to and activates MEK1/2 (Jacob et al., 2002). This then in turn results in activation of ERK1/2 (MAP kinase family proteins) (Jacob et al., 2002). ERK is activated via phosphorylation by threonine/tyrosine kinase activity of MEK, resulting in phosphorylation of Thr202/Tyr204 (Jacob et al., 2002). Activated/phosphorylated ERK phosphorylates ribosomal S6 kinases (S6Ks) (Roux et al., 2007). Also, nuclear translocation of ERK proteins results in the phosphorylation of transcription factors, one of which is MYC (Marampon et al., 2006). Phosphorylation of MYC at Ser62 results in its stabilisation and activation as a transcription factor, where it is involved in the transcription of genes involved in proliferation and survival (Sears et al., 2000).

Stimulation of B cells via CD40-CD40L Tfh cell interactions in the LN also activates NF-κB and MAPK signalling pathways, resulting in the activation of ERK (Mizuno and Rothstein, 2005, Homig-Holzel et al., 2008). MEK/ERK signalling regulates apoptosis via phosphorylation of BCL2 family proteins, which regulate the mitochondrial pathway of apoptosis (Tamura et al., 2004). The balance of expression of the pro-survival and the pro-apoptotic BCL2 family proteins is critical in determination of a cells fate (Fulda and Debatin, 2006). It has more recently also been demonstrated that ERK signalling plays a role in BCR-induced survival and the CD40-mediated survival of GC B cells following co-stimulation (Adem et al., 2015). During early BCR signalling, GC B cells experiencing CD40-CD40L co-stimulation survive and differentiate into memory or plasma B cells (Grewal and Flavell, 1996). If this help is not received, ERK1/2 is inhibited and thus cell death occurs. Therefore, co-stimulation of CD40 and the BCR results in both immediate and sustained ERK1/2 signalling (Adem et al., 2015).

Another key pathway of downstream BCR signalling responses is the AKT/mTOR cascade. AKT is recruited to the cell membrane following stimulation of the BCR and CD19 –dependent activation of PI3K (Aman et al., 1998, O'Rourke et al., 1998, Pogue et al., 2000). Downstream of this, AKT activates the mTORC1 complex (Pogue et al., 2000). mTORC1 is comprised of mTOR, regulatory-associated protein of mTOR (RAPTOR), DEP domain-containing mTOR-interacting protein isoform-2 (DEPTOR) and other proteins (Limon and Fruman, 2012). RAPTOR is involved in phosphorylation of substrates for mTORC1, whereas DEPTOR suppresses the action of kinases (Limon and Fruman, 2012). This pathway and its relevance in mRNA translation will be discussed in further depth in section 1.4.5.3.

1.3 Mature B cell malignancies

Malignancies of mature B cells, including various types of leukaemia and lymphoma, are becoming increasingly common. Mature B-cell malignancies can arise at different stages of B cell development and therefore have distinct B-cells-of-origin (Johnsen et al., 2014). For example, follicular and Burkitt's lymphoma derives from GC B cells, whereas myeloma originates from an antibody-secreting (post-GC) B cell (Johnsen et al., 2014, Seifert et al., 2013).

Diffuse large B-cell lymphoma (DLBCL), the most common subtype of non-Hodgkin's lymphoma, consists of two major subtypes with differing cell of origins (Seifert et al., 2013). Germinal center B-cell DLBCL (GCB-DLBCL) is derived from B-cells in the light zone of the GC, whereas activated B-cell DLBCL (ABC-DLBCL) is derived from activated B cells at a later stage of differentiation (Johnsen et al., 2014, Seifert et al., 2013). The differing cell of origin impacts on the clinical outcomes and treatments of DLBCL patients (Johnsen et al., 2014, Seifert et al., 2013). This is similar to CLL, which

can also be divided into two main subtypes with pre and post-GC cells of origin (Hamblin et al., 1999). This seminal discovery had a significant impact on the treatment and research landscape for CLL and is a major determinant for clinical outcome, and will be discussed in greater depth below. Figure 1-9 depicts the developmental stages from which certain B cell malignancies develop (figure is non-exhaustive).

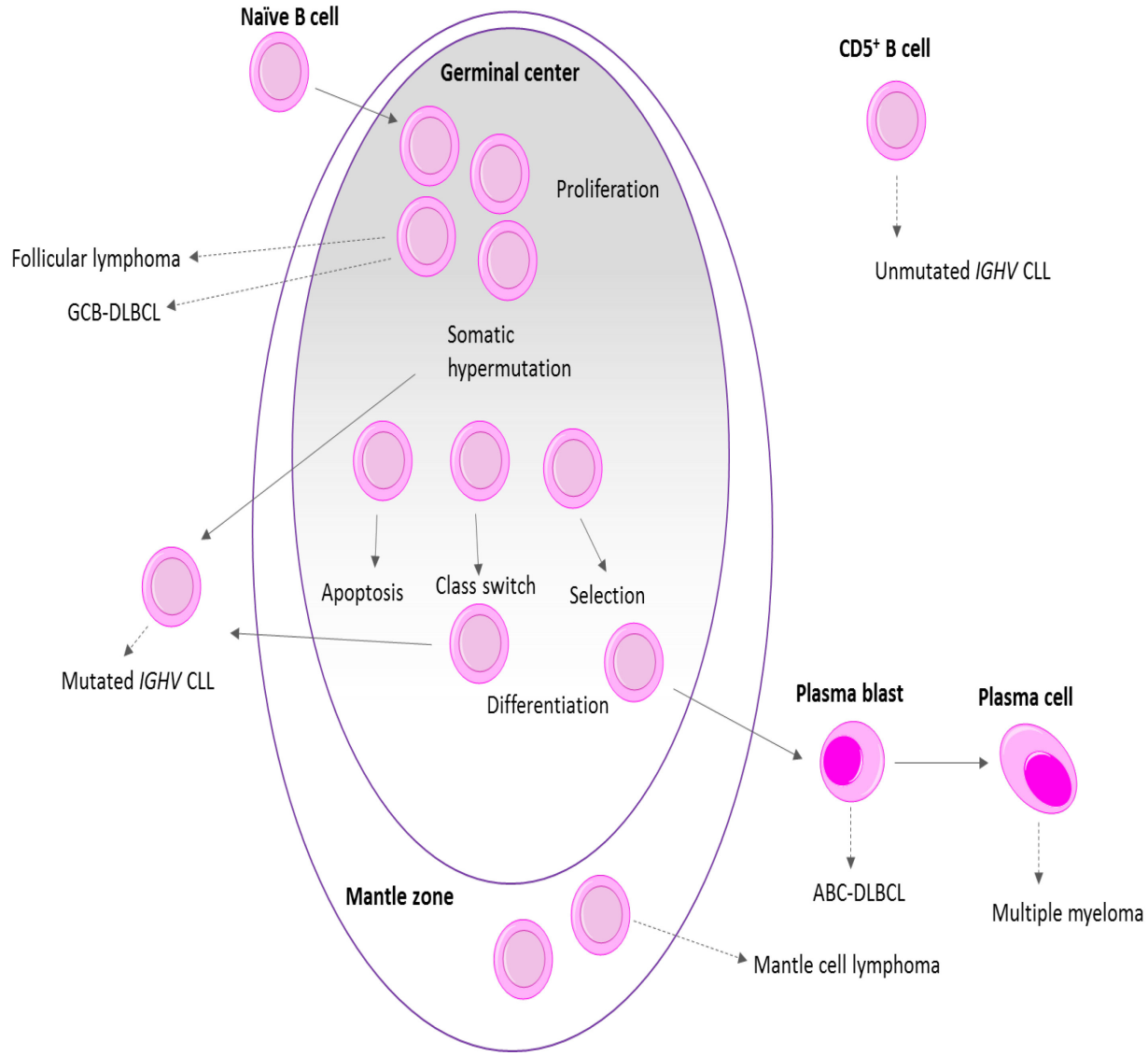

Figure 1-9. Simplified diagram of the origin of B-cell neoplasms.

The diagram demonstrates the GC reaction and the main steps involved in the differentiation of mature B cells, depicting the cellular origin of a selection of B cell tumours and their stage of development before tumorigenesis. GC B cells can undergo transformation to develop into follicular lymphoma or GCB-DLBCL. By contrast, ABC-DLBCL derives from more differentiated plasma blasts. Myeloma derives from antibody-secreting plasma cells. CLL derives from either pre-GC or post-GC B cells (U-CLL and M-CLL respectively). Mantle zone B cells can give rise to mantle cell lymphomas. Image produced using ChemDraw professional ® v16.0. Figure adapted from (Seifert et al., 2013).

1.3.1 Chronic lymphocytic leukaemia

CLL is a cancer of mature $CD5^+$ B cells characterised by the presence of malignant lymphocytes in the peripheral blood, bone marrow and secondary lymphoid tissues, such as the lymph nodes (Hallek, 2017). It is the most common leukaemia in the Western world and thus has a significant disease burden (Hallek, 2017). The median age of patients with CLL is around 70 years of age (Parikh et al., 2014) and CLL is more common in men. Presentation of CLL can include swollen lymph nodes, splenomegaly, recurrent infections and typical 'B symptoms' which consist of fevers, chills and weight loss (Hallek, 2017). However, due to its relatively indolent nature, many CLL patients present with no symptoms and are diagnosed upon investigation for other conditions. Prognosis and disease progression varies substantially between patients due to a multitude of factors.

The pre-cursor to CLL is monoclonal B lymphocytosis (MBL) (Strati and Shanafelt, 2015, Hallek et al., 2018). MBL is defined by the presence of CLL cells in the peripheral blood and the absence of other diagnostic CLL features, such as recurrent infection, a B cell count lower than $5x10^9$/L , and a lack of nodal involvement (Strati and Shanafelt, 2015). MBL is known to precede almost all cases of CLL (Landgren et al., 2009, Strati and Shanafelt, 2015). MBL is also a precursor to small lymphocytic lymphoma (SLL), a non-Hodgkin's lymphoma which presents similarly to CLL albeit with more substantial evidence of nodal disease (Swerdlow et al., 2016).

At diagnosis, CLL is categorised using the Binet or Rai disease grading systems (Binet et al., 1981, Rai et al., 1975). Both systems grade the disease based upon lymphocytosis and the enlargement of secondary lymphoid organs, amongst other conditions such as anaemia and platelet count (Binet et al., 1981, Rai et al., 1975). Rai staging is numerical, ranging from 0 to IV (Rai et al., 1975). Stage 0 patients show lymphocytosis, stage I have enlarged LNs, stage II patients demonstrate splenomegaly or hepatomegaly, stage III is defined by anaemia due to reduced bone marrow function and stage IV patients present with thrombocytopenia (Rai et al., 1975). Earlier stages (0, I and II) have significantly longer survival rates than those in stages III and IV (Rai et al., 1975). Binet staging uses simpler alphabetical grouping (groups A,B and C) (Binet et al., 1981).

Simplicity in diagnosis and disease staging was required to improve access to clinical trials and would only require data from haematological investigation and clinical examination. Group A patients are defined by the lack of anaemia and thrombocytopenia, similar to that of group B patients who additionally have at-least three areas of disease present, such as the LNs, spleen and liver (Binet et al., 1981). Finally, group C patients present evidence of anaemia and/or thrombocytopenia, and have a shorter survival time than groups A and B (Binet et al., 1981).

CLL may also progress further and undergo transformation to other diseases, such as Richter's transformation (also known as Richter's syndrome). Richter's transformation describes the development of an aggressive high-grade lymphoma in a CLL patient, most commonly DLBCL (Lortholary et al., 1964, Michelis et al., 2012). Richter's transformation occurs in between three and ten percent of CLL cases (Michelis et al., 2012) and its development is associated with CLL cases that have high CD38 expression, acquired mutations leading to aberrant MYC activation, unmutated *IGHV*, ZAP-70 expression and other factors (Rossi et al., 2008).

1.3.2 Subsets of CLL

Like many B-cell malignancies, CLL is a heterogeneous entity and can be divided into subsets with distinct biological and clinical features, which can significantly affect prognosis and proposed treatments for patients.

1.3.2.1 *IGHV* mutational status

CLL can be divided into two major subsets dependent on whether the tumour cells express mutated or un-mutated *IGHV* genes. (U-CLL or M-CLL) (Hamblin et al., 1999). U-CLL arises from a B cell that has not undergone SHM within the GC, whereas M-CLL originates from a B cell that has undergone SHM (and in a small proportion of cases, may also have undergone CSR) (Hamblin et al., 1999, Seifert et al., 2013). U-CLL cases have at least 98% sequence homology between the expressed *IGHV* sequences and germline sequences, whereas M-CLL have with less than 98% sequence homology (Hamblin et al., 1999). The development of M-CLL cells is therefore similar to normal B cell development in that they undergo SHM of the *IGHV* as part of affinity maturation. Importantly, these different cells-of-origin are linked to different clinical behaviour. Thus, U-CLL is associated with a worse prognosis and more aggressive disease, whereas M-CLL is often more indolent and has a more favourable outcome (Hamblin et al., 1999).

U-CLL and M-CLL have differential gene expression profiles for both mRNA and microRNA (miRNA) (Rosenwald et al., 2001, Ferrer et al., 2004). For mRNA, *ZAP70* is the most differentially regulated gene discovered between the two subsets, with U-CLL commonly expressing more *ZAP70* than M-CLL (Rosenwald et al., 2001, Ferrer et al., 2004). ZAP70 expression is a prognostic marker discussed in more detail in section 1.3.2.2. On the other hand, *CD44* and *PAX5* are more highly expressed in M-CLL than U-CLL (Ferrer et al., 2004). CD44 is a cell membrane glycoprotein involved in lymphocyte activation and lymph node homing, whilst PAX5 is a transcription factor involved in B-cell

differentiation and is a regulator of isotype/class switching (Ferrer et al., 2004). Further studies are needed to determine the impact of this on clinical outcome.

With regards to miRNA expression, M-CLL is associated with the upregulation of miR-150, miR-29c, miR-143 and miR-223 and the downregulation of miR-15a, compared to U-CLL (Papakonstantinou et al., 2013). The most highly regulated in M-CLL (compared to U-CLL) is the downregulation of miR-15a. miR-15a is a tumour suppressor which regulates proliferation and apoptosis (Cimmino et al., 2005, Klein et al., 2010). In contrast, miR-101 is downregulated in U-CLL (compared to M-CLL) which is associated with overexpression of *EZH2* (Papakonstantinou et al., 2013). In B cell lymphomas, high expression of *EZH2* is linked to a more aggressive disease (Papakonstantinou et al., 2013, Tagawa et al., 2013).

DNA methylation patterns via genome-wide studies have been profiled in CLL, by comparison to normal B cell populations (Rush et al., 2004). Methylation of DNA is the addition of a methyl-group to cytosine, commonly in CpG dinucleotides. Most CpG dinucleotides are enriched in non-coding and more repetitive regions of the genome (Rush et al., 2004). Gene foci enriched in CpG dinucleotides within promoter regions (CpG islands) are generally unmethylated (Rush et al., 2004). Studies revealed that the majority of the epigenome in CLL reflects that of the cell of origin, and that minimal alterations in the epigenome are CLL-specific (Rush et al., 2004). With the development of the DNA 'methylome' profiling in CLL, it was noted that there are at least three differential methylation profiles between disease subgroups, likely due to different cell of origin (Rush et al., 2004). With this, higher levels of heterogeneity in epigenetic changes are seen in more aggressive subgroups of CLL (Rush et al., 2004). Methylation/hypermethylation of CpG islands within promoters results in gene silencing, and thus methylation patterns can be used to understand further genetic changes driving disease evolution.

Notably, CLL cells have hypermethylated CpG islands compared to normal B cells (Rush et al., 2004). U-CLL have a different methylation pattern to M-CLL. U-CLL have hypermethylated and thus 'silenced' tumour suppressor genes (Kanduri et al., 2010). Examples of these genes are *ABI3* and *IGSF4* (Kanduri et al., 2010). U-CLL also demonstrated hypomethylation, and consequential expression, of genes with roles in cell proliferation (such as *ADORA3*) (Kanduri et al., 2010). This study identified that U-CLL cases, M-CLL cases and CLL with *IGHV3-21* (regardless of mutational status) all demonstrated differential methylation patterns (Kanduri et al., 2010). The majority of differences were noted to be outside of CpG islands and in non-coding regions (Cahill et al., 2013). This study also demonstrated that methylation patterns were stable over disease progression/time and this implies that methylation changes occur early in CLL development (Cahill et al., 2013).

1.3.2.2 Other prognostic markers in CLL

ZAP-70 expression is associated with a poor prognosis (compared to CLL not expressing ZAP-70), and is expressed most typically in U-CLL (Durig et al., 2003). ZAP-70 is a tyrosine kinase normally expressed near the cell surface of T and natural killer cells (Wang et al., 2010). ZAP-70 enhances BCR signalling in CLL cells via the prolonged phosphorylation of SYK, although this effect is independent of kinase activity of ZAP-70 (Gobessi et al., 2007). *ZAP-70* is commonly hypermethylated in M-CLL, compared to U-CLL (Cahill et al., 2013). Hypermethylation of *ZAP70* results in gene silencing, reducing ZAP-70 expression and associated enhanced BCR signalling, thus resulting in a more favourable outcome for patients (Cahill et al., 2013).

CD38 is another prognostic indicator for CLL, associated with more aggressive disease and occurring more commonly in U-CLL cases (Damle et al., 1999). In normal B cells, CD38 expression varies throughout their developmental stages, dependent upon maturation and activation (Malavasi et al., 1994, Oertel et al., 1996). CLL cases with a high percentage of $CD38^+$ cells (>30%) have reduced overall survival compared to those with low $CD38^+$ percentage (Damle et al., 1999). $CD38^+$ B cells demonstrated an increased responsiveness to BCR stimulation via a more efficient response to cross-linking of sIgM (Cutrona et al., 2008). They also have enhanced rates of migration (Cutrona et al., 2008). Activation of CD38 *in vitro* increases CLL cell proliferation via ZAP-70 and ERK1/2, and increased homing via CXCR4 and CD49d (Deaglio et al., 2010). $CD38^+$ cells are also thought to have a clear survival advantage due to their increased expression of anti-apoptotic BCL2 family protein, MCL1 (Pepper et al., 2007), resulting in a more aggressive disease.

CD49d is also associated with poor prognosis in CLL. CD49d expression correlates with $ZAP\text{-}70^+$, $CD38^{hi}$ expression and unmutated *IGHV* (Shanafelt et al., 2008). CD49d is involved in the migration of CLL cells and helps to retain CLL cells in the LN and BM for exposure to growth/survival signals in the microenvironment (Dal Bo et al., 2016). CLL can be defined as $CD49d^{hi}$ or $CD49d^{lo}$ through flow cytometry of peripheral blood CLL samples, using a 30% cut-off (Shanafelt et al., 2008).

1.3.2.3 Genetic alterations in CLL

Numerous genetic alterations have been described in CLL, including mutations and large chromosomal alterations (Table 2). Some genetic alterations are also associated with increased heritable risk of developing CLL (Berndt et al., 2013, Di Bernardo et al., 2008).

Table 2. Key genetic aberrations in CLL, their clinical impact and suggested treatment (adapted from (Dohner et al., 2000))

GENETIC ABBERATION	RISK	CLINICAL IMPACT	THERAPY
17p DELETION	Very high	Around 40% of refractory CLL cases have 17p13 deletion (Le Garff-Tavernier et al., 2011) Approx. 80% of patients with del(17p13) have loss of p53 (Zenz et al., 2008a)	BTK inhibitors, p53-independent drugs
***TP53* MUTATION**		Reduced expression of mir-34a (Zenz et al., 2009)	Allogeneic stem cell transplant
***BIRC3* MUTATION**		Loss of function *BIRC3* mutations in 2-4% of CLL cases, but 24% of fludarabine-refractory cases (Rossi et al., 2012)	
11q DELETION	High	18% of CLL patients have 11q deletion at diagnosis (Dohner et al., 2000)	FCR (fludarabine, cyclophosphamide and rituximab)
***ATM* MUTATION**		Point-mutations and 11q deletion can result in reduced ATM function and dysregulated p53 (Dohner et al., 2000)	
***NOTCH1* MUTATION**		8.3% CLL cases have activating *NOTCH1* mutations, associated with treatment resistance (Fabbri et al., 2011)	
***SF3B1* MUTATION**		5% cases at diagnosis have *SF3B1* mutation, present in 17% fludarabine-refractory cases (Rossi et al., 2011)	
TRISOMY 12	Intermediate	Present in 20% of CLL cases at diagnosis (Matutes, 1996)	'watch and wait'
13q14 DELETION	Low	Most common genetic aberration, detected in around 50% of CLL patients at stage of first-line treatment (Dohner et al., 2000) Can lead to over expression of *BCL2* (Cimmino et al., 2005)	watch and wait'

1.3.2.3.1 Chromosomal aberrations

Studies have demonstrated that over three quarters of CLL patients have at least one of the following chromosomal aberrations; deletions in 13q, 11q, 17p and trisomy of chromosome 12 (Dohner et al., 2000).

Deletion of 13q (del(13q)) is detected in around 50% of CLL patients requiring first-line treatment and is associated with a favourable prognosis when it occurs as a sole abnormality (Dohner et al., 2000, Shanafelt et al., 2006). This deletion results in the loss of the *miR-15/16* gene cluster (Calin et al., 2002). *miR-15/16* represses expression of BCL2 and so del(13q) is an important mechanism that can contribute to reduced apoptosis susceptibility in CLL cells (Majid et al., 2008). Del(13q) is also associated with increased expression of other BCL2-family proteins, such as myeloid cell leukaemia-1 (MCL1), a key anti-apoptotic protein associated with CLL cell survival and resistance to chemotherapy (Calin et al., 2008, Pepper et al., 2008). A mono-allelic deletion is sufficient for a complete loss of function (Mertens et al., 2006). Del(13q) also results in the activation of the *miR34* cluster, which reduces expression of ZAP-70, resulting in a favourable prognosis for CLL patients (Rassenti et al., 2004).

Del(13q) can also have a negative outcome, depending upon the size of the deletion (Parker et al., 2011). Smaller deletions are of favourable outcome whilst larger deletions at diagnosis are associated with disease progression (Parker et al., 2011). When a larger deletion occurs in U-CLL this results in a treatment-free survival of around 3 months compared to 18 months for cases with smaller deletions (Parker et al., 2011). 13q deletion has also been described in MBL at a frequency similar to CLL, implying that this aberration occurs early in the development of disease (Dohner et al., 2000).

Del(17p) is much less common, occurring in around 7% of CLL cases requiring first-line treatment (Dohner et al., 2000). 17p deletions are associated with an adverse prognosis and rapid disease progression (Dohner et al., 2000). This deletion results in the loss of tumour suppressor *TP53*, encoding P53 (Zenz et al., 2008b, Rossi et al., 2012) . P53 is a key factor in the recognition of DNA damage, control of cell cycle progression and apoptosis (Adimoolam and Ford, 2003). Interestingly, more than 80% of patients with del(17p) also express mutated *TP53* from the other allele, losing P53 function completely (Zenz et al., 2008a, Malcikova et al., 2009). Around 40% of patients with relapsed/refractory CLL have del(17p), implying that the loss of p53 is a selective advantage during clonal evolution for CLL cell survival (Le Garff-Tavernier et al., 2011). This often occurs after the original development of CLL, as large clonal shifts can occur after chemotherapy due to these selective advantages.

Del(17p) is associated with aggressive disease in U-CLL, although M-CLL cases with del(17p) may still experience indolent disease (Gladstone et al., 2011). Therefore, fluorescence in-situ hybridisation (FISH) analysis of chromosomes is necessary when predicting disease outcome in patients, regardless of mutational status. Clonal loss of P53 has a selective advantage for CLL cells (Rossi et al., 2014), and is associated with a worse prognosis, but sub-clonal mutations in *TP53* also have the same impact on prognosis as clonal mutations (Rossi et al., 2014). These small sub-clones tend to become the clonal CLL population at the stage of relapse after chemotherapy and can be identified early in disease progression to predict the course of disease (Rossi et al., 2014).

Another deletion associated with an adverse outcome in CLL is del(11q), found in around 18% of cases requiring first treatment (Dohner et al., 2000). 11q deletions result in the deletion of/alterations in *ataxia-telangiectasia mutated* (*ATM*) (Dohner et al., 2000). Patients with this deletion develop severe lymphadenopathy and have a poor response to treatment, thus del(11q) is associated with a more aggressive disease course (Dohner et al., 1997, Pflug et al., 2014). ATM is a serine/threonine kinase implicated in DNA repair and is activated following the recognition of a double strand break (DSB) in DNA (Marechal and Zou, 2013). Once activated, ATM phosphorylates and activates target proteins, such as P53 (Marechal and Zou, 2013). Loss of ATM therefore results in reduced recognition of DNA damage and the reduced function of P53 (Westphal et al., 1997). In relapsed cases of CLL, deletion of 11q occurs in around 40% of cases and so is also a selective advantage for clonal evolution of CLL cells (Dohner et al., 2000). Loss of ATM and del(11q) are most common in U-CLL and these cases often present with aggressive disease (Dohner et al., 2000).

Del(11q) also results in the loss of the *miR-34* locus (Zenz et al., 2009). *miR-34* is responsible for reducing *ZAP-70* expression (Fabbri et al., 2011), so loss of this cluster increases *ZAP-70* expression and has a worse outcome for patients. Low expression of *mir-34a* in CLL is associated with P53 inactivation and in refractory CLL (Zenz et al., 2009), inactivated P53 is associated with an impaired response to DNA damage and increased resistance to apoptosis (Mraz et al., 2009), regardless of other genetic abnormalities (Zenz et al., 2009).

Trisomy of chromosome 12 (an extra 12^{th} chromosome) is present in 16% of CLL patients undergoing first-line treatment, with an intermediate effect on prognosis (Dohner et al., 2000). Trisomy 12 results in the increased expression of integrins on the surface of CLL cells, particularly CD11a and CD49d, enhancing transendothelial migration of CLL cells to the LNs (Riches et al., 2014). Trisomy 12 CLL cases often have increased CD38 expression (Riches et al., 2014), a factor involved in cellular adhesion and is responsible for the augmentation of BCR signalling (Lund et al., 1996, Funaro and Malavasi, 1999). Trisomy 12 is also associated with high CD49d expression, a further determinant of shorter time-to-treatment in these patients (Zucchetto et al., 2013).

Trisomy 12 is another aberration that has been described in MBL (Dohner et al., 2000), and has been noted in 50% of CLL patients who ultimately develop Richter's syndrome (Rossi et al., 2008). Thus, trisomy 12 often has a negative impact on a patients prognosis, and as with many of the most common chromosomal aberrations in CLL, trisomy 12 is more commonly associated with U-CLL cases (Athanasiadou et al., 2006).

1.3.2.3.2 Somatic mutations

Somatic mutations are important determinants of the pathogenesis of CLL and response to treatment. These mutations are most commonly found in genes encoding proteins involved in DNA damage, mRNA processing, NOTCH signalling and inflammatory pathways. Some of the most commonly mutated genes have been identified as being *p53*, *NOTCH1, ATM, BIRC3*, *XPO1* and *MYD88* (Puente et al., 2011, Landau et al., 2015).

Somatic mutations have been identified in *SF3B1* (Rossi et al., 2011). SF3B1 (encoded by *SF3B1)* is a component of the RNA splicing machinery, whereby it catalyses the removal of introns from mRNA of genes involved in cell cycle control (Kaida et al., 2007). Mutations in *SF3B1* are associated with more aggressive disease and a worse prognosis (Rossi et al., 2011). The majority of mutations occur within the C-terminal domain, a highly conserved region, meaning they are likely to have functional significance and thus mutated *SF3B1* results in an aberrant RNA splicing response in these cases, but only on specific targeted transcripts rather than having a global effect (Rossi et al., 2011, Quesada et al., 2011). A target transcript of SF3B1 is *FOXP1.* In CLL with mutated *SF3B1, FOXP1* expression is three-times higher than in cases without *SF3B1* mutations (Quesada et al., 2011). FOXP1 is a transcription factor and is known to be linked with a negative outcome in DLBCL (Barrans et al., 2004). Importantly, CLL cells have been shown to express higher SF3B1 than normal B cells (Rossi et al., 2011), and thus it is likely that mutations in *SF3B1* are responsible for driving disease and the lack of cell-cycle control in some cases. *SF3B1* mutations occur in 5% of CLL cases at diagnosis, but also in 17% of fludarabine-refractory cases of CLL, implying that *SF3B1* mutations are a selective advantage (Rossi et al., 2011).

NOTCH1 mutations are also common in CLL, particularly being more common in U-CLL than M-CLL (Fabbri et al., 2011). NOTCH1, encoded by *NOTCH1*, is a transmembrane protein that functions as a transcription factor (Fabbri et al., 2011). When activated by its ligand, NOTCH1 is cleaved and translocates to the nucleus for roles in differentiation, proliferation and apoptosis, ultimately activating transcription of target genes. A key target gene of NOTCH1 is *MYC* (Palomero et al., 2006). The majority of *NOTCH1* mutations in CLL are 2-base deletion frameshifts which lead to the

production of a truncated, and constitutively activated, NOTCH1 protein (Fabbri et al., 2011). Other mutations in *NOTCH1* were also present in the same region as this frameshift, but instead result in the generation of a premature stop codon, which results in the production and accumulation of a more stable form of NOTCH1 lacking its C-terminal domain (Puente et al., 2011). This is particularly important, as NOTCH1 is constitutively expressed in CLL (Rosati et al., 2009). Around 42% of U-CLL cases with trisomy 12 also have *NOTCH1* mutations (Balatti et al., 2012). These aberrations may potentially result in the increased activation of MYC, downstream of constitutively active NOTCH1, which can contribute to a poorer outcome.

Non-coding mutations in the 3' untranslated region (UTR) of *NOTCH1* have also been demonstrated in two percent of untreated CLL and MBL patients (Puente et al., 2015). These mutations are associated with aberrant RNA splicing, resulting in the increased activity of NOTCH1 and a more aggressive disease (Puente et al., 2015). *NOTCH1* is commonly hypermethylated in M-CLL, compared to U-CLL and normal B cells (Cahill et al., 2013), which results in the silencing of *NOTCH1* and thus consequentially reduces NOTCH1 expression and signalling. This methylation pattern can result in a favourable outcome for CLL patients (Cahill et al., 2013).

Puente and colleagues (Puente et al., 2011) also identified mutations in *XPO1,* which encodes Exportin 1 (XPO1). XPO1 is a nuclear transport factor which mediates the nuclear export of proteins, RNAs and ribonucleoproteins (Fornerod et al., 1997). Various mutations in *XPO1* have been found in the same codon, in position 571 (Puente et al., 2011). These are found in a highly conserved region, indicating that these mutations affect the function of XPO1. *XPO1* mutations occur most commonly in U-CLL, and are often associated with mutations in *NOTCH1,* which implies that these mutations may have synergistic roles in the development of CLL (Puente et al., 2011). The consequences of these mutations in *XPO1* are not yet understood in terms of functionality, but the role of XPO1 in B-cell malignancies and nuclear export will be discussed in greater depth in section 1.5.

Interestingly, at the time of first treatment, around three percent of CLL cases have mutations in *MYD88* (Puente et al., 2011). This mutation has also been identified in lymphomas (Ngo et al., 2011). *MYD88* encodes myeloid differentiation primary response-88 (MYD88), an adaptor protein involved in signalling pathways downstream of toll-like receptors (TLR) and IL-1 during the innate immune response (Coste et al., 2010, O'Neill and Bowie, 2007). Downstream effectors of the MYD88 pathway are highly phosphorylated in *MYD88* mutated cases, compared to those without this mutation (Puente et al., 2011). These effectors include signal transducer and activator of transcription-3 (STAT3), IκBα and the p65 subunit of NF-κB. Mutated *MYD88* cases also exhibit enhanced DNA binding by NF-κB (Puente et al., 2011). Altogether, these findings imply that

mutations in *MYD88* are activating mutations which drives disease, allowing MYD88 to act as a proto-oncogene.

The final somatic mutation discussed in this section is that of *BIRC3*. BIRC3, also known as cellular inhibitor of apoptosis-2 (cIAP2), is an ubiquitin ligase which regulates the non-canonical pathway of NF-κB signalling and innate immune pathways via TLR and nucleotide oligomerisation domain (NOD)-like receptor (NLR) signalling (Dubrez-Daloz et al., 2008). All *BIRC*3 mutations discovered in CLL disrupt the C-terminal domain (Rossi et al., 2012), which inactivates BIRC3, preventing downregulation of NF-κB signalling via MAP3K14 (Rossi et al., 2012). As a consequence of this, *BIRC3* mutated CLL cases have augmented and constitutive NF-κB activation (Rossi et al., 2012). These cases have a poor outcome, regardless of the presence of other risk factors (Rossi et al., 2012). Between two and four percent of CLL cases (at time of diagnosis) have loss of function mutations in *BIRC3* (Rossi et al., 2012). Also, 24% of fludarabine-refractory CLL cases have inactivating *BIRC3* mutations (Rossi et al., 2012) implying a selective advantage for *BIRC3* mutations in sub-clones following therapy.

1.3.2.3.3 Single nucleotide polymorphisms

A range of genome-wide association studies (GWAS) have been performed in the past decade which have demonstrated the role of genetic variation in development of CLL. A person with a relative diagnosed with CLL is around eight-times more likely to develop CLL (Goldin et al., 2009) and inherited genetic variation may therefore also contribute to increased risk.

Four single nucleotide polymorphisms (SNPs) have been identified in *IRF8,* which encodes interferon regulatory factor-8 (IRF8), within the 16q24.1 locus (Slager et al., 2011). Notably, these SNPs are associated with an increase in the expression of *IRF8* and increases an individual's risk for CLL, likely due to the role of IRF8 in regulating B cell lineage and differentiation (Wang et al., 2008).

An SNP at 18q21.32 was discovered 51kb downstream from *PMAIP1* (Berndt et al., 2013). This gene encodes NOXA, a BCL2-family pro-apoptotic protein. NOXA regulates apoptosis and is necessary for B-cell expansion following antigen exposure (Wensveen et al., 2012). NOXA is a key factor in maintaining the balance between pro/anti-apoptotic proteins to influence cell survival or death, with anti-apoptotic MCL1 (Smit et al., 2007). If NOXA expression is down-regulated, the balance shifts increasing the persistence/survival of CLL cells in the lymph node (Smit et al., 2007). This SNP was identified to increase risk of developing CLL (Berndt et al., 2013).

1.3.3 The role of the BCR in CLL

Multiple lines of evidence indicate that the BCR plays an important role in the development of CLL.

1.3.3.1 Immunogenetics

As described above (section 1.3.2.1), the seminal finding was that the *IGHV* mutation status of the CLL clone (i.e. U-CLL versus M-CLL) was tightly correlated with disease outcome (Hamblin et al., 1999). However, other lines of immunogenetic evidence have linked features of the BCR to variable disease behaviour in CLL. For example, there is evidence for biased V-gene usage whereby individual V-genes, or families of V-genes, are used at a significantly different frequency from the normal B-cell repertoire (Fais et al., 1998, Tobin, 2005). A clear example of this is the overuse of *IGHV1-69*, occurring in around ten percent of CLL versus around four percent in the normal repertoire (Potter et al., 2003, Murray et al., 2008), most commonly in U-CLL (Forconi et al., 2010). *IGHV4-34* is also overrepresented, mainly in M-CLL (Fais et al., 1998). The presence of a biased V-gene repertoire provides evidence for a restricted repertoire of driving antigens (including viral) acting on CLL BCRs. The use of *IGHV3-21* appears to 'overrule' mutational status, since it is associated with poor prognosis independent of *IGHV* mutational status (Ghia et al., 2005).

There is also evidence for a functional influence of the BCR in CLL progression, particularly between U- and M-CLL subsets (Mockridge et al., 2007). This is mainly attributable to a varied signalling capacity, with U-CLL having retained signalling capacity in comparison to M-CLL, which may account in part to the more aggressive disease associated with U-CLL (Mockridge et al., 2007). This signalling capacity is also influenced by somatic mutations, as described in section 1.3.2.3.2 and can further influence disease outcome and progression regardless of *IGHV* mutational status.

1.3.3.2 BCR signalling in CLL

In CLL, BCR signalling appears to be driven predominantly by (auto)antigen. Whilst the antigen inducing CLL signalling *in vivo* is unknown, it is likely that BCR activation occurs within the tumour microenvironment, since B cells are activated within secondary lymphoid organs (such as the LNs), where they encounter antigen (Harwood and Batista, 2010b). It has more recently been discovered that CLL B cells engage antigen within the PCs, in LNs, demonstrated by the overexpression of BCR target genes in CLL cells residing within the LNs, compared to circulating CLL cells (Packham et al., 2014, Herishanu et al., 2011).

A multitude of (auto)antigens have been identified as potential antigens for BCR signalling in CLL, such as markers on apoptotic cells like cytoskeletal proteins, as well as bacterial antigens (Lanemo Myhrinder et al., 2008). Other potential antigens include viral and fungal antigens (Steininger et al., 2012, Hoogeboom et al., 2013), although the antigens which stimulate established CLL cells are not necessarily the antigen which stimulated the originating B cell (Packham et al., 2014). Autonomous signalling (driven by BCR-BCR self-recognition) has also been described for CLL cells (Duhren-von Minden et al., 2012, Ghia et al., 2008) but its significance *in vivo* is unclear.

The ability of individual CLL samples to signal via sIgM is highly variable and this variation has been linked to distinct disease subsets and clinical outcome (Mockridge et al., 2007, Lanham et al., 2003, D'Avola et al., 2016). Overall, the expression of sIgM is low on CLL cells compared with other B-cell malignancies, and BCR signalling responses are generally weak (Efremov et al., 1996). However, U-CLL samples tend to retain a degree of sIgM expression and signalling capacity. sIgM expression and signalling is more strikingly down-modulated in M-CLL samples (Mockridge et al., 2007, Lanham et al., 2003, D'Avola et al., 2016).

The link between retained sIgM expression/signalling capacity *in vitro* and poor disease outcome for patients has contributed to the idea that antigen-driven BCR signalling is an important driver of CLL pathogenesis (Mockridge et al., 2007, Lanham et al., 2003, D'Avola et al., 2016). Consistent with this, the activation of sIgM on signal responsive CLL samples *in vitro*, engages various malignancy-promoting pathways, including the activation of upstream signalling responses via PI3K, NF-κB and ERK, and downstream responses, including the induction of *MYC* expression (Krysov et al., 2014, Krysov et al., 2012). Importantly, stimulation of sIgM also increases rates of global mRNA translation in CLL samples (Yeomans et al., 2015). Immobilised-anti-IgM treatments *in vitro,* triggers stronger and longer-lasting signal responses, compared to soluble anti-IgM (Petlickovski et al., 2005). Soluble anti-IgM promotes apoptosis of CLL cells, whereas engagement of the BCR by immobilised-anti-IgM results in repression of apoptosis by induction of MCL1 (Petlickovski et al., 2005).

The natural downregulation of sIgM expression/function that characterises all CLL samples (but is particularly evident in M-CLL), appears to be due the induction of anergy following engagement of the BCR *in vivo* (Figure 1-10) (Packham et al., 2014). Thus, culturing CLL cells *in vitro* leads to recovery of sIgM expression and signalling capacity. Induction of anergy is an expected response to engagement of CLL BCRs by autoantigen in the absence of T-cell help (Pepper et al., 1997, Packham et al., 2014). Although normal anergic B cells are especially susceptible to apoptosis, anergic CLL cells appear to be protected by increased anti-apoptotic protein BCL2 expression (Pepper et al., 1997).

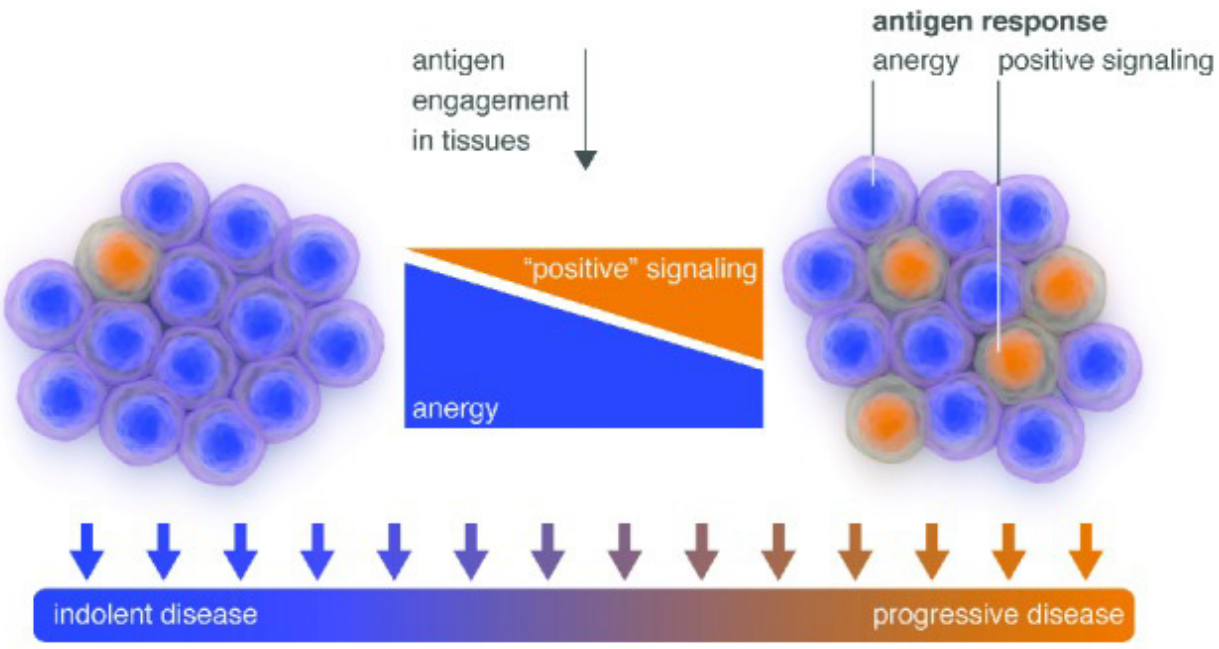

Figure 1-10. Balance between 'positive' BCR signalling and anergy in CLL

BCR signalling results in varied effects on anergy and 'positive signalling, leading to a varied clinical outcome, dependent upon the balance of these signalling responses. Anergy is the most common outcome in CLL following antigen engagement, resulting in indolent disease. Increased levels of 'positive' (growth-promoting) BCR-signalling may result in more progressive CLL. The balance can be tipped by intrinsic factors (such as mutational status and ZAP-70 expression) and extrinsic factors (potentially via T-cell help and TLR activation). Figure taken from (Packham et al., 2014).

Stimulation of the BCR also modulates the expression of certain miRNAs. In more aggressive cases of U-CLL, stimulation of the BCR induces upregulation of *miR-17/92* (Psathas et al., 2013, Balatti et al., 2015). This cluster is overexpressed in many lymphoid malignancies and inhibits expression of PTEN, a tumour suppressor, and the pro-apoptotic BCL-2 family protein, BIM (Xiao et al., 2008).

miRNA are also implicated in the consequences of BCR signalling in CLL. Dysregulated *miR-155* expression is associated with clonal expansion in B cell malignancies and modulates BCR signalling via SHIP1 (Costinean et al., 2006). Reduction of SHIP1 expression by *miR-155* enhances BCR signalling responses (Cui et al., 2014). Overexpression of *miR-155* has been noted in refractory CLL, linked to enhanced BCR signalling, proliferation and lymphomagenesis (Guinn et al., 2015).

In contrast to sIgM, relatively little is known about the function of IgD in CLL cells. sIgD does not appear to be reversibly down-modulated on CLL cells and the vast majority of samples retain the ability to signal downstream of sIgD (Krysov et al., 2012). This appears to reflect the overall anergic phenotype of CLL cells since IgM, but not IgD, is down-regulated by chronic antigen engagement in mouse models of anergy (Packham et al., 2014). However, although signal responsiveness is most commonly retained, the responses tend to be short-lived and fail to effectively engage downstream pathways, such as MYC induction (Krysov et al., 2012) or mRNA translation (Yeomans et al., 2015). Studies investigating the role of IgD have implicated that IgD activation contributes to the initiation of IgM signalling (Ten Hacken et al., 2016), as demonstrated by the co-stimulation of IgM and IgD resulting in the increased activation of proximal BCR signalling markers, such as ERK-phosphorylation, although not with longer-term responses such as cell survival (Ten Hacken and Burger, 2016).

1.3.4 Current therapies for CLL

Decisions to initiate treatment in CLL are influenced by the presence of anaemia, thrombocytopenia, lymphadenopathy and typical B symptoms (Hallek et al., 2018). The choice of therapy for CLL is also determined by a range of factors. Genetic aberrations such as del(17p), *IGHV* mutational status, age and overall wellness of the patient, amongst other parameters, play a significant role. Patients with indolent CLL are often managed on a 'watch and wait' treatment approach due to minimal symptoms; these patients undergo regular blood tests to monitor disease progression (Hallek et al., 2018). When disease begins to progress, or in more aggressive cases, treatment is initiated (Hallek et al., 2018). Historically, chemotherapy combinations were the initial choice of treatment for CLL, as with many other cancers. Fludarabine, or other purine analogues, and alkylating agents such as chlorambucil are some of the key agents used in chemotherapy for

CLL (Hallek, 2015). The lack of specificity of these agents for tumour cells result in a range of complications for patients, such as myelosuppression and the development of secondary cancers (Ricci et al., 2009).

More recent developments in treatment include combination therapies of chemotherapy with anti-CD20 monoclonal antibodies, such as rituximab, in combination with classic chemotherapy agents, named chemoimmunotherapy (CIT) (Hallek, 2015). These treatments are typically used for cases of progressive/aggressive CLL. CIT can be associated with severe side effects that are detrimental to a patient's quality of life. Initial CIT regimens for patients able to withstand the associated toxicity often include a combination of fludarabine, cyclophosphamide and rituximab (FCR) (Hallek, 2015). Whilst not curative, studies suggest that FCR may provide long-term progression-free survival in a subset of M-CLL patients, with no del(17p) or del(11q) (Thompson et al., 2016). Notably, FCR-treated patients have longer progression-free survival and higher response rates than those on chemotherapy alone (Hallek, 2010). However, patients with del(17p) or del(11q) are unlikely to gain significant benefit from CIT due to the inactivation of DNA damage response pathways in these patients' tumour cells.

Development of therapies for CLL and other B-cell tumours is necessary due to the resistance and toxicity associated with current therapeutic strategies. Therefore, there has been a strong focus on the development of new treatments for CLL, such as BCR-signalling kinase inhibitors and BCL2 homology domain-3 (BH3)-mimetics.

The BTK inhibitor ibrutinb was the first kinase inhibitor approved for use in therapy against CLL (de Claro et al., 2015). A pivotal randomised trial of ibrutinib showed improved progression-free survival and overall survival in patients without del(17p), compared to chlorambucil chemotherapy (Burger et al., 2015a). Ibrutinib is used as a single-agent therapy in the treatment of CLL, and functions by inhibition of BTK (and likely other targets), resulting in the inhibition of signalling via the BCR and other cell surface receptors (Burger et al., 2015b). Side-effects of ibrutinib include gastro-intestinal disturbances, fatigue, myalgia and atrial fibrillation, amongst others. Patients must continue on ibrutinib indefinitely, and so it is not a curative treatment, but it does provide significant improvement in many cases of CLL (Hallek et al., 2018).

Ibrutinib also inhibits the homing of CLL cells to the LNs by inhibition of chemokine receptor signalling (Ponader et al., 2012). Redistribution of CLL cells into the blood, following shrinkage of the lymph nodes causes an increase in the lymphocyte count in the blood (Byrd et al., 2013). This increased lymphocytosis subsides throughout treatment as the tumour burden reduces over time, and often resolves within 8 months of treatment (Woyach et al., 2014, Byrd et al., 2013).

Resistance to ibrutinib treatment has been demonstrated. One method of which is the mutation of a cysteine residue at position 481 within the active site of BTK, which renders the enzyme resistant to drug inhibition (Woyach et al., 2014). Mutations have also been described in PLCγ2 which are gain-of-function (Woyach et al., 2014), bypassing requirements for BTK. Refractory CLL is also associated with clonal evolution (acquired genetic aberrations) having poor prognostic consequences, such as *TP53* mutations. Targeting of tyrosine kinases, such as BTK, with inhibitors such as ibrutinib show efficacy in relapsed/refractory CLL (Byrd et al., 2013). Relapsed CLL patients treated with Ibrutinib have an overall survival of 83% following 26 months therapy (Byrd et al., 2013), independent of the presence of any high-risk genetic features such as del(17p). A complete response by Ibrutinib treatment is very rare, at around two percent in previously treated CLL cases (Byrd et al., 2013).

PI3K inhibitors, such as idelalisib, also result in rapid lymphocytosis upon initiation of treatment (Furman et al., 2014). Idelalisib is a small molecular inhibitor of PI3Kδ and was approved for therapy in Europe following trials demonstrating its ability to increase progression-free survival when in combination with rituximab, in comparison to rituximab alone (Furman et al., 2014). A notable issue with idelalisib treatment is the development of severe complications, such as enterocolitis and hepatotoxicity, which can have such a significant impact on quality of life that the treatment has to be ended, which renders it unsuitable as front-line treatment (Lampson et al., 2016). Aside from these toxic side effects, inhibition of PI3Kδ by idelalisib may also have implications on genomic stability (Compagno et al., 2017). In particular, there is an increase in genomic instability, due to increased AID expression (Compagno et al., 2017). AID is an enzyme known to induce genomic translocations and mutations (Compagno et al., 2017). With this in mind, further PI3K inhibitors are under-development, such as ACP-319.

BH3-mimetics which inhibit BCL2, such as venetoclax, have been investigated as a treatment for CLL. Venetoclax induces apoptosis of CLL cells by preventing the sequestration of BIM by BCL2 (Anderson et al., 2016). BIM is pro-apoptotic and so increasing the availability of BIM results in increased apoptosis. A substantial side-effect of venetoclax treatment is tumour lysis syndrome, the risk of which can be mitigated by a slow dose-escalation of venetoclax (Cheson et al., 2017). FDA approval of venetoclax was issued for patients with relapsed/refractory CLL or those with del(17p), as studies have demonstrated improved progression-free survival with eight percent of patients achieving complete response to treatment (Roberts et al., 2016, Stilgenbauer et al., 2016).

With these treatments demonstrating a minimal curative ability and side effects that reduce quality of life, novel treatments are key for improving disease outcomes in CLL. Currently, allogeneic stem cell transplantation is the main treatment for curative intent in some cases (Hallek et al., 2018),

examples of which are those with relapsed/refractory CLL or with del(17p), although this is rarely undertaken, due to the advanced age and poor health of most patients. With this in mind, the resistance and lack of curative ability of current treatments means that other pathways critical for CLL proliferation and survival need to be explored.

Also of significance for treatment is del(17p) and the consequential loss of P53, associated with mutations in *TP53* on the remaining allele in more than 80% of patients with a 17p deletion (Dohner et al., 2000). To overcome the loss of P53, treatment must induce cell death independent of P53. Inhibitors of BCR signalling, such as ibrutinib have been used to treat P53 deficient cases. Although, despite the favourable responses of ibrutinib as described previously (Byrd et al., 2013), responses to ibrutinib in P53-deficient CLL deficient were less effective, as del(17p) patients demonstrated progression-free survival of 50% at 28 months (Byrd et al., 2015). Whereas, those without del(17p) had 87% progression free survival (Byrd et al., 2015). This difference is substantial and more work into novel treatments is necessary for high-risk CLL.

1.3.5 *In vivo* models for CLL

In order to progress therapeutic interventions from *in vitro* studies into clinical trials, they must first be investigated using *in vivo* models that aim to recapitulate human CLL. Although models will never truly incorporate all of the complexities of human malignancy, it is important to use preclinical models as a method to develop knowledge and understanding, whilst taking into account potential disease, species and immunity differences. Many models have been developed and the two most commonly used in recent studies will be discussed below; the Eμ-*TCL1* transgenic mouse and patient-derived xenografts (PDX).

1.3.5.1 Eμ-*TCL1* transgenic mouse model

In this model the *TCL1* gene is under the control of Ig regulatory elements, resulting in clonal expansion of $CD5^+$ IgM^+ B cells with an enforced expression of human *TCL1* (Bichi et al., 2002). TCL1 is involved in the normal development of both B and T cells (Teitell, 2005) and modulates transcription, by enhancing the phosphorylation of AKT and signalling via the NF-κB pathway. This results in increased cellular proliferation and survival (Laine et al., 2000). Enhanced TCL1 expression consequentially results in similar biological responses to those seen following BCR stimulation in CLL (Bichi et al., 2002). In human CLL, high TCL1 expression is often associated with poor prognostic markers, such as a diagnosis of U-CLL (Mansouri et al., 2010), and so this murine model is likely to mimic more aggressive cases of CLL as the tumour cells in this model express unmutated *IGHV*

(Bresin et al., 2016). Of course, murine models do not have the same immune complexities as human patients, but this model can provide an insight into the impact of certain treatments on CLL-like disease pathology. One major pitfall of this technique is that simple over-expression of *TCL1,* whilst key in modelling human CLL, does not account for the complexity of genetic aberrations in the human disease.

This model can be used in adoptive transfer experiments. Eμ-*TCL1* leukaemic cells can be transferred into non-tumour bearing C57BL/6 mice which can provide quicker access to this model than waiting for tumours to develop *de novo,* and gives more consistent tumour development. The fact that these animals are immunocompetent provides a significant advantage in experiments investigating new therapies, as it can demonstrate the impact of the immune system on the efficacy of these treatments and more fully recapitulates human disease.

1.3.5.2 Patient-derived xenografts (PDX)

Patient-derived xenografts (PDX) are models that involve the insertion of human tumour cells into immune-deficient mice. Implantation of patient tumour samples into this murine model allows for similar clinical and molecular responses seen in the human disease. These models are beneficial in comparison to transgenic models, as it recapitulates to a greater depth the complexities of human disease.

With this in mind, PDX models have their own limitations, particularly that studies need to be performed using immunocompromised animals and that tumour engraftment can be highly variable (Simonetti et al., 2014). Establishing a model this way is therefore largely more time-consuming and complicated. Historically, the main issues in PDX development, were the development of mice immunodeficient enough to prevent the rejection of human tumour cells, as any residual immune response in these mice will target implanted xenogeneic cells (Simonetti et al., 2014). The development of disease in xenograft models depend greatly upon the cells transplanted, for example, transplantation of CLL-PBMCs into nonobese diabetic/severe combined immunodeficiency (NOD/SCID) mice recapitulates similarities with the patients clinical features within the murine organs (Durig et al., 2007). NOD/SCID mice are characterised by the absence of mature B and T cells, but still have NK cell activity (Durig et al., 2007). This led to the development of the NSG (NOD/Sci-scid ILRrg$^{-/-}$) mouse model, which is absent of mature B, T and NK cells (Simonetti et al., 2014). Implantation of CLL-PBMCs into the NSG mouse highlighted the need for an allogeneic transplant of normal antigen presenting cells to allow the CLL cells to fully engraft (Bagnara et al., 2011).

The requirement for antigen presentation implies the need for T cell help, and the study found a direct correlation between the presence of T cells with proliferation of the leukaemic cell population (Bagnara et al., 2011). Therefore, as with many developed murine models, the complexities become further away from the reality of human disease but still can be used as a model to mimic disease *in vivo*.

1.4 mRNA translation

Both the transcription and the translation of mRNA is critical in the regulation of protein synthesis, allowing cells to vary protein expression in response to both internal and external stimuli. mRNA translation is highly regulated at the initiation, elongation and termination steps (Baker and Coller, 2006), allowing for rapid changes in the expression of specific proteins independent of changes in their associated mRNA expression. Translation initiation can occur via 'cap-dependent' or 'cap-independent' mechanisms, and can be regulated by phosphorylation of eukaryotic initiation factors (eIFs) (Sonenberg and Hinnebusch, 2009). Studies have suggested that variation in mRNA translation accounts for approximately the same level of regulatory control over protein expression as variation in mRNA expression (Schwanhausser et al., 2011).

1.4.1 The structure of mRNA

The mRNA code is read by the ribosome in the 5' to the 3' direction. Post-transcriptional modifications of most RNA involves the 'capping' of the 5' end; this consists of the methylation of a guanosine nucleoside by a methyltransferase on the 7th position (Sonenberg and Hinnebusch, 2009). The presence of this cap may alter the rates of mRNA translation (Sonenberg and Hinnebusch, 2009) (Figure 1-11). The 5' and 3' UTRs are not translated as part of the coding sequence and are thought to have roles attributing to gene expression, such as providing stability of mRNAs (Mignone et al., 2002). Surrounding the start codon there is usually a Kozak consensus sequence (Kozak, 1987). This is the position where the 40S ribosomal subunit recognises the translational start site and begins the process of 60S recruitment, and subsequent translation elongation (Kozak, 1987).

The 40S ribosomal subunit will bind to the mRNA at the 5' UTR cap (for cap-dependent translation) or an internal ribosome-entry site (IRES, for cap-independent translation) (Sonenberg and Hinnebusch, 2009). The most common start codon in mRNA is an AUG, which encodes for the amino acid methionine; this is where the complete 80S ribosome initiates translation of the mRNA, and begins to form a polypeptide chain of amino acids (Sonenberg and Hinnebusch, 2009). Once the

ribosome has fully scanned the coding sequence of the mRNA it will reach a stop codon prior to the 3' UTR (Sonenberg and Hinnebusch, 2009). The 3' UTR plays a role in post-transcriptional regulation and attached to it is the poly-A tail, a chain of adenines which is implicated in the export of RNA and mRNA stability (Sonenberg and Hinnebusch, 2009, Huang and Carmichael, 1996).

Although often depicted as a simple single strand, mRNA can be highly structured. Examples of mRNA secondary structures are hairpins, stem loops and G-quadruplexes (Sonenberg and Hinnebusch, 2009). Secondary structures in the 5' UTR require RNA helicase action to allow for binding and scanning of the ribosome (Sonenberg and Hinnebusch, 2009).

The mRNA coding sequence is comprised of nucleotide triplets called codons which encode for the sequence of amino acids within a protein after translation (Sonenberg and Hinnebusch, 2009). This occurs via the recognition of this code by the ribosome, which selects a tRNA molecule specific for the anti-codon complementary to that codon (Sonenberg and Hinnebusch, 2009). The amino acid corresponding to the tRNA molecule is covalently linked to form a nascent polypeptide chain, before releasing the tRNA (Sonenberg and Hinnebusch, 2009). There are multiple defined stages to mRNA translation, namely translation initiation, elongation and termination.

Figure 1-11. The simplified structure of mRNA.

The structure of a mature mRNA is read in the 5' to 3' direction. At the 5' end there exists a 5' cap which is implicated in cap-dependent translation initiation, and is followed by the 5' untranslated region (UTR). During ribosome scanning, the ribosome will then find the start codon (commonly AUG) at the beginning of the coding sequence (CDS) and will continue to translate the mRNA until the ribosome reaches the stop codon at the end of the CDS. Following from this, there is a 3' UTR and a poly-A tail, which has a role in RNA export and stability.

1.4.2 Cap-dependent translation initiation

During cap-dependent translation, the 5' m^7G cap on the mRNA is recognised and bound by the eIF4F initiation complex, which comprises eIF4A, eIF4G and eIF4E (Figure 1-12). eIF4E binds the 5' cap on the mRNA in an ATP-independent manner (Gingras et al., 1999b). Following this, eIF4G binds to eIF4E, to act as a scaffold to which eIF4A is attracted (Sonenberg and Hinnebusch, 2009). Once the eIF4F complex is formed alongside the 5' cap, eIF4A can act as an RNA helicase to unwind complex secondary structures within the 5' UTR of the mRNA to be translated (Sonenberg and Hinnebusch, 2009). This process facilitates the attraction of the 43S pre-initiation complex (PIC), comprised of the 40S ribosomal subunit bound to methionyl-tRNA (met-tRNA), eIF3 and eIF2 (Sonenberg and Hinnebusch, 2009).

Following this, the 43S PIC then scans the 5' UTR of the mRNA for a Kozak sequence containing a start codon, to begin translation (Sonenberg and Hinnebusch, 2009, Kozak, 1987). The closer to the optimal Kozak consensus, the more efficiently the initiation codon is recognised (Hinnebusch, 2011). There are also a number of other accessory factors involved, particularly eIF4B and eIF4H, which facilitate the recruitment of the ribosome by stimulating the activity of eIF4A as an RNA helicase (Sonenberg and Hinnebusch, 2009). There are two mammalian isoforms of eIF4A involved in mRNA translation, eIF4A1 and eIF4A2 (Lin et al., 2008). These isoforms have a high level of amino acid conservation and are therefore highly similar. eIF4A1 is the most abundant and its expression is at least partly under the transcriptional control of MYC (Lin et al., 2008).

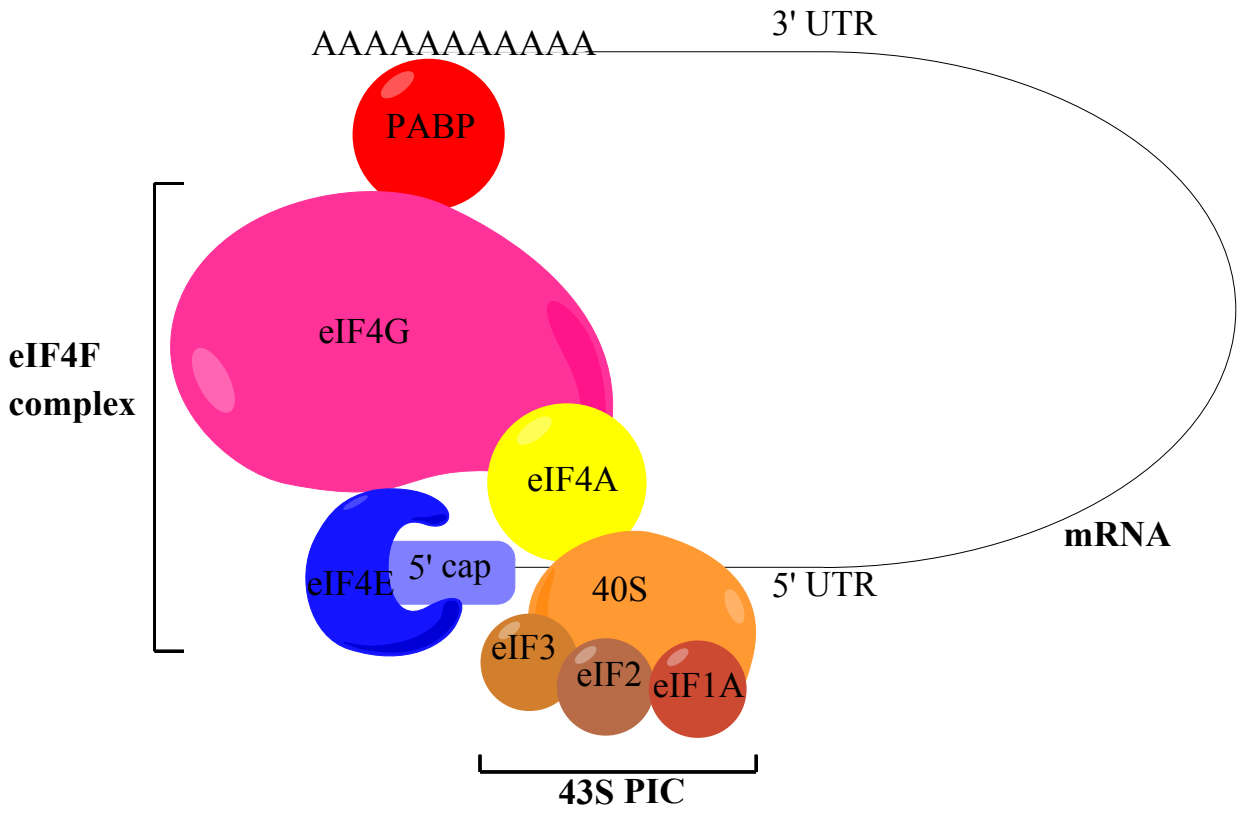

Figure 1-12. Cap-dependent translation initiation.

During cap-dependent translation initiation, the 7'methylguanylate cap (m^7G) on the 5' end of the mRNA is recognised and bound by the eIF4F complex, comprised of eIF4G, eIF4E and eIF4A. eIF4E is the 5' cap-binding protein, which is bound by eIF4G, a scaffold protein acting to hold the eIF4F complex together. Also bound to eIF4G is eIF4A, an RNA helicase which unwinds secondary structures in the 5' UTR of the mRNA. Another protein bound to eIF4G is poly(A) binding protein (PABP) which is bound to the poly(A) tail and is responsible for the stabilisation and the circularisation of the mRNA, to allow for the initiation of translation. Formation of the eIF4F complex allows for formation of the 43S pre-initiation complex (PIC). Following scanning and recognition of the start codon, the eIFs dissociate from the 40S subunit, which subsequently attracts the 60S large ribosomal subunit and allows for translation to begin. Image produced using ChemDraw professional ® v16.0.

1.4.3 Cap-independent translation initiation

Cap-independent translation occurs without the recognition of the 5' cap on the mRNA. This mechanism relies on the presence of internal ribosome entry sites (IRES) within the mRNA, often nearby to the AUG start codon in the 5' UTR (Sonenberg and Hinnebusch, 2009). IRES are structural elements within the mRNA that are recognised by the 40S ribosomal subunit (Sonenberg and Hinnebusch, 2009). This method of initiation requires the presence of binding proteins, such as polypyrimidine-tract-binding proteins, and other IRES trans-activating factors (ITAFs) (Sonenberg and Hinnebusch, 2009). IRES sequences have been identified within the sequences of viral mRNAs (Kieft, 2008), and cap-independent translation is suggested to occur in the translation of select eukaryotic mRNAs during cellular stress, or when cap-dependent translation is inhibited (Martinez-Salas et al., 2012). One of the first identified human genes containing an IRES was *MYC* (Stoneley et al., 1998), which provides *MYC* with an alternative method of translation initiation.

1.4.4 Elongation and termination of translation

Following the initiation of translation, elongation steps occur (Figure 1-13). Eukaryotic translation elongation factor eEF-1 forms a complex with aminoacyl-tRNAs in the presence of guanosine triphosphate (GTP) and moves into the A-site of the ribosome, next to the already placed initiator Met-tRNA in the ribosomal P-site (Sonenberg and Hinnebusch, 2009). The aminoacyl-tRNA brought into the site is the anticodon complementary to the codon of the mRNA in the A-site of the ribosome (Sonenberg and Hinnebusch, 2009). Pairing of the correct tRNA codon:mRNA anticodon causes hydrolysis of the GTP bound to eEF1, and the release of this factor, which fully "relaxes" the aminoacyl-tRNA into the A site. This is followed by a peptidyl-transferase reaction whereby the bond between methionine and tRNA is broken and a peptide bond is formed between the two adjacent amino acids (Sonenberg and Hinnebusch, 2009). The ribosome then moves along the mRNA by three bases in the 5'-3' direction, catalysed by hydrolysis of GTP associated with eEF2, this moves the used tRNA into the E site, where it is ejected from the ribosome, thus leaving the new peptidyl-tRNA in the P-site and opening up the A-site for incoming aminoacyl-tRNAs (Sonenberg and Hinnebusch, 2009). This process repeats, forming a polypeptide chain, until a stop codon, such as UAA, UAG or UGA which cannot be recognised by any tRNA molecules, is presented in the A-site of the ribosome (Sonenberg and Hinnebusch, 2009). The stop codons are instead recognised by release factors, such as eukaryotic release factor-1 (eRF1) (Kisselev and Frolova, 1995), which can recognise all three stop codons and release the peptide chain from the tRNA in the P-site of the ribosome by hydrolysis (Sonenberg and Hinnebusch, 2009). The ribosome is then re-used for the translation of other mRNA molecules.

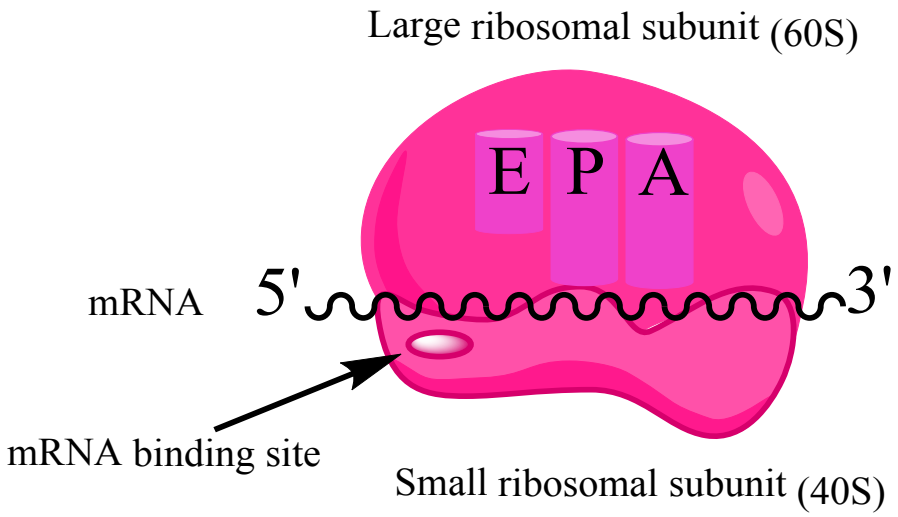

Figure 1-13. Schematic diagram of ribosome showing E, P and A sites.

mRNA is read in the 5' to 3' direction and binds to the mRNA binding site on the small ribosomal subunit (40S). The large ribosomal subunit (60S) contains three tRNA binding sites: the E, P and A sites. The A-site is the amino-acyl tRNA binding site, the P-site is the peptidyl-tRNA binding site and the E-site is the exit site of tRNA after it has donated an amino-acid to the peptide chain. Image produced using ChemDraw professional ® v16.0.

1.4.5 Regulation of mRNA translation

Translation is a highly regulated process due to the high energy demand that translation puts on the cell (Buttgereit and Brand, 1995). Many mechanisms are exploited by the cell to control the levels of translation, either at a global or mRNA-specific level. These may be implemented under conditions of stress to reduce the synthesis of proteins and to prolong cell survival (Holcik et al., 1999), but also to modify the expression of individual proteins dependent upon their requirements in the cell.

In malignant cells, altered translational control can lead to aberrant cell survival and proliferation, for example, over-expression of proteins involved in cellular proliferation, or to reduce the expression of pro-apoptotic proteins. The regulation of translation can be also specific for certain mRNAs. The translation of mRNAs with short and unstructured 5' UTRs is more efficient, due to the ease of scanning and binding of the eIF4F complex, known as 'strong' mRNAs (De Benedetti and Graff, 2004). These mRNAs are often highly expressed house-keeping genes, such as β-actin (De Benedetti and Graff, 2004). 'Weak' mRNAs are those which have longer and more complex 5' UTRs (De Benedetti and Graff, 2004). The translation of these mRNAs is rate-limited by the availability of the eIF4F complex, thus experiencing less efficient initiation of translation (De Benedetti and Graff, 2004) (Figure 1-14). Examples of these 'weak' translating mRNAs are often implicated in driving malignancy, such as *MYC* (De Benedetti and Graff, 2004). Another way in which translation is regulated is by the limited availability of certain amino acids, which can slow translation rates and affect the expression of some mRNAs (Kimball, 2002).

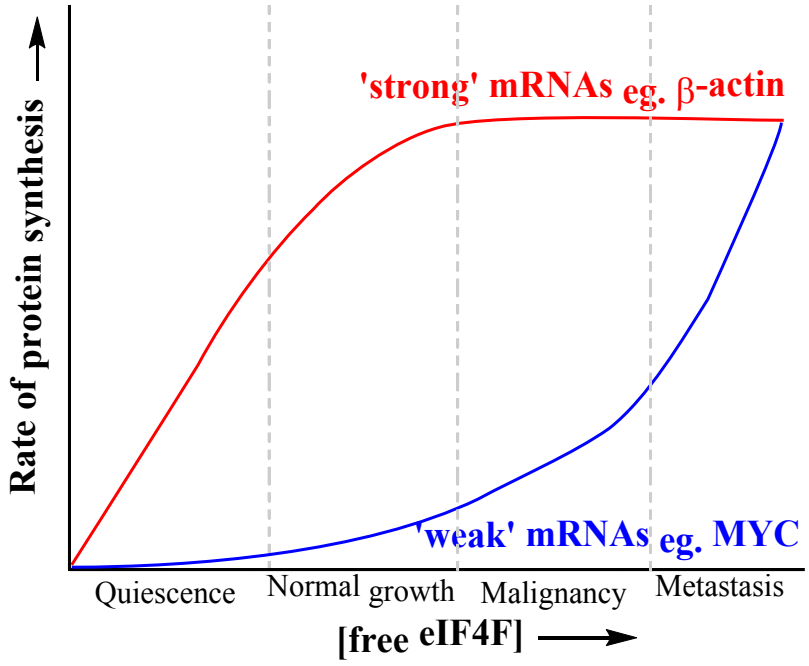

Figure 1-14. Rates of translation of 'strong' versus 'weak' mRNAs.

'Strong' mRNAs have short and simple structured 5' UTR, which are easily scanned and bound by the eIF4F complex to initiate translation. In contrast, 'weak' mRNAs often have complex 5' UTR. These mRNAs are less efficiently translated and can be rate-limited by eIF4F complex levels. In malignancy, increased eIF4F can result in an increase in translation of 'weak' mRNAs such as MYC. Image adapted from (De Benedetti and Graff, 2004).

1.4.5.1 Signalling pathways

Certain signalling pathways can influence rates of translation following their stimulation or under conditions of cellular stress. mTOR is a major regulatory factor for cap-dependent mRNA translation initiation (Figure 1-15) (Gingras et al., 2001). Under energy and amino-acid abundant cellular conditions, mTOR promotes the formation of the eIF4F complex and therefore facilitates ribosome binding for translation to occur (Gingras et al., 2001). mTOR is a serine/threonine kinase and occurs in 2 protein complexes, mTORC1 and mTORC2. mTORC1 facilitates proliferation via protein and lipid synthesis, whereas mTORC2 facilitates cell survival and reorganisation of the cytoskeleton (Gingras et al., 2001). As mTORC1 is more involved in the regulation of mRNA translation it is important to understand its role. mTORC1 consists of mTOR, the catalytic subunit, and other proteins such as RAPTOR, DEPTOR and RHEB (Gingras et al., 2001). RHEB is a GTPase which activates mTORC1 when bound to GTP (Gingras et al., 2001). To regulate translation, mTORC1 phosphorylates key members of the translational machinery, notably eIF4E-binding proteins (4E-BPs) and ribosomal S6Ks (Gingras et al., 2001, Magnuson et al., 2012, Laplante and Sabatini, 2012). S6K activation by mTORC1 results in the stimulation of both protein and lipid synthesis, whereas phosphorylation of 4E-BPs by mTORC1 blocks their ability to bind and suppress eIF4E (Gingras et al., 1999a, Silvera et al., 2010). Both of these actions further stimulate mRNA translation following signalling (Donahue and Fruman, 2007). mTORC1 is de-activated during hypoxia and energy-depletion, allowing for regulation of energy-intensive processes such as translation (Gingras et al., 2001).

During quiescence, 4E-BPs are hypo-phosphorylated and therefore strongly bind to eIF4E, preventing its binding in the eIF4F complex. This is because the binding motif on eIF4E where 4E-BP1 binds is the same motif to which eIF4E binds eIF4G (Gingras et al., 1999a). Downstream of activation, mTORC1 phosphorylates 4E-BP1 at Thr37/46 (Gingras et al., 1999a). This phosphorylation primes 4E-BP1 for further phosphorylation at Ser65 and Thr70 (Gingras et al., 1999a), resulting in hyperphosphorylation. Hyperphosphorylation of 4E-BP1 leads to the release of eIF4E, allowing formation of the eIF4F complex and the consequential initiation of cap-dependent translation (Gingras et al., 1999a). Over-expression of S6Ks inhibits the phosphorylation of 4E-BP1 by mTORC1 as both substrates compete for the same binding site on mTORC1 (Gingras et al., 1999a) which can reduce rates of translation.

Another mechanism by which mTORC1 regulates mRNA translation is through ribosomal S6Ks and PDCD4 (Figure 1-15) (Carayol et al., 2008). mTORC1 phosphorylates S6Ks to activate them, facilitated by eIF3 (Holz and Blenis, 2005). The S6Ks then phosphorylate PDCD4, the natural inhibitor of eIF4A, leading to its ubiquitination and subsequent degradation by the proteasome (Carayol et al., 2008). Degradation of PDCD4 allows eIF4A to bind as part of in the eIF4F complex and for

translation to be initiated (Carayol et al., 2008). mTORC1 signalling and the subsequent phosphorylation/activation of S6Ks also results in the phosphorylation of ancillary factor eIF4B, which enhances the RNA helicase activity of eIF4A (Bi and Goss, 2000, Dennis et al., 2012). These regulatory processes influence the translation of eIF4E-sensitive and eIF4A-dependent mRNAs, with complex 5' UTRs. These mRNAs often encode known disease drivers in CLL, such as MYC and MCL1 (Volpon et al., 2016).

mTORC1 is also regulated by ERK activity (Gingras et al., 2001). ERK phosphorylates tuberosclerosis complex-2 (TSC2) to deactivate it (Ma et al., 2005). TSC2 inhibits mTORC1 activity, unless it is deactivated via phosphorylation (Laplante and Sabatini, 2012). ERK also indirectly regulates translation via synthesis of transfer RNAs (tRNAs) and ribosomal RNAs (rRNAs) (Wang and Proud, 2002). ERK also phosphorylates MAPK-interacting kinase proteins (MNK1 and 2) at Thr197/Thr202 (Waskiewicz et al., 1997). Activation of MNK1 modulates the activity of eIF4E via phosphorylation at Ser209, which increases the affinity of eIF4E for binding of the 5' cap on mRNA (Shveygert et al., 2010). Transcription factor and known oncoprotein, MYC, is also responsible for increasing the transcription of translation initiation factors such as eIF4E and eIF4A, inducing mRNA translation (Ruggero, 2009, Lin et al., 2008, Chu and Pelletier, 2015). MYC also regulates mRNA translation by regulating the expression of rRNA and ribosomal subunits to increase availability of ribosomes for translation (Ruggero, 2009).

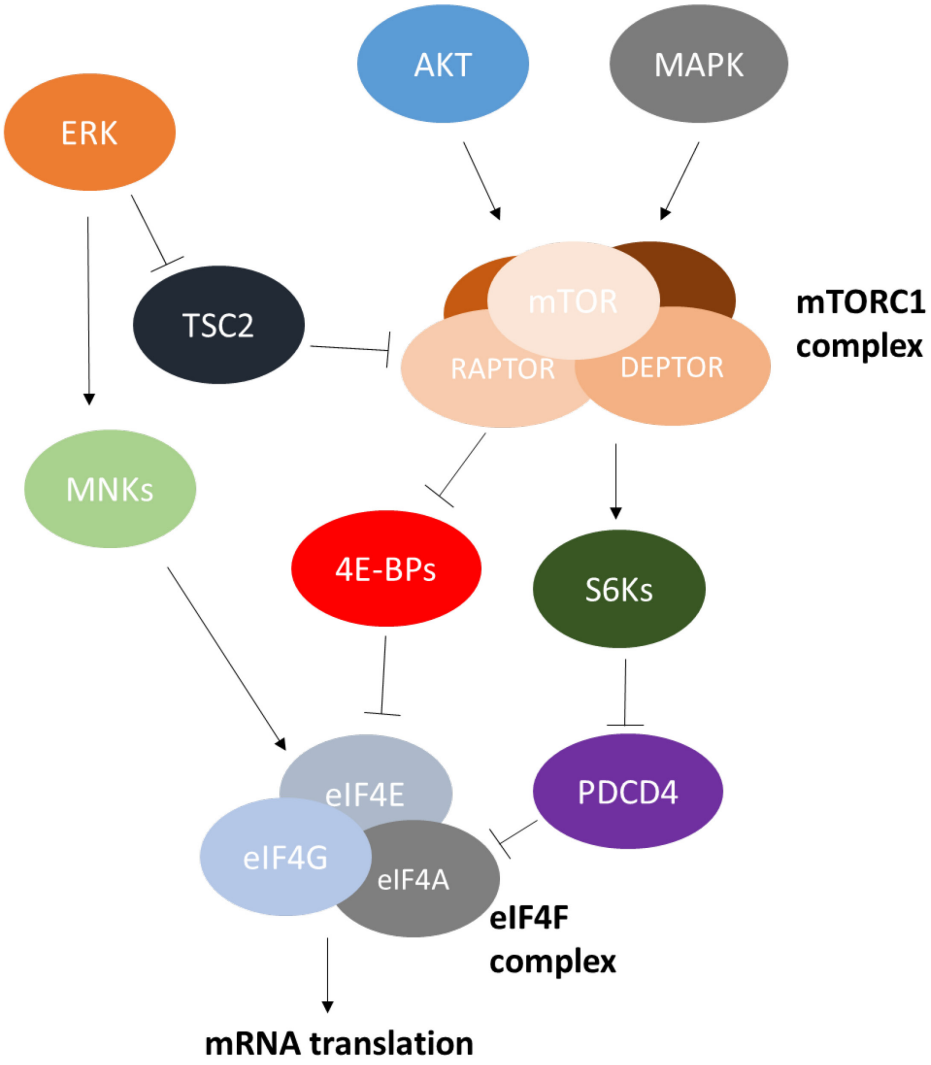

Figure 1-15. Control of mRNA translation by signal transduction

Downstream of stimulation and the consequential activation of ATK and MAPK, mTOR promotes the formation of the eIF4F complex. mTOR is a serine/threonine kinase and occurs in two protein complexes, mTORC1 and mTORC2. mTORC1 facilitates proliferation via protein and lipid synthesis. mTORC1 consists of mTOR, the catalytic subunit, and other proteins such as RAPTOR, DEPTOR and Rheb. Rheb is a GTPase which activates mTORC1 when bound to GTP. mTORC1 phosphorylates key members of the translational machinery, 4E-BPs and S6Ks. When 4E-BPs are hypo-phosphorylated they bind eIF4E, preventing eIF4E binding in the eIF4F complex. Following BCR-engagement, mTORC1 phosphorylates 4E-BP1 at Thr37/46 which primes 4E-BP1 for further phosphorylation at Ser65 and Thr70. Hyperphosphorylation of 4E-BP1 results in the release of eIF4E, allowing eIF4F formation to occur and the initiation of cap-dependent translation can begin. mTORC1 also phosphorylates S6Ks to activate them. S6Ks phosphorylate PDCD4, leading to its ubiquitination and subsequent degradation by the proteasome. This allows eIF4A to join the eIF4F complex and translation to be initiated. ERK phosphorylates TSC2. TSC2 inhibits mTORC1 unless it is phosphorylated by ERK which deactivates it. ERK also phosphorylates MNKs to phosphorylate eIF4E, increasing the affinity of eIF4E for the 5' cap of an mRNA.

1.4.5.2 miRNAs

A key method of translational regulation is called RNA interference (RNAi) by miRNA, which are small single-stranded RNA molecules comprised of short nucleotide sequences that play a key role in the action of the RNA-induced silencing complex (RISC) (Gregory et al., 2005). To form the RISC complex, miRNA associate with Argonaut (Ago) proteins (Gregory et al., 2005). Dependent upon the sequence complementarity between the miRNA and the target mRNA. Regulation of expression can occur via three processes; (i) cleavage of mRNA, (ii) enhanced degradation of mRNA and (iii) inhibition of mRNA translation (Gregory et al., 2005). miRNA with perfect complementarity to the target mRNA undertake RNAi via Ago2 protein to cleave the target mRNA (Gregory et al., 2005). miRNA with mismatch sequences or imperfect complementarity repress translation via non-cleavage methods through destabilisation of the target mRNA or inhibition of translation (Gregory et al., 2005). miRNA with imperfect complementarity tend to bind to the 3' UTR, resulting in the inhibition of translation rather than cleavage of the mRNA (Gregory et al., 2005). An example of miRNA regulation is that the RISC complex has been shown to promote the release of eIF4A from its target mRNAs (Fukao et al., 2014). Treatment with an eIF4A inhibitor, silvestrol, was shown to overcome this translational repression by forcing mRNA binding with eIF4A (Fukao et al., 2014).

1.4.5.3 Regulation of eIF4F complex formation

Another method of translational control involves altering of the 5' cap recognition by the eIF4F complex. As described previously (section 1.4.5.1), 4E-BPs can compete for binding of eIF4E with eIF4G, thus preventing formation of the eIF4F complex (Gingras et al., 1999a). Importantly, 4E-BP binding of eIF4E would only temporarily inhibit cap-dependent translation initiation and would have no effect on the initiation of translation from IRES sites, and so the translation of some mRNAs could still occur.

Another method of regulation of mRNA translation is via the phosphorylation of a subunit of an eIF involved in translation initiation, eIF2α (Sonenberg and Hinnebusch, 2009). This occurs during cellular stress, such as amino acid starvation (Sonenberg and Hinnebusch, 2009). Phosphorylation of eIF2α at the Ser51 residue prevents the formation of the 43S PIC and thus reduces mRNA translation (Sonenberg and Hinnebusch, 2009). This phosphorylation can occur by any of four kinases, which are GCN2, HRI, PERK and PKR (Sonenberg and Hinnebusch, 2009). eIF2α phosphorylation also results in the formation of stress granules, which are storage vesicles that sequester mRNA to prevent its degradation during stress (Anderson and Kedersha, 2002).

1.4.6 mRNA translation in B-cell tumours

Translation is highly regulated and commonly dysregulated in a variety of tumour types, including B-cell cancers. Control of translation is necessary as protein synthesis is highly energy consuming for the cell (Buttgereit and Brand, 1995) and upregulation of translation is associated with increased cellular proliferation and survival. Translation initiation is a highly regulated process. However, dysregulation can occur during both cap-dependent and -independent initiation mechanisms.

Overexpression of eIF4E and eIF2α has long been associated with aggressive disease and tumorigenesis in non-Hodgkin's lymphomas (NHL) (Wang et al., 1999). eIF4E overexpression has also been demonstrated in other B cell tumours, including CLL (Martinez-Marignac et al., 2013). High expression of eIF4E can be driven in part by MYC, due to the presence of a MYC:MAX binding site within the promoter region of eIF4E (Lin et al., 2008). This implies that over-expression of MYC drives eIF4E expression, thus driving mRNA translation (Jones et al., 1996). eIF4E also co-operates with MYC by suppressing MYC-induced apoptosis to accelerate lymphomagenesis, demonstrated by mice engineered to overexpress MYC and eIF4E which results in rapid development of tumours (Ruggero et al., 2004). The relationship between MYC and eIF4E provides an interesting target for therapeutic intervention in B cell tumours.

A study into mRNA translation during tumorigenesis, focusing on the role of eIF4E requirements demonstrated that haploinsufficiency of eIF4E has minimal effect on global mRNA translation (Truitt et al., 2015). This study utilised heterozygote knock-out mouse models of eIF4E (*Eif4e*$^{+/-}$) (Truitt et al., 2015). In contrast, they also demonstrated that the translation of eIF4E-sensitive mRNAs is dependent upon eIF4E dose (Truitt et al., 2015). Here, eIF4E haploinsufficiency negated the ability for KRas, a potent oncoprotein, to induce tumorigenesis *in vivo.* Thus, this study demonstrates the importance of eIF4E dose in tumour development, whilst a reduced dose had minimal effect on global mRNA translation rates. Another factor involved in translation initiation, PDCD4, has been implicated in lymphoma development (Hilliard et al., 2006). PDCD4 inhibits cap-dependent initiation by inhibiting eIF4A. However, mice deficient of PDCD4 develop spontaneous B cell lymphomas and have a significantly reduced life span due to this lymphoma development (Hilliard et al., 2006).

Analysis of the translatome in DLBCL demonstrated upregulation of mRNAs encoding anti-apoptotic proteins, such as *BCL2* (Horvilleur et al., 2014). This upregulation was due to increased signalling through the mTOR pathway and consequential enhanced activation of eIF4A via eIF4B (Horvilleur et al., 2014). This dysregulated translation of eIF4A-target mRNAs would therefore lead to reduced apoptosis. This study also demonstrated that eIF4B-driven expression of proteins such as BCL2 correlated with disease outcome (Horvilleur et al., 2014).

Furthermore, components of the CBM complex, which couples BCR signalling to NF-κB activation, are dysregulated in DLBCL (Steinhardt et al., 2014). The 5' UTRs of the complex components are all complex and reliant upon eIF4A, and are all required for the constitutive NF-κB activation seen in DLBCL (Steinhardt et al., 2014). Translational regulation of the CBM complex counterparts was shown, as inhibition of eIF4A reduced expression of MALT1, BCL10 and CARD11 (Steinhardt et al., 2014).

1.4.6.1 BCR-associated regulation of mRNA translation in CLL

Yeomans and colleagues performed key studies into the regulation of mRNA translation in CLL. By combining multiple gene expression datasets, weighted gene co-expression network analysis (WGCNA) was used to demonstrate that antigen stimulation of CLL cells within PCs *in* vivo, was associated with a strong signature of translational regulation (Yeomans et al., 2015).

Treatment of CLL cells with anti-IgM coated-beads induced global mRNA translation, in signal responsive samples (Yeomans et al., 2015). Anti-IgM also increased the expression of MYC, and this was associated with increased *MYC* mRNA translation. Interestingly, anti-IgM-induced translation in CLL cells was associated with increased expression of eIF4A and eIF4G, and reduced expression of PDCD4 (Yeomans et al., 2015). Anti-IgM also increased global mRNA translation in normal B cells, but this response was not associated with altered expression of eIF4A or PDCD4 (Yeomans et al., 2015). Other studies have demonstrated low expression of eIF4E in unstimulated normal B cells which was not induced by BCR stimulation (Steinhardt et al., 2014, Urtishak et al., 2019). Moreover, it has been demonstrated that eIF4E is over-expressed in unstimulated CLL cells (Martinez-Marignac et al., 2013).

In CLL, PCs are the site of antigen engagement *in vivo* (Packham et al., 2014), and it is here that MYC is highly expressed within a small fraction of cells (Krysov et al., 2012). It is therefore not surprising that *MYC* translation is induced *in vitro* following BCR engagement (Yeomans et al., 2015). *MYC* translation is dependent upon translation initiation factors eIF4A and eIF4E due to its highly structured 5' UTR (as discussed in 1.4.5.3) and in turn drives aberrant translation in CLL. Increased MYC expression following BCR stimulation in CLL is dependent upon the MEK/ERK signalling pathway (Krysov et al., 2012). Phosphorylated ERK1/2 expression also correlated with MYC expression in the PC of CLL LNs (Krysov et al., 2012). Together, this data demonstrates the involvement of BCR signalling and MYC expression in driving mRNA translation in CLL.

Overall, studies have demonstrated a clear role of BCR stimulation in driving mRNA translation and disease progression in B cell tumours, particularly CLL, although the mechanisms and impact of this remains to be fully elucidated.

1.4.7 Inhibitors of mRNA translation

An example of a translation inhibitor that has been investigated previously in CLL is cycloheximide (Collins et al., 1991). Cycloheximide functions by blocking translation elongation, specifically by inhibiting the translocation of tRNA by binding to the E-site of the 60S ribosomal sub-unit (Schneider-Poetsch et al., 2010). Cycloheximide also induces apoptosis *in vitro* in CLL samples (Collins et al., 1991). However, this inhibitor does not show specificity to CLL cells and inhibits translation, thus inducing apoptosis in normal lymphocytes (Collins et al., 1991). Interestingly, cycloheximide increases the stabilisation of mRNAs by inhibiting the formation of cytoplasmic processing bodies, which are the sites in which mRNAs are decayed (Sheth and Parker, 2003, Wisdom and Lee, 1991, Chan et al., 2018). To reduce translation inhibitor toxicity, by limiting the off-target effects, there is a need to develop inhibitors specific to proteins which are over-expressed and drive disease progression in CLL.

Another well-established inhibitor of mRNA translation is harringtonine (and the related compound homoharringtonine). These compounds inhibit the elongation step of mRNA translation by preventing aminoacyl-tRNA from binding to the A-site of the large 60S ribosomal subunit of an initiating ribosome (Fresno et al., 1977). Homoharringtonine inhibits anti-apoptotic protein MCL1 expression in CLL samples by inhibiting its translation, resulting in apoptosis (Chen et al., 2011). Harringtonine is a licenced drug for the treatment of chronic myeloid leukaemia (CML), although many side-effects occur with this treatment.

1.4.7.1 eIF4A inhibitors

As BCR-induced eIF4A expression has been described in CLL cells, but not in their normal counterparts (Yeomans et al., 2015), eIF4A is a potential target for translational inhibition of specific mRNAs. A general inhibitor of eIF4A is hippuristanol, which acts by inhibiting the binding of eIF4A to RNA and thus, results in the loss of eIF4A action, preventing the formation of the eIF4F complex and the initiation of mRNA translation (Cencic and Pelletier, 2016, Bordeleau et al., 2006). Unfortunately, with inhibitors such as hippuristanol, there is a general non-specific inhibition of mRNA translation which may result in high levels of toxicity and side-effects (Cencic and Pelletier, 2016).

Novel eIF4A inhibitors have been described from the flavagline family of compounds which are natural-product inhibitors derived from plants of the genus *Aglaia* (King et al., 1982). Their chemical structures comprise a cyclopenta[b] benzofuran group, and various complex side chains, dependent

upon the specific compound in question (King et al., 1982). These compounds were first discovered as part of traditional Chinese herbal medicines in the 1980s. Since then, studies have focused on the characterisation of the anti-tumour and anti-leukaemic properties of specific compounds especially rocaglamide and silvestrol (King et al., 1982).

1.4.7.1.1 Rocaglamide

Rocaglamide is a flavagline compound (Figure 1-16) which inhibits the translation of specific mRNAs by increasing the affinity between eIF4A and polypurine sequences in the 5' UTR of target mRNAs, independent of ATP (Iwasaki et al., 2016). This mechanism of action is novel and suggests a specificity of mRNA translation inhibition for specific eIF4A-dependent mRNAs.

Formation of this rocaglamide-eIF4A complex, which binds to sequences in the 5' UTR means that the 43S pre-initiation complex cannot scan the 5' UTR for a start codon to begin translation and thus stalls cap-dependent translation initiation (Iwasaki et al., 2016) (Figure 1-16). Interestingly, it was shown that rocaglamide can also, to some extent, inhibit cap-independent translation from IRES elements in mRNAs, as this process still involves some scanning of the 5' UTR and thus can stall the ribosome if polypurine sequences are present and bound by an eIF4A-rocaglamide complex (Iwasaki et al., 2016).

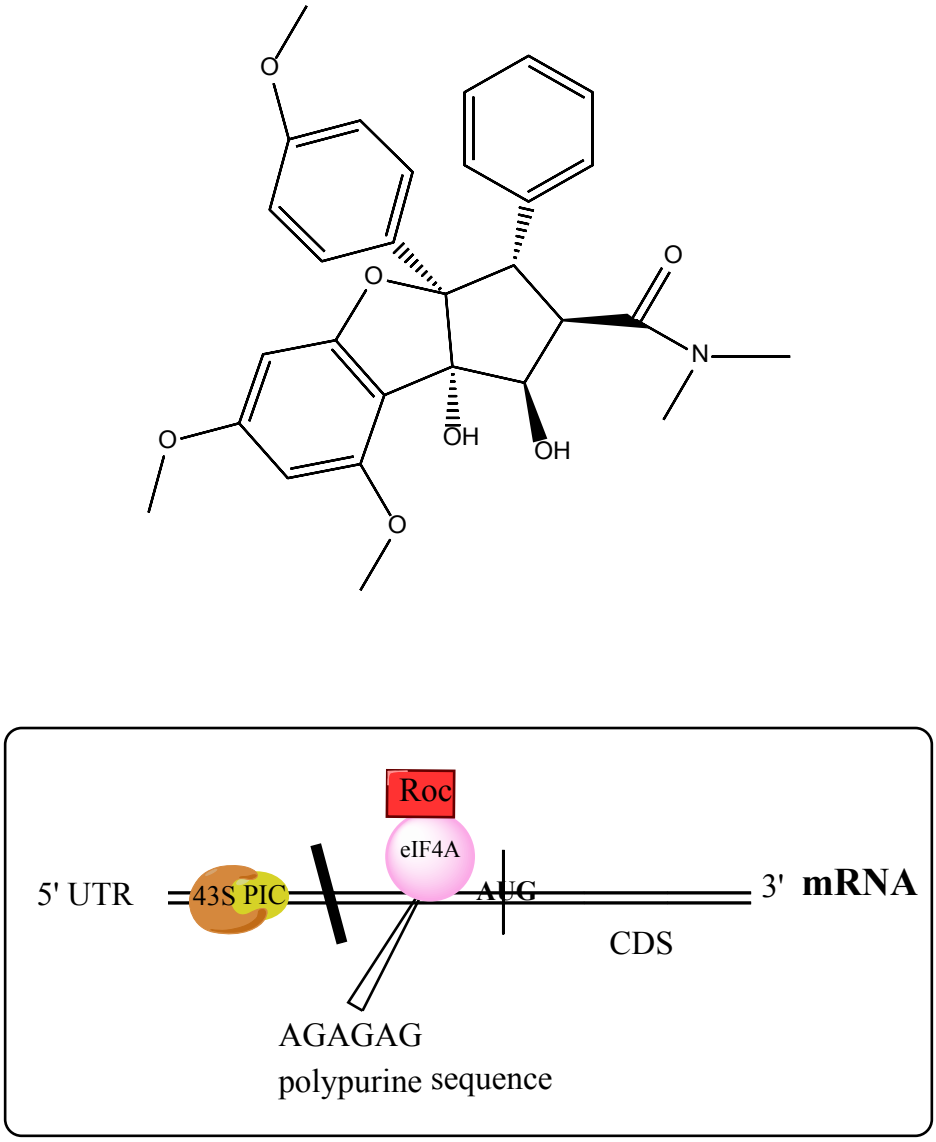

Figure 1-16. Chemical structure of rocaglamide and its mechanism of action

The top panel shows the chemical structure of rocaglamide. The bottom panel shows the mechanism of action of rocaglamide. Here, rocaglamide (Roc) forces the binding of eIF4A to AGAGAG/GAGAGA polypurine sequences in the 5' of certain mRNAs. Binding of this complex results in a block of scanning by the 43S pre-initiation complex (PIC) for the start codon (AUG), inhibiting mRNA translation. Image produced using ChemDraw professional ® v16.0.

1.4.7.1.2 Silvestrol

Another flavagline compound, suggested to have similar action to rocaglamide is silvestrol. Silvestrol contains the characteristic cyclopenta[b] benzofuran group in its chemical structure (Figure 1-17) (King et al., 1982), but with a large functional group on a side chain (featured in red on image below) resulting in a larger overall structure than rocaglamide. This side chain is a glycone group which enhances its solubility in water but is likely removed in cells. Similarities in the structure of silvestrol and rocaglamide imply the possibility that silvestrol acts through the same mechanism as rocaglamide to inhibit translation of specific mRNAs, although this is yet to be explored. One key study into silvestrol describes the cross-linking of eIF4A to mRNA by silvestrol, to be 5' cap-dependent, and suggests that silvestrol sequesters free eIF4A on a target mRNA (Bordeleau et al., 2008), which correlates with the more recently described mechanism of rocaglamide (Iwasaki et al., 2016).

Silvestrol has been shown to induce apoptosis in unstimulated primary CLL samples, at nanomolar concentrations (Lucas et al., 2009). This study also demonstrated inhibition of basal *MCL1* translation, which preceded induction of cell death (Lucas et al., 2009). Whilst this study revealed interesting consequences of silvestrol treatment, it did not investigate the impact of BCR stimulation on these outcomes. For example, anti-IgM treatment induces a pro-survival response in CLL cells (Ten Hacken et al., 2016) and so it is necessary to understand the impact of silvestrol on cell death following BCR stimulation. There is also known to be an induction of MYC and MCL1 expression following BCR-engagement (Petlickovski et al., 2005, Krysov et al., 2012) and so it would be important to understand the ability of silvestrol to overcome this induction to inhibit these disease-driving proteins in CLL.

The CBM complex components all have mRNA that have complex 5' UTR and are sensitive to eIF4A inhibition by silvestrol (Steinhardt et al., 2014). This implies that following BCR stimulation, silvestrol can interfere with BCR signalling pathways and reduce NF-κB activation by reducing expression of the members of the CBM complex.

In vivo studies have demonstrated that silvestrol significantly reduces B cell counts in Eμ-*TCL1* mice, with minimal effects on T cell numbers (Lucas et al., 2009). Silvestrol treatment also sensitises doxorubicin-resistant cases in the murine Eμ-*MYC* lymphoma model to induce apoptosis of their derived lymphomas (Bordeleau et al., 2008). This shows that silvestrol holds promise as a therapeutic intervention in B-cell tumours.

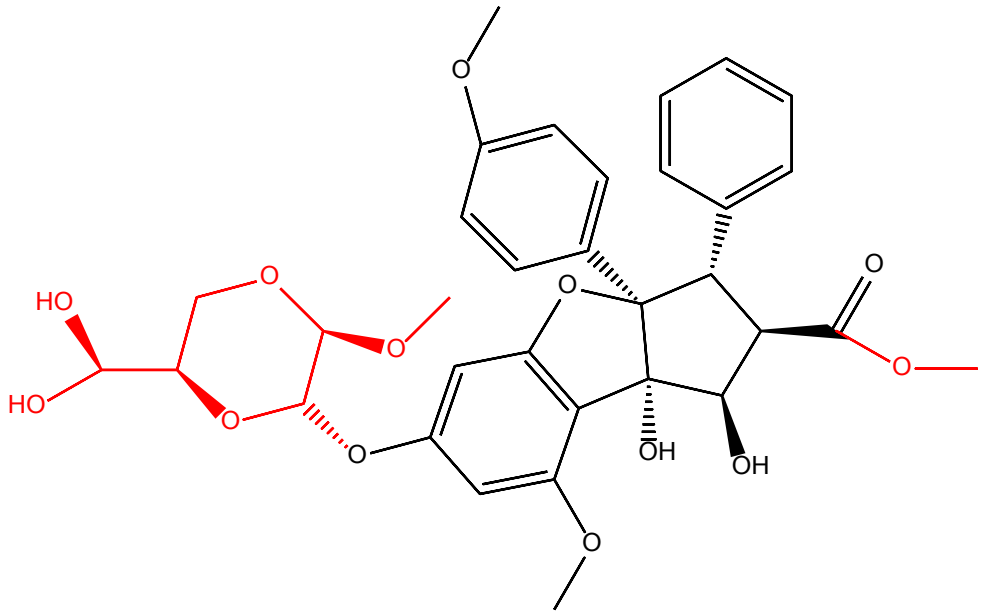

Figure 1-17. Chemical structure of silvestrol.

Differences between silvestrol structure and similar compound rocaglamide structure shown in red. Image produced using ChemDraw professional ® v16.0.

1.4.7.2 eIF4E inhibitor, ribavirin

Overexpression of eIF4E has long been known to induce oncogenic transformation (Lazaris-Karatzas et al., 1990) and is linked to a poor prognosis in many cancers (Khosravi et al., 2015, Zhou et al., 2006). eIF4E is over-expressed in CLL, resulting in aberrant rates of mRNA translation (De Falco et al., 2015). eIF4E in normal B cells is rate-limiting, to regulate of rates of translation (Raught and Gingras, 1999). Importantly, overexpression of eIF4E does not result in increased global rates of mRNA translation, but only that of mRNAs with complex 5' UTRs (Borden, 2016). These mRNAs were generally involved in cell survival and malignancy, such as *CCND1* and *MYC* (Borden, 2016).

Ribavirin is a nucleoside analogue that acts to inhibit the function of eIF4E by acting as an analogue of the m^7G cap of mRNA (Kraljacic et al., 2011) (Figure 1-18). Within this complex, eIF4E is rate-limiting, implying that the initiation of mRNA translation is reliant upon the expression of eIF4E and thus targeting eIF4E may have a use therapeutically. Ribavirin therefore prevents translation initiation and the formation of the eIF4F complex (Kraljacic et al., 2011).

Ribavirin is currently used in patients as part of a combination anti-viral therapy for hepatitis C infection, but has shown potential as a translational inhibitor and has shown some activity in acute myeloid leukaemia clinical trials (Assouline et al., 2009), with poor prognosis patients achieving complete or partial remission. Another report has described the treatment of a patient with follicular lymphoma being treated with ribavirin for hepatitis C therapy achieving full remission of lymphoma (Maciocia et al., 2016), demonstrating the exciting potential for this drug in B cell tumours. Ribavirin is well profiled clinically, and if it shows promise in CLL samples *in vitro,* this compound would be a promising candidate to move forward into clinical trials more quickly than other less-well defined compounds.

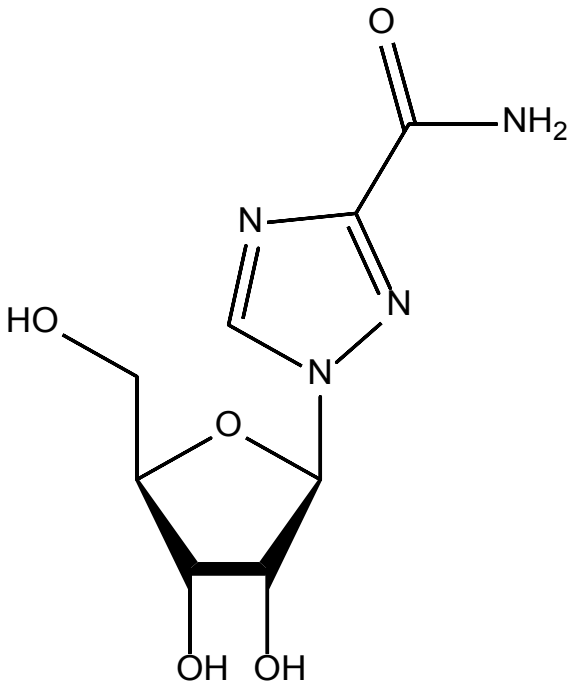

Figure 1-18. Chemical structure of ribavirin.

Image produced using ChemDraw professional ® v16.0.

1.5 eIF4E and nuclear export

In addition to its role in translation initiation, eIF4E is also involved in the nuclear export of RNA (Iborra et al., 2001). Around 70% of cellular eIF4E exists within the nucleus (Iborra et al., 2001), where eIF4E promotes the transport of specific mRNAs. Some mRNAs are only regulated by export, by translation, or by both (Culjkovic et al., 2005). mRNAs to be exported from the nucleus by eIF4E contain a 50-nucleotide sequence in their 3' UTR called an eIF4E-sensitivity element (4E-SE) (Topisirovic et al., 2009). The importance of a 4E-SE is not sequence dependent, but is based on the recognition of its secondary structure, which is often a stem-loop, implying that target mRNAs must not only have a complex 5' UTR for export, but also a complex 3' UTR secondary structure (Culjkovic et al., 2006). eIF4E also requires a 5' cap on an mRNA to facilitate its nuclear export, as well as mRNA translation (Culjkovic et al., 2005). A key example of an mRNA regulated only at the level of transport is *CCND1* (encoding cyclin D1) (Culjkovic et al., 2005), whereas an mRNA that isn't regulated by eIF4E is *GAPDH* (Culjkovic et al., 2006).

During nuclear export, mRNAs are transported through the nuclear membrane, via the nuclear pore complex (NPC), into the cytoplasm where they engage the translational machinery (Schmidt-Zachmann et al., 1993). Export of mRNAs is mediated via the active transport of karyopherin proteins (Schmidt-Zachmann et al., 1993). Karyopherin proteins are either importin proteins for nuclear export, exportins for nuclear export or transportin proteins (Ullman et al., 1997).

One of the most common exportin proteins is CRM1/XPO1, which can export mRNAs and proteins (Volpon et al., 2017). Common cargoes of XPO1 include P53 and eIF4E (Xu et al., 2012, Culjkovic et al., 2006), which in turn can lead to the upregulation of expression of key disease-driving oncoproteins, such as MYC. For an mRNA to be eligible for export from the nucleus via XPO1, it must interact with an adaptor protein, as XPO1 is not an RNA binding protein (Culjkovic et al., 2006). XPO1 interacts with adaptor protein leucine-rich pentatricopeptide repeat protein (LRPPRC) (Volpon et al., 2017) (Figure 1-19). LRPPRC interacts with eIF4E (bound to the 5' cap of the target mRNA) and the 4E-SE in the 3' UTR of the mRNA (Volpon et al., 2017). XPO1 then binds LRPPRC to export this complex out of the nuclear pore into the cytoplasm (Volpon et al., 2017). XPO1-associated nuclear export of mRNAs has been implicated in cancers, notably CLL and other B cell malignancies (Camus et al., 2017, Lapalombella et al., 2012, Zhang et al., 2013).

Export of mRNAs via LRPPRC and XPO1 requires hydrolysis of Ran-GTP to Ran-GDP as it is an active export process (Culjkovic et al., 2006). Following export of the target mRNA into the cytoplasm, the export factors must be recycled and returned back into the nucleus for further export of target mRNAs. Importin 8 is a protein known to engage with free eIF4E and LRPPRC and import them back into the nucleus following dissociation of the mRNA, through the NPC (Volpon et al., 2017).

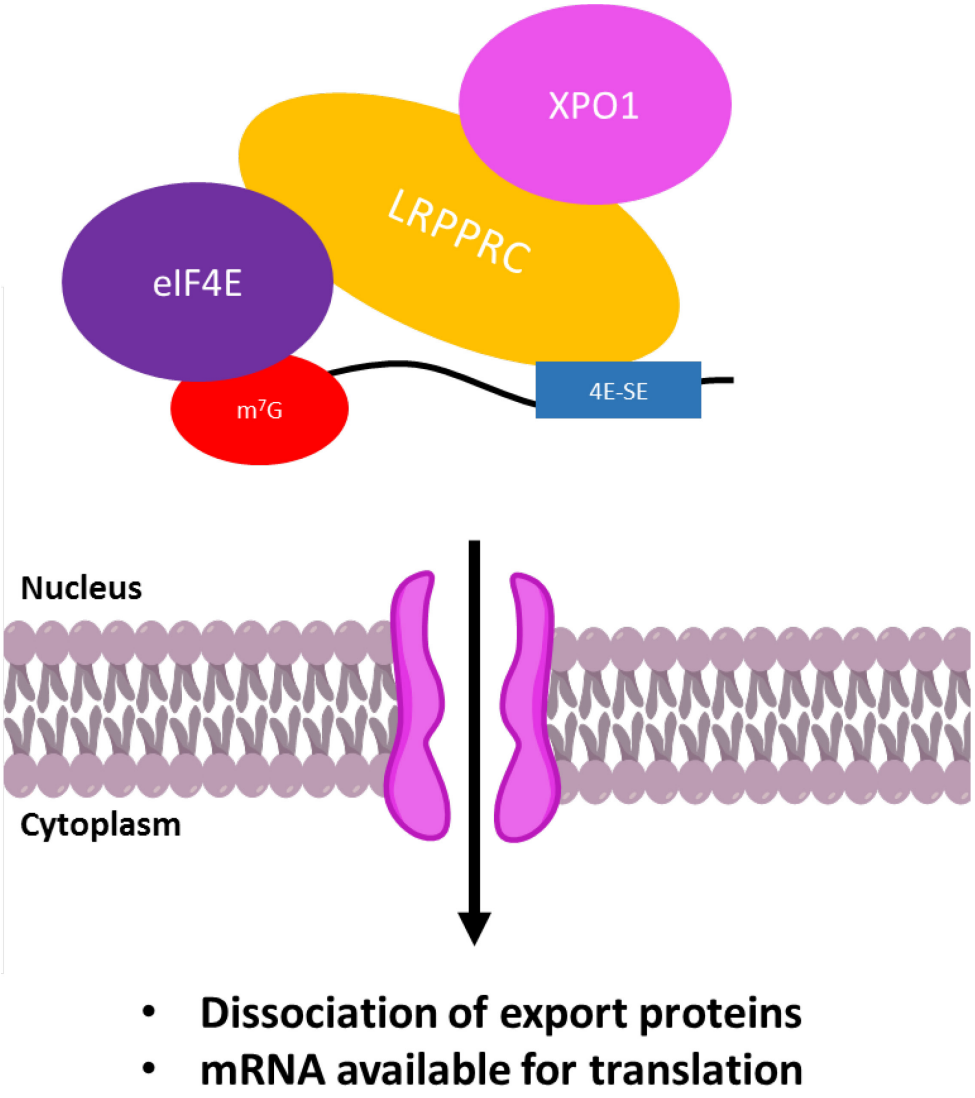

Figure 1-19. XPO1 and eIF4E-dependent nuclear export of mRNAs.

mRNAs in the nucleus are transported through the nuclear membrane into the cytoplasm for mRNA translation. The mRNA form a complex with an exportin protein, such as XPO1, and Ran-GTP. This complex translocates into the cytoplasm, resulting in the hydrolysis of Ran-GTP to Ran-GDP. This results in dissociation of the mRNA cargo, making it available for translation. Some mRNAs require adaptor proteins for their export. eIF4E is a key adaptor protein for mRNA export via XPO1. Leucine-rich pentatricopeptide repeat protein (LRPPRC) associates with eIF4E and with the 4E-SE RNA. LRPPRC then binds to XPO1 for the active export of mRNA via Ran-GTP. The export factors are then recycled and returned back into the nucleus for further export of target mRNAs, via importin 8, which engages with free eIF4E and LRPPRC to import them back into the nucleus. Image produced using ChemDraw professional ® v16.0.

1.5.1 The importance of nuclear export in B-cell malignancies

High expression of XPO1 in AML patients has been associated with a poor prognosis (Kojima et al., 2013). The same has been identified for mantle cell lymphoma (MCL) patients (Camus et al., 2017), and in many haematological malignancies, including CLL, *XPO1* mutations have been identified which can result in a gain-of-function mutation and thus over-active XPO1-dependent nuclear export pathways (Puente et al., 2011, Jain et al., 2016).

XPO1 is over-expressed at both the protein and mRNA level in CLL cells, in comparison to normal B cells (Lapalombella et al., 2012). Over-expression of XPO1 may be due to mutations in this gene which drive its expression, or due to increased requirements for XPO1 as a nuclear export protein (Lapalombella et al., 2012). This implies that the dysregulation of XPO1-dependent nuclear export may play a role in tumorigenesis in CLL. Some key protein cargo of XPO1 are known tumour suppressor proteins, such as P53 and IκB (Xu et al., 2012). Export of tumour suppressors from the nucleus during normal regulation allows for signalling to occur through NF-κB and prevents P53 activation, in the absence of genetic insults (Xu et al., 2012). Overexpressed XPO1 results in the export of tumour suppressors out of the nucleus, allowing for aberrant NF-κB signalling and the dysregulated function of P53 (Lapalombella et al., 2012).

As eIF4E is over-expressed in CLL, the majority of eIF4E is present within the nucleus (Iborra et al., 2001, Martinez-Marignac et al., 2013), implying that eIF4E's role in the export of certain mRNAs is likely to play a significant role in CLL disease progression. Known mRNAs exported by eIF4E include key disease drivers such as *MYC, BCL2* and *BCL6* (Culjkovic-Kraljacic et al., 2016). This implies a potential for the use of therapeutics that target eIF4E/XPO1-dependent nuclear export for the treatment of B-cell malignancies.

1.5.2 Inhibitors of nuclear export

As eIF4E is known to function as an adaptor protein for XPO1-dependent nuclear export of complex mRNAs (Culjkovic-Kraljacic et al., 2016), as well as its role as a member of the eIF4F translation initiation complex, it is clear that ribavirin may impact the levels of nuclear export of its target mRNAs, as well as selectively inhibiting mRNA translation. Particularly, it has been shown that eIF4E regulates the export of *BCL2, MYC* and *BCL6* mRNA, and when eIF4E is over-expressed there is a corresponding increase in the protein expression of the proteins encoded by these mRNAs (Culjkovic-Kraljacic et al., 2016). In studies using DLBCL cell lines, ribavirin treatment reduced the cytoplasmic abundance of *MYC, BCL2* and *BCL6* mRNA (calculated as a ratio of cytoplasmic to nuclear expression) (Culjkovic-Kraljacic et al., 2016). This implies that targeting eIF4E via ribavirin

can inhibit the nuclear export of these mRNAs by preventing eIF4E function as an export adaptor protein (Culjkovic-Kraljacic et al., 2016). Interestingly, as ribavirin acts as a m^7G cap analogue and binds to eIF4E, this prevents the recycling of eIF4E back into the nucleus by importin 8, as importin 8 can only transport free-eIF4E (Volpon et al., 2016), leading to the depletion of eIF4E from the nucleus and its accumulation within the cytoplasm.

Selective inhibitors of nuclear export (SINE) compounds have recently been developed, of particular interest are inhibitors of XPO1. Inhibiting XPO1-dependent export of mRNAs will not only inhibit those mRNAs associated with eIF4E, but also a larger variety of cargoes that function as tumour suppressor proteins. Inhibition of the export of these proteins will encourage them to act as tumour suppressors in the nucleus, and so clearly these inhibitors will have potential for the therapy of some cancers. An XPO1 inhibitor of interest is selinexor, a first-in-class inhibitor of XPO1, which forms a slowly reversible covalent bond with XPO1 (Etchin et al., 2013). This ultimately renders XPO1 inactivated and unable to undertake nuclear export (Etchin et al., 2013). Selinexor induces the activation of tumour suppressor proteins and reduces the expression of oncoproteins, such as MYC, in early-stage trials for relapsed/refractory NHL (Kuruvilla et al., 2017). This treatment was also associated with significant side effects, including reduced neutrophil count, reduced platelet count and anaemia (Kuruvilla et al., 2017). In CLL, XPO1 is over-expressed (Lapalombella et al., 2012) and thus a key target for potential therapeutic strategies. Selinexor induces apoptosis in CLL samples *in vitro* and more recent data suggests that SINE may also inhibit ribosomal biogenesis and mRNA translation (Lapalombella et al., 2012, Tabe et al., 2015). With this in mind, selinexor is a promising choice for investigative comparisons to ribavirin, to understand further the impact of XPO1 and eIF4E inhibition on nuclear export and other mechanisms in CLL.

1.6 Hypothesis and aims

1.6.1 Hypothesis

The main hypothesis of this thesis was that the inhibition of translation initiation factors in CLL is promising as a potential therapeutic strategy, due to its ability to deprive CLL cells of the expression of tumour-promoting oncoproteins, such as MYC and MCL1, following stimulation of sIgM.

1.6.2 Aims

To investigate this hypothesis, the project aimed to characterise pathways of mRNA translational control in CLL and to investigate the effects of inhibitors of eIF4A and eIF4E.

The main aims of this project were to:

- Characterise the effect of eIF4A inhibitors on both global mRNA translation and expression of key disease drivers, MYC and MCL1 in primary CLL cells
- Investigate the consequences of eIF4A inhibition for MYC RNA accumulation and stability
- Characterise the effect of the eIF4E inhibitor ribavirin on both global mRNA translation and expression of key disease drivers, MYC and MCL1
- Investigate the effect of ribavirin on nuclear export of RNA in CLL cells
- Investigate potential anti-tumour effects of ribavirin using an *in vivo* model of CLL

Chapter 2

Materials and Methods

2.1 Cell culture

2.1.1 Cell culture materials

Table 3. Cell culture materials and their individual components with supplier information described where available.

MATERIAL	COMPONENTS AND ORDERING INFORMATION
COMPLETE RPMI-1640 MEDIA	RPMI-1640 media (Sigma Aldrich, Missouri, USA), supplemented with 10% (v/v) foetal calf serum (PAA laboratories Ltd, Somerset, UK), 2 mM L-glutamine (PAA laboratories) and 1% (v/v) penicillin/streptomycin (PAA laboratories)
PHOSPHATE BUFFERED SALINE (PBS)	137 mM NaCl, 2.7 mM KCl, 10 mM Na_2HPO_4, 2 mM KH_2PO_4
DYNABEADS	ThermoFisher Scientific, Massachusetts, USA, #14311D
'CONTROL' ANTIBODY – UNCONJUGATED GOAT F(ab')$_2$ IgG	Cambridge Bioscience, Cambridge, UK, #0110-01
ANTI-IGM ANTIBODY – UNCONJUGATED GOAT F(ab')$_2$ ANTI-HUMAN IgM	Cambridge Bioscience, #2022-01
Q-VD-OPh	Sigma Aldrich, #SML0063
CELL CULTURE PLATES	Sigma Aldrich, #CLS3595

Table 4. Drugs/compounds used in this study and their ordering information.

DRUG/COMPOUND	ORDERING INFORMATION
ROCAGLAMIDE	Sigma Aldrich, #SML0656
SILVESTROL	MedChemExpress, New Jersey, USA, #HY-13251
CYCLOHEXIMIDE	Sigma Aldrich, #C7698
CpG-ODN	Source Bioscience, Nottingham, UK, #ODN2006-1
DIMETHYL SULFOXIDE (DMSO)	Sigma Aldrich, #D8418
ACTINOMYCIN D	ThermoFisher Scientific, USA, #11805017
SELINEXOR (KPT-330, XPO1i)	Selleckchem, Texas, USA, #S7252
RIBAVIRIN	MedchemExpress, #HY-B0434

2.1.2 CLL cell recovery and treatment

CLL patients were diagnosed based on IWCLL-NCI guidelines (Hallek et al., 2008) and diagnosis was confirmed via flow cytometry. Patients gave the necessary written informed consent prior to donation of whole blood samples. All experiments performed using CLL samples had ethical approval from Southampton and South West Hampshire Research Ethics committee (228/02/t). All CLL samples were taken at the point of diagnosis or subsequent clinic visits. Samples were only selected for this study if patients had not received any therapy in the 6 month period prior to sample donation.

Peripheral blood mononuclear cells (PBMCs) were isolated by lymphoprep centrifugation (Axis-Shield Diagnostics, Dundee, UK) before cryopreservation in 10% DMSO and 90% foetal calf serum (FCS, PAA laboratories). Before use, all samples were characterised for *IGHV* mutational status, tumour population ($CD19^+CD5^+$%), ZAP70 expression, CD38 expression, surface IgM (sIgM) expression and intracellular Ca^{2+} mobilisation (%). This was performed by research technicians in the University of Southampton Cancer Sciences Tissue Bank and CLL group. Samples used in this study were chosen based upon their ability to signal through sIgM, determined by intracellular Ca^{2+} mobilisation of over 5% and tumour population over 85% (Table 5). Following cryopreservation, CLL samples were defrosted and recovered in complete RPMI-1640 (see Table 3) for 1 hour at 37˚C. Cells were then diluted with complete RPMI to $1x10^7$ per ml before use in assays. Where stated, cells were treated with Dynabeads (Invitrogen, Massachusetts, USA) coated with goat $F(ab')_2$ anti-human IgM antibody (Cambridge Bioscience, Cambridge, UK) or goat $F(ab')_2$ IgG (Cambridge Bioscience) as a control antibody as described previously (Coelho et al., 2013).

2.1.3 CLL samples

Table 5. CLL samples used in this study and their associated characteristics.

SAMPLE ID	TUMOUR POPULATION (% $CD19^+$, $CD5^+$)	IGHV GENE	*IGHV* MUTATIONAL STATUS	ZAP-70 (%)	CD38 (%)	*IGM EXPRESSION (MFI)*	Ca^{2+}MOBILISATION (% CELLS)
222D	91	3-72*01	M	4	92	*162*	38
276D	95	3-23*01	M	0	2	*307*	78
279A	89	3-30-3*01	M	1	2	*47*	74
281D	88	3-23*01	M	1	8	*11*	16
343F	85	3-48*03	U	2	6	*370*	86
348C	96	3-15*01	M	3	0	*36*	21
351C	96	3-66*01	M	20	99	*96*	79
368D	97	3-15*05	M	9	62	*86*	35
466A	90	4-38-2*02	U	5	2	*51*	6
475C	91	1-3*01	M	5	9	*12*	10
483	90	2-5*10	M	3	1	*49*	5
500C	92	3-48*03	U	32	56	*68*	12
511B	89	3-72*01	U	24	24	*36*	48
523D	95	3-72*01	M	1	0	*57*	65
525B	90	3-23*01	M	5	0	*21*	19
563C	87	3-30-3*01	M	0	0	*62*	81
575E	95	3-15*01	M	0	1	*115*	69
588B	90	3-23*01	M	3	11	*42*	10
598B	86	3-7*01	M	1	0	*46*	66
604G	89	3-30*03	M	0	3	*163*	40
609A	88	3-72*01	M	0	18	*25*	57
621B	93	1-3*01	M	23	1	*134*	49
629B	94	3-49*03	M	0	14	*25*	19
630D	91	3-49*03	M	1	0	*12*	6

SAMPLE ID	TUMOUR POPULATION (% $CD19^+$, $CD5^+$)	IGHV GENE	*IGHV* MUTATIONAL STATUS	ZAP-70 (%)	CD38 (%)	*IGM EXPRESSION (MFI)*	Ca^{2+}MOBILISATION (% CELLS)
635C	90	3-21*01	U	7	2	*134*	89
639B	89	3-74*01	M	22	3	*16*	8
643C	88	6-1*01	M	1	0	*31*	32
654	85	1-69*01	M	0	1	*21*	36
668A	92	3-30*03	U	18	1	*175*	47
674C	85	3-21*01	U	35	35	*562*	88
681	96	3-7*02	M	0	6	*304*	60
684D	94	3-15*07	M	5	11	*27*	21
686A	88	3-11*01	M	23	18	*99*	78
689	96	3-48*03	U	8	92	*59*	15
716B	88	3-7*01	M	1	4	*34*	65
766	89	3-30*01	M	11	0	*92*	78
774A	97	1-69*01	U	15	5	*118*	25
780B	98	3-21*01	U	30	98	*122*	81
781	95	1-8*01	M	3	0	*62*	51
784	98	3-48*01	U	0	11	*151*	85
791A	87	3-7*03	M	5	33	*53*	28
794A	86	4-4*02	M	8	5	*50*	37
803C	95	1-69*01	U	56	33	*62*	31
815	85	3-33*01	M	55	42	*141*	32
816C	86	1-18*01	U	1	5	*145*	80
875A	88	3-48*02	M	1	10	*496*	86
888	94	3-21*01	U	81	86	*139*	65
929	80	1-69*01	U	25	75	*268*	58
1011	94	3-53*01	U	2	88	*190*	71

Mutational status of the *IGHV* gene; M indicates mutated (M-CLL) or U indicating unmutated (U-CLL). Ca^{2+} signalling is the response as a percentage of cells following stimulation with soluble anti-IgM antibody. CLL samples were characterised by research technicians in the tumour bank and CLL group.

2.2 Flow cytometry

2.2.1 Materials

Table 6. Materials used in flow cytometry and their associated components

MATERIALS	COMPONENTS/ORDER INFORMATION
ANNEXIN-V BUFFER (10X)	0.1 M HEPES pH 7.4, 1.4 M NaCl, 25 mM $CaCl_2$
FACS BUFFER	1% BSA, 4 mM EDTA, 0.15 mM Sodium azide
CLICK-IT PLUS OPP ALEXA FLUOR 647 PROTEIN SYNTHESIS ASSAY KIT	ThermoFisher Scientific, USA, #C10458
BD CYTOFIX/CYTOPERM FIXATION/PERMEABILIZATION SOLUTION KIT	ThermoFisher Scientific. #15747847
ANNEXIN-V-FITC	Protein Core Facility, University of Southampton
PROPIDIUM IODIDE	1 mg/ml solution, Invitrogen, #P3566
FLUO-3-AM	Invitrogen #F1242
PLURONIC ACID F-127	50 mg/ml in sterile H_2O, Sigma Aldrich, #P2443

Table 7. Antibodies used for flow cytometry and their ordering information

ANTIBODIES	ORDERING INFORMATION
PERCP-CY5-5-CONJUGATED ANTI-HUMAN CD5	Biolegend, #300620
PACIFIC BLUE-CONJUGATED ANTI-HUMAN CD19	Biolegend, #302232
ALEXA FLUOR 647-CONJUGATED OPP	ThermoFisher Scientific, USA, #C10458
PE-CONJUGATED GOAT ANTI-HUMAN IgM	Biologend, #314507
PE-CONJUGATED ISOTYPE MOUSE IgG1	Biolegend, #400112

2.2.2 *O*-propargyl-puromycin (OPP) incorporation

Cells were plated at $1x10^6$ cells per well in a 96-well plate (flat bottom, Sigma Aldrich) with Q-VD-OPh (10 µM, Sigma Aldrich). Q-VD-OPh is a pan-caspase inhibitor and was used to prevent spontaneous apoptosis of CLL cells *in vitro*. Cells were pre-treated with inhibitors or DMSO for one hour at 37˚C. Following this, cells were treated with control antibody, anti-IgM or CpG-ODN (7.5 µg/ml, Source Bioscience), for a further 24 hours incubation at 37˚C. Next, cycloheximide (CHX, 10 µg/ml, Sigma Aldrich) was added for five minutes as a control to pause translation. This was followed by addition of O-propargyl-puromycin (OPP, 20 µM) reagent to all cells for 30 minutes at 37˚C, according to the manufacturers' specification (ThermoFisher Scientific, Essex, UK). OPP is a puromycin analogue that is incorporated into newly synthesised polypeptide chains, and its incorporation is measured as a rate of translation.

Cells were then moved into flow cytometry plastic tubes and spun at 350 g for 5 minutes before washing with cold PBS twice and repeating the above centrifuge step. Cells were then washed and fixed with BD Cytofix/Cytoperm Fixation/Permeabilisation Kit (ThermoFisher Scientific) before addition of OPP reaction mixture at room temperature for 30 minutes. Following this, staining of incorporated OPP was undertaken using Alexa Fluor-647 (APC) antibody (ThermoFisher Scientific), and CLL samples stained with anti-human CD19-Pacific blue and anti-human CD5-PerCyP5.5 antibodies on ice, in the dark for 30 minutes (Biolegend, California, USA). Samples were then centrifuged as above, and resuspended in 300 µl FACs buffer. Data was acquired using a BD FACSCanto (BD Biosciences, California, USA) and analysed using FlowJo® software version 9.9.6 (BD Biosciences). The fluorescence value for CHX-treated cells was subtracted from all other values during analysis to correct for background fluorescence. Live cells were first gated, followed by gating of the $CD5^+/CD19^+$ CLL population, and APC measured as incorporation of OPP, as below (Figure 2-1).

Results from a pilot OPP labelling experiment are shown in Figure 2-1 to illustrate the gating procedure. The multiple live cell populations with differing side scatter shown in Figure 2-1 have been reported previously (Coelho et al., 2013) and are due to binding of increasing numbers of anti-IgM beads.

For analysis, mean fluorescence intensity (MFI) was calculated via FlowJo® software and exported to Microsoft Excel. Average MFI was calculated per duplicate of each condition. The MFI value for the CHX-treated control was subtracted from the average MFI of each condition. Values were then set to the DMSO control normalised to 1 (basal) or 100 (anti-IgM-induced). This allowed for improved visibility of the effects of sIgM-stimulation and the effects of inhibitors on this response.

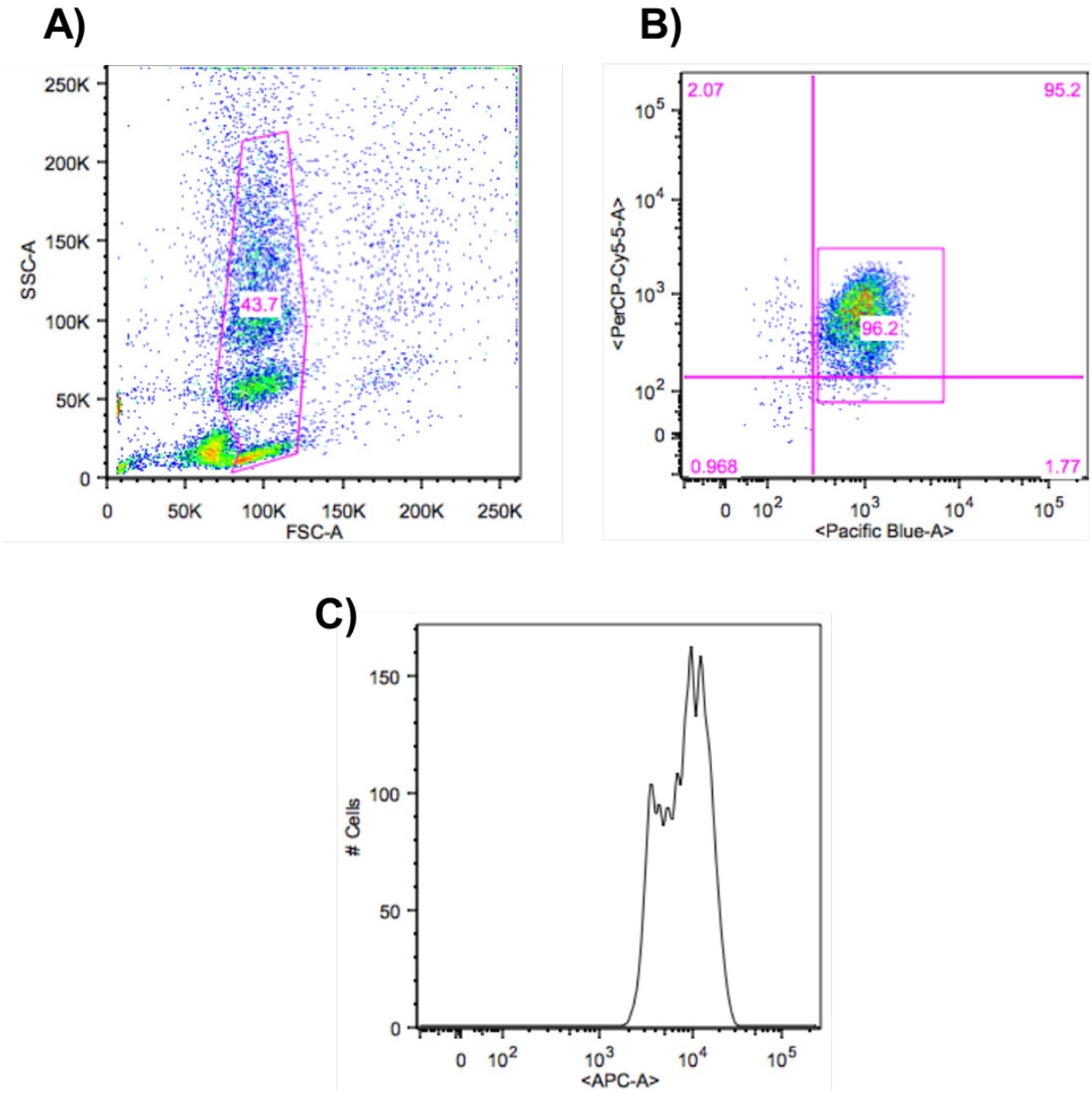

Figure 2-1. OPP-incorporation flow cytometry gating strategy

Representative FACS plots shown for OPP-incorporation assay. FACS OPP-incorporation assay was performed on the BD FACSCanto™ and data analysed using FlowJo® software v10.3. Gating was performed by initially selecting live and bead-bound cells based upon their forward scatter (FSC-A) and side-scatter (SSC-A) profiles (A). These cells were then further gated for positive CD19 expression (Pacific Blue-A) and CD5 expression (PerCP-Cy5-5-A), thus selecting only CLL cells (B). This subset of cells was then measured for APC expression, which measured OPP-incorporation (C). These gates were replicated across all conditions per experiment and APC MFI used as a measure of OPP-incorporation/ mRNA translation.

2.2.3 Annexin-V/propidium iodide (PI) staining

Annexin-V/propidium Iodide (PI) FACS staining was used to analyse viability of CLL cells following the treatments stated, with or with-out Q-VD-OPh (10 µM, Sigma Aldrich). Annexin-V/PI staining works on the basis that on the cytoplasmic surface of the plasma membrane of viable cells there is a phospholipid, phosphatidylserine (PS), actively held by an enzyme, flippase. When the cell undergoes apoptosis, scramblase enzyme catalyses the movement of PS to the outer-side of the plasma membrane, where PS can be recognised by macrophages for phagocytosis. Annexin-V staining can be used to bind and identify PS on the external cellular membrane of apoptotic cells. Propidium iodide (PI) is a fluorescent dye that intercalates into DNA when a cell is undergoing apoptosis. PI cannot permeate through the cell membrane of viable cells and so PI staining can only occur in apoptotic cells.

Cells were plated at $1x10^6$ cells per well in a 96-well plate and treated with the relevant inhibitor compound (as stated per experiment) for 24 hours (or longer in the case of ribavirin experiments, up to 72 hours). Cells were collected into flow cytometry tubes and spun at 300 g for 5 minutes before washing with cold PBS twice. Cells were then incubated in 300 µl of 1x Annexin-V buffer containing 2.5 µg/ml of Annexin-V-FITC (Protein Core Facility, University of Southampton) and 12.5 µM PI (Invitrogen, USA) per sample tube in the dark before analysis using a BD FACSCanto and analysed using FlowJo® software. Cells gated as in Figure 2-2, and percentage of live cells was recorded (Annexin V^-/PI^-). Percentage of live cells were then normalised with DMSO-control set to 100 and other conditions made relative to this before presentation in GraphPad Prism software v7.

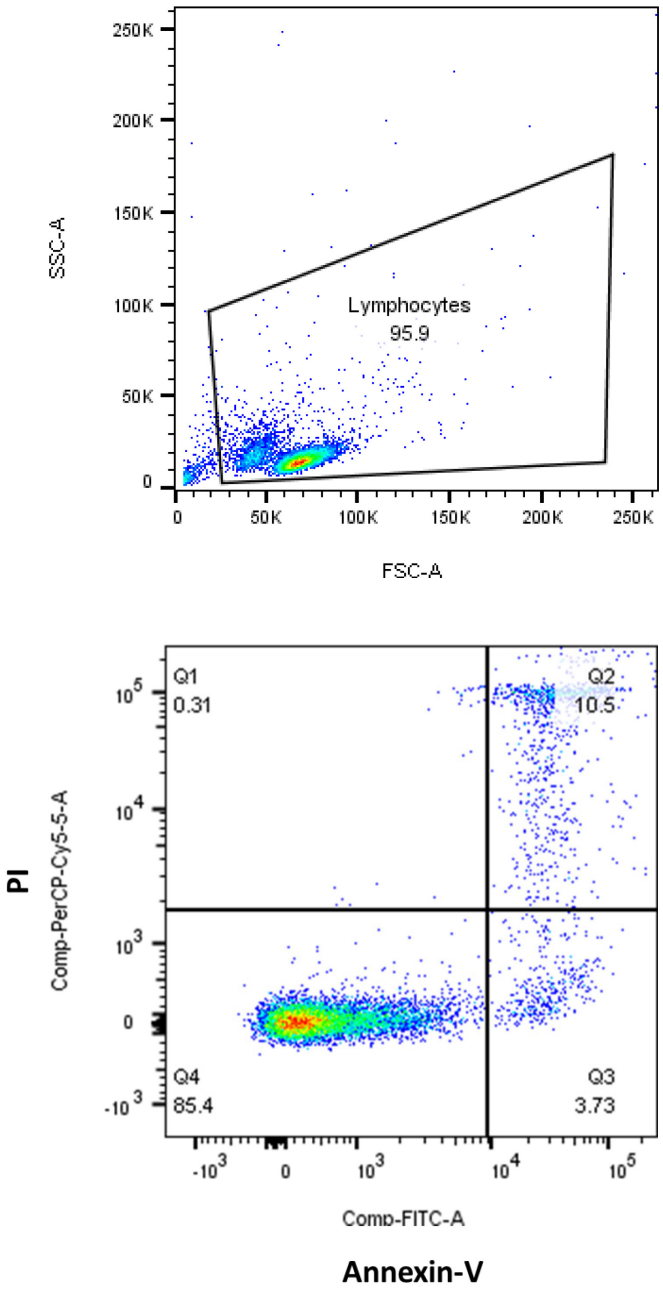

Figure 2-2. Gating strategy of Annexin-V/PI flow cytometry assay

Representative FACS plots shown for Annexin-V/PI assay, performed on the BD FACSCanto™ and data analysed using FlowJo® software v10.3. Gating was performed by initially selecting lymphocytes based upon their forward scatter (FSC-A) and side-scatter (SSC-A) profiles, removing debris from analysis. These cells were then further gated for Annexin-V (FITC-A) and PI (PerCP-Cy5-5-A). Plots were gated into quadrants of Annexin-V positive/negative and PI positive/negative. Q1 shows percentage of Annexin-V^-/PI^+ cells, Q2 is Annexin-V^+/PI^+ cells, Q3 is Annexin-V^+/PI^- cells and Q4 is Annexin-V^-/PI^- cells. Q4 is therefore the live cell population and provides a percentage of total cells per sample that are live. Percentage of cells were then normalised with DMSO-control set to 100 and other conditions made relative to this.

2.2.4 Calcium-flux (Ca^{2+})/ mobilisation flow cytometry

Calcium (Ca^{2+}) mobilisation was investigated as a marker of BCR signalling capacity. CLL cells were recovered as in section 2.1.2 and plated at $1x10^7$ cells in 1ml in a 1.5 ml Eppendorf and treated with the relevant drug for one hour. Cells were then treated with Pluronic acid F-127 at 0.02% of total volume (Sigma Aldrich, Poole, UK) and Fluo3-AM dye (4 μM, Invitrogen, UK) for 30 minutes at 37˚C. Cells were washed and resuspended in fresh room temperature RPMI (with relevant drugs re-added). Each tube was warmed to 37˚C for 5 minutes prior to acquisition. The flow cytometer ran for 30 seconds to record background/baseline fluorescence, after 30 seconds tubes were carefully removed whilst the flow cytometer was still recording and 20 μg/ ml $F(ab')_2$ soluble anti-human IgM or 'control' antibody, goat $F(ab')_2$ IgG was added and the tube replaced back on the flow cytometer. Following five minutes of data acquisition, the Ca^{2+} ionophore ionomycin (1 μM) was added, to determine full Ca^{2+} releasing capacity of the sample. Data acquisition was performed using the BD FACSCanto flow cytometer and analysed using FlowJo® software. Percentage of responding cells was calculated by [peak response – mean Y (baseline) / %$CD19^+$ cells] x 100. Percentage of $CD19^+$ cells per sample was taken from phenotyping data provided and described in Table 5. Example plots of calcium mobilisation assay can be seen in Figure 5-8.

2.2.5 Surface IgM (sIgM) expression

Flow cytometry staining was also used to determine sIgM expression on CLL cells following ribavirin treatment. Cells were plated at $1x10^6$ in 100 μl media per well in a 96-well plate, after recovery for one hour. The relevant wells were treated with the relevant drug for 24-hours at 37˚C. Cells were then collected in FACs tubes and washed twice in cold PBS by centrifugation. Samples were then stained with anti-human CD19-Pacific blue, anti-human CD5-PerCyP5.5 and PE-conjugated anti-human IgM (or a PE isotype control antibody, Biolegend) for 30 minutes on ice, in the dark. Cells were then washed in 1 ml FACS buffer by centrifugation then resuspended in 300 μl FACs buffer for analysis on the BD FACSCanto and analysed using FlowJo® software. Gating was performed as demonstrated in Figure 2-3. Staining controls are demonstrated in Figure 2-4. MFI was made relative to DMSO-treated control set to 100 for analysis. Statistical analysis performed using paired T-tests.

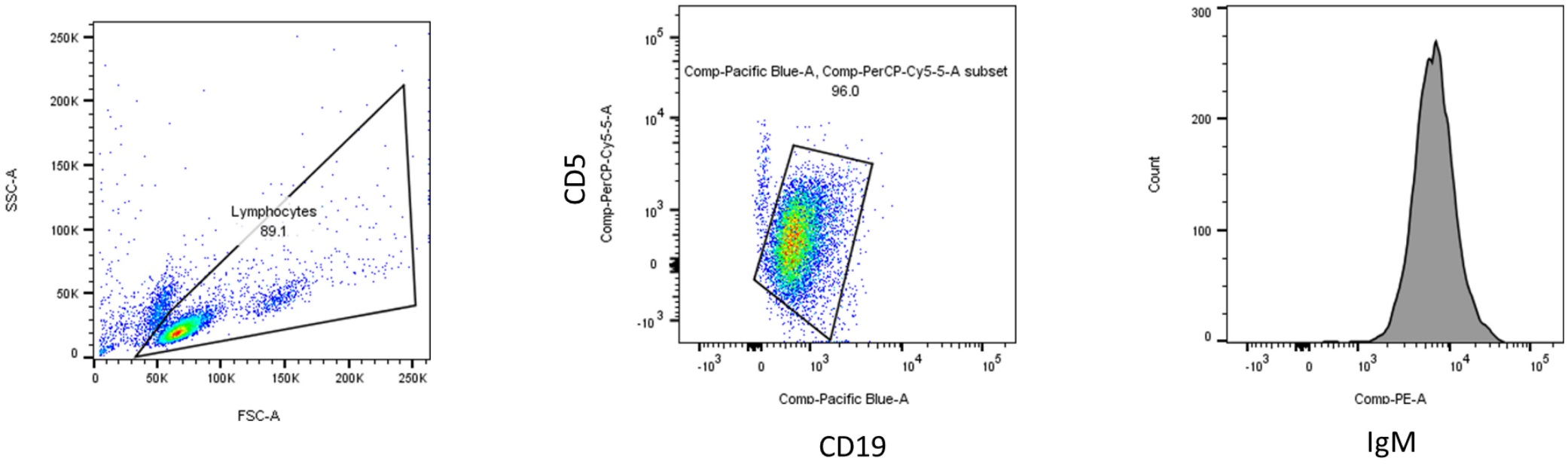

Figure 2-3. Gating strategy of sIgM expression

Representative FACS plots shown for sIgM staining assay, performed on the BD FACSCanto™ and data analysed using FlowJo® software v10.3. Gating was performed by initially selecting lymphocytes based upon their forward scatter (FSC-A) and side-scatter (SSC-A) profiles, removing debris and dead cells from analysis. These cells were then further gated for positive CD19 (Pacific Blue-A) and CD5 (PerCP-Cy5-5-A) expression to identify CLL cells. These CLL cells were then measured for sIgM expression (PE-A) and MFI calculated. sIgM MFI expression was then normalised with DMSO-control set to 100 and other conditions made relative to this.

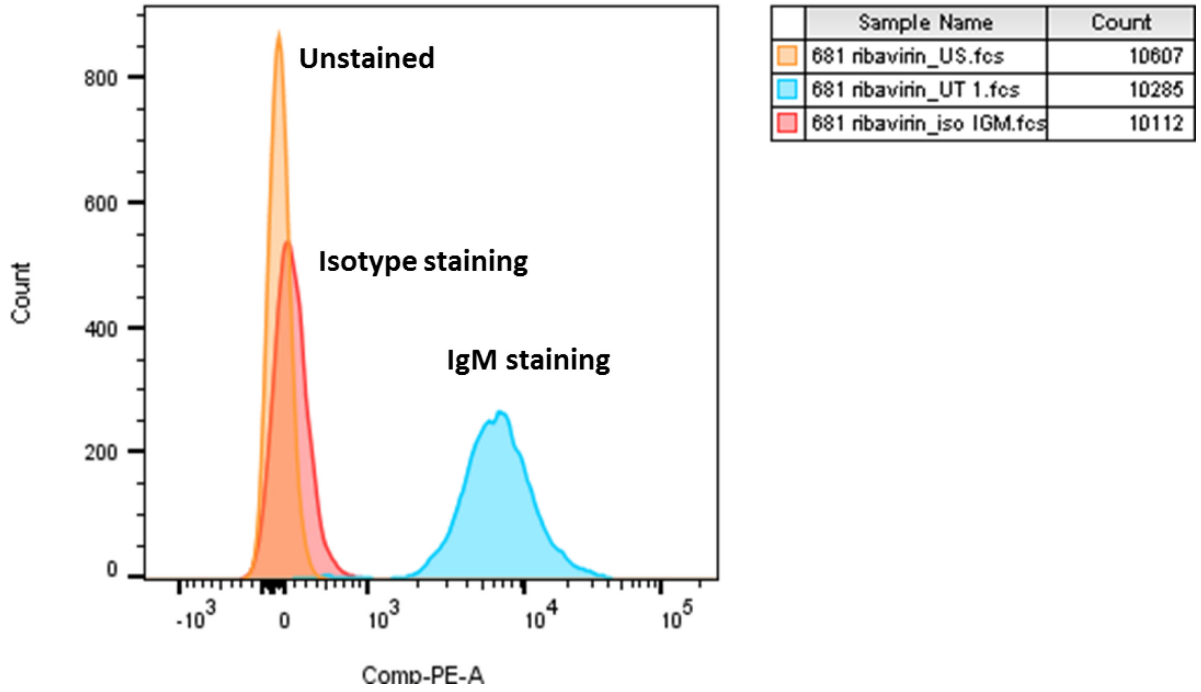

Figure 2-4. Overlay of PE expression in IgM stained or PE- isotype stained or unstained cells

Representative FACS histogram overlays shown for sIgM staining assay, using sample M-681, performed on the BD FACSCanto™ and data analysed using FlowJo® software v10.3. Gating was performed by initially selecting lymphocytes based upon their forward scatter (FSC-A) and side-scatter (SSC-A) profiles, removing debris and dead cells from analysis. These cells were then further gated for positive CD19 (Pacific Blue-A) and CD5 (PerCP-Cy5-5-A) expression to identify CLL cells. These CLL cells were then measured for sIgM expression (PE-A). Overlays demonstrated to show binding of PE-conjugated IgM stain and PE-conjugated isotype control stain and unstained cells.

2.3 Western blotting

2.3.1 Materials

Table 8. Materials used for western blotting and their components.

MATERIAL	COMPONENTS/ORDER INFORMATION
RUNNING BUFFER (10X)	250 mM Tris-base, 1.9 M Glycine , 35 mM SDS
TRANSFER BUFFER	25% (v/v) ethanol, 10 % (v/v) running buffer (10x), 65% (v/v) deionised H_2O
TRIS-BUFFERED SALINE – TWEEN (TBST)	20 mM Tris pH7.6, 137 mM NaCl, 0.1% (v/v) Tween-20 (Sigma Aldrich)
POLYACRYLAMIDE RESOLVING GEL (10%)	deionised H_2O, 30% acrylamide mix (Sigma Aldrich), 1.5 M Tris pH8.8, 10% SDS, 10% ammomium persulfate, 0.0004% (v/v) TEMED
POLYACRYLAMIDE STACKING GEL (6%)	deionised H_2O, 30% acrylamide mix (Sigma Aldrich), 1.0 M Tris pH6.8, 10% SDS, 10% ammomium persulfate, 0.001% (v/v) TEMED
RIPA LYSIS BUFFER (5X)	0.75 M NaCl, 5% (v/v) NP40, 2.5% (v/v) deoxycholate (DOC), 0.5% (w/v) SDS, 0.25 M Tris pH8.0
5% BSA-TBST	TBST (as above) supplemented with 5% bovine serum albumin (w/v, BSA, Sigma Aldrich, #A7906)
PROTEASE INHIBITOR COCKTAIL	Sigma Aldrich, #8340
PHOSPHATASE INHIBITOR COCKTAIL 2	Sigma Aldrich, #5726
PHOSPHATASE INHIBITOR COCKTAIL 3	Sigma Aldrich, #0044
DTT AND SDS-LOADING DYE KIT	Cell Signaling Technology, London, UK, #7723
SUPERSIGNAL™ WEST FEMTO CHEMILUMINESCENT SUBSTRATE	ThermoFisher Scientific, #34094

Table 9. Antibodies used for western blotting and their order information.

ANTIBODY	COMPANY & ORDER NUMBER
POLYCLONAL GOAT ANTI-MOUSE HORSERADISH PEROXIDASE (HRP)	Agilent Technologies, Santa Clara, USA, #PO44701-2
POLYCLONAL GOAT ANTI-RABBIT HRP	Agilent Technologies, #D048701-2
ANTI-c-MYC MOUSE MONOCLONAL (CLONE 9E10)	Merck, Watford, UK, #MABE282
POLYCLONAL RABBIT ANTI-eIF4E	Cell Signaling Technology, #9472
POLYCLONAL RABBIT ANTI-PHOSPHO-eIF4E (Ser209)	Cell Signaling Technology, #9741
MONOCLONAL RABBIT ANTI-4E-BINDING PROTEIN-1 (4E-BP1)	Cell Signaling Technology, #9644
MONOCLONAL MOUSE ANTI-MCL1	Santa Cruz Biotechnology, Texas, USA, #12756
POLYCLONAL RABBIT ANTI-eIF4A	Abcam, Cambridge, UK, #ab31217
MONOCLONAL RABBIT ANTI-PDCD4	Cell Signaling Technology, #9535
MONOCLONAL RABBIT ANTI-CYCLIN D1	Cell Signaling Technology #2978
MONOCLONAL MOUSE ANTI-HSC70	Santa Cruz Biotechnology, #7298
MONOCLONAL MOUSE ANTI-PARP	BD Biosciences, #556494
POLYCLONAL RABBIT ANTI-ERK1/2	Cell Signaling Technology, #9102
POLYCLONAL RABBIT ANTI-PHOSPHO-ERK1/2 (THR202/TYR204)	Cell Signaling Technology, #9101
MONOCLONAL RABBIT ANTI-BETA-ACTIN	Cell Signaling Technology, #4970

All antibodies were used as a 1:1000 dilution in 5% BSA in TBST buffer.

2.3.2 Protein extraction

Proteins were extracted from cell pellets by treatment with 1X RIPA buffer (Table 8) supplemented with protease and phosphatase inhibitors (Sigma Aldrich) for 20 minutes on ice followed by centrifugation at 16,100 g at 4˚C for 5 minutes. The supernatant, containing proteins, was then transferred to a fresh 1.5 ml Eppendorf tube and the pellet discarded.

2.3.3 Protein quantification by Bradford assay

Protein concentration was calculated using the Bradford colorimetric assay (Biorad, Watford, UK). Bradford reagent was diluted and added to a 96 well plate and 1 mg/ml bovine serum albumin (BSA) used for the standard curve, alongside samples of unknown protein concentration. The plate was then read by the Varioskan Flash plate reader (ThermoFisher Scientific) by measuring the wavelength of light at 595nm. Protein concentrations were then calculated using the standard curve method. Following quantification, equal concentrations of each sample were mixed with 30X dithiothreitol (DTT) and SDS loading dye (Cell signaling technology, Hertfordshire, UK), and boiled at 95˚C for 5 minutes then stored at -20˚C before gel electrophoresis.

2.3.4 Gel electrophoresis

Proteins were separated by gel electrophoresis using a 10% Tris/Glycine gels were made and resolved at 120V for ~1 hour in running buffer (Table 8). The proteins were then transferred onto a nitrocellulose membrane at 100V for 1 hour in transfer buffer (Table 8). The membrane was then incubated for 1 hour in 5% (w/v) BSA in TBST (Table 8) to prevent any non-specific binding of antibodies during the following incubation steps.

2.3.5 Visualisation of proteins

Primary antibodies were incubated (Table 9) with membranes in 5% BSA overnight at 4˚C, before washing with TBST (Table 8) and then incubated with the relevant horseradish peroxidase (HRP) secondary antibodies in 5% BSA for 2 hours at RT. Imaging of Western blot membranes was carried out by adding Supersignal™ West Femto chemiluminescent substrate (ThermoFisher scientific) and imaging performed using the UVP ChemiDoc-IT imaging system (Analytik Jena, California, USA). Image J software (NIH) was used to calculate band densitometries for graphs shown and all calculations are made relative to HSC70 or other relevant protein expression, as stated.

2.4 Molecular biology techniques

2.4.1 Materials

Table 10. Materials used for molecular biology and their ordering information

MATERIAL	ORDERING INFORMATION
RELIAPREP RNA EXTRACTION MINIKIT	Promega, Southampton, UK, #Z6011
RNASEZAP RNASE DECONTAMINATION SOLUTION	ThermoFisher Scientific, #AM9780
EPPENDORF LOBIND MICROCENTRIFUGE TUBES 2ML	Sigma Aldrich, #Z666556
OLIGO-$(dT)_{15}$ PRIMERS	Promega, #C1101
M-MLV REVERSE TRANSCRIPTASE AND M-MLV BUFFER KIT	Promega, #M5313
RNAISIN RIBONUCLEASE INHIBITOR	Promega, #N2111
dNTP'S (dATP, dCTP, dGTP, dTTP)	Promega, #U1130
FAST 96-WELL HARDSHELL CLEAR PLATES	ThermoFisher Scientific, #4483485
MICROAMP CLEAR ADHESIVE FILM PLATE SEALS	ThermoFisher Scientific, #4306311
TAQMAN FAST ADVANCED MASTERMIX	ThermoFisher Scientific, #4444963

Table 11. Primers/probes used in qPCR

PRIMER/ GENE NAME	SPECIES	AMPLICON LENGTH	ORDER CODE
MYC	Human	107	Hs00153408_m1
MCL1	Human	89	Hs01050896_m1
B2M	Human	64	Hs00187842_m1
GAPDH	Human	157	Hs02786624_g1
EIF4E	Human	191	Hs00854166_g1
CCND1	Human	57	Hs00765553_m1

All primers were sourced from ThermoFisher Scientific UK and used according to the manufacturers' instructions. Probes of each primer were produced known to span the exons of the mRNA in question.

2.4.2 RNA extraction

CLL cells were recovered and plated at $1x10^7$ cells per well in a 12 well plate and treated as stated per experiment. Following this incubation cells were collected as pellets after washing with PBS and RNA then extracted following the manufacturers protocol using the Reliaprep RNA extraction minikit (Promega). RNA was eluted in RNAse-free water and then quantified using the Nanodrop 1000 spectrophotometer (ThermoFisher Scientific).Techniques involving RNA were carried out in an RNase-free environment and all surfaces and equipment were pre-treated with RNaseZAP RNase decontamination solution (ThermoFisher Scientific). DNase/RNase free Eppendorf tubes (Sigma Aldrich) and filter tips were used to prevent contamination/degradation of RNA.

2.4.3 Synthesis of first strand complementary DNA

1 μg of RNA was used to synthesise single-stranded complementary DNA (cDNA) for all experiments excluding polysome profiling which used 300 ng RNA due to experimental limitations. RNA was diluted to a total volume of 14 μl with RNase-free H_2O. To this, 1 μl oligo-$(dT)_{15}$ primer (Promega, Southampton, UK) was added to RNA before heating to 70˚C for 5 minutes to allow the oligo-(dT) primer to bind to the polyA tail of the RNA. Next, samples were cooled to 4˚C and a mixture of 1 μl M-MLV reverse transcriptase (Promega), 0.625 μl RNaisin ribonuclease inhibitor (Promega), 1.25μl 10 mM dNTP, 5 μl M-MLV buffer (Promega) and 2.125 μl RNase-free H_2O added to each sample. Samples were then placed in a thermal cycler set to 42˚C for 60 minutes which allows generation of the cDNA complementary to the mRNA sequence, with optimal reverse transcriptase enzyme activity. This was followed by heating to 95˚C for 5 minutes, to inactivate the reverse transcriptase enzyme before cooling to 4˚C. Samples were diluted with 75 μl sterile-filtered H_2O and stored for future use in qPCR at -20 ˚C.

2.4.4 Quantitative polymerase chain reaction (qPCR)

cDNA synthesised as described above was used for Taqman® quantitative polymerase chain reaction (qPCR) using gene-specific Taqman® primers (Table 11) and the Quant-Studio Flex 7 Real-Time PCR System (ThermoFisher Scientific). Taqman® primers contained both forward and reverse primers specific to the gene of interest, as well as a probe with a fluorophore and quencher. Probes are DNA oligonucleotides which bind downstream of a forward or reverse primer during PCR. The probes 5' end has a fluorophore, and the 3' end has the quencher. The quencher is used to 'quench'

the fluorophore when close to one another. When the probe is intact, a process called fluorescence resonance energy transfer (FRET) occurs. FRET is the transfer of energy between two dye molecules, during which excitation/energy is transferred from the donor molecule (in this case, the fluorophore) to an acceptor molecule (the quencher) without emission of a photon. Therefore, the quencher absorbs the fluorescence produced by the fluorophore when they are in close proximity. When the probe has bound to the target sequence, it gets cleaved by the Taq polymerase enzyme in the Taqman Mastermix during the extension phase of the PCR cycle, which separates the probe and fluorophore, resulting in increased fluorescence. Thus, with every PCR cycle, more probe is cleaved and an increasing level of fluorescence is produced.

Cleavage of the probe also removes the probe itself from the target sequence, allowing primer extension to continue and not preventing exponential accumulation of the PCR product. With each PCR cycle, additional fluorophores are cleaved from the probes resulting in increased fluorescence which is proportional to the concentration of the target cDNA in the reaction, as gene-specific primers and probe were used.

Based upon baseline fluorescence, the software produces a threshold value, often an average of the fluorescence detected between early cycles (usually between cycles three to 15). When fluorescence in the reaction is detected over this threshold value a threshold cycle (Ct) value is produced for each sample. The Ct value is the fractional cycle number of which the fluorescence reaches the threshold, and correlates with more template cDNA at the start of the PCR reaction leading to a smaller Ct value. The Ct value occurs during the exponential phase of the PCR reaction. Once the components in the reaction mixture become sparse, and rate limiting, the rate of amplification decreases until the PCR reaction undergoes the plateau phase, whereby the reaction template is no longer being generated exponentially. Stages of the qPCR cycle are illustrated in Figure 2-5, and repeated 40-times.

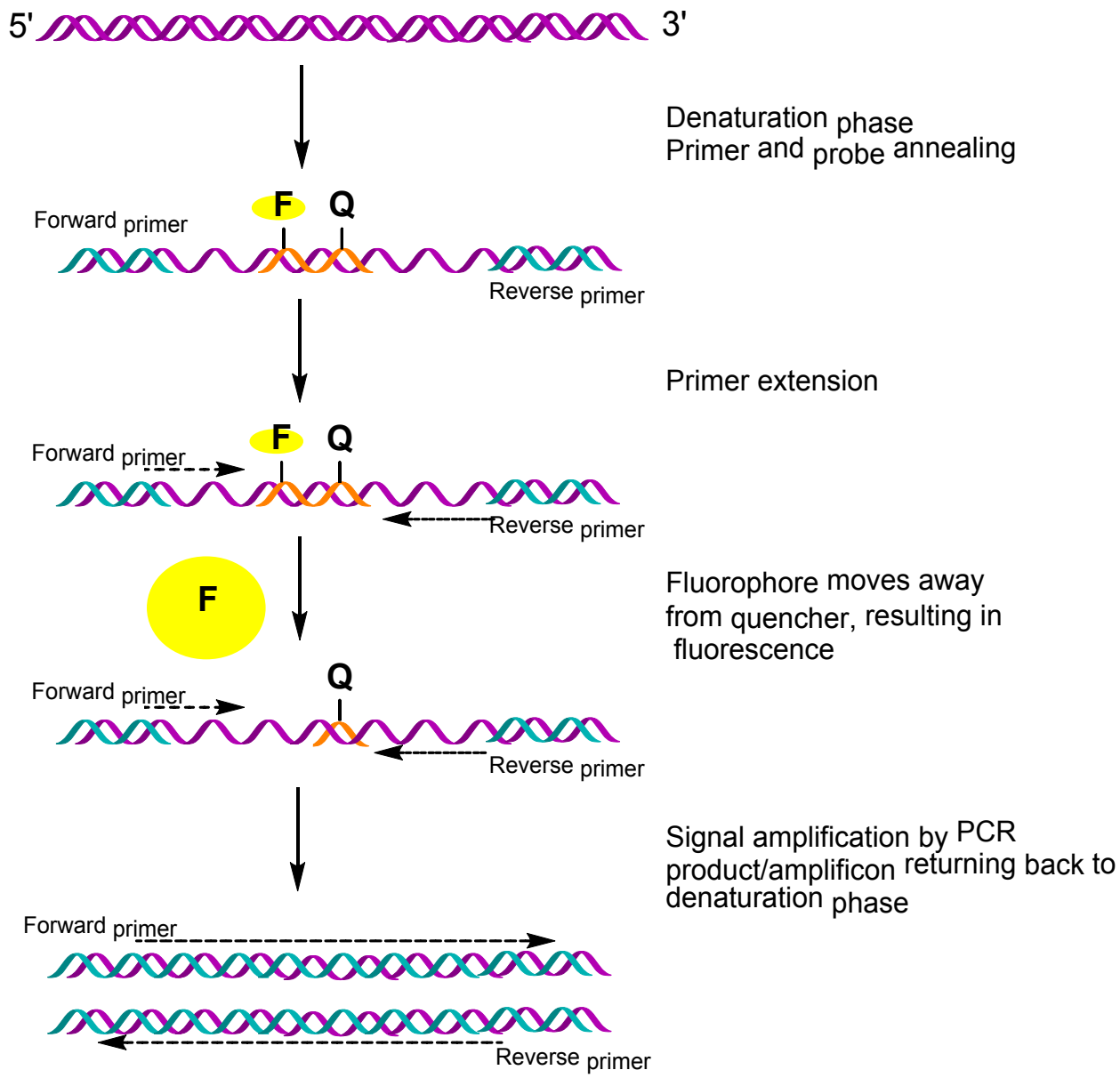

Figure 2-5. Stages of a Taqman qPCR cycle.

Diagram of the stages of a Taqman qPCR. F indicates the fluorophore and Q represents the quencher of the probe. The initial stage of PCR involves heating to 95°C for denaturing of the cDNA, to allow primers and probes access to individual strands. The temperature then is reduced to 60°C for extension of the primers in the 5'-3' direction, resulting in Taq polymerase enzyme meeting the 5' end of the probe, where the fluorophore is attached. Taq polymerase then degrades the probe, resulting in the fluorophore moving away (no longer near the quencher) and producing fluorescence. The polymerase can continue to extent the primer. This cycle then repeats with more PCR product produced. Image produced using ChemDraw Professional v16.

For the qPCR reaction, 5 μl of cDNA, 1 μl of the gene-specific Taqman primer/probe mix and 10 μl of Taqman mastermix were added per well of a 96-well qPCR plate (Thermofisher Scientific). A clear plate seal was applied to the plate, before brief centrifugation to collect all of the qPCR reaction mix to the bottom of the well. Within the plate, each sample was added in duplicate and a duplicate standard curve was also added. This standard curve was generated from RNA extracted from cells of the HBL1 cell line. RNA was extracted and cDNA synthesised as in 2.4.2 and 2.4.3 and serial dilutions were performed to create a standard curve of the following concentrations; 10, 5, 1, 0.5, 0 ng/μl. Once the qPCR had been performed, the Ct values produced were exported to Microsoft Excel. The higher the Ct value, the lower abundance of the target-gene, as more PCR cycles occurred to reach the fluorescence threshold (Figure 2-6). To quantify cDNA, the standard curve was used to correlate Ct values with the known cDNA concentration. Ct values of the samples measured with unknown concentrations of cDNA were calculated against those of the standard curve to calculate the cDNA concentration present in each sample. The duplicate results were then used to calculate the average concentration. mRNA expression was then calculated by making the cDNA values relative to the B2M (housekeeping control) cDNA expression of each sample. Data was then statistically and graphically analysed using GraphPad prism software v7.0 and using students T-tests.

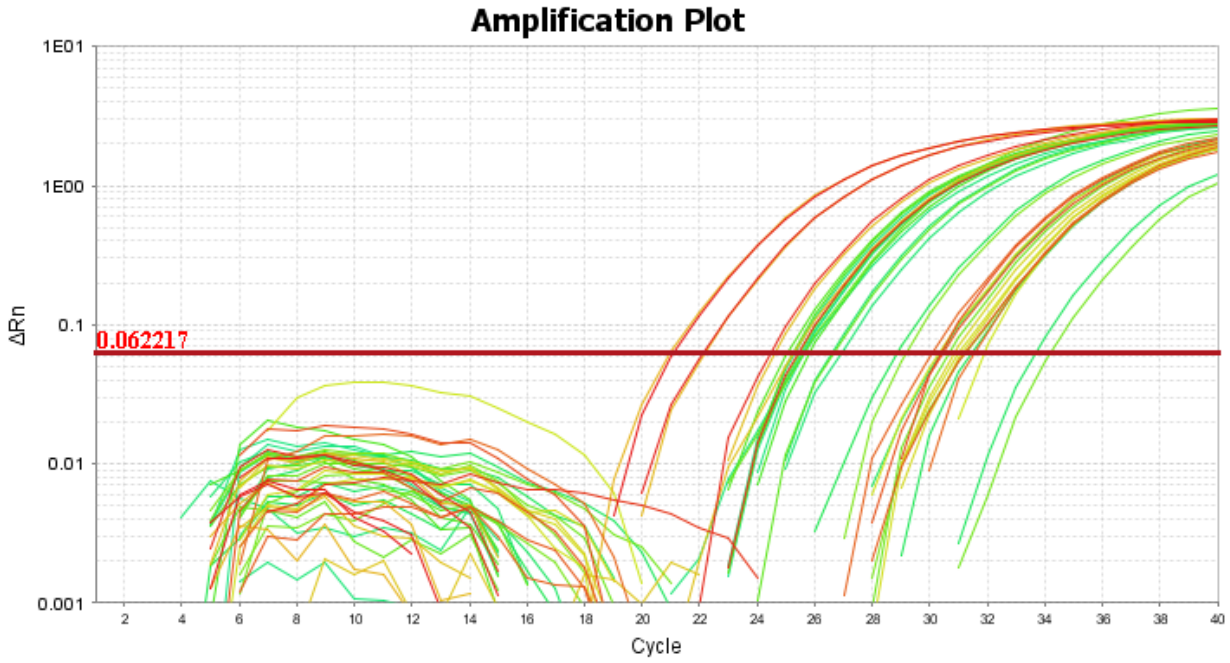

Figure 2-6. Amplification plot from a qPCR experiment

Example of a typical amplification plot produced following a qPCR experiment. Threshold line can be seen in red with threshold value (0.062217). The threshold value is the ΔRn at which the fluorescence of a sample must reach to exceed background fluorescence. The cycle at which a sample reaches the threshold is classed as its threshold cycle (or Ct). Each coloured line represents a single sample, duplicates are shown in the same colour for that sample. The qPCR experiment which this plot was taken from was measuring *MYC* expression in untreated, isotype control-bead and anti-IgM bead treated CLL cells. Plot was obtained using the QuantStudio Flex 7 Real-Time PCR software v1.3 (ThermoFisher Scientific).

2.5 Polysome profiling

2.5.1 Materials

Table 12. Materials used for polysome profiling and their components/ordering information

MATERIAL	COMPONENTS/ORDER INFORMATION
CELL LYSIS BUFFER	10 mM Tris-HCl pH 7.5, 100 mM NaCl, 100 mM $MgCl_2$, 10% Triton X-100 and sodium deoxycholate (DOC) (1:1 mix), 1 M DTT and 40U RNasin Ribonuclease Inhibitor (Promega, Wisconsin, USA, #N2111)
PROTEINASE K	Thermo Fisher Scientific, #AM2546
CARRIER tRNA FROM BAKERS YEAST	Sigma Aldrich, #R9001
PHENOL-CHLOROFORM	Sigma Aldrich, #77618
CHLOROFORM	Sigma Aldrich, #25666
POLYSOME GRADIENT BUFFER	30 mM Tris-HCl pH7.5, 100 mM NaCL, 10 mM $MgCl_2$

2.5.1 Preparation of CLL samples and treatments

Cells were recovered as in 2.1.2 and treated with QVD-O-Ph (5 µM, Sigma Aldrich) before being split into T25 flasks at $5x10^7$ per condition. Cells were treated as required per experiment then following incubation, cells were treated with 10 µg/ml CHX (Sigma Aldrich) for 5 minutes to arrest the ribosomes. Cells were then collected and washed in PBS (with CHX added) before centrifugation at 300 g and 4˚C for 5 minutes. Cell pellets were then incubated in cell lysis buffer (see Table 12) for 2 minutes on ice before centrifugation at 16,100 g at 4˚C for 5 minutes. The resulting supernatant containing polysomes was snap-frozen and stored at -80˚C.

2.5.2 Ultracentrifugation, fractionation and visualisation of polysome profiles

Sucrose solutions of 20%, 26%, 32%, 38%, 44% and 50% (made up in distilled H_2O) were layered and snap-frozen at each layer in ultracentrifugation tubes, with the most concentrated solution at the base of the tube, before defrosting overnight at 4˚C to form continuous gradients. Polysome lysates were then thawed and equal volumes gently pipetted atop continuous sucrose gradients in

ultracentrifugation tubes. These samples were then centrifuged at 234,745 g for 2.5 hours at 4˚C with no brake using the Beckman Coulter Optima XPN-80 ultracentrifuge. Samples were run through the piston gradient fractionator (Biocomp instruments) and absorbance measured at 254 nm. Waveforms were measured and analysed using Windaq DATAQ software (DATAQ Instruments, Ohio, USA). Technique demonstrated in Figure 2-7. Fractions were collected for 45 seconds into Eppendorf tubes containing 5 mg/ml proteinase K (to remove proteins, ThermoFisher Scientific) and 0.25 µg/µl carrier tRNA (to aid precipitation of the mRNA) from bakers' yeast (Sigma Aldrich) followed by two hours incubation at 37˚C then stored at -20˚C.

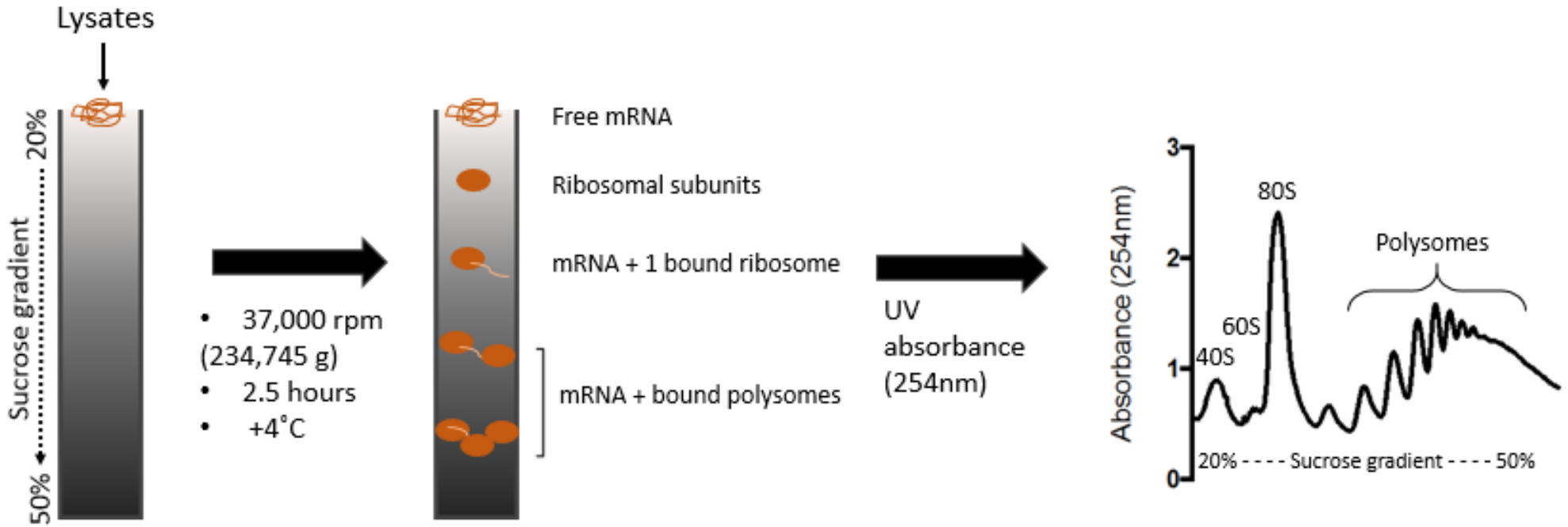

Figure 2-7. Polysome profiling.

Polysome lysates pipetted on top of a continuous sucrose gradient (20-50%) before ultracentrifugation at 234,745 g (37,000rpm) for 2.5 hours. This results in more dense fragments at bottom of tube, such as mRNA bound to multiple polysomes, whereas lighter fragments would be towards the top such as free mRNA or ribosomal subunits. Sample is taken up from the top and pumped through polysome profiling machine where UV absorbance is measured and produces profile as shown.

2.5.3 Phenol-chloroform RNA extraction of polysome fractions

Fractions were defrosted on ice before mixing with phenol-chloroform (pH 4.5, ratio 1:1, Sigma Aldrich) and vortexed thoroughly. Fractions were centrifuged at 13,700 g for 10 minutes at 4˚C to separate the aqueous phase which contains nucleic acids from the organic phase of proteins and lipids. The aqueous phase was then combined with chloroform and vortexed again. Fractions were then centrifuged again as above, then the top layer taken was and mixed with isopropanol to precipitate RNA. Fractions were then inverted 5 times and stored at -20˚C for 2 hours. Next, samples were centrifuged at 13,700 g for 30 minutes at 4˚C, and the pellet then re-suspended in 80% ethanol. Finally, samples were spun again at 13,700 g for 30 minutes, ethanol removed and pellet air-dried on ice for 10 minutes before dissolving in RNase free water. The extracted RNA from each fraction was then quantified using the Nanodrop 1000 spectrophotometer (ThermoFisher Scientific). 300 ng of RNA per sample was then used for synthesis of cDNA as in section 2.4.3, and qPCR performed as in section 2.4.4.

2.5.4 Analysis of polysome profiling data

Following qPCR, cDNA from each of the 10 fractions per sample was quantified using the standard curve method as described (section 2.4.4). Image depicts the collection of fractions 1-10 against a polysome profile (Figure 2-8).

Using the cDNA values obtained, total cDNA (ng) per condition was calculated as a sum of the 10 fractions. Monosome associated cDNA was calculated as a sum of the fractions 1-4, while polysome-associated cDNA was calculated as a sum of fractions 5-10 for each condition. The percentage of RNA per fraction of each condition was calculated by dividing the amount of RNA in each fraction by the total RNA and multiplied by 100 to generate a percentage. The percentage of RNA in the polysomes or monosome peak was calculated by using the polysome or monosome-associated cDNA (respectively) and divided by the total RNA to generate a percentage. The percentage of RNA per fraction was then used to calculate the RNA per polysome fractions relative to monosome fractions, and normalised with anti-IgM DMSO treated sample set to 1.

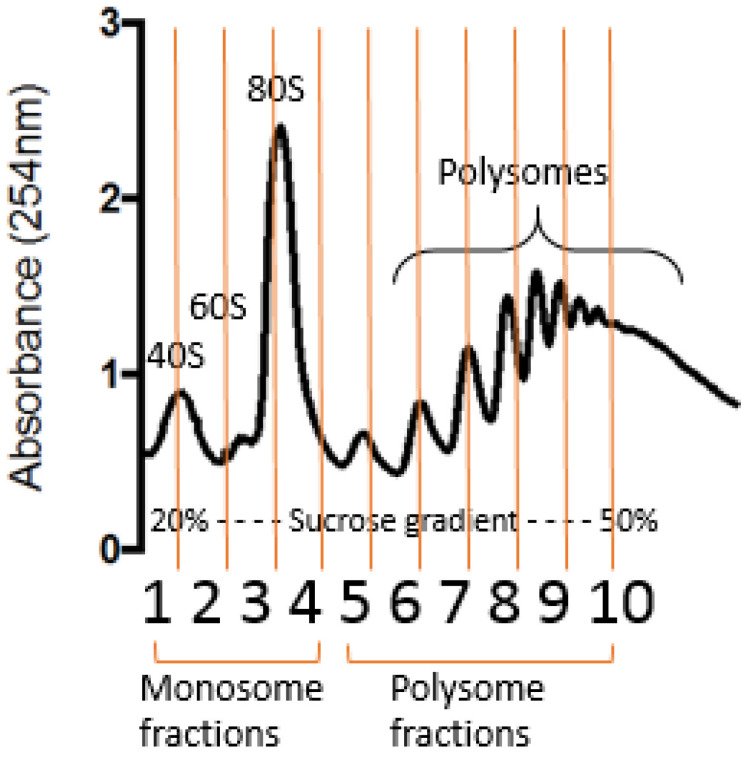

Figure 2-8. Fractions collected during polysome profiling

Equal fractions during polysome profiling were collected for 45 seconds into 1.5 ml Eppendorf tubes containing 5 mg/ml proteinase K (ThermoFisher Scientific) and 0.25 µg/µl carrier tRNA (Sigma Aldrich).

2.6 Bioinformatical analysis of 5' UTR of *MYC* and *MCL1*

Sequences of target genes were taken from National Center for Biotechnology Information (NCBI) Genbank, using RefSeq accessions – NM_002467 (*MYC)* and NM_021960 (*MCL1)*. Sequences were truncated at the start codon and length determined (as base pairs). Presence of polypurine sequences was determined by counting of individual 6mers (A/G). Presence of G-quadruplexes was determined using QuadBase2 online software. Finally, free energy of the most stable predicted secondary structure was determined using RNAFold online software.

2.7 Subcellular fractionation

2.7.1 Materials

Table 13. Materials used for subcellular fractionation and their components or ordering information

MATERIAL	COMPONENTS/ORDER INFORMATION
FRACTIONATION BUFFER 1	10 mM HEPES pH 7.5, 10 mM KCl, 0.1 mM EDTA, 0.5% IGEPAL, 1 mM DTT
FRACTIONATION BUFFER 2	20 mM HEPES pH 7.5, 400 mM NaCl, 1 mM EDTA, 1 mM DTT
SUPERASEIN RNASE INHIBITOR	Invitrogen, USA, #AM2696

2.7.2 Fractionation of nuclear and cytoplasmic RNA

$4x10^6$ CLL cells were incubated in T25 flasks in 4 ml complete RPMI media. Cells were recovered as in section 2.1.2 before treatment with the relative drug for 1-hour at 37˚C and then control or anti-IgM beads added for 24 hours. Following treatments, cells were collected in cold PBS and centrifuged for five minutes at 300 g. Pellets were then resuspended in cold PBS and re-centrifuged. The supernatant was removed and 400 μl Buffer 1 (containing SUPERaseIn RNase inhibitor 1:100, to prevent degradation of RNA) was added to the remaining cell pellet. Samples were then scraped across an Eppendorf rack to gently disrupt the pellet. The samples were incubated on ice for 20 minutes, and then vortexed before centrifugation at 12,000 g for 10 minutes at 4˚C. Supernatant (cytosolic fraction) was collected in a fresh 1.5 ml Eppendorf tube and stored on ice before RNA extraction.

The remaining pellet was washed twice in 200 µl Buffer 1 by centrifugation at 12,000 g for 2 minutes at 4˚C. The pellet was then resuspended in 150 µl Buffer 2 (including RNase inhibitor as above for buffer 1) and incubated on ice for 30 minutes. Then the samples were centrifuged at 12,000 g for 15 minutes at 4˚C, and the supernatant collected as the nuclear fraction.

To extract RNA from the cytoplasmic and nuclear fractions, phenol-chloroform RNA extractions were performed as described in section 2.5.3. To determine success of the fractionation protocol, the integrity of the RNA and the quantity of RNA extracted, I used the Agilent 2100 Bioanalyzer system (Agilent, Santa Clara, USA) according to the manufacturer's instructions. RNA integrity could be confirmed by the presence of peaks produced by electrophoresis, representing 18S and 28S rRNA, with the software producing an RNA integrity number (RIN) based upon the relative abundance of these peaks. Demonstration of successful fractionation can be shown via the gel electrophoresis image, showing the presence of tRNA in the cytoplasmic fraction (at ~27 s), and not in the nuclear fraction. Finally, RNA concentration in the samples were determined via the software, by comparison to a ladder of known RNA concentration. An example report produced by the Agilent 2100 Bioanalyzer from a representative fractionation experiment is shown below (Figure 2-9).

Once RNA concentration was determined, RNA was used to synthesise cDNA and perform qPCR as described in section 2.4.3 and 2.4.4. Ct values were exported from the qPCR software and standard curve analysis used to calculate mRNA expression. cDNA expression was then made relative to housekeeping control (*GAPDH*). The resulting mRNA expression was then used to calculate relative cytoplasmic/nuclear ratio and normalised with DMSO-control set to 1. Statistical significance determined by paired T-test.

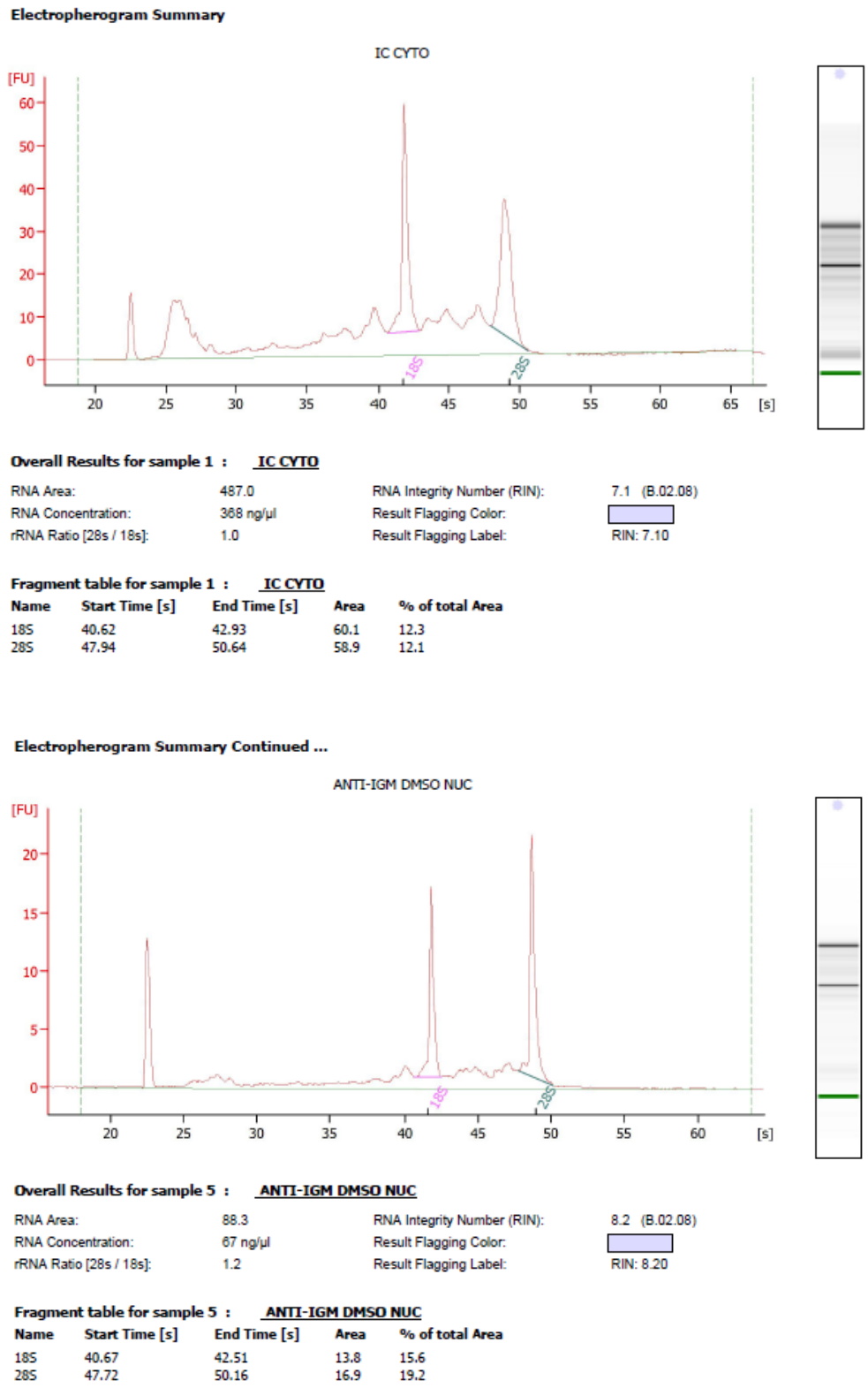

Figure 2-9. Determination of fractionation success, RNA integrity and RNA concentration using the Agilent 2100 Bioanalyzer

Read-outs from the Agilent 2100 Bioanalyzer shown. Top report shows electrophoresis of representative cytoplasmic RNA sample, with 28S, 18S and tRNA peaks. RIN number describes the integrity of the RNA, and electrophoresis peaks used against ladder of known RNA concentrations to determine RNA concentration. Bottom graph shows nuclear RNA sample with no significant presence of tRNA peak.

2.8 Adoptive transfer of Eμ-*TCL1* leukaemic cells into C57BL/6 mice

2.8.1 Materials

Table 14. Materials used and their ordering information

MATERIAL	ORDER INFORMATION
PBS pH 7.4	Severn Biotech, Kidderminster, UK , #20-74-05
BRILLIANT VIOLET 510™ ANTI-MOUSE CD45 ANTIBODY	Biolegend, London, UK #103138
FITC ANTI-MOUSE CD5 ANTIBODY	Biolegend, #100606
APC ANTI-MOUSE CD19 ANTIBODY	Biolegend, #152410
PE ANTI-MOUSE/HUMAN CD45R/B220 ANTIBODY	Biolegend, #103208
RED BLOOD CELL LYSIS SOLUTION	Bio-Rad Laboratories, California, USA, #BUF04C

2.8.1 *In vivo* manipulation

C57BL/6 mice were bred within the animal breeding facilities in house. Mice were then maintained in house and experiments were approved by local ethical committees and under the relevant licences (Home Office license PPL30/2964). Mice were inoculated with $1x10^7$ Eμ-*TCL1* leukaemic cells (Eμ-*TCL1* 020 (T1)) and blood monitored weekly for evidence of disease by flow cytometry. After 21 days, tumour was evident in the blood (at around 10% of total lymphocyte population) and mice were randomised for treatment of either 80 mg/kg ribavirin dissolved in PBS, or PBS as a vehicle control. There were 3 animals per arm. All animal handling and treatments were performed by Dr Mathew Carter, Dr Laura Karydis and animal handling technicians in the animal facilities of the Centre for Cancer Immunology, Southampton. Treatment was once daily by intraperitoneal injection.

2.8.2 End-point analysis

Weekly monitoring of tumour burden in the peripheral blood was performed, measuring total $CD5^+B220^+$ lymphocyte count by flow cytometry. After a further 21 days, all mice were euthanized and organs harvested, as they all met two out of the three humane end-point (HEP) criteria defined by the Home Office licence; $CD5^+B220^+$ B cells present over 80% of peripheral blood lymphocytes, spleen size greater than 30 mm (measured by palpation), total lymphocyte count over $5x10^7$ per ml blood.

Following harvesting, spleens were weighed and photographed to document relative size comparisons between treatment arm. The spleens were then disrupted to a single cell suspension using mechanical pressure, and washed in complete RPMI by centrifugation. Along with this, peripheral blood and the contents of the peritoneal cavity were harvested. $2x10^6$ cells from each anatomical site were transferred into a flow cytometry tube, and 86 µl FACS buffer added (Table 6). To this, 1 µl of each flow cytometry stain antibody was added (anti-mouse CD5 antibody, anti-mouse CD19, anti-mouse B220, anti-mouse CD45 (Table 14) and kept on ice in the dark for 30 minutes. Following this, 1 ml of 1X RBC lysis solution (Table 14) was added per tube. Tubes were then quickly vortexed and centrifuged at 1,520 g for five minutes. Supernatant was removed by flicking, then cells were resuspended in a further 1 ml of FACs buffer. Centrifugation step was then repeated and cells resuspended in 300 µl FACs buffer. Data were acquired using the BD FACSCanto and analysed using FlowJo® software. Live cells were first gated, followed by gating of the CD45 and B220 positive populations. Total cell number was calculated per tissue, before analysis, to calculate tumour burden per tissue. The presence of $CD5^+B220^+$ lymphocytes in each of these compartments were calculated by flow cytometry. CD5 is used as a marker of leukaemic cells in this model, and B220 is a pan B-cell marker in mice.

Chapter 3

The effects of eIF4A inhibitors on anti-IgM-induced mRNA translation and expression of MYC and MCL1 in CLL cells

3.1 Introduction

Silvestrol and rocaglamide are both naturally occurring flavagline compounds that act as eIF4A inhibitors. Rocaglamide was the first of this family to be discovered (King et al., 1982), and has since been shown to selectively inhibit the translation of mRNAs with complex 5' UTR that contain polypurine sequences by forcing an interaction between them and eIF4A, therefore blocking scanning of the 43S PIC (Iwasaki et al., 2016). As silvestrol also contains the characteristic cyclopenta[b] benzofuran group in its chemical structure, it is likely that this compound acts through a similar mechanism. Indeed, initial studies into its mechanism described dimerization between free-eIF4A and RNA in the presence of silvestrol (Bordeleau et al., 2008, Cencic et al., 2009) and more recent studies have demonstrated that silvestrol preferentially inhibits translation of mRNAs with more complex 5' UTRs (Wolfe et al., 2014, Rubio et al., 2014, Raza et al., 2015), potentially due to the requirement of high levels of eIF4A helicase activity for the translation of these mRNAs (Kogure et al., 2013, Wolfe et al., 2014).

In CLL cells, anti-IgM-induced mRNA translation is associated with induction of eIF4A and reduced expression of the natural eIF4A inhibitor, PDCD4 (Yeomans et al., 2015). By contrast, anti-IgM-induced mRNA translation in healthy donor B cells is not associated with changes in expression of eIF4A/PDCD4. These observations suggest a potential utility for eIF4A inhibitors to specifically block anti-IgM-induced translational responses in CLL cells compared to normal B cells. Potential eIF4A-dependent targets in CLL cells include *MYC* and *MCL1* which are induced following sIgM stimulation, and are mRNAs with complex 5' UTRs (Krysov et al., 2012, Petlickovski et al., 2005). MYC and MCL1 are important disease drivers which are linked to proliferation and cell survival, respectively. Therefore, the experiments in this chapter focused on characterising the effect of eIF4A inhibitors, silvestrol and rocaglamide, on the induction of global mRNA translation and the expression of MYC and MCL1 following sIgM stimulation in CLL cells. I also compared responses in CLL and healthy donor B cells to determine whether effects of eIF4Ai on translation were specific for CLL.

One previous study has investigated the effects of silvestrol in CLL samples (Lucas et al., 2009). This work demonstrated that relatively long-term (72 hours) exposure to silvestrol induced CLL cell apoptosis and reduced expression of MCL1 (Lucas et al., 2009). Although encouraging, a major drawback of this prior work is that experiments were performed in the absence of sIgM stimulation. Thus, it is not clear whether silvestrol will exert similar effects in stimulated cells, where levels of mRNA translation (and expression of MCL1 and MYC) are elevated, and where susceptibility to apoptosis is reduced. However, this study did demonstrate that silvestrol reduced leukaemic cell growth *in vivo* in the Eμ-*TCL1* model at well-tolerated doses (Lucas et al., 2009), providing strong support to the idea that eIF4A inhibition is an attractive potential therapeutic approach for CLL.

3.2 Hypothesis and aims

3.2.1 Hypothesis

The primary hypothesis addressed in this chapter was that eIF4A inhibitors (eIF4Ai) effectively reduce anti-IgM-induced mRNA translation, and the induction of MYC and MCL1 protein expression, in CLL samples. The secondary hypothesis was that inhibitory effects of eIF4Ai on anti-IgM-induced mRNA translation are specific for CLL cells compared to B cells from healthy donors.

3.2.2 Aims

The specific aims of this chapter were:

- Investigate the effect of eIF4Ai on global mRNA translation in CLL cells
- Determine the effects of eIF4Ai on anti-IgM-induced upstream signalling and regulation of translation initiation factor expression
- Investigate the effects of eIF4Ai on anti-IgM-induced MYC and MCL1 expression
- Determine the effects of eIF4Ai on CLL cell viability
- Characterise the effect of eIF4Ai on global mRNA translation in B cells from healthy donors

3.3 Results

3.3.1 The effect of eIF4Ai on global mRNA translation within the malignant CLL population

I used the OPP-incorporation assay to investigate the effects of eIF4Ai on basal and anti-IgM-induced global mRNA translation in CLL cells. This is a quantitative assay whereby flow cytometry is used to measure the incorporation of a synthetic puromycin analogue into the polypeptide chain during translation. By gating on cell sub-populations identified through staining for cell surface markers, it is possible to specifically quantify mRNA translation within the malignant cell population (Yeomans et al., 2015).

Previous comparison between soluble and bead-bound anti-IgM showed that bead-bound anti-IgM resulted in a stronger and more sustained signalling response (Krysov et al., 2012) and a greater induction of mRNA translation compared to soluble anti-IgM (Yeomans et al., 2015). Thus, bead-bound anti-IgM was used for stimulation of sIgM in this experiment and throughout the project. It has also been shown that sIgM signalling non-responders (defined by the ability of soluble anti-IgM to induce intracellular Ca^{2+} mobilisation in less than 5% of malignant cells (Mockridge et al., 2007)) do not show a substantial increase in MYC expression (Krysov et al., 2012) or mRNA translation following anti-IgM treatment (Yeomans et al., 2015), so all studies were performed using samples that were all considered anti-IgM responsive (Table 5). This included both signal responsive M-CLL and U-CLL samples. Finally, experiments of duration exceeding and including 24-hours were performed in the presence of Q-VD-OPh, a pan-caspase inhibitor, to minimise potentially confounding effects of spontaneous cell death in culture. However, Q-VD-OPh was not used in experiments which set out to determine the effect of anti-IgM or inhibitors directly on cell death. Finally, CpG-ODN treatment was used as a comparator for anti-IgM in some experiments.

To investigate the effects of rocaglamide on anti-IgM-induced mRNA translation, cells were pre-treated with rocaglamide for one hour and then stimulated with anti-IgM for an additional 24 hours. The time period for anti-IgM stimulation was based on the study of Yeomans et al, which demonstrated that anti-IgM resulted in robust induction of mRNA translation at this point (Yeomans et al., 2015). Experiments were also performed in the presence of control antibody coated beads (dynabeads coated with goat $F(ab')_2$ IgG) to investigate the effects of rocaglamide on basal mRNA translation in unstimulated cells. Rocaglamide was used at 10 or 20 nM. These concentrations were selected as they have been shown to be effective in other studies (Callahan et al., 2014). DMSO was used as a solvent control. Raw histogram example of OPP experiment with rocaglamide can be found in Appendix A.

In experiments measuring basal mRNA translation, results for the control antibody/DMSO-treated sample was set relative to 1. This allows for clearer evaluation of the effect of rocaglamide on basal translation. In contrast, in experiments measuring anti-IgM-induced mRNA translation, results for the anti-IgM/DMSO-treated sample were set to 100. This allows for easier analysis of the induction of mRNA translation, and any potential inhibition by rocaglamide.

As demonstrated previously (Yeomans et al., 2015), anti-IgM (and CpG-ODN) significantly increased OPP-incorporation (by ~4-fold) in $CD5^{+}CD19^{+}$ CLL cells (Figure 3-1). Anti-IgM-induced OPP-incorporation was significantly reduced by rocaglamide at both concentrations tested, although 20 nM rocaglamide inhibited translation to a greater extent (Figure 3-1B). Rocaglamide modestly reduced the low levels of basal mRNA translation seen in unstimulated CLL cells, but these differences did not reach statistical significance (Figure 3-1A). Therefore, the eIF4A inhibitor rocaglamide inhibited anti-IgM-induced mRNA translation in CLL cells.

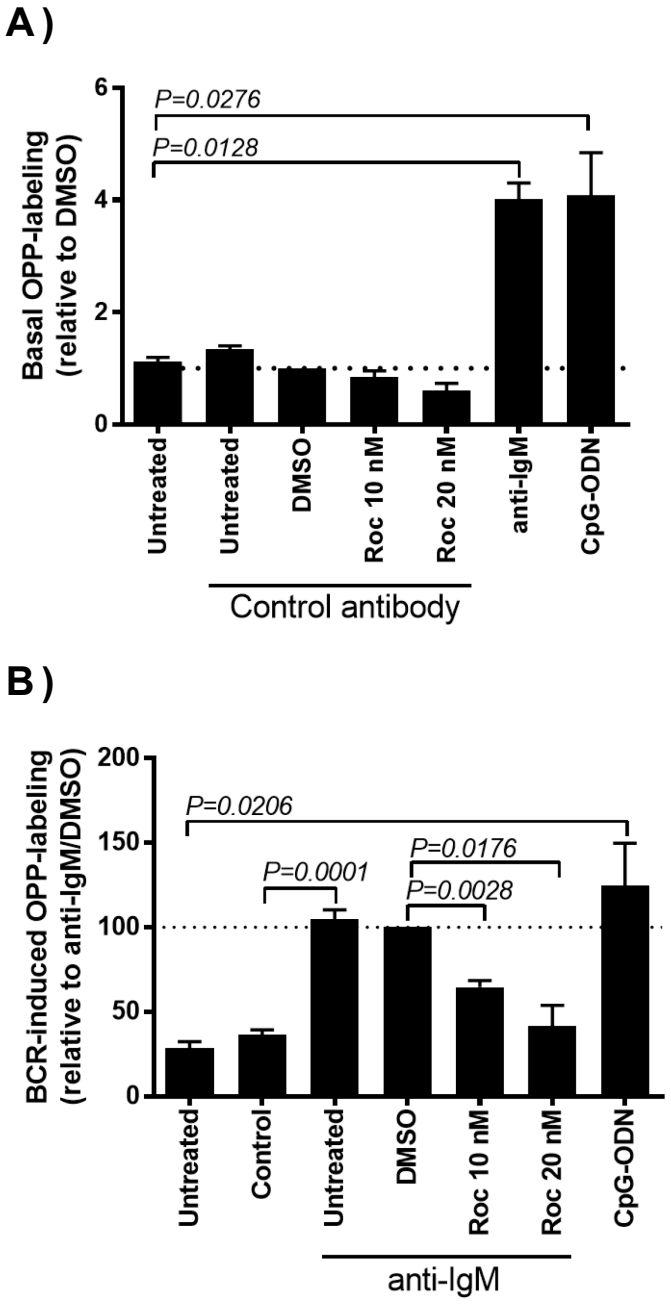

Figure 3-1. Inhibition of basal and anti-IgM-induced mRNA translation in CLL cells by rocaglamide

CLL samples (n=4) were pre-treated with rocaglamide (Roc) or DMSO as a control, or left untreated for one hour. Cells were then treated with control antibody, anti-IgM or CpG-ODN as indicated, for a further 24 hours. Values for control antibody/DMSO-treated cells were set to 1 (A) and values for anti-IgM/DMSO-treated cells were set to 100 (B). Error bars show SEM and any statistical significance indicated was determined between conditions using paired t tests.

Parallel analysis of the effects of silvestrol on OPP-labelling was performed by Dr Alison Yeomans and are shown here for comparison (Figure 3-2). Silvestrol was tested at the same concentrations (10 and 20 nM), which is also in-line with concentrations used in previously published studies (Lucas et al., 2009).

Similar to rocaglamide, silvestrol significantly inhibited anti-IgM-induced OPP-labelling at both concentrations tested (Figure 3-2B). Basal OPP-labelling was perhaps reduced at 20 nM silvestrol, but the differences between silvestrol and DMSO treated cells was not statistically significant (Figure 3-2A). The overall potency of the rocaglamide and silvestrol for inhibition of anti-IgM-induced translation appeared to be very similar. Therefore, silvestrol and rocaglamide have similar inhibitory effects on anti-IgM-induced RNA translation in CLL cells.

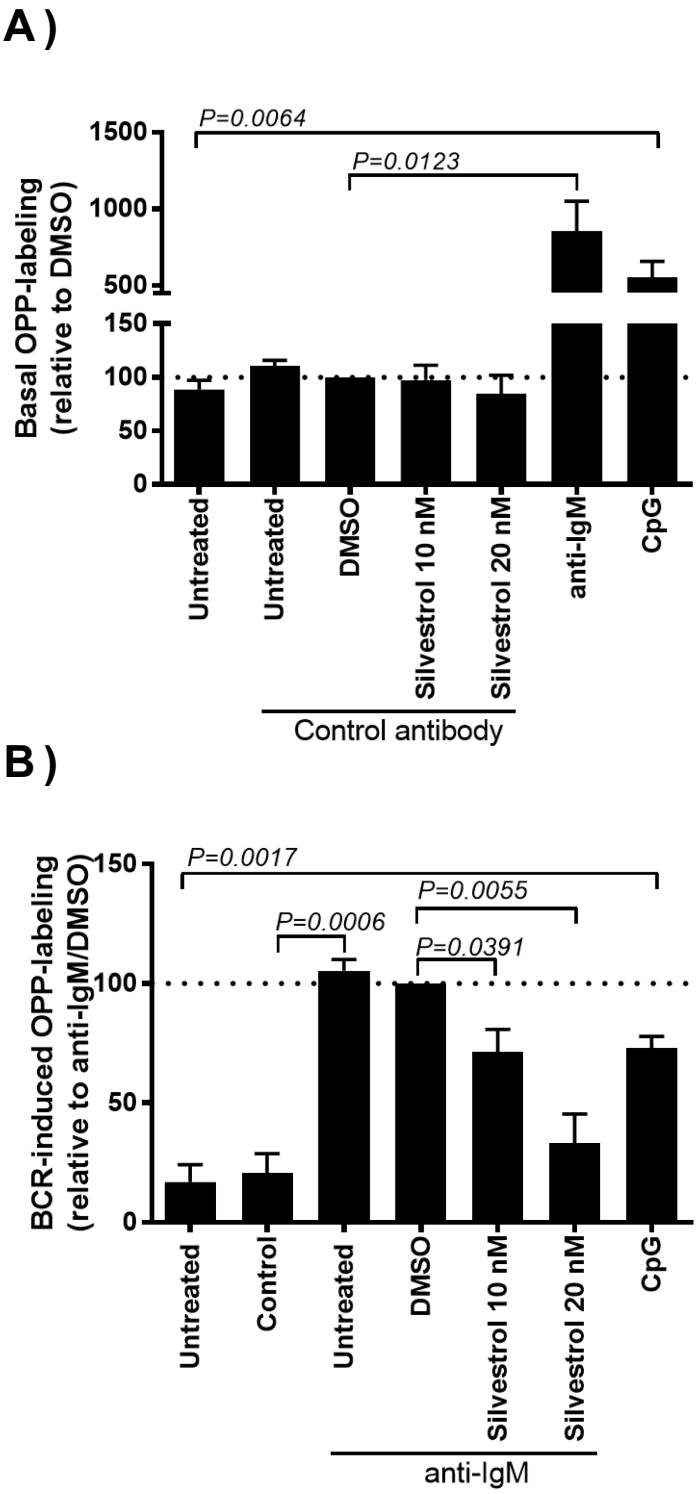

Figure 3-2. Inhibition of basal and anti-IgM-induced mRNA translation in CLL cells by silvestrol

CLL samples (n=6) were pre-treated with silvestrol, DMSO as a control, or left untreated for one hour. Cells were then treated with control antibody, anti-IgM or CpG-ODN as indicated, for a further 24 hours. Values for control antibody/DMSO-treated cells were set to 1 (A) or anti-IgM/DMSO treated cells set to 100 (B). Error bars show SEM and the statistical significance of the indicated differences was determined using paired t tests. Data supplied by Dr Alison Yeomans and shown to allow comparison to Figure 3-1.

3.3.2 The effects of silvestrol on mRNA translation – polysome profiling

I next investigated the ability of eIF4Ai to inhibit anti-IgM-induced polysome-associated mRNA translation in CLL cells using polysome profiling assays. The principles behind this technique are described in section 2.5. These experiments were performed using silvestrol only, due to the large cell numbers required for these experiments.

Figure 3-3 and Figure 3-4 show polysome profiles derived from a representative CLL sample (M-523D). To allow for easier comparison, the polysome profiles from this sample were overlaid (Figure 3-4) to show any changes in the profiles between treatments. The results for the other samples studied (5 in total) are shown in Appendix A.

Overall, the levels of global translation of the untreated and control samples was very low, indicated by the abundant 80S peak and sparse polysomes. There was a clear increase in mRNA translation (polysome abundance) in cells following treatment with anti-IgM which is most apparent in the overlays (Figure 3-4A). The response to anti-IgM was reduced by silvestrol (Figure 3-4B). In sample M-523D, this was evident as a reduction in size of the polysome peaks and a left-shift of the polysome peaks. There was a slight shift after DMSO treatment. However, this was very modest and is likely due to experimental variation. Thus, consistent with the OPP-labelling analysis, the eIF4Ai silvestrol inhibits global anti-IgM-induced mRNA translation in CLL samples.

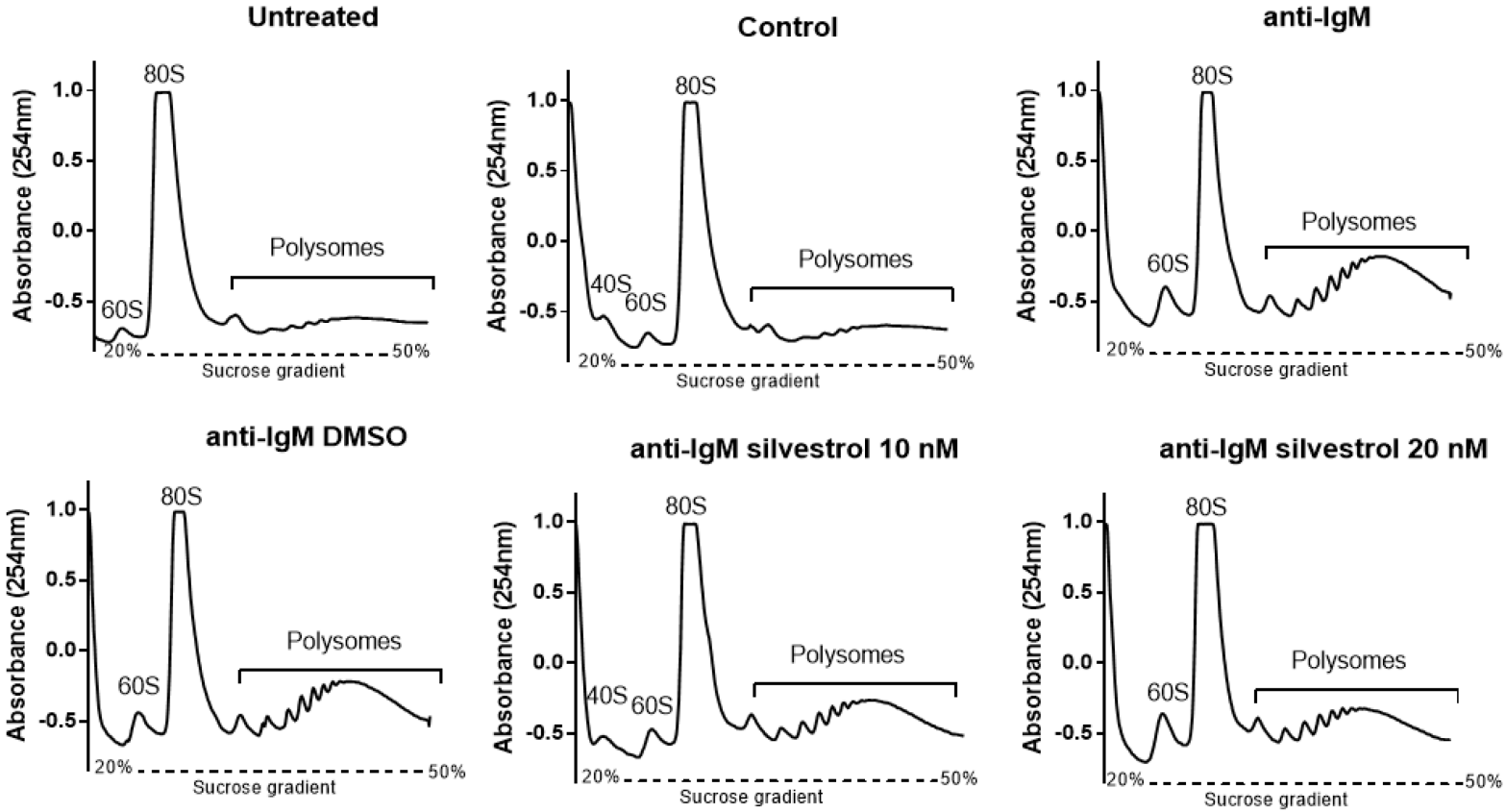

Figure 3-3. Polysome profiling following anti-IgM and silvestrol treatment (10 and 20 nM)

CLL cells were pre-treated with silvestrol (10 or 20 nM), DMSO or left untreated for one hour. Cells were then incubated with control antibody or anti-IgM for 24 hours as indicated. Polysome lysate samples were then collected and analysed by polysome profiling, as described in sections 2.5.1 and 2.5.2. Representative polysome profile of M-523D shown. Polysome profiles obtained for other samples can be found in the appendix.

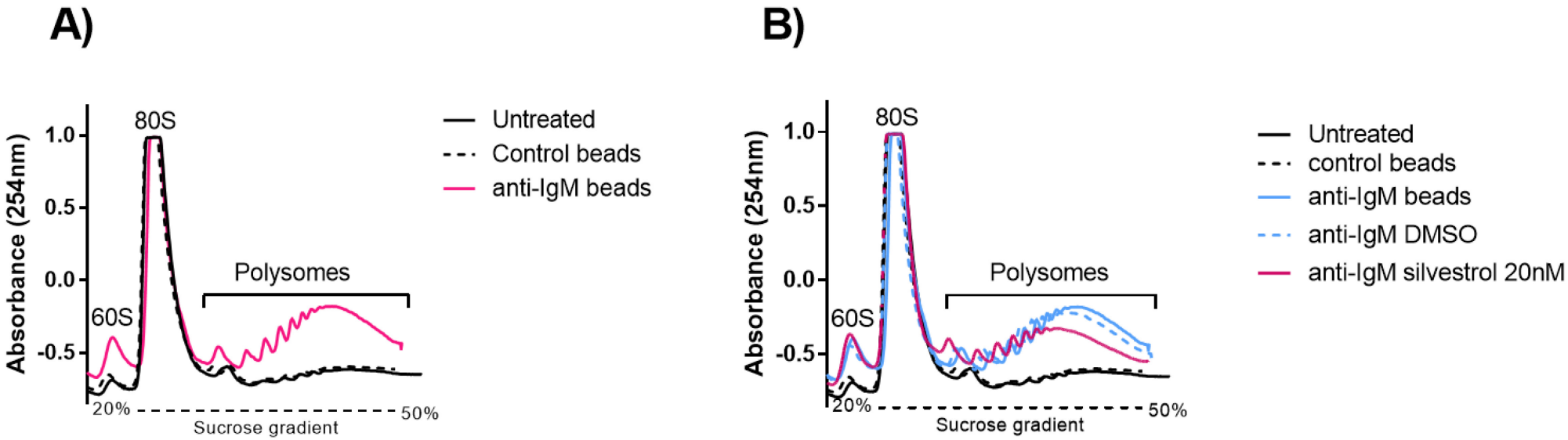

Figure 3-4. Overlaid polysome profiles of M-523D following anti-IgM and silvestrol treatment (20 nM)

Polysome profiles from Figure 3-3 were overlaid to allow for comparison, and aligned based upon the 80S peak. A) An overlay of untreated, control treated and anti-IgM treated polysome profiles. B) An overlay of anti-IgM, anti-IgM DMSO and anti-IgM silvestrol 20 nM treated sample polysome profiles. Anti-IgM silvestrol 10 nM profile excluded from overlays for simplicity.

3.3.3 The effects of eIF4Ai on anti-IgM-induced ERK phosphorylation

It was important to determine whether the effects of eIF4Ai on global mRNA translation were a direct consequence of translational inhibition or were mediated by reduced sIgM function. For example, eIF4Ai-mediated translational inhibition might reduce expression of sIgM or key signalling intermediates. To investigate this, the effects of eIF4Ai on ERK phosphorylation were analysed. ERK phosphorylation which is strongly activated following sIgM stimulation of CLL cells, and acts as a sensitive readout for signalling (Krysov et al., 2012). Moreover, studies have shown that sustained ERK pathway activity, following BCR stimulation, is required for optimal induction of MYC expression and mRNA translation (Krysov et al., 2012, Yeomans et al., 2015). Although ERK phosphorylation is induced rapidly following BCR stimulation, more sustained ERK activation is required for signal propagation downstream of the BCR (Murphy et al., 2004). Thus, analysis of ERK-phosphorylation was performed at a relatively late time-point (24 hours).

For this experiment, CLL cells were pre-treated with silvestrol or rocaglamide for one hour, then stimulated with anti-IgM for an additional 24 hours, before cells were collected and proteins extracted for immunoblotting. Blots were probed with antibodies specific for ERK, phosphorylated-ERK and HSC70. There was a significant induction in the phosphorylation of ERK following sIgM-stimulation at this time-point (Figure 3-5). However, this induction was unaffected by either compound (Figure 3-5). Interestingly, there is a reduction in expression of total ERK, visible in the immunoblot but not represented in the densitometries. This reduction of total ERK correlates with the reduction of phosphorylated-ERK, thus overall ERK-phosphorylation is not reduced. Further studies will be needed to understand the reduction of total ERK with rocaglamide or silvestrol treatment (Figure 3-5). Thus, inhibition of anti-IgM-induced translation by eIF4Ai is not a consequence of inhibition of upstream signalling.

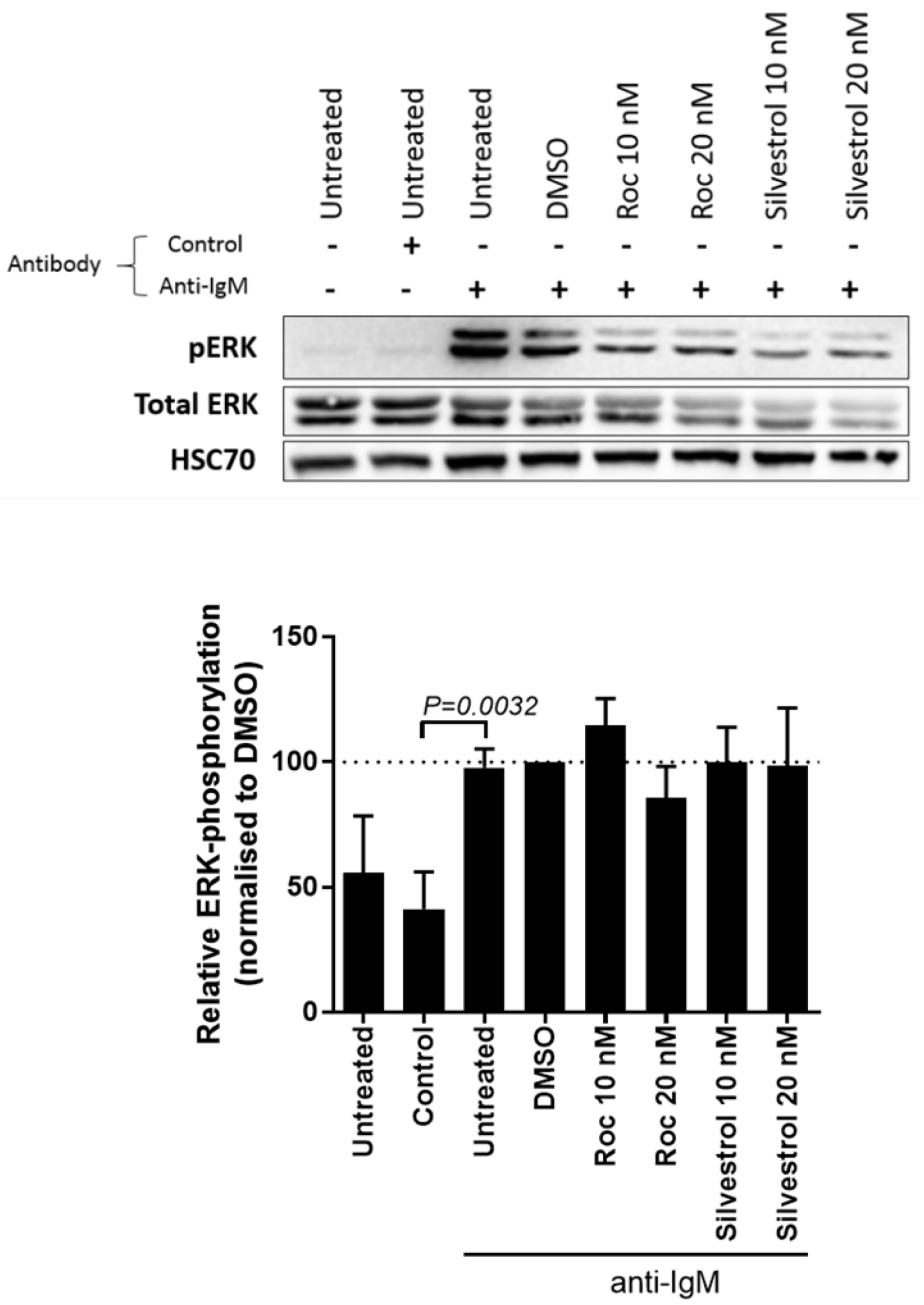

Figure 3-5. ERK-phosphorylation following anti-IgM and eIF4Ai treatment

CLL samples (n=6) were pre-incubated with silvestrol or rocaglamide for one hour, before treatment with anti-IgM or control antibody for an additional 24 hours. Immunoblotting was undertaken and blots probed for ERK, phosphorylated ERK and HSC70 as a loading control. Western blot of representative sample M-281D (top panel). ERK-phosphorylation with values for anti-IgM/DMSO treated cells set to 100 (bottom panel). Error bars show SEM and the statistical significance of the indicated differences was determined using paired t tests.

3.3.4 The effect of eIF4Ai on translation initiation factor expression

Previous studies have demonstrated that anti-IgM induces eIF4A and eIF4G expression in CLL cells, and reduces expression of PDCD4 (Yeomans et al., 2015). It was therefore necessary to investigate the effects of eIF4Ai on the expression of these factors. CLL samples were pre-treated with silvestrol or rocaglamide for one hour and then treated for 24 hours with anti-IgM as in the previous study (Yeomans et al., 2015). Cells were collected and eIF4A, PDCD4, eIF4G and eIF4E expression was analysed by western blot (Figure 3-6).

Following sIgM stimulation, there was a significant induction of eIF4A expression (Figure 3-6A), confirming previous studies (Yeomans et al., 2015). The induction of eIF4A expression was significantly reduced by eIF4Ai (Figure 3-6A). At the highest concentration tested (20 nM), both drugs essentially returned eIF4A expression to the same as detected in control treated cells. At the lower concentration (10 nM), the effects of silvestrol were partial, whereas the response to rocaglamide was similar to that of the high concentration (Figure 3-6A). Therefore, silvestrol and rocaglamide counteracted the induction of eIF4A in anti-IgM-treated cells.

In contrast to eIF4A, eIF4Ai did not reverse down-modulation of PDCD4 in anti-IgM-treated cells (Figure 3-6B). In fact, at 20 nM, the compounds appeared to further reduce PDCD4 expression in anti-IgM treated cells, although differences in PDCD4 expression between anti-IgM/DMSO and anti-IgM/eIF4Ai treated cells were not statistically significant (Figure 3-6B).

Anti-IgM treatment did not alter eIF4E expression (Figure 3-6C). There was a modest and weakly statistically significant reduction in eIF4E expression in cells treated with 20 nM rocaglamide, but overall, eIF4E expression was relatively unaffected by anti-IgM or eIF4Ai (Figure 3-6C).

eIF4G expression was induced upon sIgM engagement (Figure 3-6D) and this was reversed in cells treated with eIF4Ai, especially at the higher concentration tested. However, overall changes in eIF4G were rather modest (~40% increase with anti-IgM compared to ~60% increase for eIF4A) and none of the differences in eIF4G expression were statistically significant (Figure 3-6D).

Overall, these experiments confirm that eIF4A, PDCD4 and eIF4G (but not eIF4E) are regulated following sIgM stimulation. Moreover, both eIF4Ai strongly interfere with the ability of anti-IgM to induce eIF4A expression.

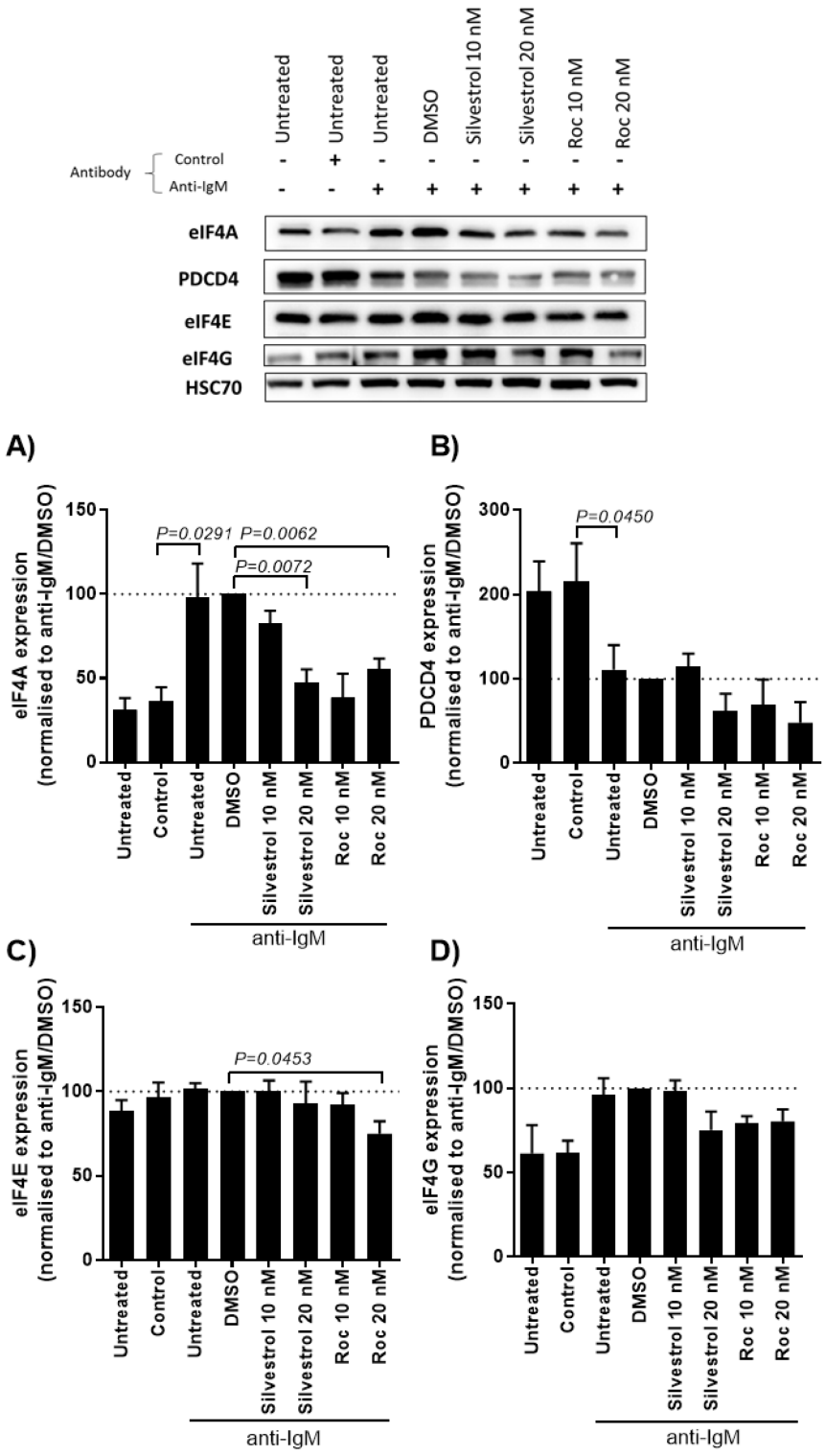

Figure 3-6. Expression of eIF4A, PDCD4, eIF4E and eIF4G following anti-IgM and eIF4Ai treatment

CLL samples (n=3) were pre-incubated with silvestrol or rocaglamide for one hour, before stimulation with anti-IgM or control antibody for an additional 24 hours. Immunoblotting was undertaken and blots probed for eIF4A, PDCD4, eIF4E, eIF4G and HSC70 as a loading control (top panel, representative sample M-281D). Relative densitometries of eIF4A (A), PDCD4 (B), eIF4E (C) and eIF4G (D) protein expression calculated following immunoblotting. Values for anti-IgM/DMSO treated cells set to 100. Error bars show SEM and the statistical significance of the indicated differences was determined using paired T tests.

3.3.5 Inhibition of anti-IgM-induced MYC and MCL1 protein expression by eIF4Ai

Having demonstrated inhibition of anti-IgM-induced global mRNA translation by both silvestrol and rocaglamide, in the absence of effects on upstream ERK phosphorylation, it was next necessary to analyse the effects of eIF4Ai on the expression of key BCR target proteins that play an important role in CLL disease pathogenesis/progression. I focused on MYC and MCL1, which are known to be strongly induced following BCR stimulation in CLL cells (Petlickovski et al., 2005, Krysov et al., 2012).

MYC is a transcription factor which regulates cell proliferation and promotes cell cycle progression (Amati et al., 2001). MYC expression is tightly regulated by mRNA translation and degradation (Wisdom and Lee, 1991). This is largely due to the highly structured 5' UTR of *MYC* mRNA, thus meaning its translation is highly-dependent upon cap-dependent initiation by eIF4F complex family members (De Benedetti and Graff, 2004, Rubio et al., 2014). MYC has been shown to be highly expressed within some cells in the PC of CLL lymph nodes, which are suggested to be sites of antigen-induced proliferation in CLL (Krysov et al., 2012). Key studies have shown that stimulation of sIgM in CLL samples induces *MYC* mRNA expression and its translation (Krysov et al., 2012, Yeomans et al., 2015). Whilst *MYC* translation is reliant in part upon cap-dependent initiation, there is also an IRES in the 5' UTR of *MYC*, although studies have shown IRES-dependent translation of *MYC* also requires eIF4G and eIF4A in part for initiation (Spriggs et al., 2009).

MCL1 is an anti-apoptotic member of the BCL-2 family of proteins, which also has a complex 5' UTR in its mRNA (Wendel et al., 2007), thus implying its translation is dependent upon eIF4A. MCL1 is thought to be responsible in part for fludarabine-resistance in some CLL cases (Johnston et al., 2004) and its expression correlates with poor outcome (Pepper et al., 2008). Silvestrol has been shown to inhibit MCL1 expression in CLL previously, although this study was not performed in the presence of sIgM stimulation (Lucas et al., 2009).

3.3.5.1 The effects of eIF4Ai on anti-IgM-induced MYC protein expression

CLL cells were pre-treated with silvestrol or rocaglamide for one hour followed by six hour treatment with anti-IgM. This time-point was chosen as previous studies have shown that following six hour stimulation of sIgM there is a clear increase in MYC expression in the majority of signal-competent CLL samples (Krysov et al., 2012). After stimulation of sIgM there was a strong induction of MYC protein expression which was significantly inhibited at 20 nM by silvestrol and rocaglamide (Figure 3-7).

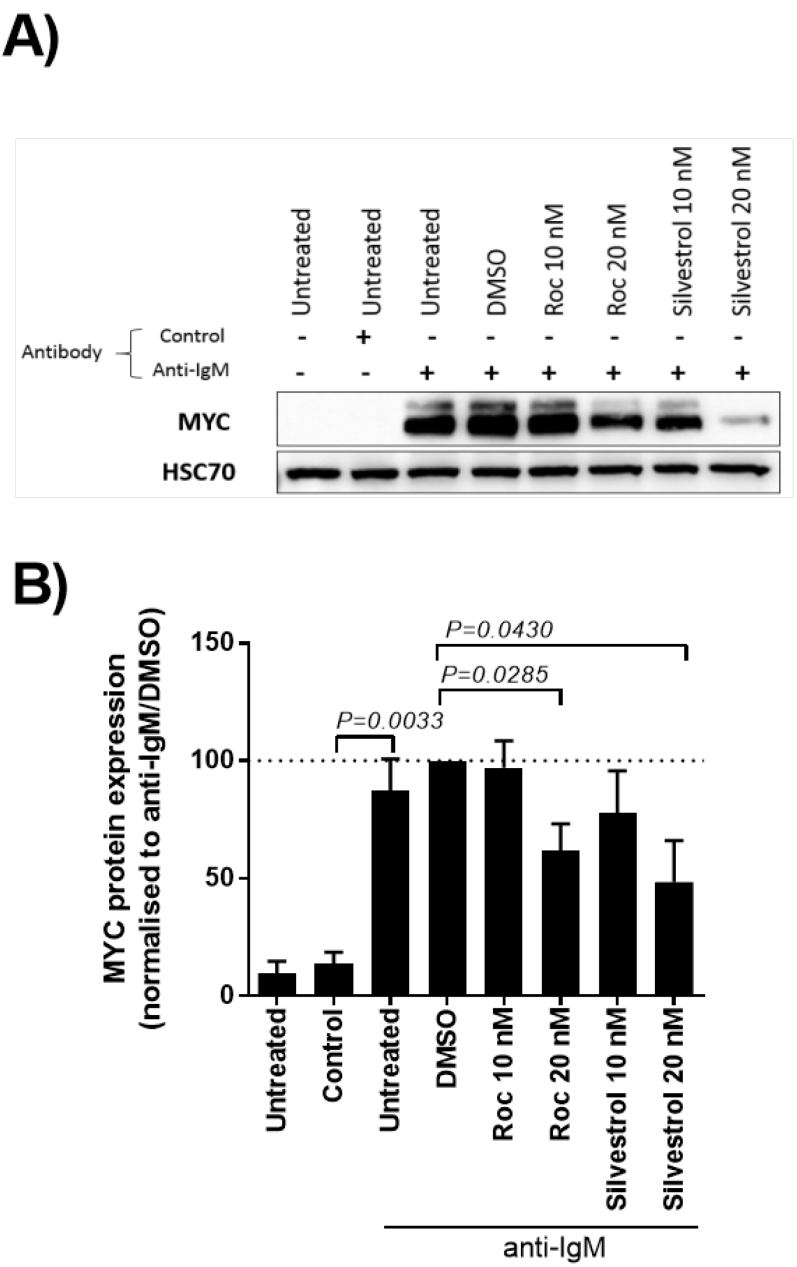

Figure 3-7. MYC expression following anti-IgM and eIF4Ai treatment

CLL samples (n=5) were pre-treated with rocaglamide or silvestrol for one hour. Samples were then stimulated with control antibody or anti-IgM for an additional six hours. After collection, cells were lysed and proteins extracted then immunoblotting was undertaken and blots probed for MYC and HSC70 as a loading control. Representative western blot shown of sample M-604G (A). Relative densitometries of MYC protein expression calculated following immunoblotting with values for anti-IgM/DMSO treated cells set to 100 (B). Error bars show SEM and the statistical significance of the indicated differences was determined using paired T test.

3.3.5.2 The effects of eIF4Ai on anti-IgM-induced MCL1 protein expression

Next, it was important to investigate the effects of anti-IgM and eIF4Ai treatment on MCL1 protein expression. 24 hour anti-IgM treatment was chosen to measure MCL1 expression as changes following sIgM engagement are best seen at this time (Petlickovski et al., 2005).

After 24 hour sIgM engagement there was a strong (~4-fold) and significant induction of MCL1 expression (Figure 3-8). This anti-IgM-induced MCL1 expression was significantly reduced by silvestrol (20 nM, Figure 3-8). However, inhibitory effects by rocaglamide were less clear than those obtained with silvestrol and did not reach statistical significance (Figure 3-8). Overall, induction of MYC expression appeared to be somewhat more effectively inhibited by eIF4Ai compared to MCL1. These data demonstrate that eIF4Ai prevent induction of both pro-growth (MYC) and pro-survival (MCL1) effectors in CLL cells following stimulation of sIgM, without substantial effects on upstream signalling (ERK1/2 phosphorylation).

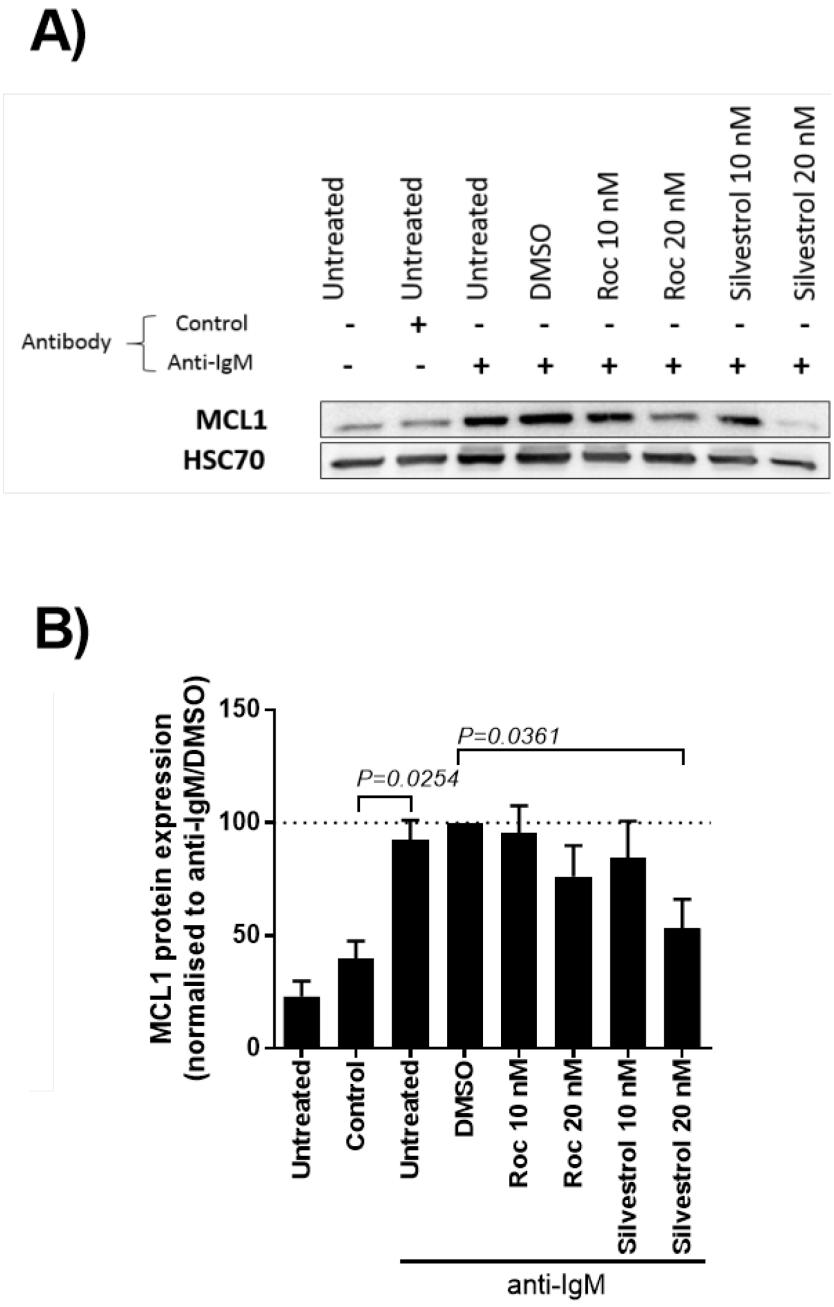

Figure 3-8. MCL1 protein expression following anti-IgM and eIF4Ai treatment

CLL samples (n=6) were pre-treated with rocaglamide or silvestrol for one hour. Samples were then stimulated with control antibody or anti-IgM for an additional six hours. After collection, cells were lysed and proteins extracted then immunoblotting was undertaken and blots probed for MCL1 and HSC70 as a loading control. Representative western blot shown of sample M-525B (A). Relative densitometries of MCL1 protein expression calculated following immunoblotting with values for anti-IgM/DMSO treated cells set to 100 (B). Error bars show SEM and the statistical significance of the indicated differences was determined using paired T tests.

3.3.6 Comparison of *MYC* and *MCL1* 5' UTRs

Although the *MYC* and *MCL1* mRNAs are both considered to have complex 5' UTRs it was interesting to note that induction of MYC protein expression appeared to be somewhat more effectively inhibited by eIF4Ai compared to MCL1 (Figure 3-7, Figure 3-8). Therefore, bioinformatical analysis of the 5' UTRs of *MYC* and *MCL1* mRNAs was performed to identify any potential features that might account for these differences (Table 15), as described in section 2.6. Features analysed included the presence of a stable secondary structure and G-quadruplexes, both of which have been linked to increased dependency on eIF4A for translation (Wolfe et al., 2014). I also analysed the presence of polypurine tracts which have been shown to confirm susceptibility of individual mRNA for inhibition of translation by rocaglamide (Iwasaki et al., 2016). RNA helicases such as eIF4A make contact with sequences up to 6 nucleotides long/6mers (Linder and Jankowsky, 2011), therefore to identify polypurine tracts, I calculated the total number of polypurine 6mers, which are enriched for inhibition by rocaglamide (Iwasaki et al., 2016).

Overall, compared to *MCL1*, the *MYC* RNA 5' UTR was longer, had more polypurine tracts and was predicted to form more stable secondary structures (Table 15). The *MCL1* RNA 5' UTR was also predicted to lack G-quadruplexes, although this analysis correctly predicted the presence of a known, functional G-quadruplex sequence in the *MYC* RNA 5' UTR (Siddiqui-Jain et al., 2002). Therefore, increased complexity of the *MYC* RNA 5' UTR compared to the *MCL1* RNA 5' UTR might account for differences in the extent to which expression of MYC and MCL1 are inhibited by eIF4Ai in anti-IgM-treated cells (Figure 3-7, Figure 3-8).

Table 15. Features of the 5' UTRs of *MYC* and *MCL1* RNAs

	MYC	***MCL1***
LENGTH (BP)	1160	208
NUMBER OF POLYPURINE TRACTS (6MERS)	72	10
NUMBER OF PREDICTED QUADRUPLEXES	1	0
FREE ENERGY OF MOST STABLE PREDICTED STRUCTURE (KCAL/MOL)	-465	-72

Data calculated as described in section 2.6.

3.3.7 The effect of silvestrol and rocaglamide on CLL cell viability

Since eIF4Ai reduced MCL1 protein expression, it was important to investigate the effect of these inhibitors on CLL cell apoptosis. A previous study of silvestrol demonstrated induction of apoptosis following 72-hours exposure in CLL cells with an IC_{50} of ~10 nM (Lucas et al., 2009). However, it is not known whether eIF4Ai induces CLL apoptosis at earlier time points. Moreover, immobilized anti-IgM has been shown to modestly increase the viability of CLL cells *in vitro* (Petlickovski et al., 2005) and the effects of eIF4Ai on apoptosis in anti-IgM stimulated CLL cells has not been examined previously. To address these questions, the effects of eIF4Ai on CLL cell viability were measured in either the absence or presence of anti-IgM. Analysis was performed at 24 hours to match the OPP-labelling experiments, but in the absence of Q-VD-OPh.

Annexin V/PI staining demonstrated that neither eIF4Ai induced apoptosis in CLL samples when tested alone at 10 nM (Figure 3-9). At 20 nM, both compounds did modestly reduce cell viability (~10%), but these differences were not statistically significant.

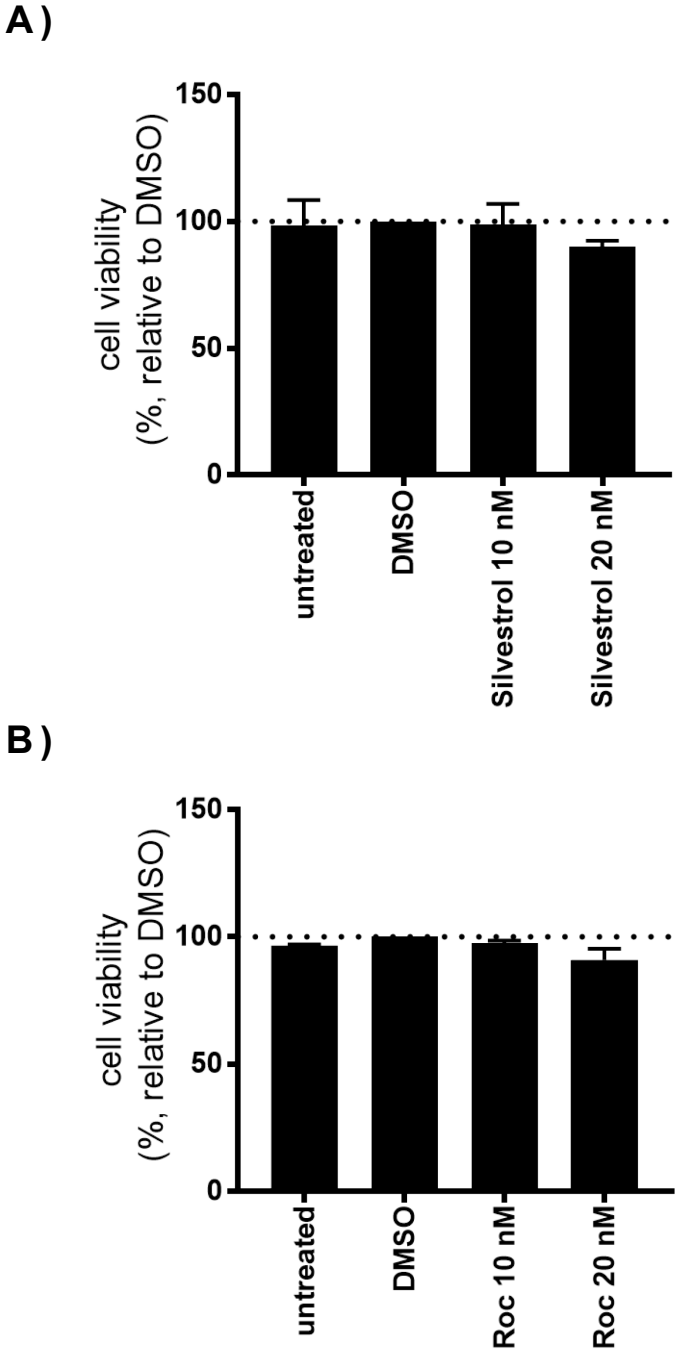

Figure 3-9. The effects of silvestrol and rocaglamide on CLL cell viability

CLL samples (n=3) were treated with silvestrol (A), rocaglamide (B), DMSO or left untreated for 24 hours. Cells were collected and cell survival was analysed via Annexin V-PI flow cytometry in the $CD5^+$ $CD19^+$ cell population. Data shown is relative cell viability with values for DMSO treated cells set to 100. Error bars show SEM and any statistical significance of the indicated differences was determined using paired T tests.

For analysis of effects of eIF4Ai in the presence of anti-IgM, CLL samples were pre-incubated with silvestrol or rocaglamide for one hour, before treatment with anti-IgM or control antibody for 24 hours. Proteins were extracted and used in western blotting for poly (ADP-ribose) polymerase (PARP) cleavage, which is indicative of caspase activation. The effect of anti-IgM on apoptosis *in vitro* following eIF4Ai exposure was not performed with Annexin V/PI flow cytometry due to the auto-fluorescence of dynabeads, as previously described (Coelho et al., 2013).

In control antibody treated cells, there was some evidence of PARP cleavage, indicating spontaneous caspase activation (Figure 3-10). Anti-IgM reduced any spontaneous PARP cleavage, consistent with protection from spontaneous cell death (Petlickovski et al., 2005). eIF4Ai co-treatment with anti-IgM induced modest amounts of PARP cleavage relative to anti-IgM-only treated cells (Figure 3-10). These differences did not reach significance in rocaglamide/anti-IgM treated cells, but did reach significance in silvestrol/anti-IgM treated cells (Figure 3-10). Thus, although eIF4Ai do not promote apoptosis alone, they may be capable of reversing the survival-promoting effects of anti-IgM. However, the ability of anti-IgM to suppress the spontaneous apoptosis of CLL cells was modest and it was hard to draw firm conclusions from these experiments, due to considerable sample-to-sample variation in the extent of spontaneous apoptosis and protection by anti-IgM.

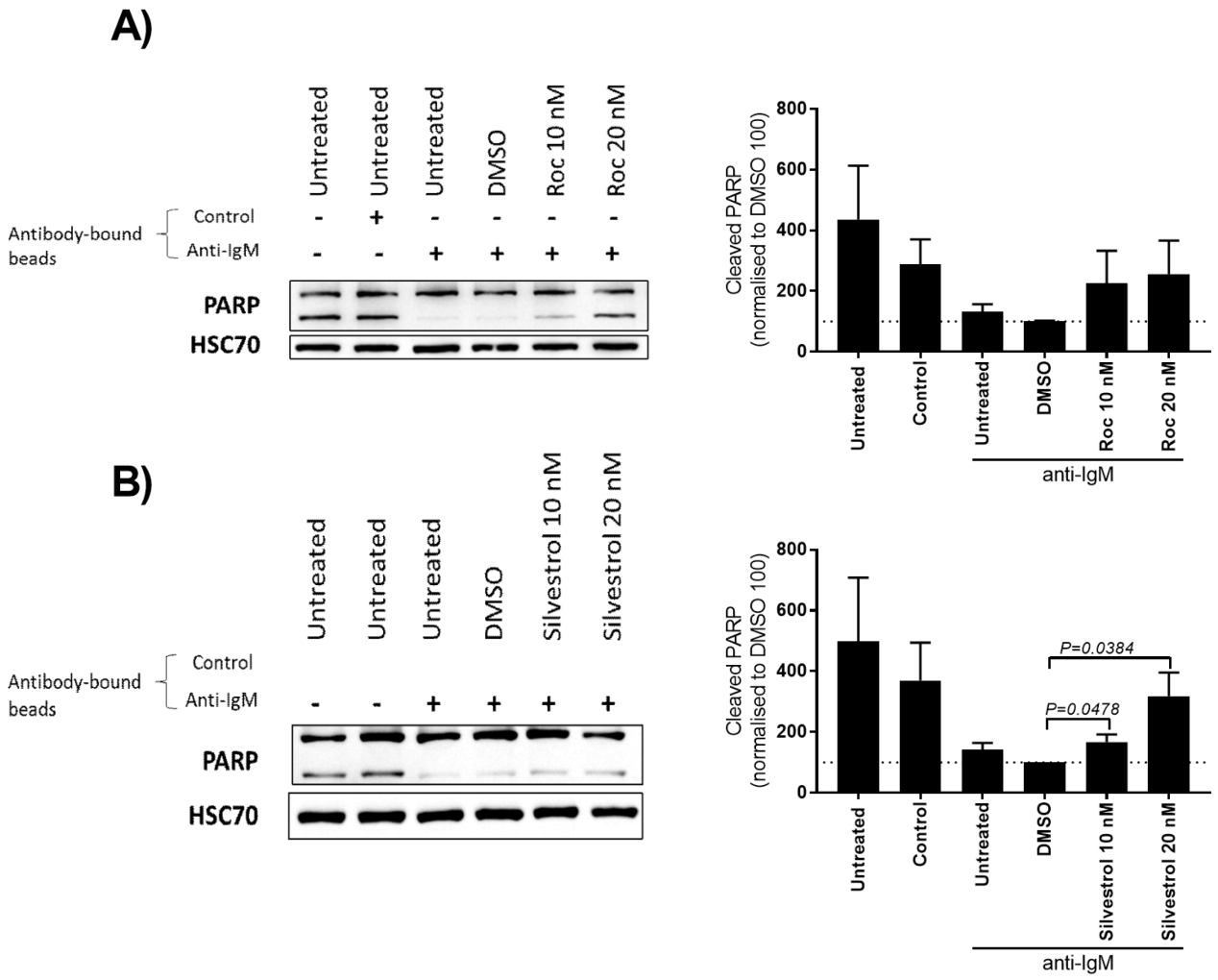

Figure 3-10. PARP cleavage following sIgM stimulation and silvestrol or rocaglamide treatment

CLL samples (n=6) were pre-treated for one hour with rocaglamide, silvestrol or DMSO, and incubated for an additional 24 hours with control antibody or anti-IgM. Cells were lysed and proteins extracted then immunoblotting was undertaken and blots probed for PARP, and HSC70 as a loading control. Representative western blot of sample M-621B (A) and U-780B (B) shown. Densitometries were measured and cleaved PARP calculated as a measure of cleaved PARP (lower band) relative to total PARP (upper and lower band). Data was made relative to values for anti-IgM/DMSO treated cells set to 100. Error bars show SEM and the statistical significance of the indicated differences was determined using paired T tests.

3.3.8 The effect of silvestrol on mRNA translation in healthy donor B cells

The final experiments of this chapter investigated the effects of eIF4Ai on basal and anti-IgM-induced mRNA translation in B cells from healthy donors using the OPP-incorporation assay. Due to limitations in the availability of cells, this study was performed using only silvestrol. Antibodies were included in the FACs analysis that enabled the specific measurement of OPP incorporation in the $CD19^+$ $CD5^-$ B cell population. IgG^+ cells were excluded so the bulk of the analysed cells represented IgM^+ naïve or non-switched memory B cells. These experiments were performed in collaboration with Dr Karly-Rai Rogers-Broadway.

Silvestrol (10 nM) caused a small but statistically significant reduction in OPP-incorporation in unstimulated cells (treated with control antibody) (Figure 3-11A). As expected, anti-IgM strongly increased OPP-incorporation (by ~4-fold) (Figure 3-11B). Similar to CLL cells, silvestrol significantly reduced OPP-incorporation in anti-IgM treated samples at both concentrations (Figure 3-11B). Thus, despite selective regulation of eIF4A/PDCD4 in CLL cells following anti-IgM stimulation (Yeomans et al., 2015), both CLL and normal B cells are dependent on eIF4A function for optimal induction of global mRNA translation.

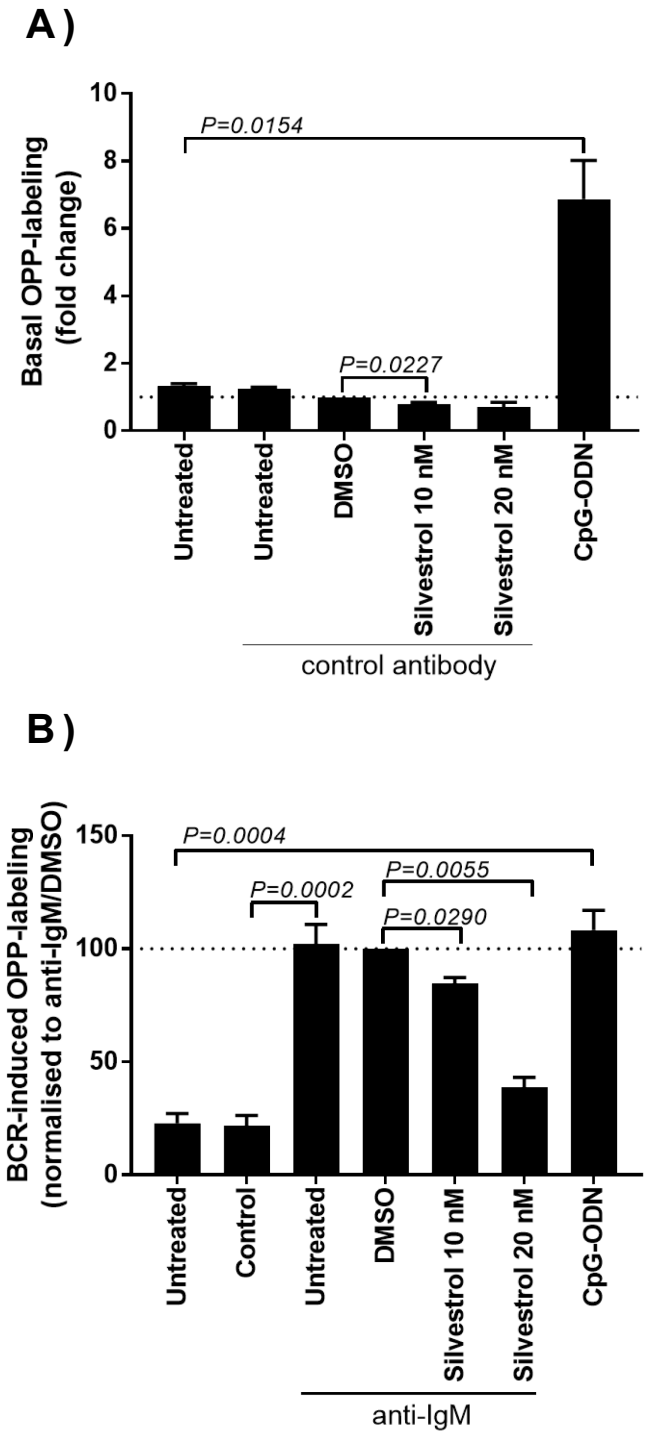

Figure 3-11. Silvestrol on basal and anti-IgM-induced OPP labelling in healthy donor B cells.

PBMCs from healthy donors (n=6) were pre-treated with silvestrol or DMSO for one hour before treatment with control antibody or anti-IgM for 24 hours. CpG-ODN was used as an additional positive control. Cells were collected and translation was analysed via OPP incorporation in the $CD19^{+}CD5^{-}IgG^{-}$ cell population. Data was made relative to DMSO-treated control set to 1 or 100. Error bars show SEM and the statistical significance of the indicated differences was determined using paired T tests. Experiments were performed in collaboration with Dr Karly-Rai Rogers-Broadway.

3.4 Summary of main findings

The overall aim of this chapter was to characterise the effects of the eIF4Ai, silvestrol and rocaglamide, on the induction of global mRNA translation and the expression of MYC and MCL1 following sIgM stimulation in CLL cells. This chapter also aimed to compare responses in CLL and healthy donor B cells to determine whether the effects of eIF4Ai on mRNA translation were specific for CLL cells.

The main findings from these experiments were;

- eIF4A inhibitors reduced anti-IgM-induced global mRNA translation in CLL samples without substantial effects on upstream ERK-phosphorylation
- eIF4Ai reduced anti-IgM-induced eIF4A expression
- eIF4Ai reduced anti-IgM-induced MYC and MCL1 protein expression
- eIF4Ai alone had minimal effects on cell viability at time-points up to 24 hours
- eIF4Ai may reverse the survival promoting effects of sIgM signalling
- Silvestrol inhibited anti-IgM-induced mRNA translation in B cells from healthy donors

Overall, these findings supported the hypothesis that eIF4Ai effectively reduce anti-IgM-induced mRNA translation, and induction of MYC and MCL1 protein, in CLL cells. However, results from the comparison of effects of silvestrol in CLL and normal B cells did not support the secondary hypothesis, that the inhibitory effects of eIF4Ai on anti-IgM-induced mRNA translation are specific for CLL cells.

3.5 Discussion

3.5.1 The effect of eIF4Ai on global mRNA translation in CLL and B cells from healthy donors

A central goal of the experiments was to determine the effects of eIF4Ai on global mRNA translation in CLL and healthy donor B cells. Although anti-IgM increased mRNA translation in both cell types, sIgM signalling results in increased expression of eIF4A (and reduced expression of PDCD4) only in CLL cells (Yeomans et al., 2015). Thus, it was possible that eIF4Ai might allow selective inhibition of anti-IgM-induced translational responses in CLL cells.

OPP-labelling and polysome profiling experiments clearly demonstrated that inhibition of eIF4A reduced global mRNA translation in anti-IgM-stimulated CLL cells (sections 3.3.1 and 3.3.2). At the higher concentration of drugs tested (20 nM), inhibition of the anti-IgM response measured by OPP-labelling was almost complete (i.e., returning OPP-labelling to pre-stimulation levels, section 3.3.1), suggesting that the bulk of the translational response in these cells was dependent on eIF4A activity. Overall, the two drugs were quite similar in terms of their effects on OPP-labelling (section 3.3.1), consistent with their close structural relationship and likely shared mechanism of action.

In contrast to anti-IgM treated cells, eIF4Ai had relatively modest effects on mRNA translation in unstimulated cells (section 3.3.1). Thus, these compounds reduced OPP-labelling by ~20% at most under these conditions, and differences between drug and DMSO treated cells were not statistically significant (section 3.3.1). Thus, in contrast to anti-IgM-induced translation, the low level of basal translation that is observed in unstimulated CLL cells appears to be less dependent on eIF4A activity.

Polysome profiling was performed to understand the effects of sIgM-stimulation and eIF4Ai on polysome-associated mRNA translation in CLL samples (Figure 3-3 and Figure 3-4). In the untreated and control- treated samples, there was a minimal presence of polysomes present visually on the polysome profiles, implying low basal levels of translation. Following sIgM-stimulation, there was an increase in the presence of polysomes (Figure 3-3 and Figure 3-4), correlating with the increased global mRNA translation demonstrated using the OPP-incorporation assay (Figure 3-1). Co-treatment with silvestrol and anti-IgM saw a partial reduction in the size and presence of polysome peaks (Figure 3-4). This is similar to that described using colorectal cancer cell lines (Wiegering et al., 2015) whereby global and mRNA-specific polysome-associated translation was inhibited by silvestrol treatment using a similar concentration as in this experiment (25 nM, in comparison to 20 nM). The partial reduction in polysome peaks implied that silvestrol inhibits the translation of select mRNAs (Figure 3-4).

Although eIF4A was not induced following anti-IgM stimulation of healthy donor B cells (Yeomans et al., 2015), it was notable that silvestrol inhibited OPP-labelling in both normal and CLL B cells (Figure 3-2, Figure 3-11). Thus, eIF4Ai did not selectively inhibit anti-IgM-induced global mRNA translation in CLL cells. It is likely that, although levels are not regulated, normal B cells retain a tight dependency on eIF4A for translational responses for stimulation.

One possible reason for this observation is that eIF4A expression is already relatively high in normal B cells, and that induction in CLL cells increases eIF4A expression from a low level to a level equivalent to that seen in unstimulated normal B cells. It would appear to be counter-intuitive that malignant cells have reduced expression of a tumour-promoting factor such as eIF4A compared to non-malignant counterparts.

However, it is interesting to note that previous studies have demonstrated reduced expression of multiple ribosome components in CLL cells compared to healthy donor B cells (Sbarrato et al., 2016). The reason why resting CLL cells may have less translational capacity compared to normal counterparts is unclear but may relate to the overall anergic features of CLL cells. Translation is highly energy dependent (Buttgereit and Brand, 1995) and both normal anergic B cells and CLL cells have reduced capacity for ATP production compared to naïve/memory B cells or normal blood B cells, respectively (Jia and Gribben, 2014, Walker et al., 2014). Thus, down-modulation of translation capacity (by reduced production of ribosomes and reduced eIF4A/increased PDCD4 expression) may represent a strategy allowing unstimulated CLL cells to match (low) energy supply and demand.

It would be interesting to address the relative differences in regulation of eIFs between normal B and CLL cells in more detail in future studies. However, it is important to consider that blood B cells are not homogeneous and comprise functionally distinct subsets. Thus, it would be necessary to separately quantify expression of eIFs and PDCD4, and their response to anti-Ig stimulation, in these different cell populations for comparison to CLL subsets (eg M-CLL versus U-CLL). The proportion of some of the populations of B cells in blood is low and analysis would be best performed using flow cytometry. Given the extended time-frame that would be required to establish these assays, it was not feasible to perform these experiments during the time available for my project.

3.5.2 Molecular effects of eIF4Ai in anti-IgM stimulated CLL cells

A series of experiments was performed to explore the molecular consequences of eIF4A inhibition on signalling responses downstream of sIgM, including (i) upstream ERK phosphorylation, (ii) expression of eIFs and PDCD4 and (iii) MYC and MCL1 expression. These demonstrated that eIF4Ai did not reduce anti-IgM-induced phosphorylation of ERK confirming that inhibition of anti-IgM-induced mRNA translation by these drugs was not an indirect consequence of inhibition of upstream signalling.

eIF4Ai did effectively reduce induction eIF4A expression in cells treated with anti-IgM (Figure 3-6). The reason for this novel finding is unclear since eIF4A inhibition *per se* would not necessarily be expected to reduce the steady state expression of eIF4A. One possibility is that the stability of eIF4A is reduced in drug treated cells, because of drug-induced conformational changes which might increase susceptibility to proteasome-mediated degradation. Alternately, it is likely that translationally inhibited mRNAs that are sequestered within eIF4A/eIF4Ai complexes are re-localised within cells, potentially to stress granules (Slaine et al., 2017) and this could also lead to destabilisation of drug-bound eIF4A. Stress granules are formed in the cytoplasm during cellular stress and contain mRNA and proteins following repression of translation initiation (Buchan and Parker, 2009). It was interesting to note that expression of the other factors analysed (eIF4G, eIF4E and PDCD4) were either unaffected or only modestly altered following eIF4Ai treatment (Figure 3-6). Thus, although the mechanism by which eIF4Ai reduce eIF4A expression in anti-IgM-treated cells is not known, these observations do perhaps point to a rather selective effect of eIF4Ai on eIF4A.

Finally, eIF4Ai reduced induction of both MYC and MCL1 in anti-IgM-treated cells (Figure 3-7, Figure 3-8), thereby depriving CLL cells of key effectors of both pro-growth (MYC) and pro-survival (MCL1) responses. Although both drugs were effective, silvestrol did appear to be somewhat more effective for inhibition of MYC/MCL1 expression compared to rocaglamide. Although the overall mechanism of action of these compounds is likely to be very similar, there may be some differences. For example, silvestrol-induced eIF4A-RNA dimerization is ATP-dependent, whereas rocaglamide does not require ATP (Cencic et al., 2009, Iwasaki et al., 2016). Such subtle differences in mechanisms of action may account for the small differences observed when comparing effects of drugs on expression of specific targets. Finally, it is worth noting that previous studies demonstrated that silvestrol inhibited induction of MYC protein expression in anti-IgM treated normal human B cells (Steinhardt et al., 2014). Thus, similar to the effects of silvestrol on global mRNA translation measured using OPP-labelling, these inhibitory effects of eIF4Ai on MYC expression are also not likely to be specific for CLL cells.

3.5.3 The effects of eIF4Ai on apoptosis

Previous studies have shown that both silvestrol and rocaglamide induced cell death in CLL samples (Lucas et al., 2009, Callahan et al., 2014). However, it was important to investigate the effects of eIF4Ai on CLL cell viability at earlier time points, and, in particular, on the ability of sIgM signalling to protect CLL cells from spontaneous apoptosis *in vitro*. Interestingly, at 24 hours, eIF4Ai did not promote apoptosis when analysed in unstimulated cells (Figure 3-9). By contrast, eIF4Ai did seem to reduce the ability of anti-IgM to suppress apoptosis of CLL cells (Figure 3-10).

However, it was hard to draw firm conclusions from these experiments where there was considerable sample-to-sample variation in the extent of spontaneous apoptosis and protection by anti-IgM. Given that the OPP-labelling and polysome profiling experiments were performed in the presence of Q-VD-OPh to suppress apoptosis, it seemed unlikely that eIF4Ai-associated reduction in mRNA translation were a secondary consequence of the induction of apoptosis.

Anti-IgM-induced CLL survival appears to be mediated primarily by induction expression of MCL1 (Petlickovski et al., 2005), so it was possible that the ability of eIF4Ai to reduce anti-IgM-induced MCL1 (Figure 3-8) expression contributed to the inhibitory effects of eIF4Ai on anti-IgM-induced survival (Figure 3-10). However, is important to recognise that apoptosis control is multi-factorial and effects of anti-IgM/eIF4Ai on apoptosis in CLL cells are likely to be complex and may involve regulation of other mediators.

Chapter 4

Detailed investigation of the effects of eIF4Ai on the translation and stability of *MYC* mRNA

4.1 Introduction

Results in the previous chapter demonstrated that eIF4Ai reduced anti-IgM-induced MYC and MCL1 protein expression, which are critical disease drivers in CLL. MYC is a key oncoprotein involved in proliferation and disease progression in CLL, known to be highly expressed in some cells within the PC of CLL lymph nodes (Krysov et al., 2012). On the other hand, MCL1 is an anti-apoptotic BCL2 family protein with a role in drug resistance in some cases of refractory CLL (Johnston et al., 2004). With this, both MYC and MCL1 are important targets for therapeutic intervention in CLL and so the mechanisms by which eIF4Ai reduce their expression need to be further understood.

Thus, the initial goal was to perform analysis of the RNA acquired by polysome profiling and that of total RNA to confirm the translational inhibition of *MYC* and *MCL1* mRNAs. These experiments provide data demonstrating the polysome association of mRNA and combining of fractions also allows for total RNA expression analysis between conditions of polysome profiling. Alongside these studies, the mRNA expression of *MYC* and *MCL1* after anti-IgM and eIF4Ai treatment was determined from whole cell lysates, in contrast to those extracted from polysome profiling fractions, to confirm translational regulation.

Previous studies of *MYC* mRNA have revealed a close linkage between the stability and translation of *MYC.* For example, cycloheximide, an inhibitor of translation elongation, inhibited *MYC* translation resulting in accumulation of *MYC* mRNA due to an increase in its stability (Wisdom and Lee, 1991). The presence of a destabilisation sequence in *MYC* requires translation for *MYC* to be degraded, thus degradation of *MYC* is coupled to its translation. Whether these responses are the same for inhibitors of translation initiation, is not yet known. Therefore, I devised further experiments to investigate the effects of eIF4Ai on *MYC* mRNA stability and probed the reversibility of these effects using drug wash-out experiments.

4.2 Hypothesis and aims

4.2.1 Hypothesis

The hypothesis for this chapter was that the reduction in anti-IgM-induced expression of MYC and MCL1 by eIF4Ai was due to inhibition of mRNA translation and not transcription, as a result of the complex 5' UTR of these mRNA and their likely dependency on eIF4A for translation.

4.2.2 Aims

In order to test this hypothesis, this chapter aimed to:

- Investigate directly the effects of silvestrol on anti-IgM-induced *MYC* and *MCL1* mRNA translation
- Characterise the effects of anti-IgM and eIF4Ai treatment on total *MYC* and *MCL1* mRNA expression
- Investigate the effects of silvestrol on *MYC* mRNA stability
- Determine the consequences of drug-removal on the effects of silvestrol on *MYC* mRNA and protein expression

4.3 Results

4.3.1 The effect of silvestrol on *MYC* and *MCL1* mRNA translation within polysome profiling fractions

Having shown that eIF4Ai inhibit anti-IgM-induced global mRNA translation (by OPP-incorporation and polysome profiling, sections 3.3.1 and 3.3.2), and reduced anti-IgM-induced MYC and MCL1 protein expression (section 3.3.5), it was important to investigate the effect of eIF4Ai directly on translation of *MYC* and *MCL1* mRNA. CLL samples were therefore pre-treated with silvestrol and then stimulated for 24 hours with anti-IgM. Polysome profiling was performed and qPCR analysis used to quantify the amount of *MYC*/*MCL1* mRNA associated with the monosome and the polysomes. These experiments were performed using only silvestrol due to the large amount of cell numbers required for this technique.

From the visual evaluation of polysome profiles in chapter 3 (Figure 3-4), it was straightforward to identify the 60S ribosomal subunit and the 80S complete ribosome peaks (i.e. monosomes; fractions 1-4). Fractions 5-10 were then classed as the polysome fractions for analysis. qPCR analysis was then used to determine the relative distribution of *MYC* and *MCL1* mRNA between monosome and polysome fractions, as previously described (Yeomans et al., 2015). Parallel qPCR analysis demonstrated that the monosome/polysome distribution of *B2M* RNA was relatively unaffected by anti-IgM/silvestrol (Appendix A) and *B2M* expression was then used for normalisation of *MYC* and *MCL1* mRNA.

4.3.1.1 The effect of silvestrol on *MYC* mRNA translation within polysome profiling fractions

To investigate whether reduced MYC protein expression by silvestrol was due to the inhibition of *MYC* mRNA association with polysomes, I investigated the total abundance and distribution of *MYC* mRNA within the polysome profiling fractions. To investigate whether *MYC* RNA is increasingly associated with polysomes for its translation following sIgM stimulation, and whether this would be inhibited by silvestrol, I analysed the expression of *MYC* RNA in the polysome fractions versus to the monosome fractions (Figure 4-1). There was a clear increase in polysome-associated translation following sIgM-engagement which was significantly reduced following silvestrol treatment (Figure 4-1), implying that silvestrol specifically reduces the polysome-associated *MYC* mRNA translation in anti-IgM-treated cells.

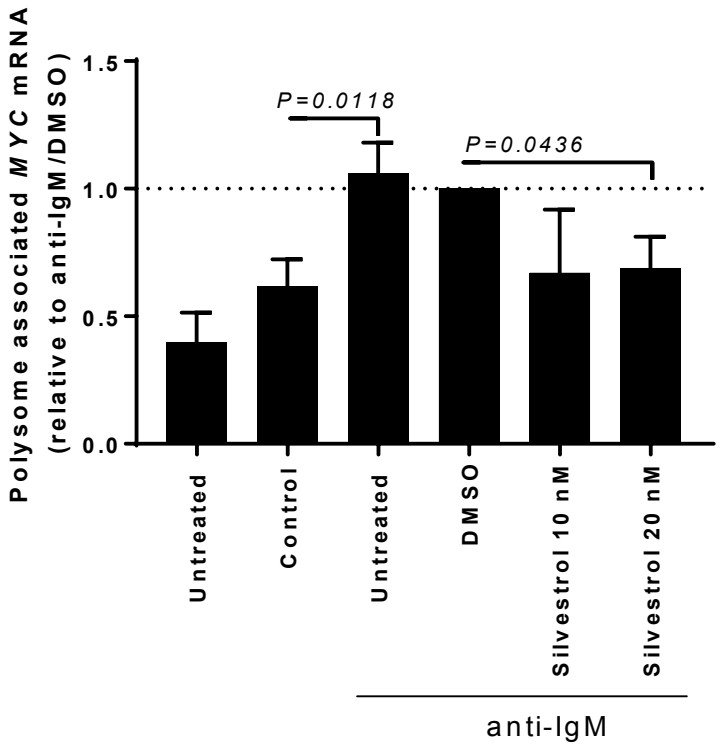

Figure 4-1. Polysome-associated *MYC* mRNA expression after anti-IgM and silvestrol treatment

CLL cells (n=5) were pre-treated with silvestrol or DMSO for one hour, followed by an additional 24 hours of control antibody or anti-IgM treatment. Cells were then lysed and used in polysome profiling as described. Polysome profiling fractions (1-10) were collected and RNA extracted. RNA was used in cDNA synthesis and qPCR using Taqman primers for *MYC*. Polysome-associated *MYC* RNA was determined by making polysome-associated (fractions 5-10) *MYC* RNA relative to monosome-associated *MYC* RNA (fractions 1-4) after normalisation to *B2M*. Values for anti-IgM/DMSO treated cells were set to 1. Error bars show SEM and the statistical significance of the indicated differences were determined using a paired T-test.

I also used these qPCR results to investigate the effect of anti-IgM and silvestrol on the overall abundance of *MYC* mRNA, by combining fractions for each condition (Figure 4-2). There was a clear induction of *MYC* mRNA expression following anti-IgM stimulation (Figure 4-2), consistent with the known transcriptional induction of MYC mRNA (Krysov et al., 2012). However, there was a surprising hyper-induction of *MYC* mRNA in cells co-treated with anti-IgM and silvestrol (10 and 20 nM, Figure 4-2). Therefore, silvestrol treatment results in a further accumulation of anti-IgM-induced *MYC* mRNA, but this mRNA is not associated with polysomes.

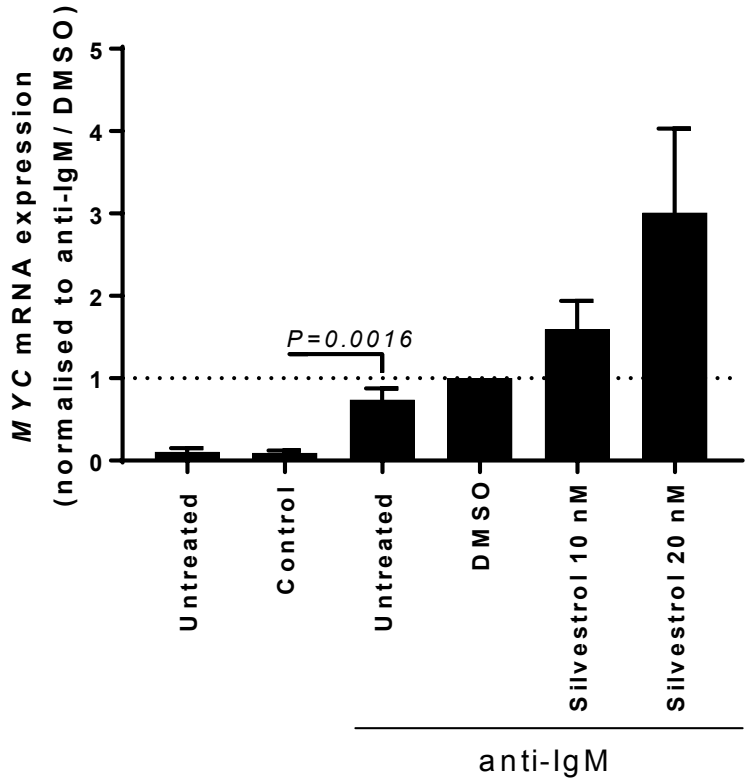

Figure 4-2. Combined polysome profiling fractions/total *MYC* mRNA expression after anti-IgM and silvestrol treatment

CLL samples (n=5) were pre-treated with silvestrol or DMSO for one hour, followed by an additional 24 hours of control antibody or anti-IgM treatment. Cells were then lysed and used in polysome profiling as described. Polysome profiling fractions (1-10) were collected and RNA extracted. RNA was used in cDNA synthesis and qPCR using Taqman primers for *MYC*. Total *MYC* expression (RNA per fraction of each condition was combined), and normalised to *B2M*. Values for anti-IgM/DMSO treated cells were set to 1. Error bars show SEM and the statistical significance of the indicated differences was determined using a paired T test.

4.3.1.2 The effect of silvestrol on *MCL1* mRNA translation within polysome profiling fractions

Similar experiments were performed to investigate the polysome association of *MCL1* mRNA. There was a significant increase in polysome-associated *MCL1* mRNA following sIgM stimulation which was significantly reduced by silvestrol treatment (10 and 20 nM, Figure 4-3). Thus, similar to *MYC,* silvestrol reduces polysome-associated *MCL1* mRNA translation in anti-IgM-treated cells.

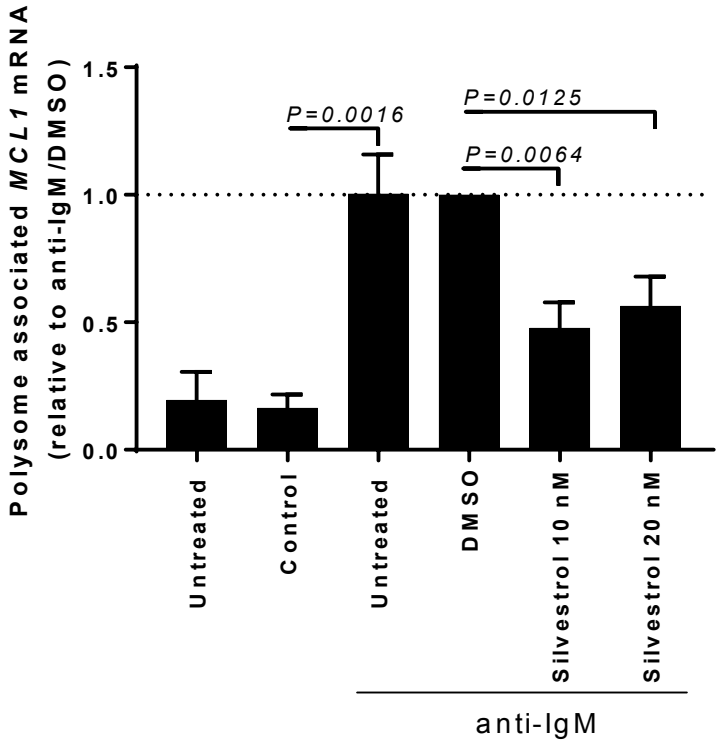

Figure 4-3. Polysome-associated *MCL1* mRNA expression after anti-IgM and silvestrol treatment

CLL samples (n=5) were pre-treated for one hour with silvestrol or DMSO, before an additional 24 hour treatment with control antibody or anti-IgM. Cells were then collected and lysed for use in polysome profiling as described previously. Polysome profiling fractions (1-10) were collected and RNA extracted. RNA was used in cDNA synthesis and qPCR using Taqman primers for *MCL1*. Polysome-associated *MCL1* RNA was determined by making polysome-associated (fractions 5-10) *MCL1* RNA relative to monosome-associated *MCL1* RNA (fractions 1-4) after normalisation to *B2M*. Values for anti-IgM/DMSO treated cells were set to 1. Error bars show SEM and the statistical significance of the indicated differences was determined using a paired T-test.

I then analysed total *MCL1* mRNA expression between conditions, by combining the qPCR results from all fractions (Figure 4-4). There was no change in *MCL1* mRNA expression following sIgM-stimulation. However, there was a subtle increase in *MCL1* expression with silvestrol treatment (Figure 4-4).

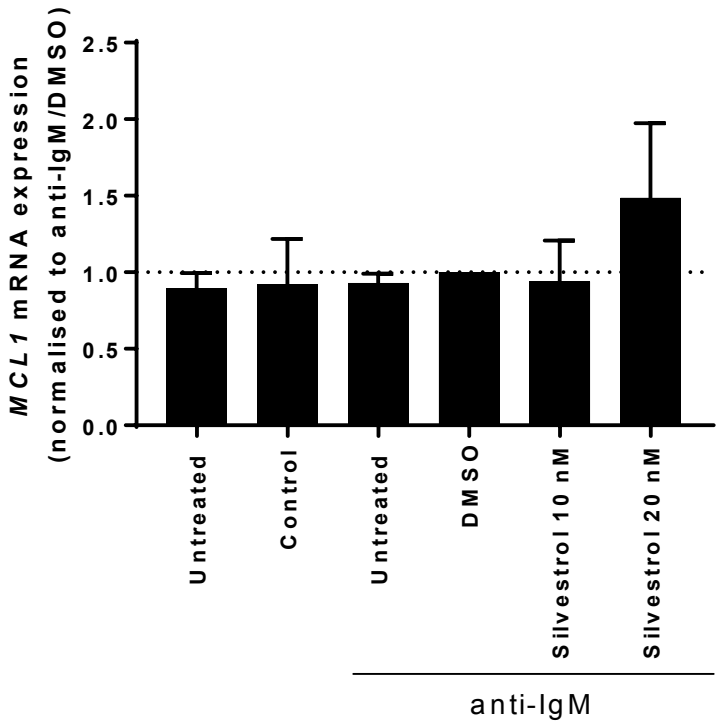

Figure 4-4. Combined polysome profiling fractions/total *MCL1* mRNA expression after sIgM-stimulation and silvestrol treatment

CLL samples (n=5) were pre-treated for one hour with silvestrol or DMSO, before an additional 24 hour treatment with control antibody or anti-IgM. Cells were then collected and lysed for use in polysome profiling as described previously. Polysome profiling fractions (1-10) were collected and RNA extracted. RNA was used in cDNA synthesis and qPCR using Taqman primers for *MCL1*. Total *MCL1* expression (RNA per fraction) of each condition was combined and normalised to *B2M*. Values for anti-IgM/DMSO treated cells were set to 1. Error bars show SEM and the statistical significance of the indicated differences was determined using a paired T-test.

4.3.2 Effect of silvestrol and rocaglamide on total expression of *MYC* and *MCL1* RNA in anti-IgM treated cells

The data above suggested a surprising increase in total *MYC/MCL1* mRNA expression in cells treated with anti-IgM and silvestrol (section 4.3.1). This was particularly striking for *MYC*. To confirm this, the expression of *MYC* and *MCL1* mRNA in total mRNA preparations was studied, to avoid potentially confounding effects associated with the polysome profiling technique whereby some RNAs may not have been recovered within the fractions. The effects of rocaglamide were also studied to determine whether this was a general effect associated with eIF4Ai or specific for silvestrol. CLL samples were treated for one hour with silvestrol or rocaglamide, followed by 24 hour anti-IgM treatment before mRNA extracted for analysis using Taqman qPCR.

Before analysis of *MYC* and *MCL1* mRNA, it was important to determine whether *B2M* mRNA could be used as an appropriate control to normalise the qPCR results in these experiments. To do so, *B2M* mRNA expression was measured by qPCR following anti-IgM and eIF4Ai treatments and quantified *B2M* expression directly by analysing the threshold cycle (Ct) values as a measure of the absolute amount of *B2M* cDNA (see Appendix A). Although there was a weak induction of *B2M* mRNA expression following sIgM-engagement, the expression of *B2M* RNA was not affected by the inhibitors in either the presence or absence of anti-IgM (Appendix A). *B2M* RNA was therefore considered suitable for normalisation of *MYC* and *MCL1* expression.

4.3.2.1 Further induction of anti-IgM-induced *MYC* mRNA expression following treatment with eIF4Ai

Following 24-hour anti-IgM stimulation, there was a significant induction of *MYC* mRNA expression (Figure 4-5A) as described previously (Krysov et al., 2012). Similar to that shown in the polysome profiling fractions, eIF4Ai treatment further increased the expression of anti-IgM-induced *MYC* mRNA (Figure 4-5B). *MYC* mRNA expression was ~10-fold higher in silvestrol (20 nM) and anti-IgM treated cells, compared to anti-IgM alone treated cells and ~3-fold higher in rocaglamide and anti-IgM treated cells compared to anti-IgM treatment alone (Figure 4-5B). Overall, this analysis confirmed that the inhibition of MYC protein expression in eIF4Ai-treated cells was not accompanied by a reduction in *MYC* mRNA expression, consistent with translational inhibition. Moreover, there was a counterintuitive and statistically significant increase in *MYC* mRNA (which remained translationally inhibited) in cells co-treated with anti-IgM and silvestrol or rocaglamide (Figure 4-5B). Neither compound had any clear effect on basal *MYC* mRNA expression (Appendix A).

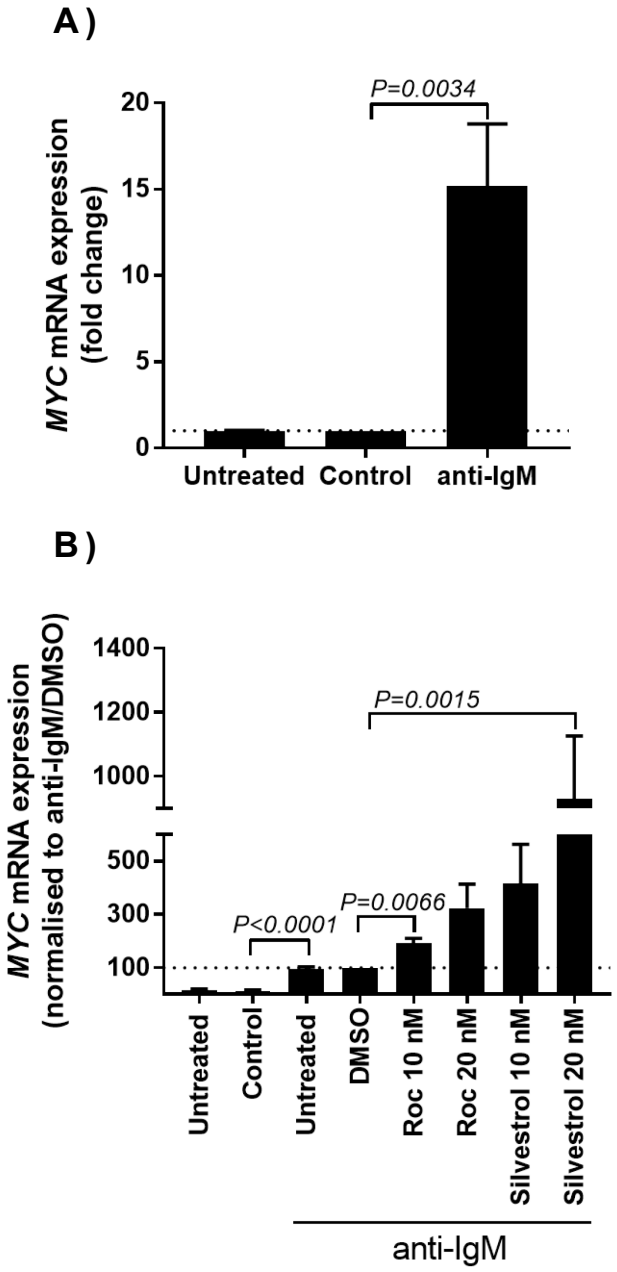

Figure 4-5. *MYC* mRNA expression following anti-IgM and eIF4Ai treatment

CLL samples (n=10) were pre-treated for one hour with silvestrol or rocaglamide (10 or 20 nM) then treated with control antibody or anti-IgM for an additional 24 hours. *MYC* and *B2M* mRNA expression measured by Taqman qPCR. A) *MYC* mRNA induction following anti-IgM treatment with data normalised to *B2M* expression with values for control antibody treated cells set to 1. Dot plot used to demonstrate the differences in induction of *MYC* expression by anti-IgM between different samples. B) *MYC* mRNA expression following anti-IgM treatment and silvestrol or rocaglamide treatment with data normalised to *B2M* expression with values for anti-IgM/DMSO treated cells set to 100. Scale set to 100 to aid visualisation of the induction of *MYC* expression whilst also showing the extent of *MYC* further induction by silvestrol. Error bars show SEM and the statistical significance of the indicated differences was determined using a paired T test.

4.3.2.2 Induction of anti-IgM-induced *MCL1* mRNA expression following treatment with eIF4Ai

Similar analysis was performed to investigate *MCL1* mRNA expression after eIF4Ai treatment and sIgM-stimulation. Again, data was normalised to *B2M*. Following 24-hour sIgM stimulation, there was a varied but significant induction of *MCL1* mRNA expression between patient samples (Figure 4-6), and when this induction was seen, it was to a lesser extent than shown with *MYC* mRNA induction following sIgM-stimulation of the same duration (Figure 4-6). Further induction of *MCL1* expression was demonstrated by eIF4Ai co-treatment with anti-IgM (20 nM, Figure 4-6), although to a lesser extent than seen with *MYC* (Figure 4-5). On average, *MCL1* RNA expression was ~2-fold higher in silvestrol and anti-IgM treated cells, and ~1.5-fold higher in rocaglamide and anti-IgM treated cells, compared to anti-IgM alone treated cells. This is substantially lower than the ~5-10-fold increase seen with *MYC* RNA following silvestrol treatment.

Overall, these data confirm that, like MYC, the inhibition of MCL1 protein expression in eIF4Ai-treated cells was not accompanied by a reduction in *MCL1* mRNA expression, consistent with translational inhibition. There was also a counterintuitive increase in *MCL1* mRNA in cells co-treated with anti-IgM and silvestrol or rocaglamide, although this was to a lesser extent than observed for *MYC* mRNA (Figure 4-5). Again, neither compound had any clear effect on basal *MCL1* mRNA expression (Appendix A).

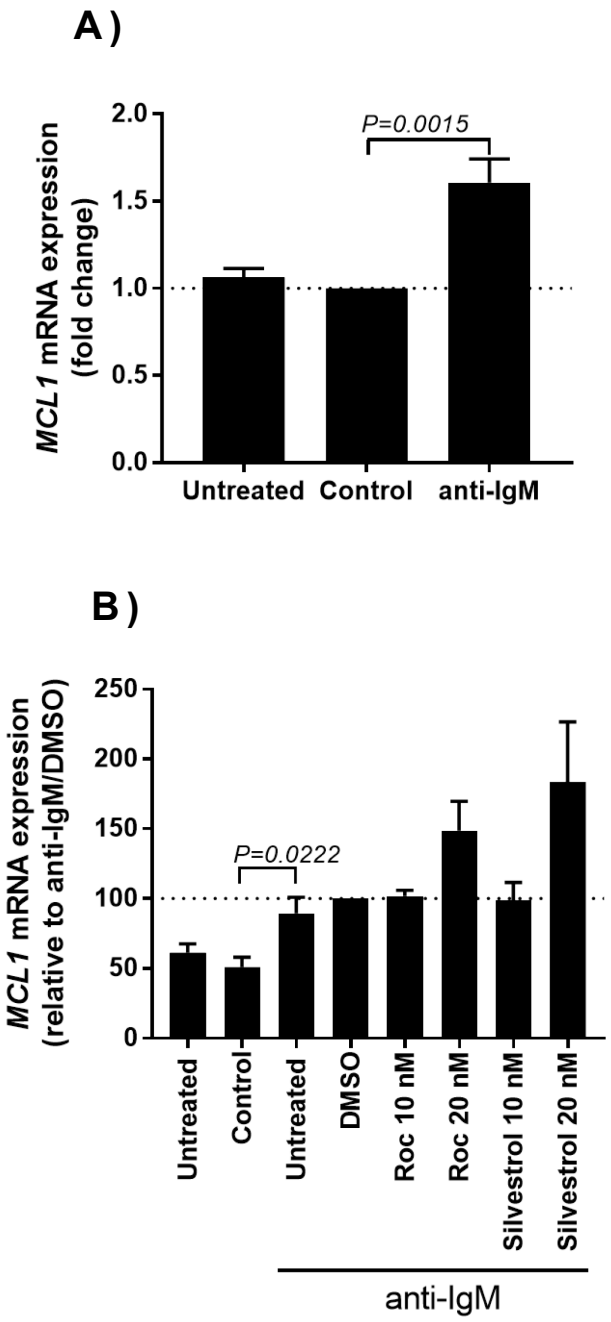

Figure 4-6. *MCL1* mRNA expression following anti-IgM and eIF4Ai treatment

CLL samples (n=11) were pre-treated with silvestrol or rocaglamide (10 or 20 nM) for one hour and then treated with control antibody or anti-IgM for an additional 24 hours. *MCL1* and *B2M* mRNA expression measured by Taqman qPCR. A) *MCL1* mRNA induction following anti-IgM treatment, data relative to *B2M* expression and normalised to control bead treated sample set to 1. B) *MCL1* mRNA expression following anti-IgM treatment and silvestrol or rocaglamide treatment with data normalised to *B2M* expression with values for anti-IgM/DMSO-treated cells set to 100. Error bars show SEM and the statistical significance of the indicated differences was determined using a paired T-test.

4.3.3 Kinetics of the induction of *MYC* and *MCL1* mRNA by anti-IgM and silvestrol

A time-course of anti-IgM and silvestrol treatment was performed, to measure the expression of *MYC* and *MCL1* mRNAs following one to 24 hour anti-IgM treatment, in order to fully understand the kinetics of the anti-IgM/silvestrol response. Data was normalised so that the anti-IgM/DMSO treated values for each time-point was normalised to 100. This allows for easier visualisation of induction of *MYC*/*MCL1* mRNA at each time-point of anti-IgM treatment and the relative further induction induced by silvestrol treatment.

Induction of *MYC* mRNA expression was evident by as early as one hour anti-IgM treatment and continued to be induced throughout the time-course up to 24 hours of anti-IgM treatment (Figure 4-7). Further induction of *MYC* mRNA by anti-IgM/silvestrol treatment was clear from three hours of treatment, but was most highly induced by 24 hours (Figure 4-7). Thus, *MYC* mRNA appears to accumulate over time following anti-IgM/silvestrol treatment.

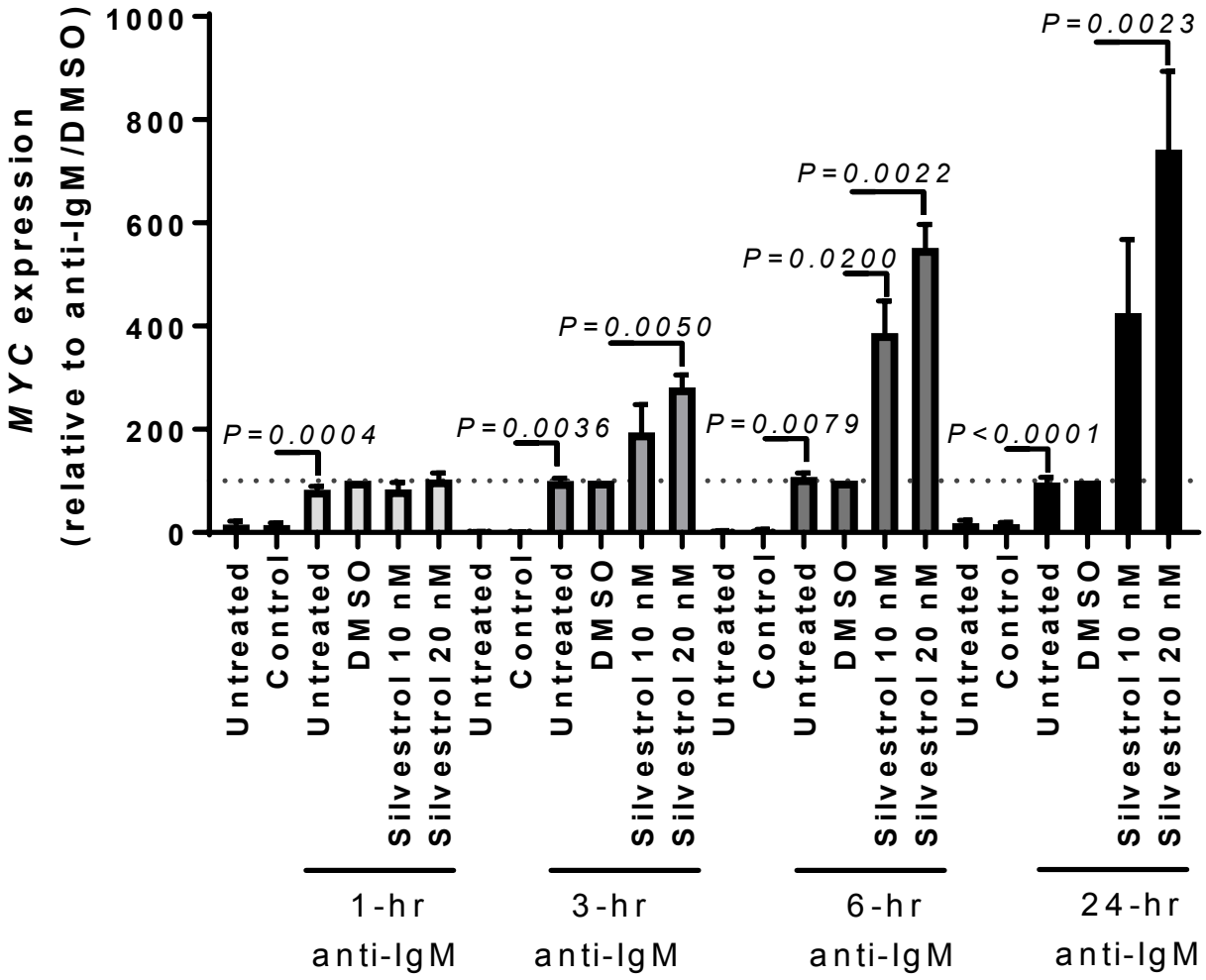

Figure 4-7. Time-course of *MYC* mRNA expression following anti-IgM and silvestrol treatment

CLL samples (n=4) were pre-treated with silvestrol or DMSO (10 or 20 nM) for another hour and then treated with control antibody or anti-IgM for an additional 1, 3, 6 or 24 hours. *MYC* and *B2M* mRNA expression measured by Taqman qPCR. *MYC* mRNA data was made relative to *B2M* expression with values for anti-IgM/DMSO sample set to 100 per time-point. Error bars show SEM and the statistical significance of the indicated differences was determined using a paired T-test.

At earlier time-points, there is a less clear induction of *MCL1* mRNA expression by anti-IgM treatment (Figure 4-8). Induction of *MCL1* mRNA expression was most clear following 24 hours of anti-IgM treatment, but even at this time-point the extent of the increase was modest (~50%) (Figure 4-8). There was a slight further induction of *MCL1* mRNA expression following anti-IgM/silvestrol treatment (20 nM) as early as one hour anti-IgM treatment, although this was most evident following six to 24 hour incubation (Figure 4-8).

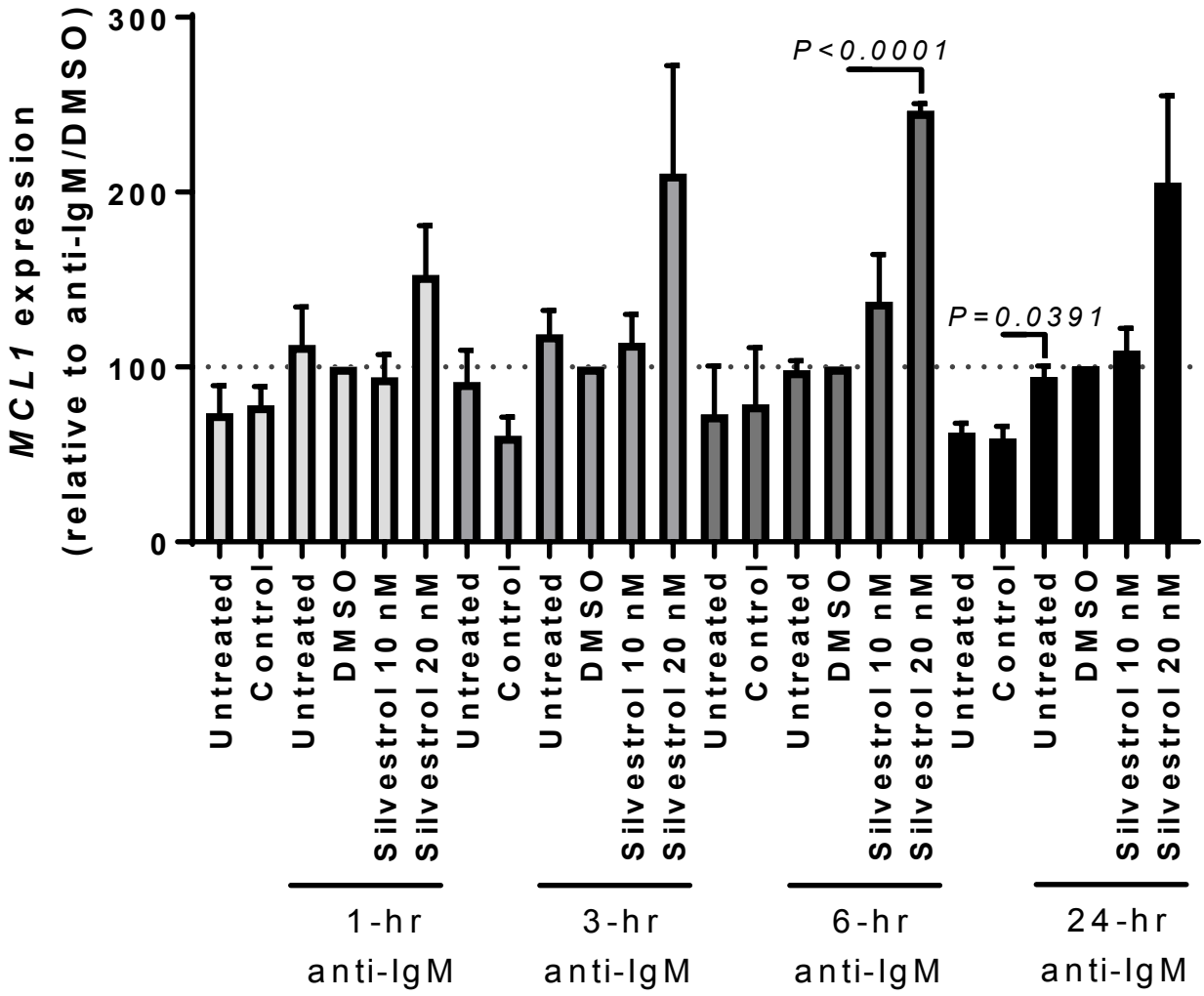

Figure 4-8. Time-course of *MCL1* mRNA expression following anti-IgM and silvestrol treatment

CLL samples (n=4) were pre-treated with silvestrol or DMSO (10 or 20 nM) for another hour and then treated with control antibody or anti-IgM for an additional 1, 3, 6 or 24 hours. *MCL1* and *B2M* mRNA levels measured by Taqman qPCR. *MCL1* mRNA data was made relative to *B2M* expression with values for anti-IgM/DMSO sample set to 100 per time-point. Error bars show SEM and the statistical significance of the indicated differences was determined using a paired T-test.

4.3.4 The effect of silvestrol on *MYC* mRNA stability

The mechanism by which eIF4Ai trigger hyper-induction of *MYC* mRNA expression (and *MCL1* mRNA to a lesser extent) was investigated in anti-IgM-treated cells. Experiments focused on *MYC* mRNA as the effects of anti-IgM/eIF4Ai treatment were much clearer than seen with *MCL1* mRNA. Due to limitations in cell numbers these experiments were performed using only silvestrol, as this compound increased expression of *MYC* mRNA to a greater extent than rocaglamide.

The abundance of an mRNA is regulated through transcription rates and rates of decay of mRNA. It is known that *MYC* mRNA contains an instability/destabilisation element in its coding region meaning that its half-life is dependent upon its translation. This means that the translation and degradation of *MYC* RNA are coupled (Lemm and Ross, 2002, Wisdom and Lee, 1991). For example, inhibition of translation elongation by cycloheximide increases *MYC* RNA expression by reducing RNA degradation through an increase in its stability (Wisdom and Lee, 1991). It could therefore be hypothesised that the increase in in *MYC* RNA expression was due to stabilisation of *MYC* mRNA secondary to inhibition of translational initiation.

The transcriptional inhibitor, actinomycin D, was used to determine the relative stability of *MYC* and *B2M* mRNAs following silvestrol treatment. In these experiments, actinomycin D was used to terminate synthesis of new pol II-dependent mRNA. Under these conditions the rate of reduction of mRNA expression is therefore a function of stability. Previous studies investigating *MYC* stability, such as the aforementioned study with cycloheximide (Wisdom and Lee, 1991), utilised actinomycin D, and so the relevant concentrations described in this study were used for these experiments. A pilot experiment was performed to investigate the effects of different concentrations and exposure times for actinomycin D on cell viability (Appendix A). Based on these results, experiments were performed using a concentration of actinomycin D of 5 µg/ml and exposures up to two hours, since actinomycin D did not induce cell death under these conditions (Appendix A).

An initial time-course was undertaken to identify a suitable time-point to study the decay of *B2M* and *MYC* mRNAs following actinomycin D treatment (Figure 4-9). Cells were treated with or without anti-IgM for 24 hours and then exposed to actinomycin D. Expression of *B2M* and *MYC* mRNAs was then quantified following up to two hours of actinomycin D treatment, using qPCR. For data shown here, expression values for each untreated sample (exposed to only control antibody or anti-IgM) was set to 1 to correct for changes in total mRNA expression due to, for example, transcriptional induction by anti-IgM. As an additional control, cells were also analysed after an additional two hours without any actinomycin D to control for changes in steady state levels in the absence of actinomycin D.

B2M expression in control antibody treated cells were not significantly affected by actinomycin D (Figure 4-9A), consistent with the idea that *B2M* mRNA is stable. The data for *B2M* was then used to normalise *MYC* mRNA data to account for any variation in loading.

In the control antibody treated samples, *MYC* mRNA expression was reduced by >50% within 30 minutes of actinomycin D treatment, and continued to reduce at up to two hours (Figure 4-9B). Thus, the half-life of *MYC* RNA was short (<30 minutes), consistent with previous studies (Herrick and Ross, 1994). Similar effects were observed for anti-IgM treated cells, suggesting that, at least at 24 hours, sIgM signalling did not substantially alter *MYC* mRNA stability. Based on these results, one hour treatment with actinomycin D was selected for further experiments.

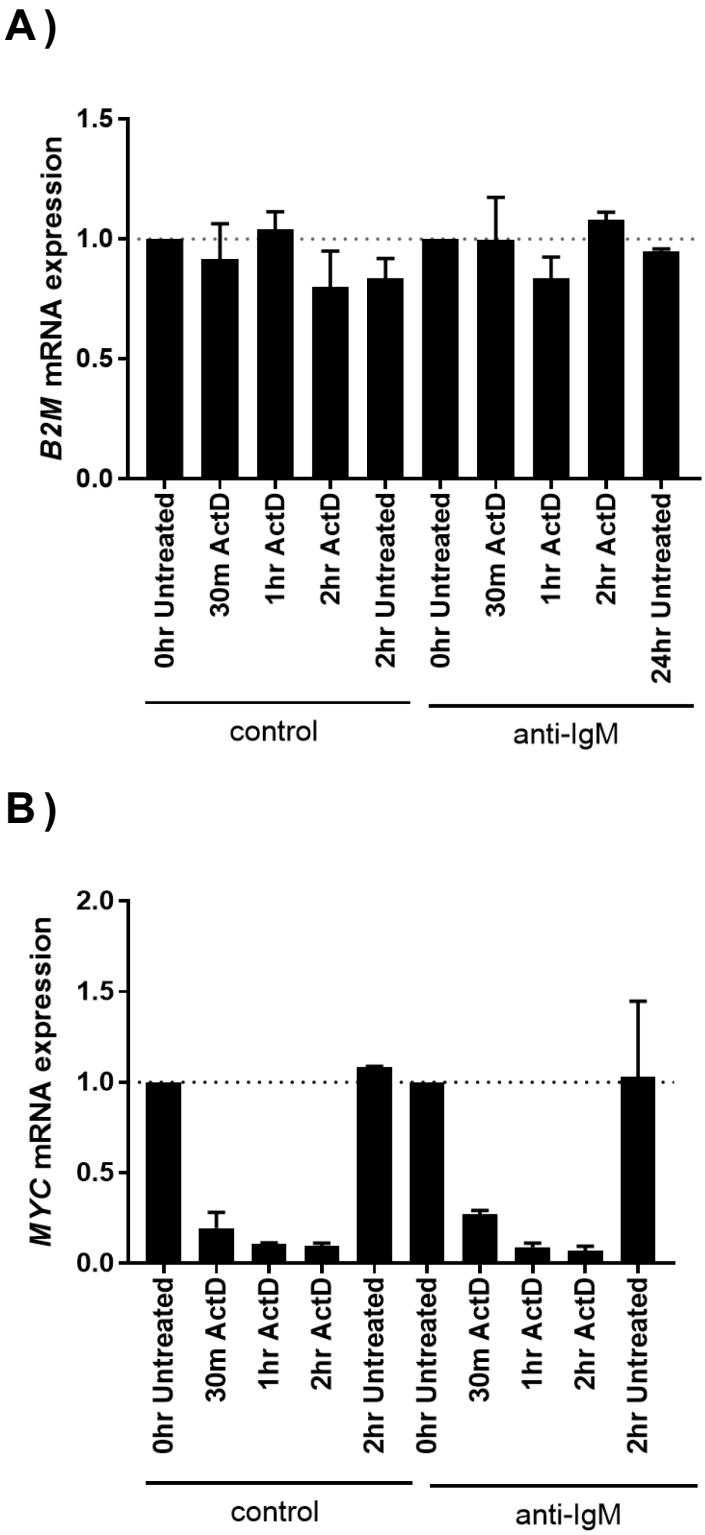

Figure 4-9. *B2M* and *MYC* mRNA expression following actinomycin D treatment as a time-course

CLL samples (n=2) were pre-treated with control antibody or anti-IgM for 24 hours, before being treated with actinomycin D (5 µg/ml) for 30 minutes, 1 or 2 hours. Cells were collected and RNA extracted before cDNA synthesised and Taqman qPCR performed. Data made relative with values for the 0 hr control-antibody and 0 hour anti-IgM-treated cells set to 1.0. A) *B2M* RNA (ng). B) *MYC* RNA normalised to *B2M* expression. Error bars show SEM.

4.3.4.1 Silvestrol increases the stability of *MYC* mRNA

To investigate the effect of silvestrol on *MYC* mRNA stability, CLL samples were incubated with silvestrol for one hour, then with control antibody or anti-IgM for an additional 24 hours, which was followed by treatment with actinomycin D for a further one hour (Figure 4-10). For this analysis, expression values for the untreated control antibody-treated sample were set to 100.

Consistent with the previous experiment, *MYC* mRNA decayed rapidly in control antibody treated cells exposed to actinomycin D, with >50% reduction at this time-point (Figure 4-10). The reduction in expression of *MYC* mRNA was actually greater in cells treated with anti-IgM in this experiment (in contrast to the previous result), which suggested some degree of destabilisation of *MYC* mRNA following sIgM-stimulation.

As described in previous experiments, anti-IgM substantially increased the overall abundance of *MYC* mRNA, and *MYC* mRNA expression was further increased in cells treated with both silvestrol and anti-IgM (Figure 4-10). In silvestrol/anti-IgM treated cells, actinomycin D did decrease *MYC* mRNA. However, the extent of reduction of *MYC* mRNA by actinomycin D was substantially less in silvestrol plus anti-IgM treated cells compared to anti-IgM-only treated cells (~49% versus ~93% reduction, Figure 4-10) indicating that silvestrol stabilises *MYC* mRNA following sIgM-stimulation.

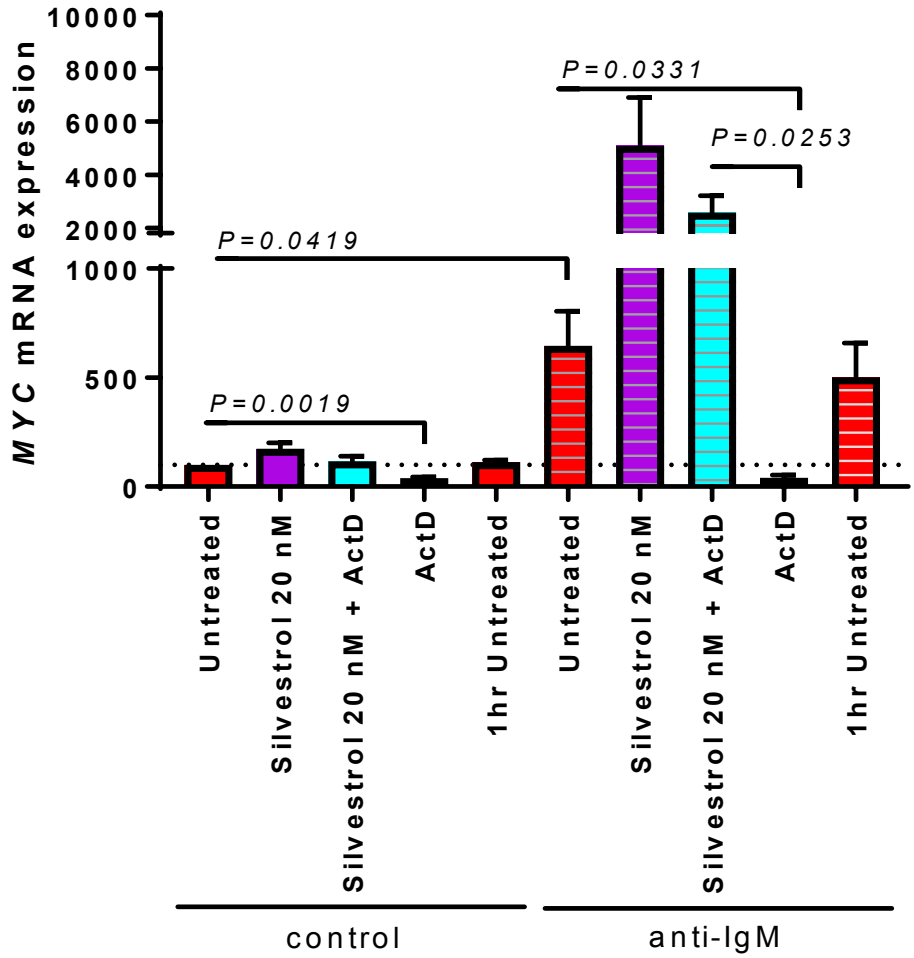

Figure 4-10. *MYC* mRNA expression following silvestrol and actinomycin D treatment

CLL samples (n=4) were pre-treated for one hour with silvestrol, followed by an additional 24 hour treatment with control antibody or anti-IgM. Cells were then treated for one hour with actinomycin D (5 µg/ml). Cells were collected and RNA extracted. *MYC* mRNA expression was measured by Taqman qPCR, normalised to *B2M* expression and values for untreated/control antibody treated cells set to 100. Error bars show SEM and the statistical significance of the indicated differences was determined using a paired T-test.

4.3.5 Wash-out of silvestrol on anti-IgM-induced MYC protein and mRNA expression

An interesting question that arose from these findings related to the fate of the *MYC* mRNA that accumulated in anti-IgM and silvestrol treated cells. For example, it is possible that, although translationally inhibited due to eIF4A inhibition, the accumulated RNA remains competent for translation if drug blockade was removed. Alternately, eIF4Ai-induced translational inhibition may render target mRNAs irreversibly blocked inhibited for translation. This is an important question to address, since, if the accumulated *MYC* mRNA remained competent for translation, intermittent or ineffective therapy with an eIF4Ai in a patient might lead to an unwanted boost in expression of tumour-driving MYC protein expression as the accumulated mRNA re-entered the translated pool. To address this, a series of wash-out experiments were performed to determine the effect of drug removal on *MYC* mRNA and protein expression.

CLL samples were pre-treated with silvestrol or DMSO for one hour, then treated with anti-IgM for three hours. Cells were then washed thoroughly (except for 'no wash' conditions), and then re-plated with either silvestrol, DMSO or no drug added. The cells were then incubated for a further three hours and then collected for lysis, proteins extracted for use in immunoblotting for MYC and HSC70 proteins. mRNA was prepared in parallel for qPCR analysis of *MYC* mRNA expression.

4.3.5.1 Removal of silvestrol reverses inhibition of MYC expression

As in previous experiments following six hour anti-IgM treatment, there is a clear induction of MYC protein expression (Figure 3-7, Figure 4-11). Cells treated with silvestrol throughout the experiment showed a strong reduction of anti-IgM-induced MYC protein expression, consistent with previous experiments (Figure 3-7). When silvestrol was removed after three hours and replaced with DMSO, MYC expression increased but only to a level similar to that detected in cells treated with anti-IgM/DMSO only (Figure 4-11). Importantly, this level of MYC expression did not reflect the elevated levels of *MYC* mRNA that had accumulated in these cells.

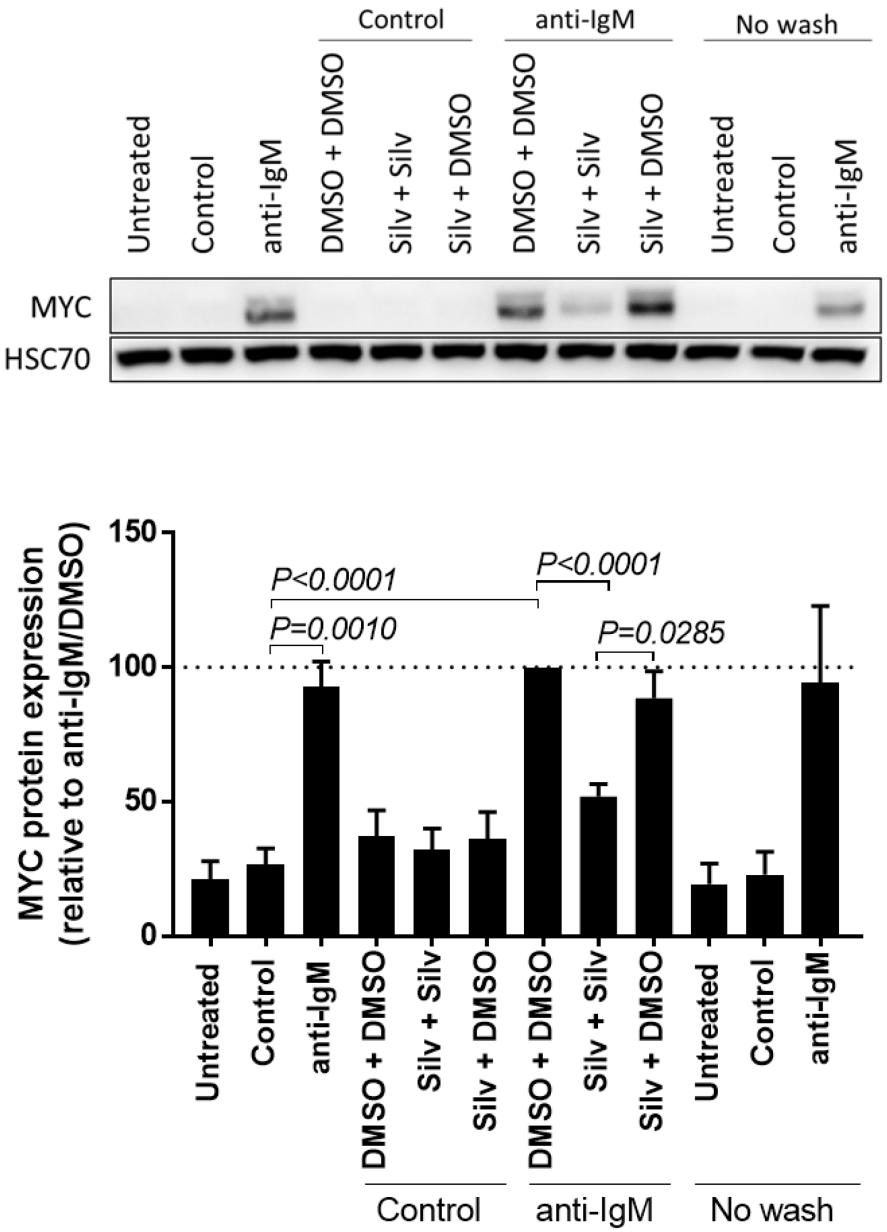

Figure 4-11. MYC protein expression following anti-IgM and silvestrol treatment followed by silvestrol wash-out

CLL samples (n=7) were pre-treated with silvestrol (20 nM) or DMSO for one hour. Samples were then treated with control antibody or anti-IgM for three hours. Cells were washed in warm medium four times (excluding the 'no wash' control cells), then re-plated with or without silvestrol or DMSO, then re-incubated for a further three hours. Cells were lysed and proteins extracted, then immunoblotting was undertaken and blots probed for MYC, and HSC70 as a loading control. Representative western blot shown of sample U-780. Relative densitometries of MYC protein expression shown with values for anti-IgM/DMSO-treated cells set to 100. Error bars show SEM and the statistical significance of the indicated differences was determined using a paired T-test.

Parallel qPCR analysis confirmed a strong induction of *MYC* mRNA expression following anti-IgM stimulation, and a further increase in cells pre-incubated with silvestrol (Figure 4-12). Upon removal of silvestrol, *MYC* mRNA expression decreased (Figure 4-12), suggesting that the accumulated mRNA is targeted for degradation. Although the decrease in mRNA expression following drug-removal was not sufficient for the expression to match that of the anti-IgM only treated cells, the decrease in mRNA expression was still statistically significant (Figure 4-12). It is likely that over longer time-points, the accumulated mRNA would have degraded and its' expression would match that of non-silvestrol treated cells. Overall, these results indicated that the accumulated *MYC* mRNA from silvestrol/anti-IgM treatment remained inhibited for translation, and upon removal of translational inhibition this mRNA was likely degraded and did not result in a large increase in MYC protein expression.

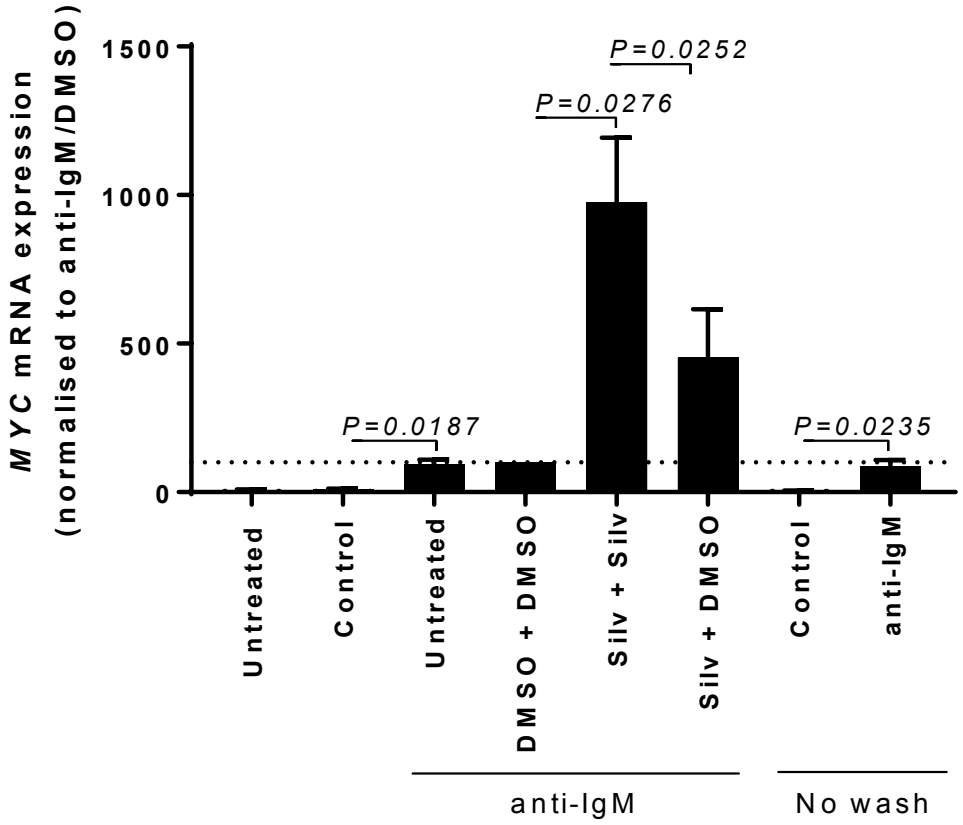

Figure 4-12. *MYC* mRNA expression following anti-IgM and silvestrol treatment followed by silvestrol wash-out

CLL samples (n=4) were pre-treated with silvestrol (20 nM) or DMSO for one hour. Samples were then treated with control antibody or anti-IgM for three hours. Cells were washed in warm medium four times (excluding the 'no wash' control cells), then re-plated with or without silvestrol or DMSO, then re-incubated for a further three hours. Cells were lysed and RNA extracted then Taqman qPCR was performed for *MYC* and *B2M*. Graph shows *MYC* mRNA expression normalised to *B2M* with values for anti-IgM/DMSO-treated cells set to 100. Error bars show SEM and the statistical significance of the indicated differences was determined using a paired T-test.

4.4 Summary of main findings

The overall aim of this chapter was to investigate in detail the effects of eIF4Ai on the translation, steady-state expression and stability of *MYC* mRNA in anti-IgM-treated CLL cells.

The main findings arising from these experiments were;

- Silvestrol reduced anti-IgM-induced polysome-association of *MYC* and *MCL1* mRNAs in CLL cells
- eIF4Ai treatment in the presence of anti-IgM resulted in an unexpected hyper-induction of *MYC mRNA (*and *MCL1* mRNA to a lesser extent)
- Hyper-induction of *MYC* mRNA in anti-IgM/silvestrol-treated CLL cells was due at least in part, in part, to increased mRNA stability
- Silvestrol treatment was reversible and removal of drug resulted in restored MYC protein expression, with reduced accumulation of *MYC* mRNA

Overall, these results support the hypothesis that eIF4Ai reduce anti-IgM-induced expression of MYC and MCL1 by inhibition of mRNA translation. Analysis of the turnover of *MYC* mRNA also confirmed the secondary hypothesis that inhibition of translational initiation by eIF4Ai was associated with stabilisation of *MYC* RNA.

4.5 Discussion

4.5.1 Inhibition of polysome-associated translation of *MYC* and *MCL1* mRNA by silvestrol

Fractions collected from polysome profiling demonstrated directly that the inhibitory effects of silvestrol on anti-IgM-induced MYC and MCL1 protein expression described in Chapter 3 were associated with inhibition of *MYC* and *MCL1* mRNA translation. Thus, there was an increase in polysome-associated *MYC/MCL1* translation by anti-IgM treatment, which was reduced by silvestrol (Figure 4-1). Thus, eIF4A activity is important for the translation of these oncoproteins following stimulation, consistent with the presence of structured 5' UTRs in their mRNAs.

4.5.2 Accumulation of *MYC* mRNA after silvestrol treatment is due to increased mRNA stability

Previous studies have shown that translation of *MYC* RNA is coupled to its degradation (Wisdom and Lee, 1991), and other translation inhibitors act to increase *MYC* RNA expression at a post-transcriptional level (Wisdom and Lee, 1991). Within the coding region of *MYC*, there is a coding region instability determinant (CRD) sequence (Lemm and Ross, 2002). When the relative binding protein (CRD-BP) binds the CRD in *MYC*, the sequence is protected from polysome-associated endonucleases (Lemm and Ross, 2002). Following dissociation of the CRD-BP, the CRD is rapidly cleaved by these endonucleases (Lemm and Ross, 2002). Another region that renders *MYC* RNA unstable is the AU-rich region in its 3' UTR (Lemm and Ross, 2002). The presence of a CRD is the reason that *MYC* RNA requires translation to be degraded, as during translation the CRD-BP dissociates from the mRNA and during a phase of ribosome pausing this CRD would be left exposed and available to endonucleases, thus resulting in destabilisation of the mRNA (Lemm and Ross, 2002). Notably, this method of decay revolves around the elongation phase of translation (Presnyak et al., 2015, Radhakrishnan and Green, 2016), and thus accounts for why inhibition of translation elongation via cycloheximide increases *MYC* mRNA stability (Lemm and Ross, 2002, Wisdom and Lee, 1991).

Another method of RNA decay described states that the stability of an mRNA is determined by competition between translation initiation factors and the decapping complex of the 5' cap, or blocking of decay factors by ribosomes on the mRNA (Chan et al., 2018). These methods have been described in yeast (Beelman and Parker, 1994, Schwartz and Parker, 1999) but provide an interesting mechanism for the increased stability of *MYC* mRNA following silvestrol treatment.

The presence of a G-quadruplex in *MYC* RNA is described as the reason for which silvestrol targets *MYC*, due to its reliance on eIF4A for translation (Wolfe et al., 2014). This study also described an increase in *MYC* mRNA expression, although only after 45-minutes of silvestrol treatment (Wolfe et al., 2014). My data demonstrated that upon silvestrol treatment *MYC* mRNA became increasingly stable even following destabilisation after anti-IgM treatment (Figure 4-10), although the extent to which this occurred did not seem to fully account for the level of increase in total *MYC* mRNA expression with silvestrol. This suggested another mechanism may also contribute to the increase in *MYC* mRNA expression observed in anti-IgM and silvestrol treated cells. Bordeleau and colleagues previously described a potential mechanism for silvestrol, involving stimulating the RNA-binding activity of eIF4A *in vivo*, which could account for the accumulation and associated increased stability of *MYC* mRNA seen in this study (Bordeleau et al., 2008). With a forced interaction between eIF4A and its target mRNAs, the mRNA will cease to be translated, thus not initiating its subsequent degradation to occur and preventing recycling of eIF4A back into the eIF4F complex for further translation to occur (Bordeleau et al., 2008).

An alternative eIF4Ai, hippuristanol, acts by preventing free and eIF4F-bound eIF4A binding to its target RNA, thus preventing initiation of translation (Bordeleau et al., 2006). More recently, Chan and colleagues described how inhibition of translation initiation destabilised mRNAs due to increased mRNA decay (Chan et al., 2018). This study was also performed using hippuristanol which inhibits eIF4A but has a distinctively different mechanism of action to compounds such as rocaglamide and silvestrol. This conclusion by Chan and colleagues is inconsistent with my data as the mechanism by which translation initiation is inhibited appears to alter the stabilisation of the mRNA in question. Forced dimerization of RNA:eIF4A by silvestrol has shown to increase stability of *MYC,* likely due to blocking degradation factors and the CRD in *MYC.* Although, my data agrees with their conclusion in that initiation efficiency can act as a determinant of RNA stability.

Earlier studies have described that treating CLL cells with silvestrol (80 nM) for up to 12 hours does not increase the expression of *MCL1* mRNA (Lucas et al., 2009). This correlates with the data presented here, in that silvestrol has no effect on basal *MCL1* expression (Appendix A), and demonstrates further that the accumulation of *MCL1* mRNA **Error! Reference source not found.**following silvestrol treatment is dependent upon stimulation of sIgM. This further demonstrates dysregulation of translation following stimulation of the BCR playing a role in CLL disease progression. It is again clear that regulation of *MCL1* by BCR-stimulation and mRNA translation is less than *MCL1* in comparison to *MYC*.

It is important to consider the use of actinomycin D in the study into RNA stability in section 4.3.4. Actinomycin D acts as a transcriptional inhibitor and thus inhibits the transcription of all pol II

dependent transcripts. This results in a global stress response (Chan et al., 2018, Sun et al., 2012) which must be considered when analysing any data produced. Whilst I demonstrated that the duration and concentration of actinomycin D treatment used in section 4.3.4 had minimal consequence on cell survival (Appendix A) and the experiments in section 4.3.4 were performed in the presence of a caspase inhibitor, it may be that cell stress and death processes were beginning to occur prior to the collection of cells.

4.5.3 Reversibility of the effects of silvestrol treatment

Bordeleau et al (2008) demonstrated reversibility of silvestrol in its ability to inhibit mRNA translation, via a ^{35}S-methionine incorporation assay (Bordeleau et al., 2008), although this study was performed using the HeLa cell line and thus may produce somewhat different results than in non-dividing primary tumour cells. To further understand the reversibility of silvestrol in inhibition of MYC protein expression and the consequence on the accumulation of *MYC* mRNA in CLL samples, a drug wash-out experiment was performed (section 4.3.5). The accumulated *MYC* mRNA, if translated following removal of silvestrol, could have major consequences. Particularly, if MYC expression was to rapidly increase it could result in cell death, or could drive proliferation and contribute to disease progression.

Here, removal of silvestrol recovered MYC protein expression, but only to a similar expression level of cells solely treated with anti-IgM/DMSO (Figure 4-11). There was also a reduction in *MYC* mRNA expression (Figure 4-12), which would be expected to slowly return over-time to similar expression of *MYC* seen in anti-IgM/DMSO-only treated cells. Thus, despite an accumulation of *MYC* mRNA in anti-IgM/silvestrol-treated cells, this was not reflected in a matching elevation of MYC protein expression following drug removal. This implied that accumulated *MYC* mRNA from silvestrol treatment remained inhibited from translation and upon removal of this silvestrol-induced blockade the mRNA was likely degraded and not sent for translation. Clinically, this would likely mean that no massive increase in MYC expression would drive disease progression following cessation/any pause of silvestrol treatment.

Chapter 5

The effects of eIF4E inhibitor, ribavirin, on anti-IgM-induced MYC and MCL1 expression and the nuclear export of RNA

5.1 Introduction

The focus for the experiments described in this chapter was to investigate the consequences of inhibition of a second translation initiation factor eIF4E, using ribavirin. eIF4E is a core component of the eIF4F translation initiation complex. Within this complex, eIF4E is rate-limiting (Gingras et al., 1999b), implying that initiation of mRNA translation is reliant upon the expression of eIF4E and thus targeting of eIF4E may have therapeutic utility. eIF4E binds the m^7G cap of mRNA during cap-dependent translation initiation to facilitate recruitment of the 40S ribosomal subunit to mRNA (Kraljacic et al., 2011). Some mRNAs are more reliant upon eIF4E for their translation than others, due to complexity in the secondary structures of their 5' UTR. Over-expression of eIF4E relieves the translational repression associated with complex secondary structures in 5' UTR of mRNA and allows for easier scanning of the 43S PIC. With this, increased eIF4E expression has been associated with increased mRNA translation of oncogenes with complex 5' UTR such as *MYC* (Koromilas et al., 1992). Thus, sensitivity to eIF4E for mRNA translation is determined by the stability and complexity of the 5' UTR of capped mRNAs (Koromilas et al., 1992). mRNAs with shorter and less complex 5' UTR are less reliant upon eIF4E for mRNA translation and are less affected by the availability of eIF4E (Wendel et al., 2007, Sonenberg and Hinnebusch, 2009).

Although the precise mechanism of action by which ribavirin interferes with eIF4E function is unclear, this synthetic nucleoside analogue may act as a mimic of the 5' m^7G cap of an mRNA and binds eIF4E, thus preventing recruitment of the eIF4F complex and the 40S ribosome to the mRNA (Kentsis et al., 2004). Although other studies have suggested that ribavirin does not act as a cap analogue (Yan et al., 2005), more recent studies have further demonstrated that ribavirin does bind eIF4E in replacement of the 5' cap and induces conformational changes in eIF4E (Volpon et al., 2013).

Ribavirin is currently used in patients as an anti-viral therapy (eg. for hepatitis C infection), but has shown potential as a translational inhibitor in clinical trials in acute leukaemia resulting in some partial and complete remissions (Assouline et al., 2009) along with a more recent trial using ribavirin in combination with chemotherapy (Assouline et al., 2015). Therefore, ribavirin is already well profiled clinically and may be promising to move into clinical trials of B-cell malignancies designed to evaluate therapeutic effects of translation inhibitors more quickly than other compounds.

In addition to its role in translation initiation, studies have demonstrated a role of eIF4E in nuclear export of some mRNAs. Around 70% of eIF4E exists within the nucleus (Iborra et al., 2001), implying that the role of eIF4E in nuclear export is significant. In aggressive lymphomas, eIF4E is required for the export of *MYC* and *BCL2* mRNAs and is linked to tumorigenesis and transformation (Culjkovic-Kraljacic et al., 2016). Thus eIF4E and its associated role in nuclear export is key in disease

progression in B-cell tumours. mRNAs exported from the nucleus by eIF4E contain a 50-nucleotide 4E-SE in their 3' UTR. One of the first mRNAs identified to be regulated by eIF4E at the level of transport is *CCND1* (encoding for cyclin D1). The function of eIF4E to facilitate nuclear export, as well as mRNA translation, also requires its cap-binding abilities and so mRNAs which are to be transported and/or translated require a 5' cap as well as a 3' 4E-SE. Notably, ribavirin interferes with eIF4E-dependent nuclear export of certain mRNAs, including *CCND1* and *MYC* (Osborne and Borden, 2015).

eIF4E is over-expressed in malignancies such as carcinomas (Kerekatte et al., 1995) and in CLL (Martinez-Marignac et al., 2013). A previous study demonstrated that ribavirin did not induce apoptosis of CLL cells *in vitro,* but did reduce expression of anti-apoptotic protein BCL2 (Martinez-Marignac et al., 2013). However, in this study, the impact of sIgM stimulation co-treatment with ribavirin was not investigated. The impact of inhibition of eIF4E by ribavirin in CLL, and the consequences on mRNA translation, MYC and MCL1 expression, and the nuclear export of RNAs following sIgM stimulation are yet to be fully elucidated.

5.2 Hypothesis and aims

5.2.1 Hypothesis

The primary hypothesis for this chapter was that the eIF4E inhibitor, ribavirin, will inhibit anti-IgM-induced expression of key target proteins, MYC and MCL1, in CLL cells potentially by reducing nuclear export of their mRNAs. The secondary hypothesis was that ribavirin would exert anti-tumour activity in an adoptive transfer model utilising Eμ-*TCL1* leukaemic cells as a model of CLL.

5.2.2 Aims

The specific aims of this chapter were to:

- Investigate the effect of ribavirin on mRNA translation in healthy donor B cells and CLL cells
- Characterise the effects of ribavirin on anti-IgM-induced MYC and MCL1 protein and mRNA expression
- Investigate the effects of ribavirin on sIgM expression and upstream signalling
- Investigate the effects of ribavirin on the regulation of translation initiation factors with anti-IgM treatment
- Determine the effects of ribavirin on CLL cell survival in the presence or absence of anti-IgM
- Characterise the effects of ribavirin on anti-IgM-induced cyclin D1 expression
- Determine the effects of anti-IgM and ribavirin treatment on mRNA nuclear export
- Compare responses seen following ribavirin treatment with that of the XPO1 inhibitor, selinexor
- Investigate *in vivo* responses to ribavirin in an adoptive transfer mouse model using Eμ-*TCL1* leukaemic cells

5.3 Results

5.3.1 The effects of ribavirin on anti-IgM-induced mRNA translation in CLL cells

I used the OPP-incorporation flow cytometry assay to investigate the effect of ribavirin on basal and anti-IgM-induced mRNA translation in CLL cells. CLL samples were pre-treated with ribavirin for one hour before treatment with anti-IgM for an additional 24 hours. Ribavirin was used at 1 or 10 μM as previous studies demonstrated that these concentrations disrupted eIF4E:mRNA binding in cells (Kentsis et al., 2004) and that these concentrations are readily clinically achievable in the plasma of patients undergoing therapy (Urtishak et al., 2019, Martinez-Marignac et al., 2013).

Ribavirin showed no effect on basal mRNA translation (Figure 5-1A). Following 24-hour anti-IgM treatment, ribavirin (10 μM) significantly inhibited anti-IgM-induced mRNA translation (Figure 5-1B). At 10 μM, ribavirin reduced anti-IgM-induced OPP labelling by ~25% (Figure 5-1B).

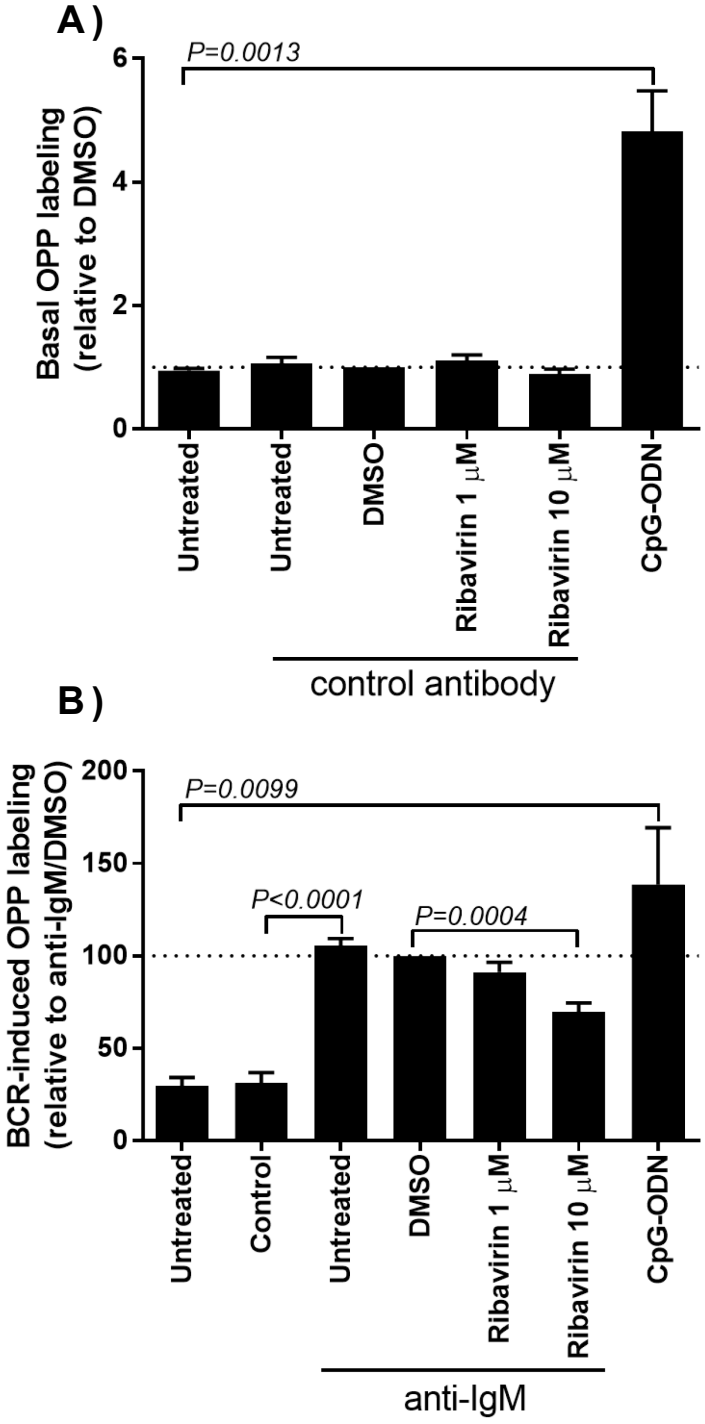

Figure 5-1. Ribavirin on basal and anti-IgM-induced OPP-labelling in CLL samples

CLL samples (n=4) were pre-treated with ribavirin or DMSO for one hour before treatment with control antibody, anti-IgM, or CpG-ODN for an additional 24 hours, as indicated. Translation was then analysed by measuring OPP incorporation in the $CD5^+$ $CD19^+$ cell population. Values for control antibody/DMSO treated cells were set to 1 (A) or anti-IgM DMSO treated cells set to 100 (B) to measure basal translation and anti-IgM-induced translation, respectively. Error bars show SEM and the statistical significance of the indicated differences was determined using paired T tests.

5.3.2 The effects of ribavirin on global mRNA translation in healthy donor B cells

The next series of experiments investigated the effects of ribavirin on basal and anti-IgM-induced mRNA translation in B cells from healthy donors using the OPP-incorporation assay. As in Figure 3-11, antibodies were included in the FACS analysis to enable specific measurement of responses in $CD19^{+}CD5^{-}IgG^{-}$ B cells.

In contrast to its effects in CLL cells, ribavirin did not reduce basal or anti-IgM induced mRNA translation in non-malignant B cells (Figure 5-2). This is in contrast to silvestrol (Figure 3-11), which significantly reduced anti-IgM-induced OPP-labelling in B cells from healthy donors. Thus, like eIF4Ai, ribavirin reduces anti-IgM-induced global mRNA translation in CLL cells. However, in contrast to silvestrol, effects of ribavirin appear to be selective for CLL cells compared to normal B cells, at least as measured using OPP-labelling.

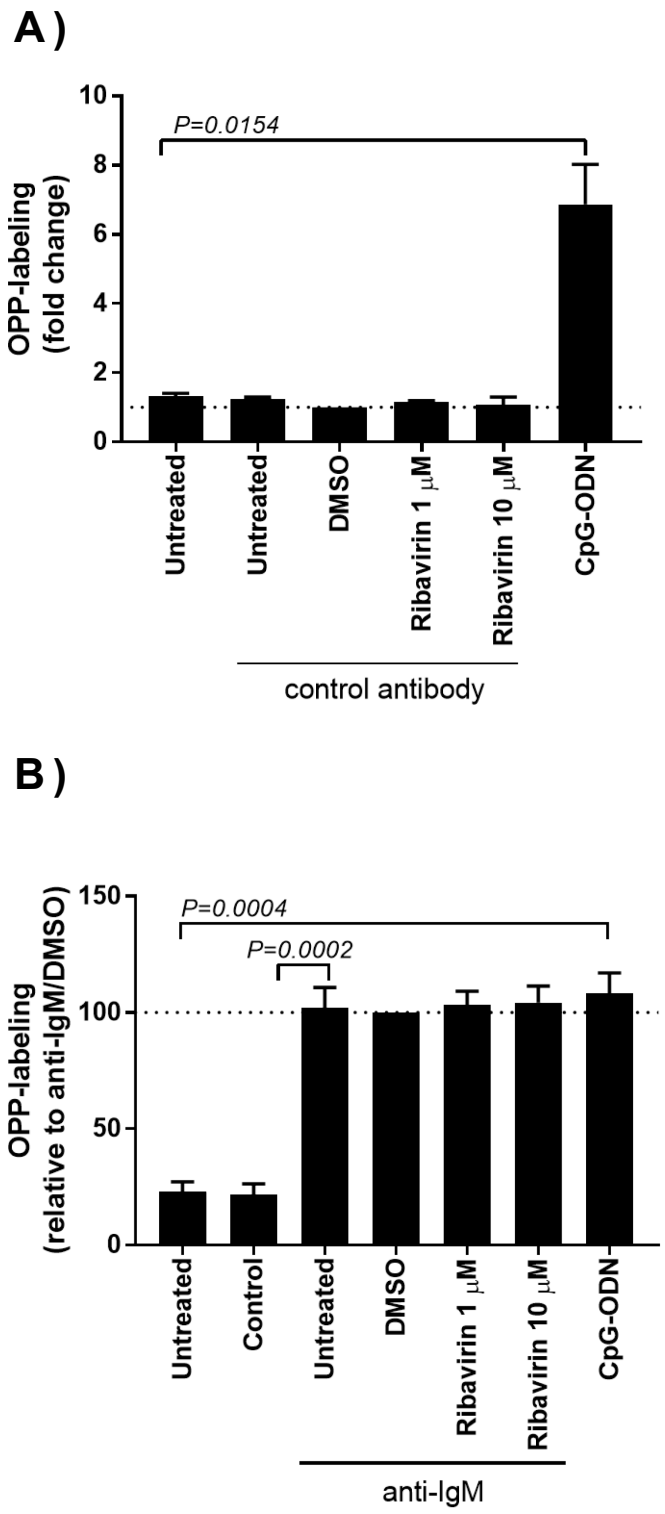

Figure 5-2. Ribavirin on basal and anti-IgM-induced OPP labelling in healthy donor B cells

PBMCs from healthy donors (n=6) were pre-treated with ribavirin or DMSO for one hour before treatment with control antibody, anti-IgM, or CpG-ODN for an additional 24 hours, as indicated. OPP incorporation was measured in the $CD19^{+}CD5^{-}IgG^{-}$ cell population. Values for control antibody/DMSO treated cells were set to 1 (A) or anti-IgM DMSO treated cells set to 100 (B) to measure basal translation and anti-IgM-induced translation, respectively. Error bars show SEM and the statistical significance of the indicated differences was determined using paired T tests. Experiments performed in collaboration with Dr Karly-Rai Rogers-Broadway.

5.3.3 The effect of ribavirin treatment on anti-IgM-induced MYC and MCL1 protein expression

I next investigated the effect of ribavirin on the expression of MYC and MCL1. Initial analysis of MYC expression was performed at six hours following anti-IgM stimulation, to match experiments performed using eIF4Ai (Figure 3-7). At this time point, ribavirin only very modestly reduced MYC expression (Figure 5-3). This was surprising, considering that ribavirin has been shown to reduce MYC expression in other cell systems (Urtishak et al., 2019).

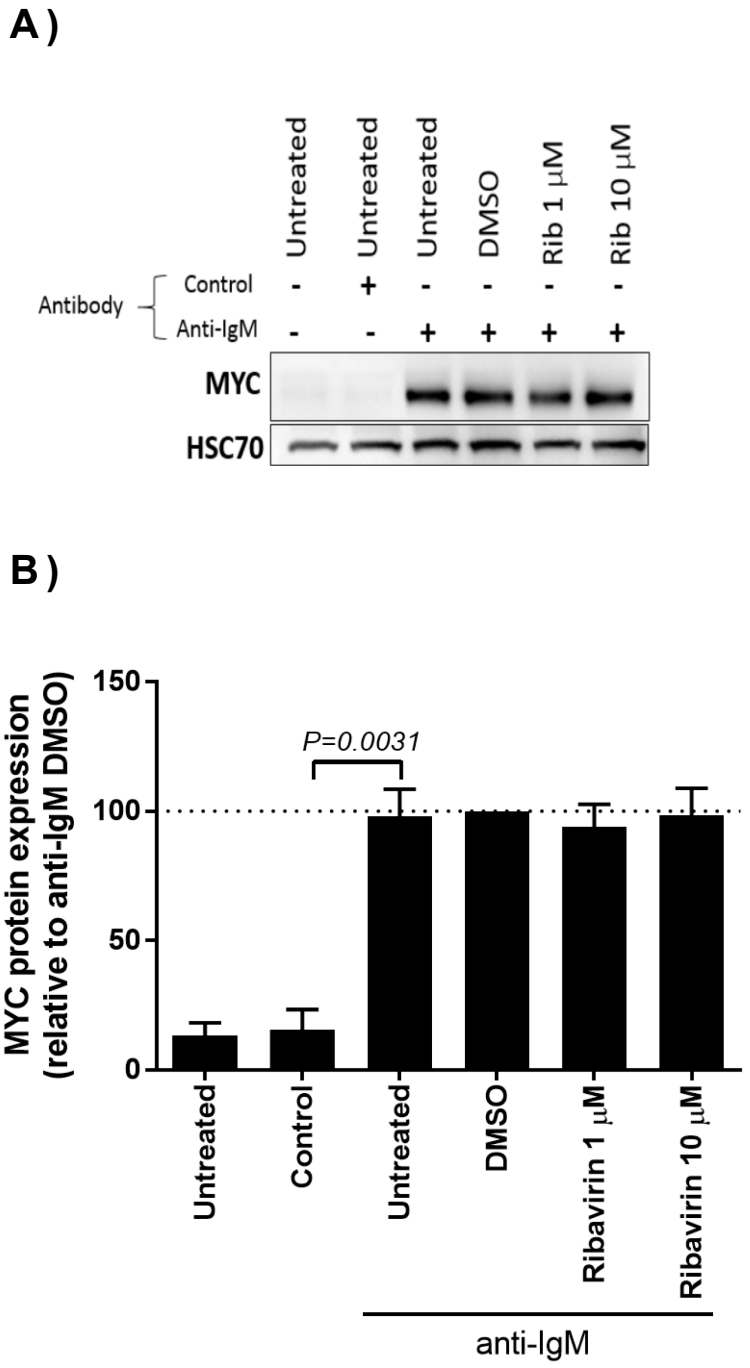

Figure 5-3. MYC expression following 6 hour sIgM-stimulation and ribavirin treatment

CLL samples (n=4) were pre-treated with ribavirin for one hour before an additional six hour treatment with anti-IgM or control antibody. After collection, cells were lysed and proteins extracted then immunoblotting was undertaken and blots probed for MYC and HSC70 as a loading control. (A) Western blot of representative sample U-929. (B) Values for MYC expression were made relative to anti-IgM/DMSO treated control set to 100. Error bars show SEM and the statistical significance of the indicated differences was determined using paired T tests.

I therefore investigated whether longer incubations with ribavirin were required to observe stronger inhibitory effects. After 24 hour anti-IgM treatment there was a strong induction of MYC protein expression (Figure 5-4B), which was significantly inhibited by ribavirin at both concentrations (1 and 10 μM). Variation in the loading in this immunoblot may be due to altered loading or small amounts of cell death. As the densitometries are normalised to the loading control (HSC70), the MYC expression is relative to this loading and takes this into account. This demonstrates that anti-IgM-induced MYC expression is sensitive to the inhibition of eIF4E, but the effects of ribavirin require relatively long incubation times, at least compared to eIF4Ai.

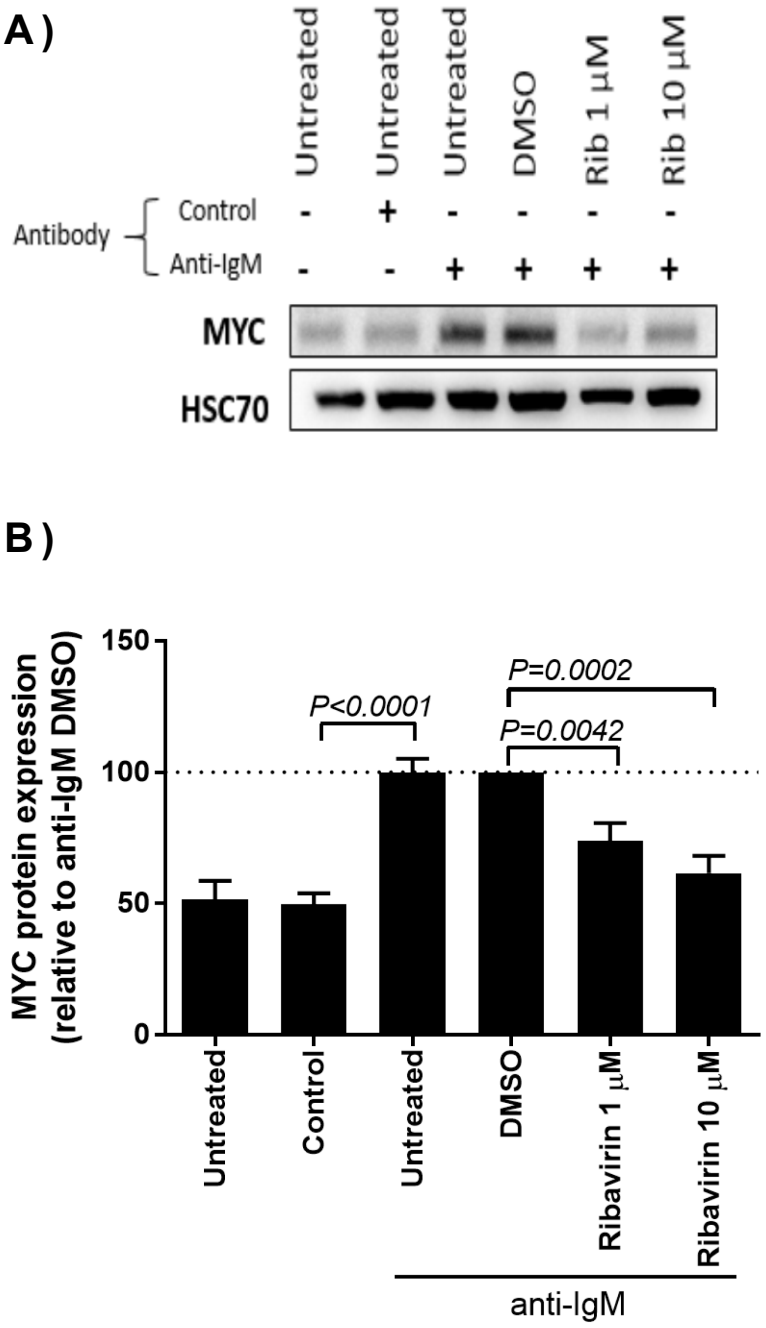

Figure 5-4. MYC expression following 24 hour anti-IgM and ribavirin treatment

CLL samples (n=10) were pre-treated with ribavirin or DMSO for one hour before treatment with control antibody or anti-IgM for an additional 24 hours. After collection, cells were lysed and proteins extracted then immunoblotting was undertaken and blots probed for MYC and HSC70 as a loading control. A) Western blot for representative sample U-816C. (B) MYC protein expression with values for anti-IgM/DMSO treated cells set to 100. Error bars show SEM and the statistical significance of the indicated differences was determined using paired T tests.

The effects of ribavirin on MCL1 expression were also examined at 24 hours, which matches the time point used to investigate effects of eIF4Ai (Figure 3-8). There was a significant induction of MCL1 protein expression following 24 hour anti-IgM treatment which was reduced by ribavirin (Figure 5-5). However, the inhibitory effects of ribavirin on MCL1 expression were very modest compared to MYC (maximal reduction in MCL1 expression of ~20% with 10 μM ribavirin) and were not statistically significant (Figure 5-5).

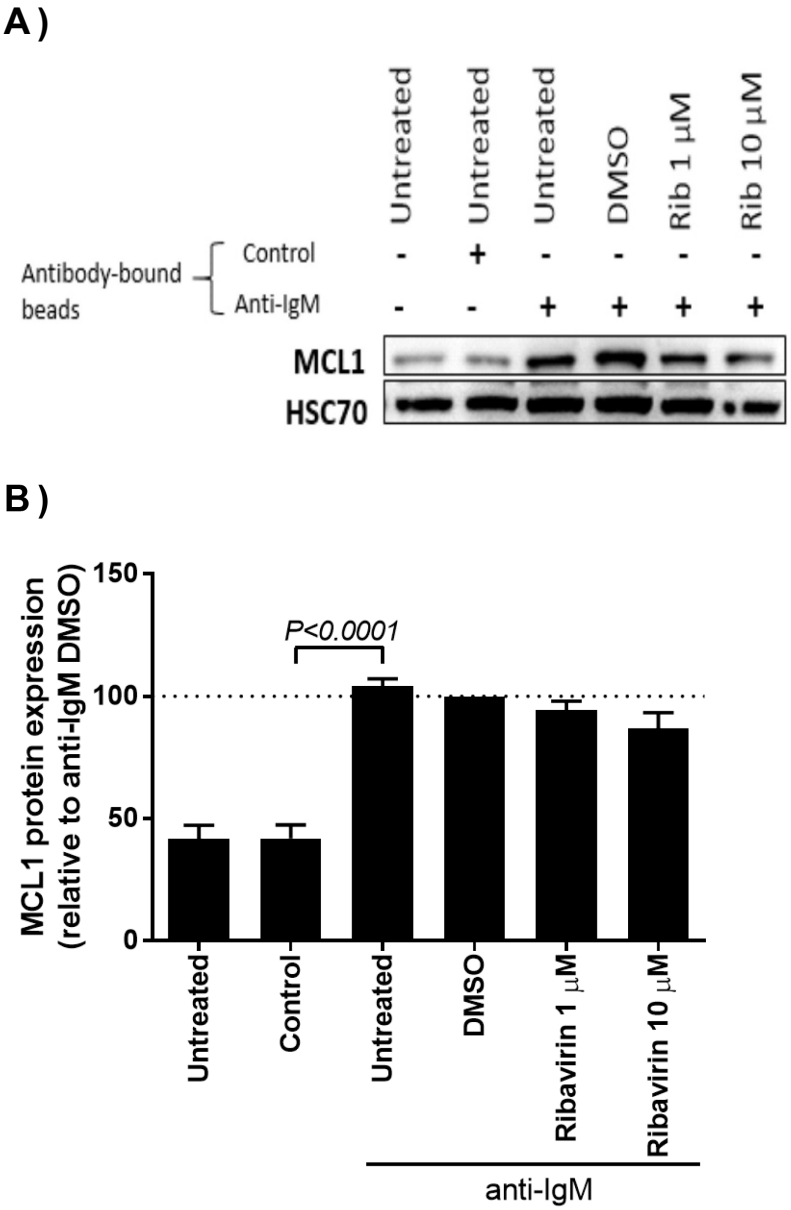

Figure 5-5. MCL1 expression following 24 hour anti-IgM and ribavirin treatment

CLL samples (n=14) were pre-treated with ribavirin or DMSO for one hour before treatment with control antibody or anti-IgM for an additional 24 hours. After collection, cells were lysed and proteins extracted then immunoblotting was undertaken and blots probed for MCL1 and HSC70 as a loading control. A) Western blot for representative sample U-929. B) MCL1 protein expression with values for anti-IgM/DMSO treated cells set to 100. Error bars show SEM and the statistical significance of the indicated differences was determined using paired T tests.

5.3.4 The effect of ribavirin on *MYC* and *MCL1* mRNA expression

To further investigate the consequences of eIF4E inhibition, the effect of ribavirin on *MYC* and *MCL1* mRNA expression was studied. CLL samples were treated for one hour with ribavirin, followed by 24 hour anti-IgM treatment. RNA was extracted and Taqman qPCR was performed to quantify *MYC, MCL1* and *B2M* mRNA expression. 24 hour anti-IgM treatment was chosen to match the analysis of the effects of ribavirin on protein expression.

There was a significant induction of *MYC* mRNA expression following 24-hour anti-IgM treatment (~75% increase), which was reduced to a small (~10%) but statistically significant extent by ribavirin (Figure 5-6A). Induction of *MCL1* mRNA expression was modest (~40% increase) and did not reach statistical significance in this series of experiments (Figure 5-6B). Ribavirin did not alter anti-IgM-induced *MCL1* mRNA expression (Figure 5-6B). Ribavirin also had no effect on *B2M* expression *per se*, by analysis of Ct values (Appendix B). Overall, these data demonstrate that reduced MYC protein induction by ribavirin is not associated with reduced *MYC* mRNA expression, consistent with a post-transcriptional mechanism of regulation. Moreover, unlike eIF4Ai, ribavirin does not hyper-induce *MYC* mRNA expression in the presence of anti-IgM.

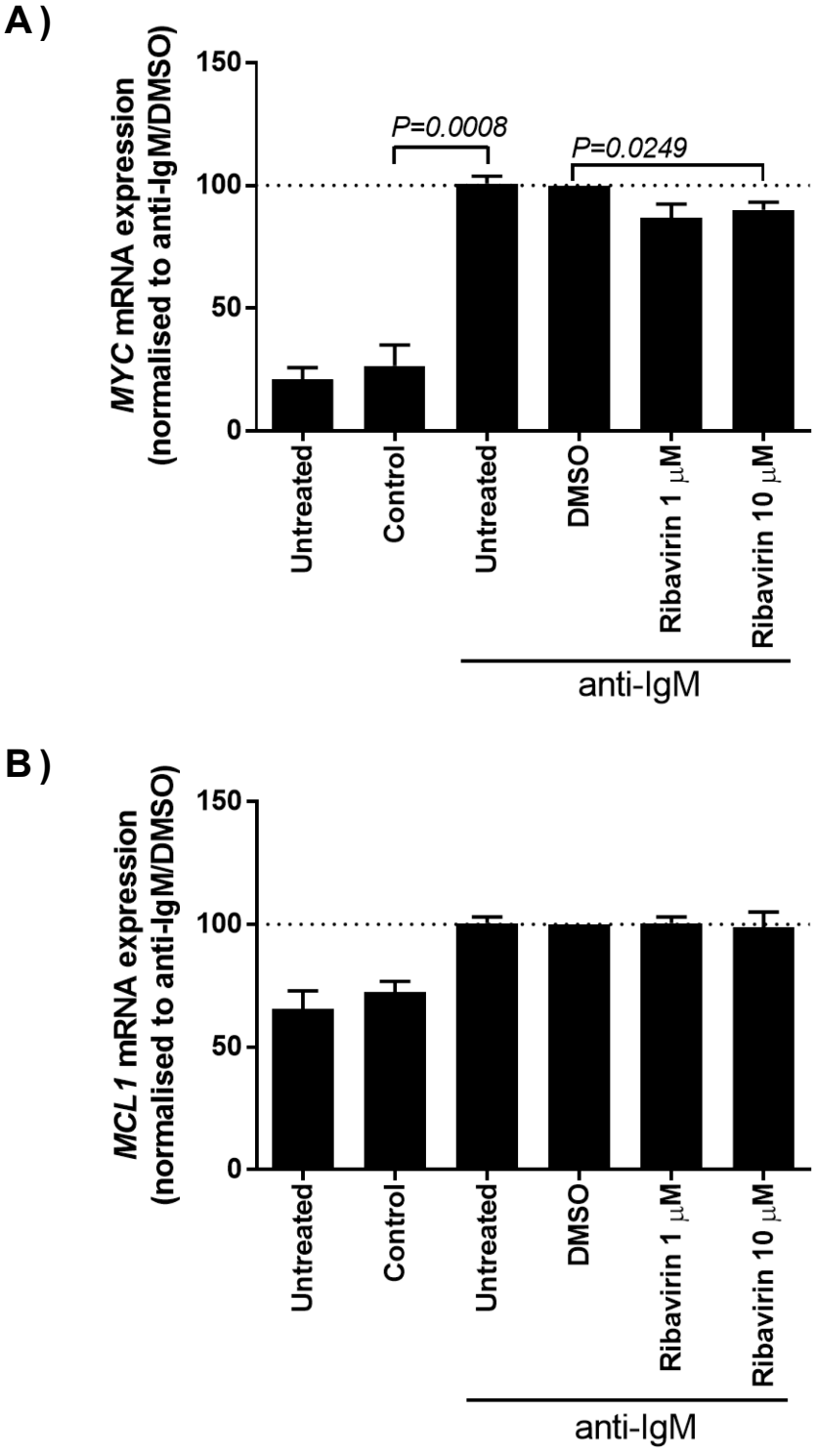

Figure 5-6. *MYC* and *MCL1* mRNA expression following sIgM-stimulation and ribavirin treatment

CLL samples (n=6) were pre-treated with ribavirin or DMSO for one hour and then treated with control antibody or anti-IgM for an additional 24 hours. *MYC, MCL1* and *B2M* mRNA expression measured by Taqman qPCR. *MYC* (A) and *MCL1* (B) mRNA expression relative to *B2M* expression with values for anti-IgM/DMSO treated cells set to 100. Error bars show SEM and the statistical significance of the indicated differences was determined using paired T tests.

5.3.5 The effect of ribavirin on sIgM expression and upstream signalling

A previous study identified multiple mRNAs associated with BCR signalling (including *CD19, BTK, LYN, PLCG2)* as potential eIF4E targets, since they were bound to eIF4E in eIF4E-RNA immunoprecipitation experiments (RIP) (Culjkovic-Kraljacic et al., 2016). It was therefore important to determine whether the reduction in MYC expression in anti-IgM treated cells was a consequence of reduced sIgM expression/function *per se*. To address this, I analysed the effects of ribavirin on sIgM expression, anti-IgM-induced ERK phosphorylation, and Ca^{2+} mobilisation as measures of sIgM function.

To investigate potential effects of ribavirin on sIgM expression, CLL samples were recovered for one hour then treated with ribavirin for 24-hours before staining for sIgM and analysis by flow cytometry (described in section 2.2.5). There was no clear effect of ribavirin on sIgM expression at either concentration tested (Figure 5-7).

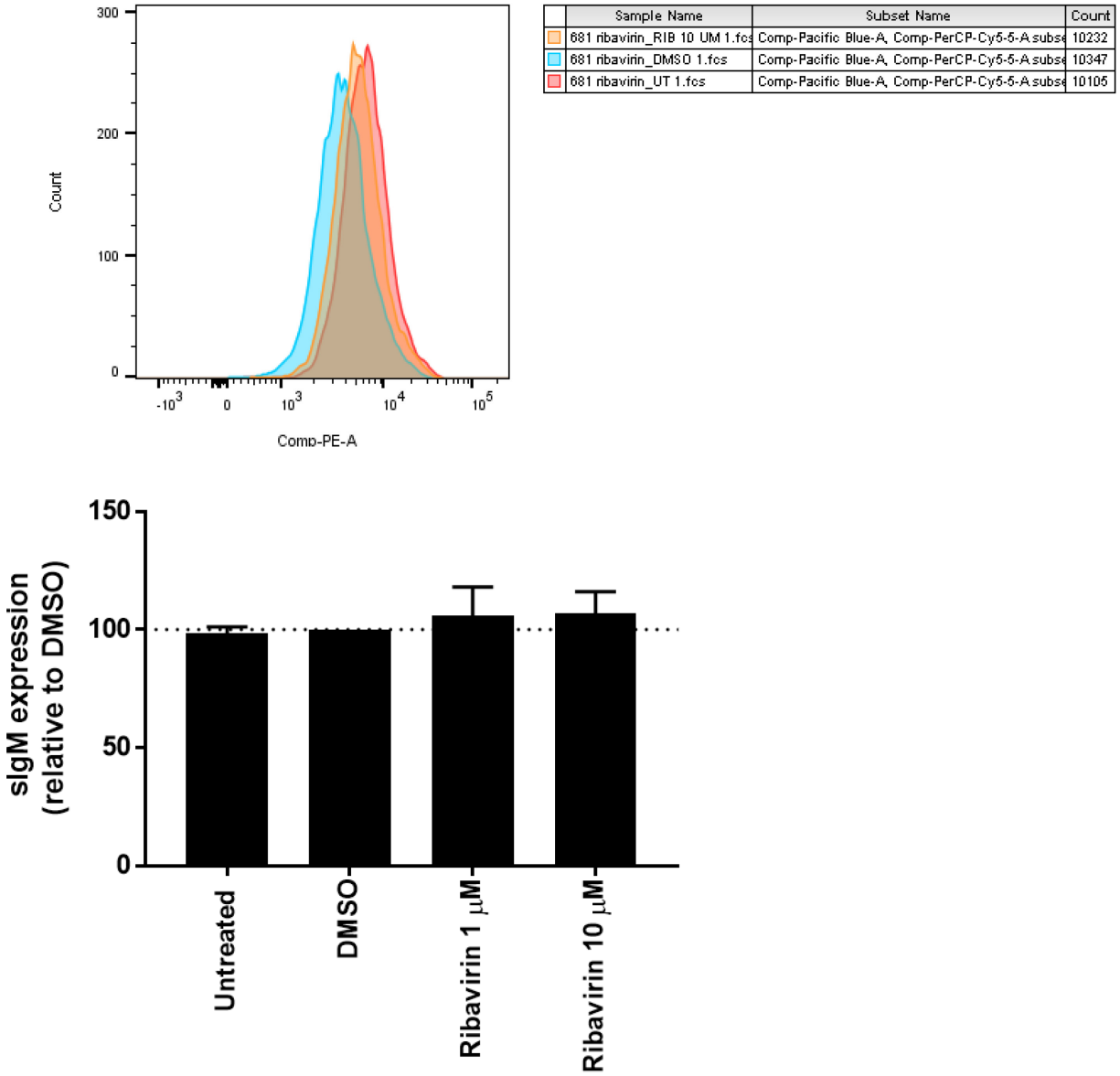

Figure 5-7. The effect of ribavirin on surface IgM expression

CLL samples (n=4) were treated with ribavirin or DMSO for 24 hours. Cells were collected and sIgM expression was analysed via flow cytometry in the $CD5^+$ $CD19^+$ cell population, as described in section 2.2.5. Top panel shows representative histogram overlays of PE fluorescence (sIgM expression) for sample M-681, for untreated (red), DMSO treated (blue) and ribavirin (10 µM) treated cells (orange). Bottom graph summarises data for all samples analysed and shows mean sIgM expression with values for DMSO treated cells set to 100. Error bars show SEM and the statistical significance of any differences was determined using paired T tests.

To investigate the effect of ribavirin on intracellular Ca^{2+} mobilisation, CLL samples were pre-treated with ribavirin for one hour before flow cytometry was performed, as described in section 2.2.4. As expected, anti-IgM induced a rapid intracellular Ca^{2+} flux in DMSO treated cells, whereas intracellular Ca^{2+} concentrations were unaffected by the control antibody. Addition of the Ca^{2+} ionophore, ionomycin, triggered intracellular Ca^{2+} flux in essentially all of the cells, confirming the competence of the sample to respond. However, ribavirin had no effect on anti-IgM-induced intracellular Ca^{2+} mobilisation in these CLL samples, at either concentration (Figure 5-8).

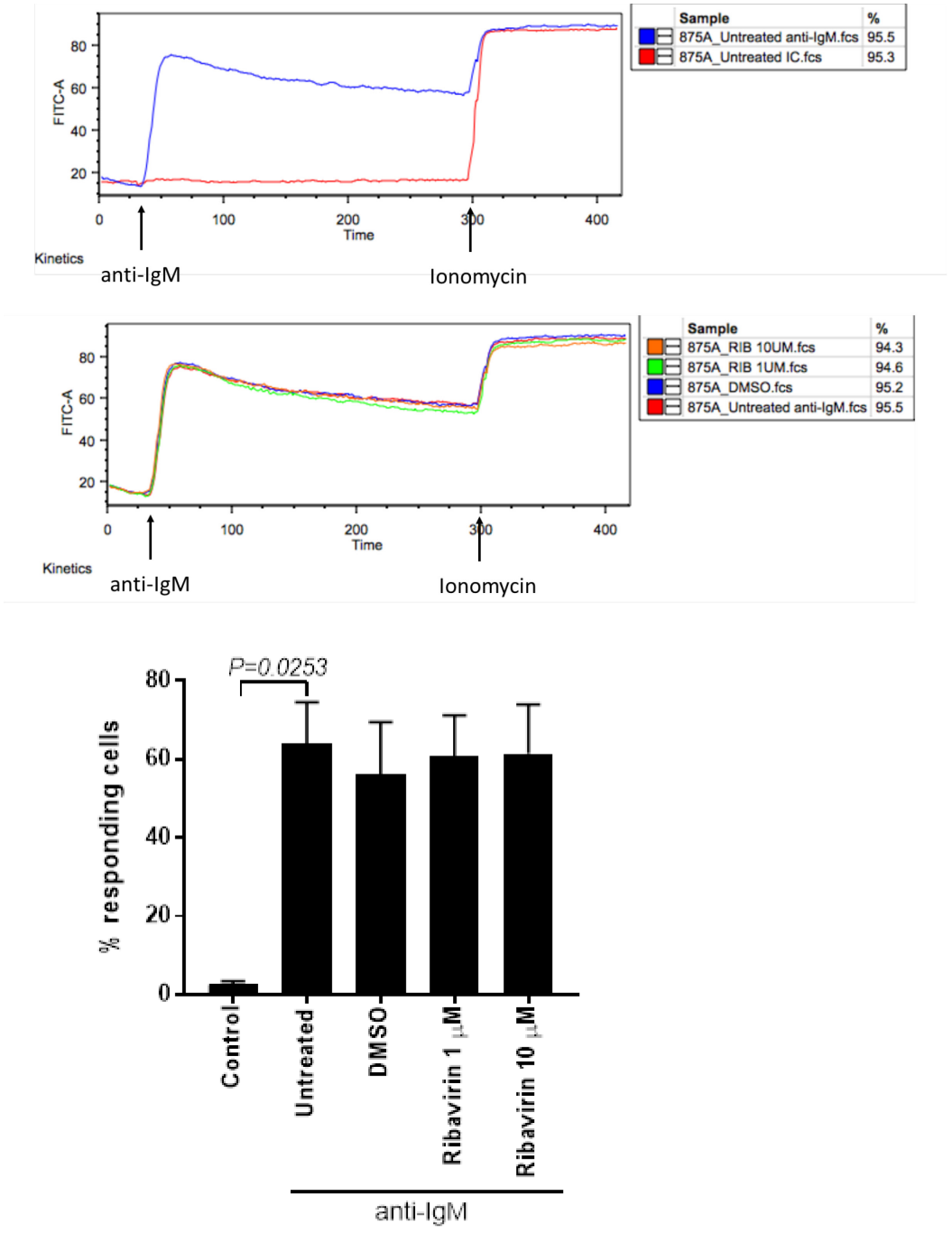

Figure 5-8. Percentage responding cells by calcium mobilisation following ribavirin and anti-IgM treatment

Anti-IgM-induced intracellular Ca^{2+} mobilisation studied after one hour ribavirin treatment (n=4). Fluorescence stained for flow cytometry using FITC-A and time measured (seconds) throughout response. Representative plots shown from sample U-875A Arrows denote anti-IgM treatment (or control/IC antibody in top graph) and ionomycin stimulation. Experiment performed as in section 2.2.4. Responding cells were calculated over the threshold (85^{th} percentile). Graph shows the percentage of cells responding to IgM stimulation by calcium mobilisation. Statistical significance of the indicated differences was determined by paired t-test.

Analysis of ERK-phosphorylation was performed following 24 hour anti-IgM treatment. There was a significant induction of ERK-phosphorylation at this time-point (Figure 5-9). There was a small (~10%) reduction in the mean increase in ERK-phosphorylation in cells pre-treated with ribavirin, but these differences were not statistically significant (Figure 5-9). In summary, ribavirin does not appear to have direct effects on sIgM signalling in CLL cells, since it did not alter sIgM expression or substantially effect anti-IgM-induced intracellular Ca^{2+} mobilisation or ERK-phosphorylation.

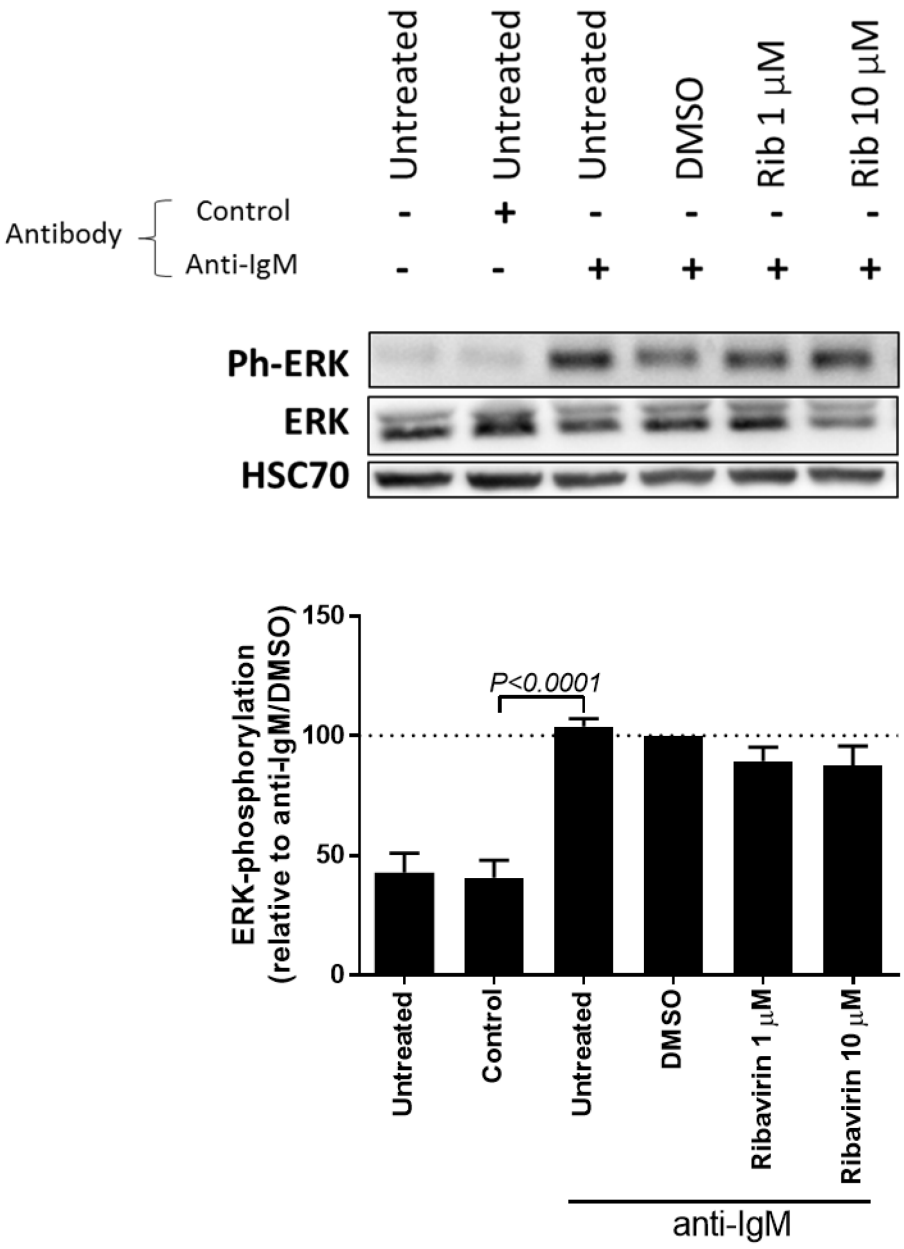

Figure 5-9. ERK-phosphorylation following sIgM-stimulation and ribavirin treatment

CLL samples (n=10) were pre-treated with ribavirin or DMSO for one hour. Samples were then treated with control antibody or anti-IgM for an additional 24 hours. After collection, cells were lysed and proteins extracted then immunoblotting was undertaken and blots probed for total ERK and phosphorylated ERK, and HSC70 as a loading control. Western blot from representative sample M-681 (top panel). Relative ERK phosphorylation with values for anti-IgM/DMSO treated cells set to 100 (bottom graph). Error bars show SEM and the statistical significance of the indicated differences was determined using paired T tests.

5.3.6 The effects of ribavirin on translation initiation factors

Since sIgM stimulation induces expression of eIF4A and eIF4G, and reduces expression of PDCD4 (Yeomans et al., 2015), it was important to investigate the effect of ribavirin on these responses. CLL samples were pre-treated with ribavirin for one hour and then treated for an additional 24 hours with anti-IgM. Expression of eIF4A, PDCD4 and eIF4G was measured using western blot.

Consistent with previous findings (Figure 3-6 and (Yeomans et al., 2015)), anti-IgM increased expression of eIF4A and eIF4G, and reduced expression of PDCD4. Ribavirin very modestly reduced the induction of eIF4A (~10%), and had no effect on eIF4G expression (Figure 5-10). Ribavirin also slightly increased PDCD4 expression in anti-IgM treated cells (~20%) (Figure 5-10). Overall, ribavirin did not substantially alter the expression of the examined proteins in anti-IgM treated cells.

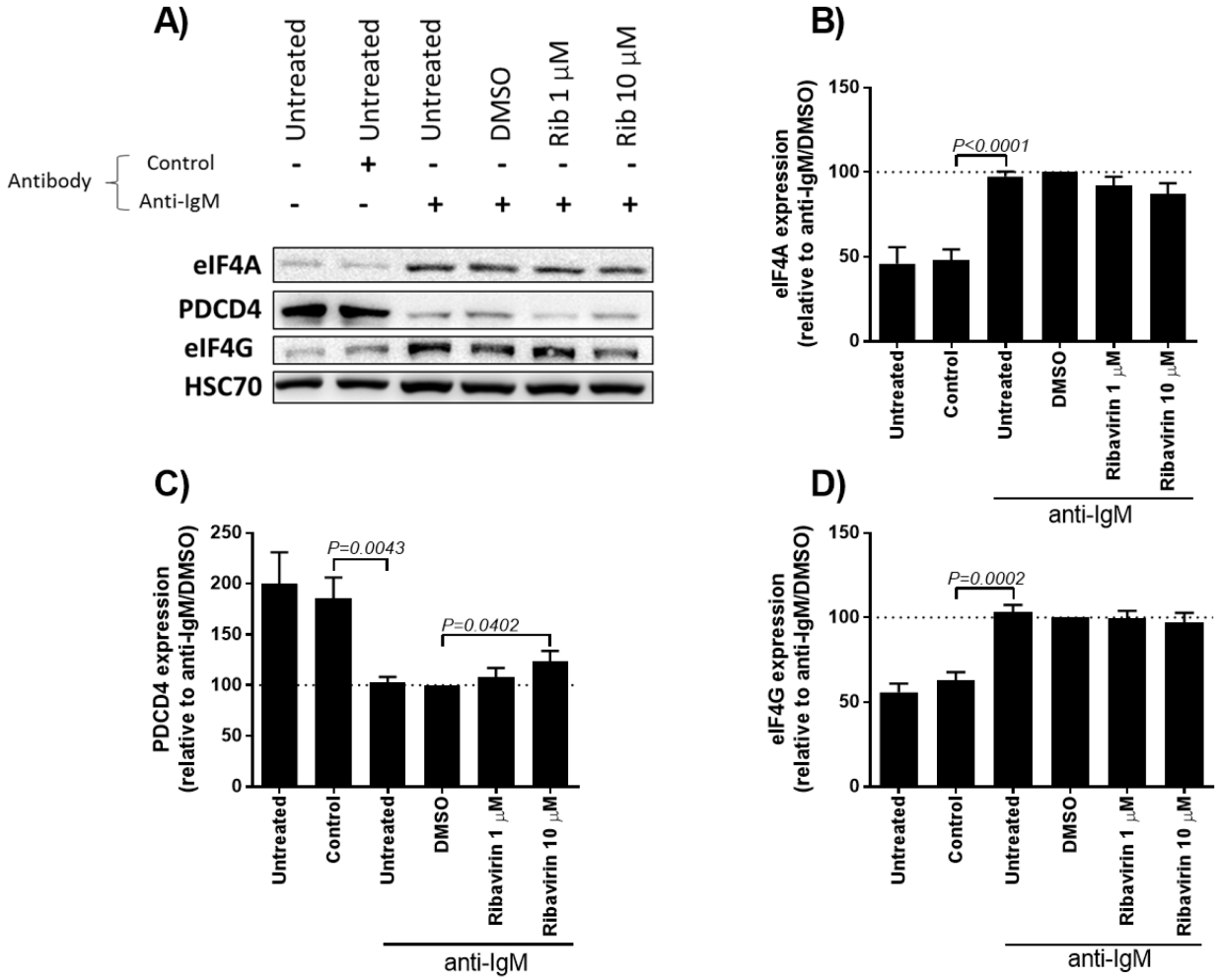

Figure 5-10. Expression of eIF4A, PDCD4 and eIF4G expression following sIgM-stimulation and ribavirin treatment

CLL samples (n=10) were pre-treated with ribavirin or DMSO for one hour then treated with control antibody or anti-IgM for an additional 24 hours. Expression of eIF4A, PDCD4, eIF4G and HSC70 (loading control) was analysed by immunoblotting. (A) Western blot from representative sample U-888B. Relative expression of eIF4A (B), PDCD4 (C) and eIF4G (D) protein expression with values for anti-IgM/DMSO treated cells set to 100. Error bars show SEM and the statistical significance of the indicated differences was determined using paired T tests.

Previous experiments have demonstrated that expression of eIF4E, the target of ribavirin, is not altered following sIgM stimulation of CLL cells (Figure 3-6). However, eIF4E function is also modulated by phosphorylation, so it was important to extend these studies to investigate the effects of anti-IgM and/or ribavirin on post-translational modification of eIF4E.

In the first experiments, CLL samples were stimulated with anti-IgM for 24 hours and expression and phosphorylation of eIF4E was analysed by immunoblotting. For phosphorylation, I used an antibody that detects phosphorylation at Ser209 which is induced by MNK1/2. Ser209 phosphorylation is thought to result in increased translation since it reduces the affinity of eIF4E for the 5' cap. One hypothesis is that phosphorylation of results in the release of initiation factors from the 5' cap after the 60S ribosome has begun scanning, allowing translation to occur and releasing the initiation factors for translation of other mRNAs (Scheper and Proud, 2002). Immunoblot analysis demonstrated that whereas overall expression of eIF4E was not regulated, anti-IgM significantly increased eIF4E Ser209 phosphorylation (~50%) (Figure 5-11A).

In addition to phosphorylation, eIF4E function can be regulated by binding of 4E-BP1 (Gingras et al., 1999a). Thus, mTORC1 dependent 4E-BP1 phosphorylation results in its dissociation from eIF4E, allowing eIF4E to be recruited to the eIF4F complex. I therefore studied expression of 4E-BP1 in these experiments (Figure 5-11). Immunoblotting revealed multiple bands for 4E-BP1 which are considered to represent hypo- (lower band) and hyper- (upper band) phosphorylated forms of 4E-BP1 (Gingras et al., 1999a) (Figure 5-11). It was not possible to reliably quantify these separate bands, so quantitation of the immunoblots was not performed. However, overall there did not appear to be substantial changes in 4E-BP1 expression/phosphorylation in anti-IgM-treated cells at this time-point (Figure 5-11).

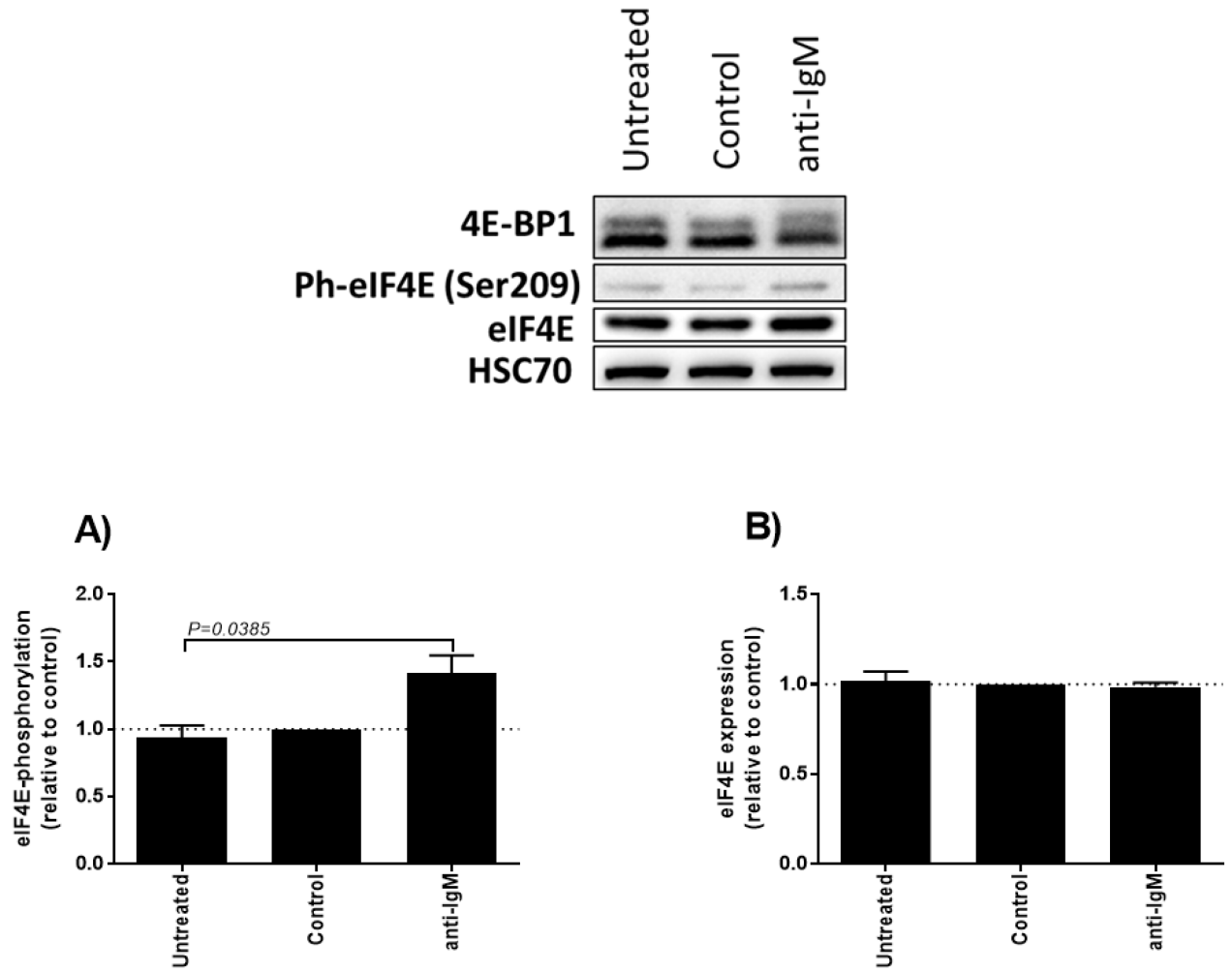

Figure 5-11. 4E-BP1, eIF4E-phosphorylation and eIF4E expression following sIgM-stimulation

CLL samples (n=7) were treated with control antibody or anti-IgM beads for 24 hours. Expression of 4E-BP1, eIF4E and phosphorylated-eIF4E (Ser209), and HSC70 as a loading control, was analysed by immunoblotting. Western blot from representative sample U-609A (top panel). (A) eIF4E-phosphorylation and (B) eIF4E expression with values for control antibody treated cells set to 1. Error bars show SEM and the statistical significance of the differences between each condition was determined using paired T tests. Quantitation was not performed for 4E-BP1 due to the difficulty of reliably resolving different protein isoforms.

Next, the effect of ribavirin on the expression of eIF4E and phosphorylation of eIF4E in anti-IgM treated cells was investigated. CLL samples were pre-treated with ribavirin for one hour and then treated for an additional 24 hours with anti-IgM. eIF4E, phosphorylated-eIF4E (Ser209) and HSC70 expression were analysed by western blot. As expected, anti-IgM did not alter eIF4E expression, but did increase phosphorylation at Ser209 (Figure 5-12). Interestingly, the increase in eIF4E-phosphorylation was effectively reduced by ribavirin (~25%) (Figure 5-12A). Ribavirin did not reduce total eIF4E expression (Figure 5-12B).

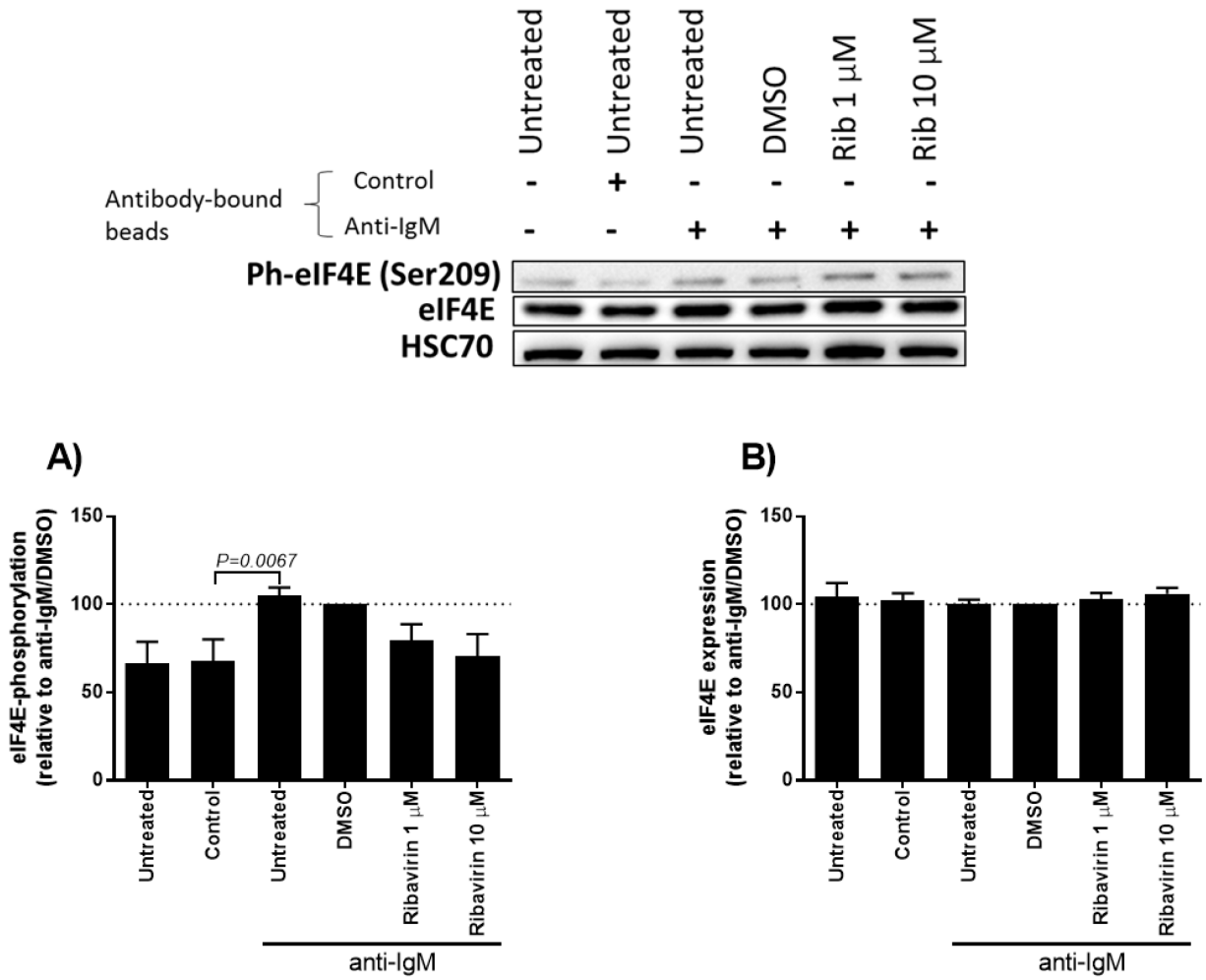

Figure 5-12. Expression of eIF4E and eIF4E-phosphorylation following anti-IgM and ribavirin treatment

CLL samples (n=7) were pre-incubated with ribavirin or DMSO for one hour, before treatment with control antibody or anti-IgM for an additional 24 hours. Expression of eIF4E and phosphorylated eIF4E, and HSC70 as a loading control, was analysed by immunoblotting. Western blot of representative sample U-609A (top panel). (A) eIF4E-phosphorylation and (B) eIF4E protein expression with values for anti-IgM/DMSO treated cells set to 100. Error bars show SEM and the statistical significance of the indicated differences was determined using paired T tests.

In summary, these studies extend previous investigations and reveal novel aspects of the effects of anti-IgM on components of the eIF4F complex in CLL cells. Although expression of eIF4E is unaltered, sIgM activation does result in increased phosphorylation of eIF4E (Figure 5-11), which has been linked to increased eIF4E activity (Scheper and Proud, 2002). Since ribavirin did not inhibit upstream signalling responses induced by anti-IgM (section 5.3.5), it was interesting to note that ribavirin did effectively reduce the increase in eIF4E phosphorylation in anti-IgM treated cells (Figure 5-12). It was somewhat surprising that anti-IgM did not alter 4E-BP1 phosphorylation (Figure 5-11), since mTORC1 is activated downstream of the BCR. However, it is possible that 4E-BP1 phosphorylation was transiently induced but had returned to background levels in these experiments performed at 24 hours post-stimulation.

5.3.7 The effects of ribavirin on apoptosis of CLL cells

The effects of ribavirin treatment for 24, 48 and 72 hours on CLL cell viability were investigated using Annexin V/PI FACs staining to probe basal apoptosis and cleavage of PARP by immunoblotting to investigate any effects in anti-IgM treated cells.

To analyse the effects of ribavirin in the absence of sIgM stimulation, CLL samples were treated with and without Q-VD-OPh, and with ribavirin (1 and 10 μM) for 24, 48 or 72 hours. Cells were then collected and stained for annexin V/PI flow cytometry (described in section 2.2.3). At all time-points it was clear that Q-VD-OPh protected CLL cells from spontaneous apoptosis (Figure 5-13), confirming the effectiveness of this caspase inhibitor. However, ribavirin did not induce cell death at up to 72 hours of treatment (Figure 5-13).

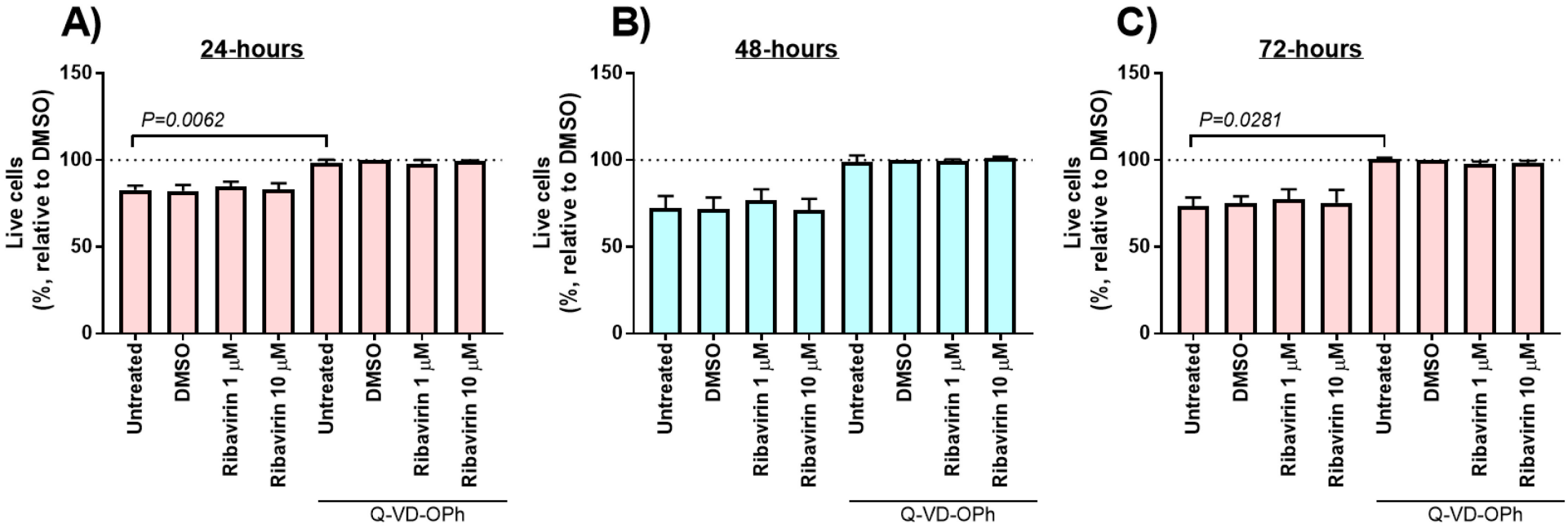

Figure 5-13. Ribavirin on basal CLL cell viability with and without Q-VD-OPh treatment

Basal cell viability (n=3) was investigated using Annexin V-PI flow cytometry. Samples were treated with or without ribavirin or DMSO, and Q-VD-OPh caspase inhibitor added where stated, and incubated for 24 (A), 48 (B) or 72 (C) hours before analysis. Cells were collected and cell survival was analysed via Annexin V-PI incorporation in the $CD5^{+}CD19^{+}$ cell population. Data shown is relative to Q-VD-OPh treated DMSO control set to 100. Error bars show SEM and the statistical significance of the indicated differences determined using paired T tests.

Next, PARP cleavage was analysed by western blot to investigate the effect of ribavirin on cell death following sIgM-stimulation. Samples were pre-incubated with ribavirin for one hour, followed by 24, 48 or 72 hour stimulation with anti-IgM (no Q-VD-OPh was added in these experiments).

Without sIgM stimulation, there was evidence of PARP cleavage at 24-hours, indicative of caspase activation associated with spontaneous cell death incubation (Figure 5-14 shows a representative sample and additional samples are shown in Appendix B). PARP cleavage was reduced with anti-IgM treatment, consistent with protection from spontaneous cell death by sIgM stimulation. However, it was notable that the extent of PARP cleavage in the unstimulated samples reduced over time (Figure 5-14). This likely reflects the presence of subpopulations of cells that underwent early spontaneous apoptosis and were rapidly deleted from the culture, leading to selection for retention of more apoptosis-resistant cells at later time-points. Consistent with the annexin V/PI data (Figure 5-13), ribavirin did not induce PARP cleavage at any time-point (Figure 5-14). Ribavirin also did not reverse the survival promoting effects of anti-IgM beads that was evident at the earlier time-points. In summary, these experiments demonstrate that ribavirin does not show strong pro-apoptotic activity in CLL cells, and does not interfere with the survival promoting effects of sIgM signalling.

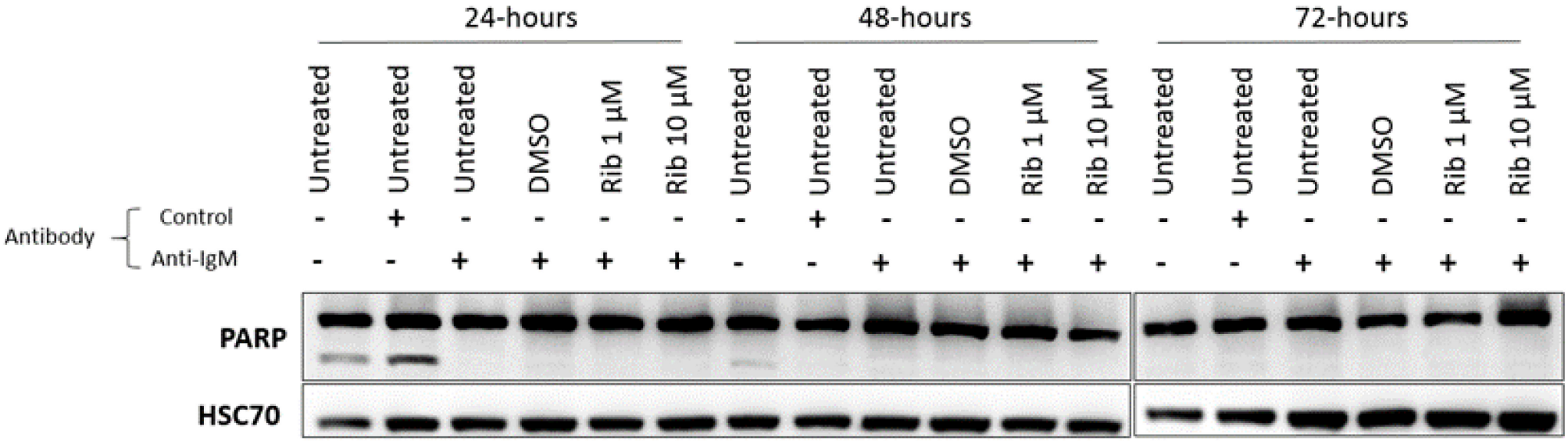

Figure 5-14. PARP cleavage following sIgM- engagement and ribavirin treatment

Sample U-780 was pre-treated with for one hour with ribavirin or DMSO, and then incubated for a further 24, 48 or 72-hours with control antibody or anti-IgM beads. The expression of PARP and HSC70 was analysed by immunoblotting. Results for additional samples are shown in Appendix B

5.3.8 The effect of ribavirin on cyclin D1 expression

Inhibitory effects of ribavirin on anti-IgM-induced MYC expression (Figure 5-4) may be mediated by inhibition of eIF4E-dependent mRNA nuclear export and/or translation. To shed further light on the potential mechanism of action of ribavirin in CLL cells, I extended analysis of the effects of ribavirin on protein expression to include cyclin D1, a major regulator of the cell cycle which is required to progress cell cycle through the G1 phase. The *CCND1* mRNA contains a 3' UTR 4E-SE. It is therefore dependent on eIF4E for nuclear export and is susceptible to inhibition by ribavirin (Culjkovic et al., 2005). By contrast, the translation of *CCND1* mRNA is relatively independent of eIF4E since it is unaffected by ribavirin (Kentsis et al., 2004, Culjkovic et al., 2005). Analysis was performed at 24 hours after sIgM stimulation, as previously described for MYC protein expression (Figure 5-4).

Anti-IgM significantly increased cyclin D1 expression (by ~3-4 fold) (Figure 5-15). This induction was partially inhibited (~25%) in cells treated with ribavirin at 10 μM (Figure 5-15). By contrast, expression of β-actin, which is not strongly dependent on eIF4E activity (Volpon et al., 2016), was unaffected by anti-IgM or ribavirin.

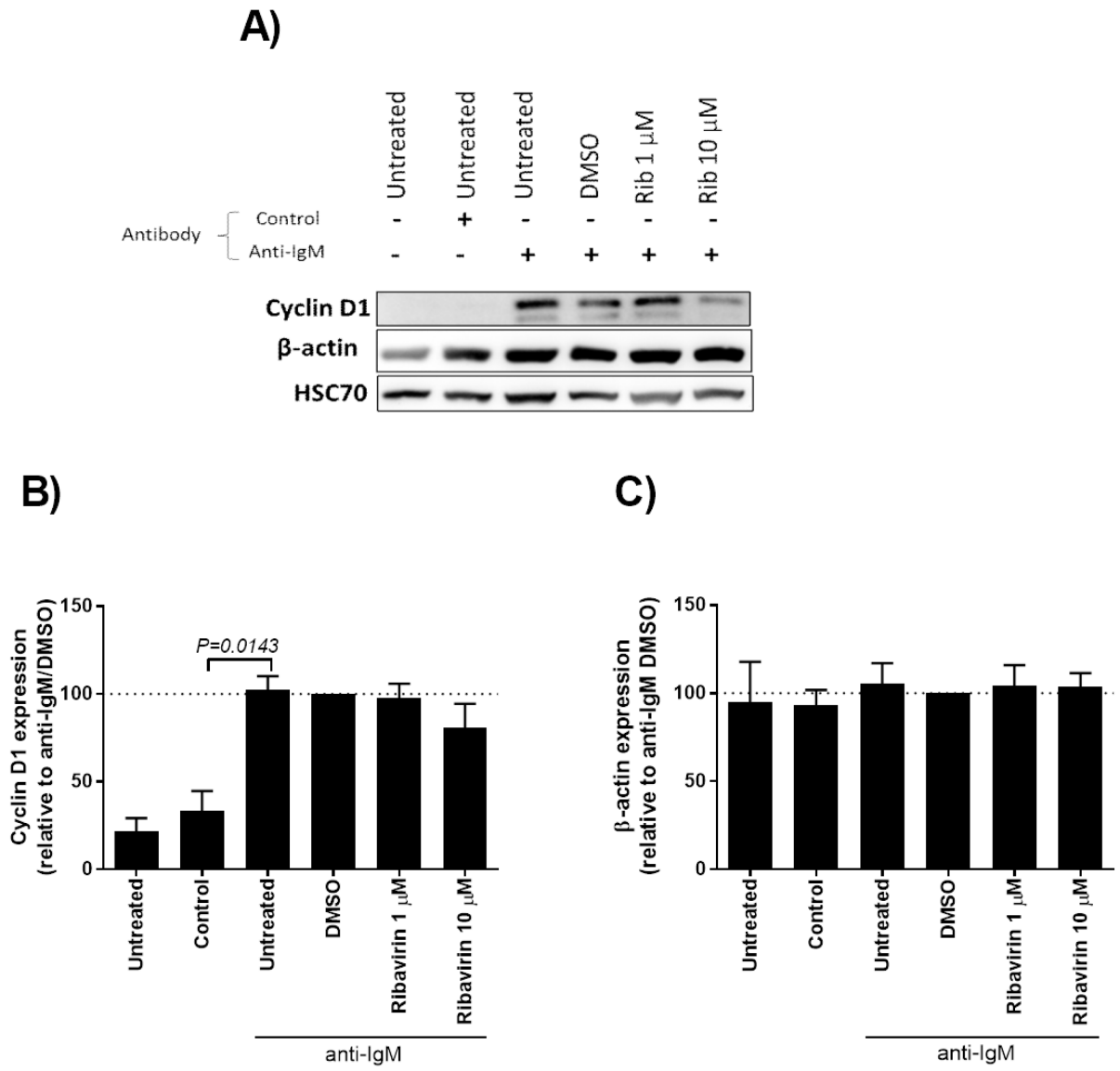

Figure 5-15. Expression of cyclin D1 and β-actin expression following sIgM-engagement and ribavirin treatment

CLL samples (n=5) were pre-incubated with ribavirin or DMSO for one hour, before treatment with control antibody or anti-IgM for an additional 24 hours. Expression of cyclin D1 and β-actin, and HSC70 as a loading control, was analysed by immunoblotting. (A) Blots from representative sample U-511B. (B) Cyclin D1 and (C) β-actin expression (relative to HSC70) was calculated with values for anti-IgM/DMSO treated cells set to 100. Error bars show SEM and the statistical significance of the indicated differences was determined using paired T tests.

5.3.9 Ribavirin on nuclear export of mRNAs

Since ribavirin reduced anti-IgM-induced cyclin D1 expression (Figure 5-15) (where eIF4E's predominant role is in mediating the nuclear export of *CCND1* mRNA), it was next necessary to study directly the effect of ribavirin on mRNA nuclear export in CLL cells. Cells were pre-treated with ribavirin for one hour and stimulated with anti-IgM for 24 hours. Subcellular fractionation was performed to isolate nuclear and cytoplasmic RNAs and the expression of *MYC, MCL1, CCND1* and *GAPDH* mRNA was analysed by qPCR. Due to the large cell numbers needed for these experiments, only control antibody, anti-IgM/DMSO and anti-IgM/ribavirin treated conditions were used. Expression of each mRNA was normalised to *GAPDH* mRNA as this mRNA is not an eIF4E target (Volpon et al., 2016).

Overall, anti-IgM appeared to increase the relative proportions of *MYC* and *CCND1* (but not *MCL1)* mRNA in the cytoplasm (Figure 5-16), indicating that sIgM signalling results in increased nuclear export of *MYC* and *CCND1* mRNA. By contrast, ribavirin reduced the relative abundance for the cytoplasmic mRNA of all three mRNAs analysed, demonstrating that the nuclear export of these mRNAs is dependent on eIF4E in CLL cells (Figure 5-16).

Further evaluation of the results revealed considerable variation in effects of anti-IgM/ribavirin between individual samples. In particular, the effect of anti-IgM on *MYC* mRNA export was very variable, with one sample showing essentially no effect (Figure 5-16A). With this, I considered an arbitrary cut off of 20% increase/decrease in relative abundance to determine any effect in individual samples. However, the inhibitory effects of ribavirin on *MYC* mRNA were observed in all samples and this difference was statistically significant (Figure 5-16A). For *MCL1,* a stimulatory effect of anti-IgM on export was only observed in one sample, whereas inhibitory effects of ribavirin were observed in three (Figure 5-16B). For *CCND1*, a stimulatory effect of anti-IgM on export was observed in two samples, whereas inhibitory effects of ribavirin were observed in three (Figure 5-16C). Overall, the inhibitory effects of ribavirin on nuclear export were more consistent than stimulatory effects of anti-IgM.

The reasons for such variation were not clear. sIgM signalling strength is likely to be important, although all samples were selected on the basis of retained signalling competence. The samples studied comprised two U-CLL and two M-CLL samples. However, variation did not seem to relative to differing cell of origin (not shown). Further studies using more samples would help to clarify the regulation of RNA nuclear export by anti-IgM and/or ribavirin, and potential reasons for this variation. However, I was unable to perform these extended studies due to the requirement for large amounts of material and time constraints.

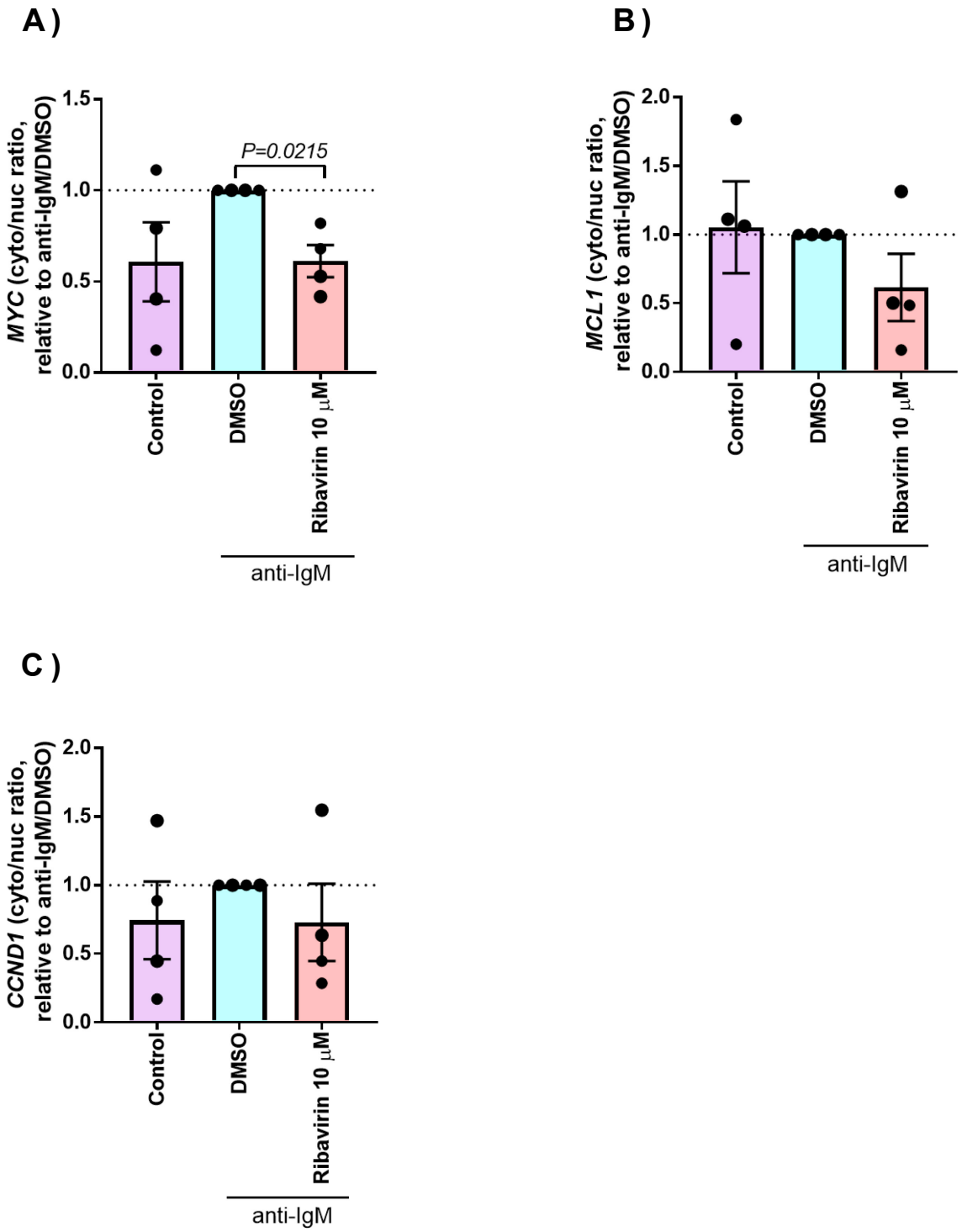

Figure 5-16. Relative cytoplasmic/nuclear ratio of MYC, MCL1 and CCND1 mRNA following sIgM-engagement and ribavirin treatment

CLL cells (n=4) were pre-treated with ribavirin or DMSO for one hour, followed by control antibody or anti-IgM treatment for a further 24 hours. Nuclear and cytoplasmic RNAs were extracted as described in section 2.7 and relative cytoplasmic/nuclear ratio of *MYC, MCL1* and *CCND1* mRNAs were calculated with values for anti-IgM/DMSO treated cells set to 1. Error bars show SEM and the statistical significance of the indicated differences was determined using paired T-tests.

5.3.10 Comparison of the effects of the XPO1 inhibitor selinexor and ribavirin

Selinexor is an XPO1 inhibitor (XPO1i) that blocks the nuclear export of multiple cargoes, including mRNAs (Kuruvilla et al., 2017, Volpon et al., 2017). Since eIF4E-mediated nuclear export of mRNAs is dependent upon XPO1 (Volpon et al., 2017), and ribavirin reduced the nuclear export of *MYC, MCL1* and *CCND1* mRNAs (Figure 5-16), the effects of selinexor and ribavirin were compared on mRNA translation in anti-IgM treated CLL cells.

I first investigated the effects of selinexor on global mRNA translation in CLL cells using the OPP-labelling assay. As before, analysis was performed at 24 hours after sIgM stimulation. Selinexor was used at 0.1 and 0.5 μM, as these concentrations were used in previous studies (Lapalombella et al., 2012) and ribavirin was used at 10 μM as a comparator. With Q-VD-OPh treatment, selinexor did not induce cell death at these concentrations (Appendix B).

Similar to ribavirin, selinexor did not affect basal mRNA translation (Figure 5-17A), but significantly inhibited anti-IgM-induced OPP-labelling (Figure 5-17B). Despite being tested at lower concentrations, selinexor was a more effective inhibitor of anti-IgM-induced translation than ribavirin, and at 0.5 μM selinexor essentially fully reversed the induction of translation by anti-IgM (Figure 5-17B). By contrast (and as shown previously in Figure 5-1), the effects of ribavirin were partial (Figure 5-17B).

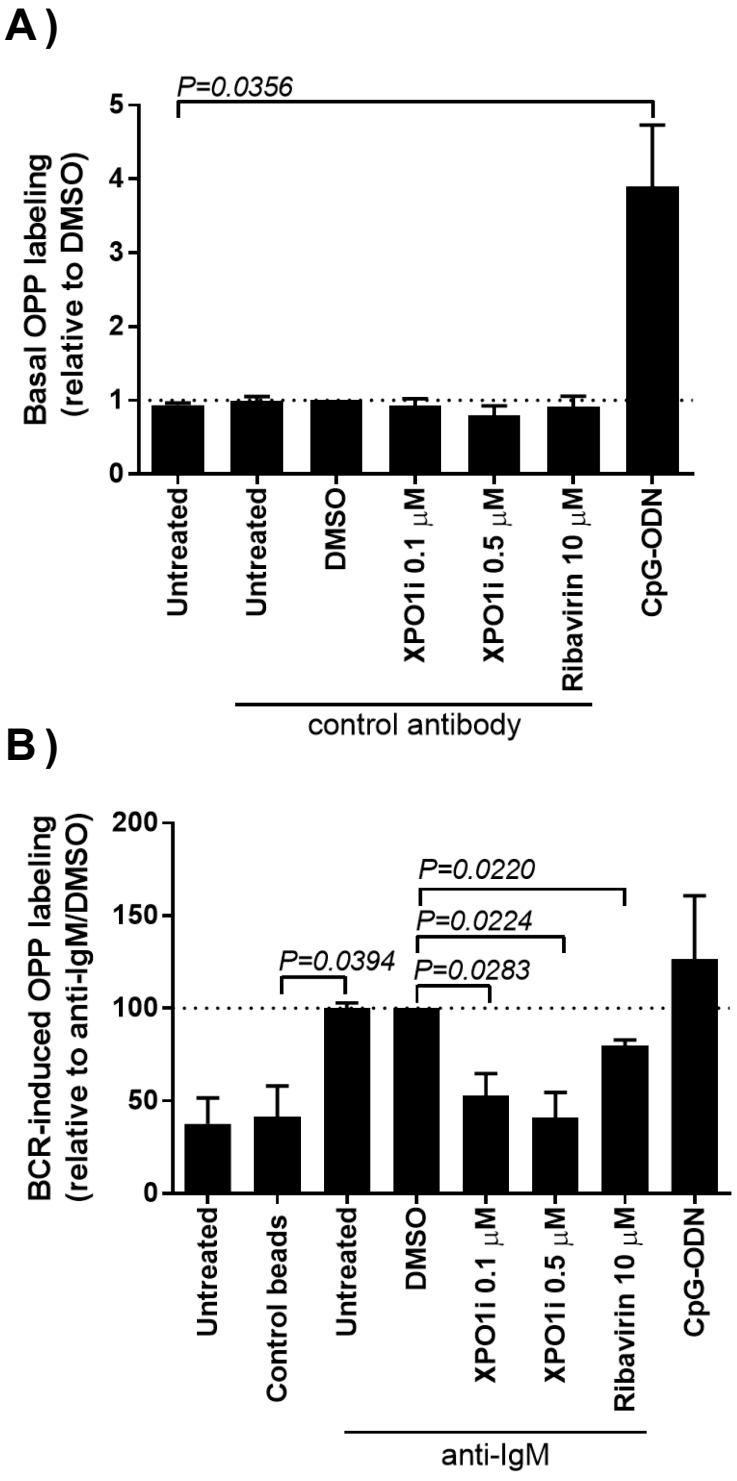

Figure 5-17. Selinexor and ribavirin on basal and anti-IgM-induced OPP labelling in CLL samples

CLL samples (n=4) were pre-treated with ribavirin, selinexor (XPO1i) or DMSO for one hour before treatment with control antibody, anti-IgM or CpG-ODN for an additional 24 hours, as indicated. Cells were collected and translation was analysed via OPP incorporation in the $CD5^{+}CD19^{+}$ cell population. Values for control antibody/DMSO treated cells were set to 1, and anti-IgM/DMSO treated cells were set to 100. Error bars show SEM and the statistical significance of the indicated differences were determined using paired T tests.

I next compared the effects of selinexor and ribavirin on MYC and MCL1 protein expression. CLL cells were pre-treated with ribavirin (10 μM) or selinexor (0.1 or 0.5 μM) for one hour before treatment with anti-IgM for an additional 24 hours. Expression of MYC, MCL1 and HSC70 was analysed by immunoblotting.

As shown previously (Figure 5-4), ribavirin significantly reduced the expression of MYC in anti-IgM treated cells, but had relatively little effect on MCL1 expression (Figure 5-18). By contrast, selinexor strongly reduced expression of both MYC and MCL1, with the expression of these in selinexor treated cells similar to those of unstimulated/ control antibody treated cells (Figure 5-18). Therefore, selinexor is a more effective inhibitor of anti-IgM-induced MYC and MCL1 protein expression compared to ribavirin.

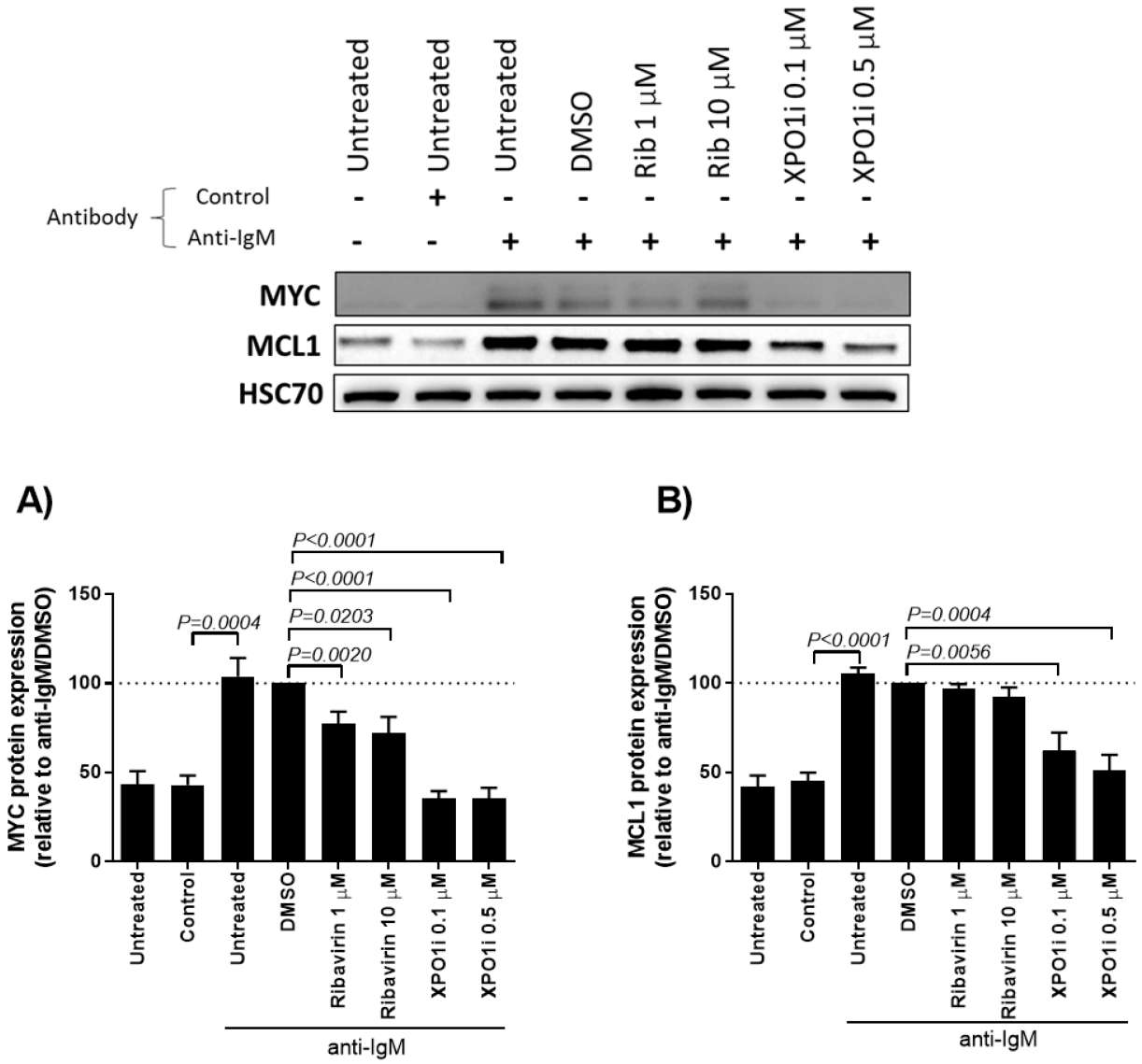

Figure 5-18. MYC and MCL1 expression following anti-IgM and ribavirin or selinexor treatment

CLL samples (n=9 for MYC, n=10 for MCL1) were pre-treated with ribavirin, selinexor or DMSO for one hour, then treated with control antibody or anti-IgM for an additional 24 hours. Cells were lysed and proteins extracted then immunoblotting was undertaken and blots probed for MYC, MCL1 and HSC70 as a loading control. Blot of representative sample U-609A (top panel). Relative expression of (A) MYC and (B) MCL1 values after anti-IgM/DMSO treated cells set to 100. Error bars show SEM and the statistical significance of the indicated differences determined by paired T tests.

It was notable in previous experiments, that the kinetics of inhibition of anti-IgM-induced MYC expression by ribavirin was relatively slow compared to eIF4Ai, with eIF4Ai inhibitory effects more readily observed at six hours post-stimulation (Figure 3-7), whereas the effects of ribavirin were more evident at 24 hours (Figure 5-3, Figure 5-4). It was therefore necessary to perform a small pilot experiment to determine the earliest time-point at which selinexor inhibited MYC protein expression. In contrast to ribavirin, selinexor inhibited MYC expression as early as three hours post-stimulation (Figure 5-19). This was the earliest time-point analysed as induction of MYC protein by anti-IgM was not reliably detected by western blot at earlier time-points (data not shown).

In summary, these results demonstrate shared responses of CLL cells to ribavirin and selinexor, consistent with the idea that they can both prevent mRNA nuclear export. Thus, like ribavirin, selinexor reduced anti-IgM-induced global mRNA translation, and the induction of MYC and MCL1 expression. Although it is difficult to make direct comparisons, since these experiments used different drug concentrations, selinexor appeared to be a more effective inhibitor of these responses compared to ribavirin. Moreover, effects on MYC expression were rapid, compared to the more delayed effects observed with ribavirin.

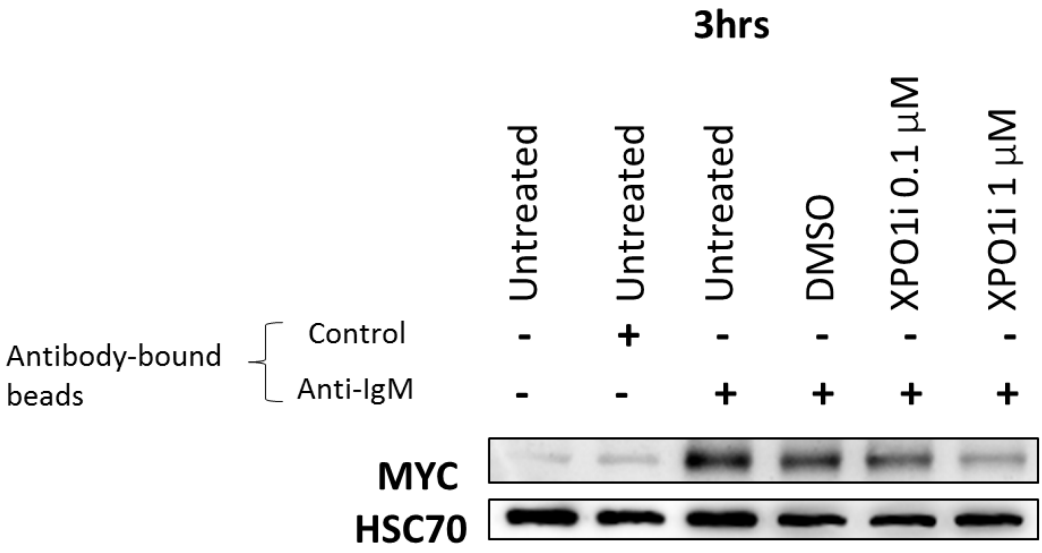

Figure 5-19. Western blot of MYC expression following 3-hour anti-IgM and selinexor treatment

CLL sample M-523H was treated with selinexor for one hour followed by a further three hour treatment with control antibody or anti-IgM. After collection, cells were lysed and proteins extracted then immunoblotting was undertaken and blots probed for MYC and HSC70 as a loading control.

5.3.11 The effects of ribavirin treatment *in vivo* using adoptive transfer of Eμ-*TCL1* leukaemic cells

Next, *in vivo* responses to ribavirin were investigated, using the adoptive transfer of Eμ-*TCL1* leukaemic cells in C57BL/6 mice. The rapid and reproducible development of disease in recipient mice makes this a widely used model to investigate therapeutic responses following drug administration.

For these experiments, C57BL/6 mice were inoculated with $1x10^7$ Eμ-*TCL1* leukaemic cells from transgenic mice bred in previous experiments performed in-house. Blood was analysed weekly to monitor the accumulation of malignant cells. Leukaemic cells were detectable in the blood of mice after 21 days and at this point mice (n=3 per arm for this initial experiment) were randomised for administration by intraperitoneal (ip) injection of ribavirin (80 mg/kg), or PBS as a vehicle control. Treatment was in seven day cycles, each comprising five consecutive days of drug/PBS administration, followed by two days without. Weekly monitoring of tumour burden in the peripheral blood was performed by flow cytometry to measure the presence of $CD5^+B220^+$ cells. After a further 23 days, all mice were euthanized and organs harvested, as all mice met two out of the three pre-determined humane end-points (HEP) as required by the Home Office Licence (PPL-P4D9C89EA, $CD5^+B220^+$ B cells present over 80% of peripheral blood lymphocytes, spleen size greater than 30 mm (measured by palpation), total lymphocyte count $>5x10^7$ per ml blood).

5.3.11.1 Ribavirin reduces the accumulation of leukaemic cells in the peripheral blood

Prior to and throughout treatment, the presence of leukaemic cells in the peripheral blood was measured by tail bleeding, performed weekly. Leukaemic cell counts were measured and calculated per ml of peripheral blood. Flow cytometry was performed and tumour cells identified by staining for CD5, CD19 and B220. CD19 is used as a B cell marker, CD5 is used as a marker of leukaemic cells in this model, and B220 is a pan B-cell marker in mice. Whereas the number of leukaemic cell counts rapidly increased in PBS-treated mice, the leukaemic counts were significantly reduced in mice treated with ribavirin (Figure 5-20). Leukaemic counts were stable during the first two weeks of treatment but then increased modestly, suggesting development of some level of resistance (Figure 5-20). Regardless, at the end of the experiment, the leukaemic cell counts in the peripheral blood of ribavirin-treated mice were ~80% lower than those in vehicle treated animals (Figure 5-20).

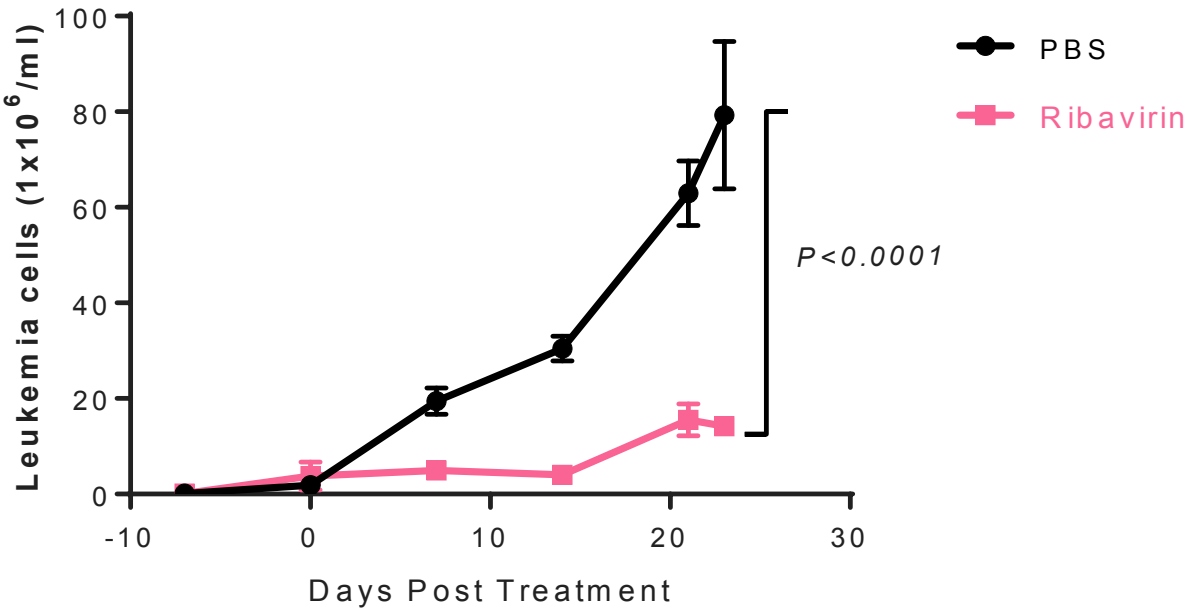

Figure 5-20. Accumulation of leukaemic cells in the peripheral blood of mice treated with ribavirin or PBS

Mice inoculated with Eμ-*TCL1* leukaemic cells (n=3 per arm) were treated with ribavirin or PBS on day 0. Cells were stained for CD19, CD5 and B220. Leukaemic cell counts in peripheral blood were determined weekly, and calculated as leukaemic cells per ml. Statistical significance was determined using a 2way ANOVA with multiple comparisons at the end of treatment only (day 23). Error bars show SEM.

5.3.11.2 The effect of ribavirin on terminal spleen weight

Following 23 days treatment, all mice were euthanized and blood, spleens and the contents of the peritoneal cavity (site of injection) were harvested. Spleens were weighed and photographed to determine the effect of ribavirin on organ size/weight. Mice bearing Eμ-*TCL1* leukaemic cells have differential splenic architecture to those seen in normal C57BL/6 mice (Blunt et al., 2015) due to the extensive infiltration of leukaemic cells. Spleens from ribavirin-treated mice were smaller than spleens from vehicle control treated mice (Figure 5-21). There was some overlap in spleen weights between the two groups but it was evident that ribavirin reduced both spleen size and weight (Figure 5-21).

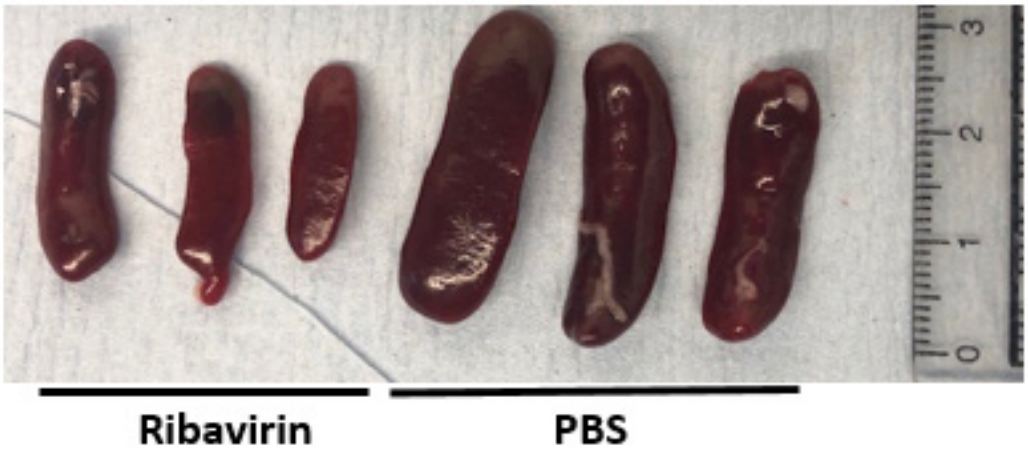

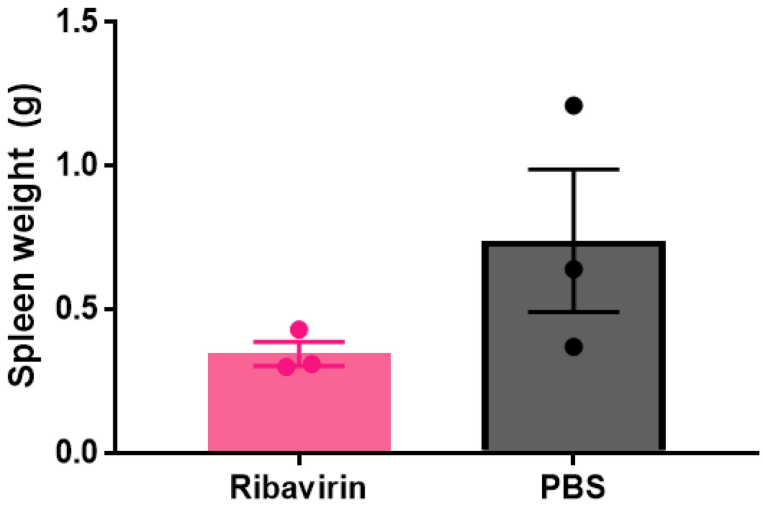

Figure 5-21. Spleen size and weights following ribavirin or PBS treatment

Mice inoculated with Eμ-*TCL1* leukaemic cells (n=3 per arm) were treated with ribavirin or PBS for 23 days. Image of spleens from mice treated with ribavirin or PBS (top panel). Graph shows weights of the spleens from ribavirin or PBS-treated mice (bottom). Any indicated differences determined to be of statistical significance was calculated by paired T test. Error bars show SEM.

Cells were collected from the blood, spleens and peritoneal cavity of these mice. The total number of leukaemic cells was then calculated per tissue. There was a clear reduction in the number of leukaemic cells in the ribavirin treated mice across all sites (Figure 5-22). Overall, whilst this study only utilised small numbers of mice, it is clear that ribavirin reduces leukaemic burden in mice inoculated with Eμ-*TCL1* leukaemic cells.

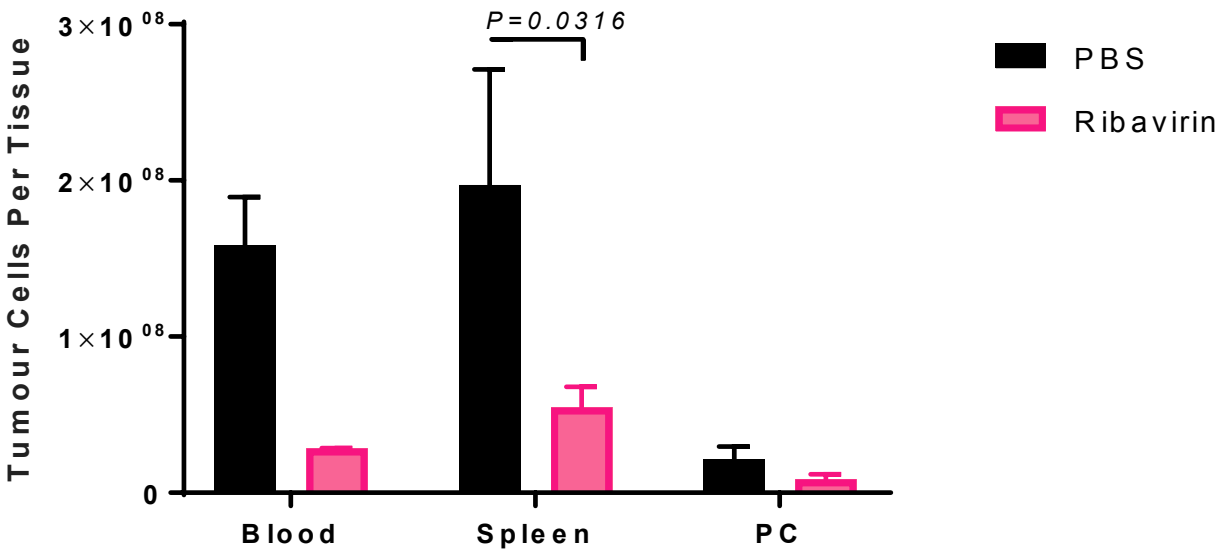

Figure 5-22. Leukaemic cells per tissue in the blood, spleen or peritoneal cavity (PC) after ribavirin or PBS treatment

Mice inoculated with Eμ-*TCL1* leukaemic cells (n=3 per arm) were treated with ribavirin (80 mg/kg/day) or PBS, after the emergence of leukaemic cells in all mice. Flow cytometry staining was used to calculate the number of leukaemic cells per tissue ($CD5^+B220^+$) in the peripheral blood, spleen and peritoneal cavity. Error bars show SEM. Statistical significance indicated determined by 2way ANOVA with multiple comparisons.

5.3.11.3 Repeat of initial ribavirin *in vivo* experiment

To confirm these results, a repeat experiment was performed to measure the accumulation of leukaemic cells in PBS or ribavirin treated mice after inoculation with Eμ-*TCL1* leukaemic cells. Treatments were identical to the previous experiment except that this experiment used six animals in each arm to allow more robust statistical analysis. Consistent with the initial experiment (Figure 5-20), ribavirin treatment resulted in a statistically significant reduction in the number of leukaemic cells (Figure 5-23).

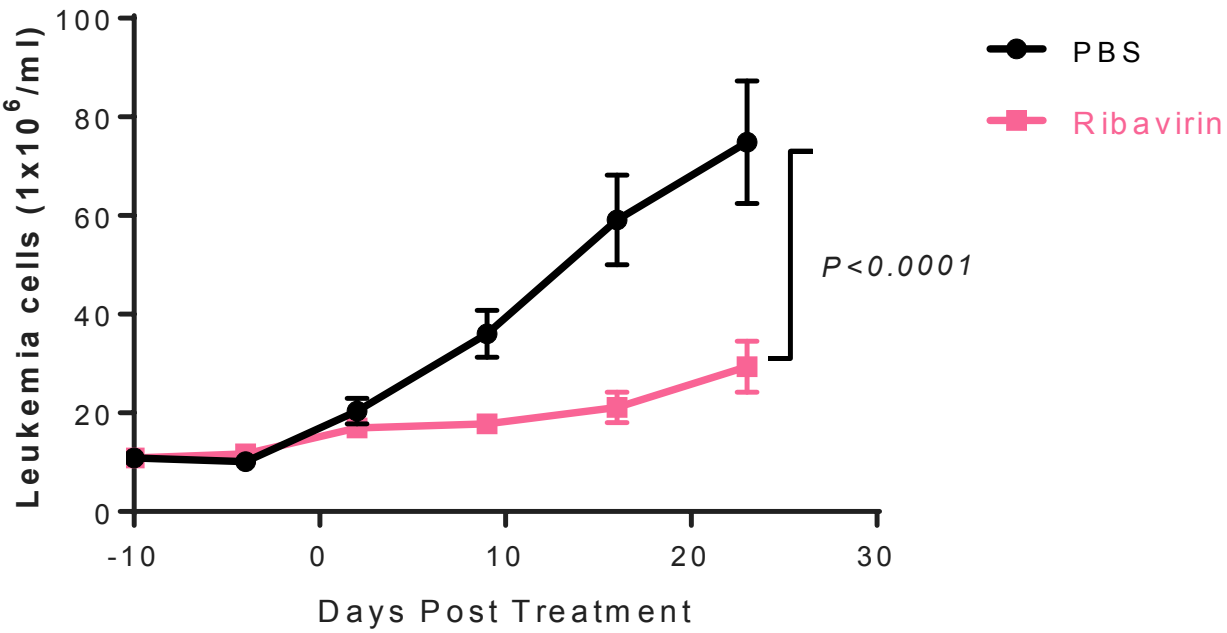

Figure 5-23. Leukaemic cells in the peripheral blood following administration of ribavirin or PBS

Mice inoculated with Eμ-*TCL1* leukaemic cells (n=6 per arm) were treated with ribavirin or PBS on day 0. Cells were stained for CD19, CD5 and B220. Total leukaemic cell counts in peripheral blood were taken weekly, by tail bleeding. Error bars show SEM. Statistical significance was determined using a 2way ANOVA with multiple comparisons at the end of treatment only (day 23). Error bars show SEM.

5.4 Summary of main findings

The overall goal of the experiments described in this chapter was to investigate the consequences of inhibition of a second translation initiation factor, eIF4E, using ribavirin. This included the effects on protein expression and nuclear export of mRNAs. I also investigated the potential *in vivo* anti-tumour activity of ribavirin using the adoptive transfer of Eμ-*TCL1* leukaemic cells.

The main findings from these experiments were;

- Ribavirin reduces anti-IgM-induced mRNA translation in CLL cells, but not in non-malignant B cells
- Ribavirin reduces the expression of MYC and cyclin D1 (but not MCL1) protein expression in anti-IgM-treated CLL cells without effects on sIgM expression or upstream signalling
- Ribavirin reduces anti-IgM-induced eIF4E phosphorylation on Ser209
- Ribavirin does not induce apoptosis of CLL cells even after protracted exposure (72 hours) and does not interfere with the ability of anti-IgM to promote CLL cell survival
- The XPO1i, selinexor, has more profound inhibitory effects on anti-IgM-induced global mRNA translation and MYC and MCL1 protein expression, than ribavirin
- Ribavirin reduces the nuclear export of *MYC, CCND1* and *MCL1* mRNAs in anti-IgM-treated cells
- Ribavirin has *in vivo* anti-tumour activity in an Eμ-*TCL1* adoptive transfer mouse model

Overall, these findings support the hypothesis that eIF4E inhibition using ribavirin reduces the expression of eIF4E-target proteins such as MYC and cyclin D1, but not MCL1, in CLL cells. At least in part, this appears to be mediated by the inhibition of nuclear export of mRNA. Importantly, ribavirin shows substantial anti-tumour activity *in vivo* in the Eμ-*TCL1* adoptive transfer model.

5.5 Discussion

5.5.1 Ribavirin selectively reduces anti-IgM-induced global mRNA translation in CLL cells

A striking finding from this study was that (in contrast to silvestrol) ribavirin appeared to selectively reduce anti-IgM-induced global mRNA translation in CLL cells but not in non-malignant B cells from healthy donors, at least as measured using OPP-labelling (Figure 5-1, Figure 5-2). This was surprising since, in contrast to the differential regulation of eIF4A/PDCD4 expression by anti-IgM in normal and CLL cells (Yeomans et al., 2015), total eIF4E expression is unaltered in either cell type following sIgM stimulation (Figure 5-11 and (Steinhardt et al., 2014)). It was interesting that inhibitory effects of ribavirin on anti-IgM induced global mRNA translation in CLL cells were partial, even at the highest concentrations tested. It is possible that higher concentrations of ribavirin would further reduce anti-IgM-induced translation (and potentially inhibit OPP-labelling in B cells from healthy donors) but it was important to restrict analysis to concentrations within a clinically achievable range. Overall, ribavirin appears to be a more selective inhibitor of OPP-labelling than eIF4Ai.

The reasons for the selective effects of ribavirin in CLL cells is not clear, but it is interesting to note that previous studies have demonstrated that eIF4E is overexpressed in CLL cells compared to normal B cells (Martinez-Marignac et al., 2013, Urtishak et al., 2019). Whether eIF4E phosphorylation, which can also influence nuclear export and translation of mRNAs, differs between normal B cells and CLL cells is not known. Increased eIF4E expression/phosphorylation may heighted the dependency of CLL cells for eIF4Es function and thereby sensitise them to the effects of ribavirin. Future studies could be developed to investigate in more detail the expression (and phosphorylation) of eIF4E in normal B-cell subsets (including anergic B cells), as outlined for analysis of eIF4A and PDCD4 in chapter 3.

Whilst it is clear that there are differential effects of ribavirin on global mRNA translation in CLL and normal B cells, the OPP assay does not reveal whether these differences are mediated by effects on mRNA translation and/or RNA export. For example, reduced RNA export from the nucleus (by ribavirin) would lead to decreases in mRNA translation due to the reduced availability of mRNA, thereby reducing OPP-incorporation. Reduced OPP-labelling could also be due to direct inhibition of translation initiation by ribavirin. To fully understand the consequences of ribavirin treatment on CLL cells it would be necessary to distinguish between both export and translation, using additional assays. For example, polysome profiling could be used to distinguish the consequences on mRNA translation of specific mRNAs, as the relative polysome/monosome association of an mRNA would be made relative to its total mRNA expression, thus measuring only a shift in its translation independent of changes in the nuclear/cytoplasmic distribution.

5.5.2 The effect of ribavirin on anti-IgM-induced MYC, MCL1 and cyclin D1 expression

Ribavirin effectively reduced expression of the cell cycle regulators MYC and cyclin D1 in anti-IgM treated CLL cells (Figure 5-4, Figure 5-15). By contrast, MCL1 expression was only very modestly affected by ribavirin (Figure 5-5). Overall, these results suggest that the consequences of ribavirin on CLL cells might be predominantly anti-proliferative, with relatively little effect on apoptosis. Consistent with this, ribavirin did not induce apoptosis of CLL cells when tested alone, even after extended duration of treatment (Figure 5-13), and in contrast to eIF4A, ribavirin did not reduce the ability of sIgM signalling to promote CLL cell survival (Figure 5-14).

The reasons why MYC and MCL1 were differently affected following ribavirin treatment of anti-IgM treated cells (i.e., reduced MYC and had little effect on MCL1) is not clear and requires further investigation. In general, MCL1 expression appears to be somewhat less susceptible to modulation by translational inhibitors compared to MYC, but it was notable that (in contrast to ribavirin) eIF4Ai did significantly reduce MCL1 expression in anti-IgM-stimulated CLL cells (Figure 3-8). Thus, the lack of effect of ribavirin on MCL1 seems to represent a specific consequence of eIF4E inhibition.

Despite the limited effects of ribavirin on MCL1 protein expression, ribavirin did appear to reduce the nuclear export of *MCL1* mRNA in anti-IgM-treated cells (Figure 5-16). One possible explanation for this apparent discrepancy is that nuclear export, but not translation of *MCL1* mRNA, is particularly dependent on eIF4E, but that the nuclear export of *MCL1* mRNA is not rate-limiting for the synthesis of MCL1 protein. Thus, ribavirin reduces the nuclear export of *MCL1* mRNA, but this does not lead to a substantial reduction in MCL1 protein. In contrast to MCL1, ribavirin reduced both the nuclear export of *MYC* mRNA and the expression of MYC protein (Figure 5-4, Figure 5-16). This suggests that, like *CCND1,* initiation of the translation of *MYC* mRNA may be relatively independent of eIF4E in CLL cells, or that ribavirin reduces both the nuclear export and translation of *MYC* mRNA. Ribavirin did not hyper-induce *MYC* mRNA expression in anti-IgM treated cells (unlike with eIF4Ai) (Figure 5-6), perhaps suggesting that *MYC* mRNA translation is not particularly sensitive to ribavirin, and that reduced MYC protein expression is largely driven by a ribavirin-mediated reduction in the nuclear export of *MYC* mRNA. However, it is important to bear in mind that MYC and MCL1 protein expression will also be controlled post-translationally, via regulation of degradation, and this could also contribute to differences in the regulation of the expression of these proteins in CLL cells.

5.5.3 Ribavirin inhibits phosphorylation of eIF4E

The data demonstrated that whilst eIF4E expression was not regulated by sIgM signalling in CLL cells (Figure 5-11), anti-IgM increased phosphorylation of eIF4E on Ser209 (Figure 5-11), thereby shedding new light on potential links between signalling and components of the eIF4F complex in CLL cells. Although not addressed in my work, increased eIF4E phosphorylation is likely to be mediated by MNK1/2 kinases (Waskiewicz et al., 1997), and results in an increased affinity between eIF4E and the 5' cap of mRNA (Shveygert et al., 2010). Phosphorylation of eIF4E has also been described to enhance the ability of eIF4E to export specific mRNAs from the nucleus (Topisirovic et al., 2004). Less is known about the role of phosphorylation of eIF4E in mRNA translation. Increased eIF4E phosphorylation in anti-IgM treated CLL cells is consistent with the ability of MEK inhibitors to reduce both global mRNA translation and MYC expression in anti-IgM treated cells (Yeomans et al., 2015, Krysov et al., 2012)

Although ribavirin did not affect sIgM expression or upstream signalling (intracellular Ca^{2+} mobilisation, ERK phosphorylation, section 5.3.5), ribavirin did substantially reduce eIF4E phosphorylation in anti-IgM treated cells (Figure 5-12). This may complicate the interpretation of how ribavirin exerts its inhibitory effects on eIF4E, since phosphorylation may enhance eIF4E function. Thus, the ability of ribavirin to reduce MYC expression, for example, might arise from direct effects of ribavirin on binding of eIF4E to 5' caps of mRNA and/or reduced eIF4E phosphorylation which would indirectly reduce the function of eIF4E. The mechanism by which ribavirin reduces eIF4E phosphorylation is not known, since ribavirin did not reduce ERK phosphorylation, which lies upstream of MNK1/2. It is possible that, when bound to ribavirin, eIF4E is less susceptible to MNK1/2-mediated phosphorylation. MCL1 is also a known eIF4E target gene, due to the presence of a complex 5' UTR and m^7G cap (Volpon et al., 2016, Urtishak et al., 2019).

Here, I demonstrated stimulation of sIgM induced MCL1 expression which was not clearly inhibited by ribavirin expression (Figure 5-5). This suggests that whilst MCL1 is regulated by translation to some extent, clearly other mechanisms are at play which have greater impact on MCL1 regulation. Investigation into the role of the proteasome and degradation would be needed to further understand regulation of MCL1 expression. This lesser inhibition of MCL1 by ribavirin may also be due to the less complex 5' UTR in *MCL1* mRNA (Table 15), compared to MYC.

5.5.4 Comparison of effects of selinexor and ribavirin

Since eIF4E-dependent nuclear export of mRNA is dependent on XPO1, it was important to compare the effects of ribavirin and the direct XPO1i, selinexor. XPO1 is one of the most commonly utilised export protein and with this it exports both mRNAs and proteins from the nucleus, most of which act as tumour suppressors (Gravina et al., 2014). For an mRNA to be eligible for export from the nucleus via XPO1, it must interact with an adaptor protein, as XPO1 does not bind mRNA (Culjkovic et al., 2006). XPO1 interacts with adaptor protein LRPPRC, which binds eIF4E and the 4E-SE of an mRNA (Volpon et al., 2017). Selinexor is currently being investigated in a phase I trial for refractory CLL in combination with ibrutinib treatment (NCT02303392), although in previous trials for solid tumours toxicity was evident with common adverse events including fatigue and nausea (Abdul Razak et al., 2016).

Consistent with shared effects on nuclear export, ribavirin and selinexor both reduced anti-IgM-induced global mRNA translation (Figure 5-17). However, compared to ribavirin, selinexor was a more effective inhibitor of mRNA translation, since it completely inhibited induction of OPP-labelling. Moreover, unlike ribavirin, selinexor also effectively inhibited anti-IgM-induced MCL1 expression (Figure 5-18). These more dramatic effects are likely to be explained by the broader role of XPO1 in nuclear export, compared to eIF4E. Although I was not able to investigate the effects of selinexor in normal B cells, it would be interesting to determine whether selinexor was able to discriminate between CLL and healthy donor B cells, as observed with ribavirin. It is likely that the less selective activity of selinexor underlies its increased pro-apoptotic activity in CLL cells compared to ribavirin (Figure 5-13, Appendix B, (Lapalombella et al., 2012)) and perhaps the high frequency of serious toxicity in selinexor versus ribavirin treated patients (Abdul Razak et al., 2016, Assouline et al., 2009, Assouline et al., 2015).

It was also interesting to note that inhibitory effects of selinexor on MYC expression appeared to be more rapid than those observed for ribavirin, where selinexor substantially reduced MYC induction at 3 hours (Figure 5-19), whereas substantial effects of ribavirin required 24 hours of drug exposure (Figure 5-4). Ribavirin requires active transport into cells via the ENT1 cell surface transporter and then intracellular phosphorylation to generate active metabolites (Iikura et al., 2012, Willis et al., 1978). I confirmed that ENT1 was expressed by CLL cells, confirming that this key uptake molecule is present in these cells (data not shown). The dependency of ribavirin on active transport and phosphorylation may explain why longer exposure to ribavirin was required to observe inhibitory effects compared to selinexor.

5.5.5 The efficacy of ribavirin *in vivo*

Eμ-*TCL1* cells were adoptively transferred into C57BL/6 model to mimic the development of CLL. Previous studies into ribavirin *in vivo* utilised PDX models of DLBCL, to demonstrate reliance on eIF4E in this B cell malignancy (Culjkovic-Kraljacic et al., 2016). This study showed reduced tumour growth with ribavirin, although not complete ablation of tumour (Culjkovic-Kraljacic et al., 2016).

PBS-treated mice had enlarged spleens in comparison to ribavirin-treated mice, although the difference in weight was not significant due to small sample size (Figure 5-21). Although, there was still a clear reduction of spleen size/weight following ribavirin treatment (Figure 5-21). Leukaemic cell counts showed that ribavirin treatment decreased the accumulation of leukaemic cells, as the PBS-treated group had around 5-fold higher leukaemic cell counts than ribavirin treated, in the final blood counts (Figure 5-20). Towards the end of treatment there was a trend for increased leukaemic counts in the ribavirin treated groups, which may develop further over longer treatment duration and would need to be studied to a greater extent before progression into clinical trials. Overall, the data suggests that ribavirin is not cytotoxic, thus not killing the leukaemic cells, but more likely to be cytostatic, and therefore inhibits the growth and proliferation of the leukaemic population. This correlates somewhat with the reduced tumour growth in PDX-DLBCL ribavirin studies (Culjkovic-Kraljacic et al., 2016). Further studies may require longer duration of treatment, bigger treatment arms, and potentially combination therapy with a pro-apoptotic agent to have greater effects on the reduction of disease burden.

Chapter 6

Final discussion

6.1 Overview of key findings

The main hypothesis of this thesis was that inhibition of mRNA translation initiation factors in CLL cells is promising as a potential therapeutic strategy, due to its ability to deprive CLL cells of the expression of tumour-promoting oncoproteins, MYC and MCL1, following stimulation of sIgM.

Aim: Characterise the effect of eIF4A inhibitors on both global mRNA translation and expression of key disease drivers, MYC and MCL1 in primary CLL cells

Findings:

- eIF4Ai effectively reduced induction of global mRNA translation, and the expression of MYC and MCL1 following the stimulation of sIgM of CLL cells
- Despite selective regulation of eIF4A following sIgM stimulation of CLL cells (Yeomans et al., 2015), silvestrol had similar effects on anti-IgM-induced translation in CLL and healthy donor B cells
- Polysome profiling confirmed that silvestrol inhibited the translation of *MYC* and *MCL1* mRNAs

Aim: Investigate in detail the consequences of eIF4A inhibition on *MYC* RNA accumulation and stability

Findings:

- Inhibition of mRNA translation by eIF4Ai in anti-IgM treated cells resulted in the stabilisation and subsequent hyper-induction of *MYC* mRNA

Aim: Characterise the effect of the eIF4E inhibitor ribavirin on both global mRNA translation and expression of key disease drivers, MYC and MCL1

Findings:

- Ribavirin reduced anti-IgM-induced mRNA translation in CLL cells but not in B cells from healthy donors
- Ribavirin reduced expression of the proliferation-promoting oncogenes MYC and cyclin D1 (but not MCL1) in anti-IgM-treated CLL cells, potentially via effects on nuclear export of RNA

Aim: Investigate potential anti-tumour effects of ribavirin, alone or in combination, in the Eμ-*TCL1 in vivo* model of CLL

Findings:

- Ribavirin showed significant *in vivo* anti-tumour activity, at well tolerated doses in the *Eμ-TCL1* mouse model of CLL

Overall, the data in this thesis supported my hypothesis, as eIF4A and eIF4E inhibitors showed potential as a therapeutic intervention in CLL, due to their ability to inhibit the expression of multiple proliferation and cell survival oncoproteins. Particularly, ribavirin demonstrated selectivity toward malignant cells for inhibition of global mRNA translation and showed promising *in vivo* activity in a mouse model of CLL.

6.2 The heterogeneity of CLL

CLL is a heterogeneous disease and this must be considered when interpreting the results in this thesis. This study used primary cells from CLL patients, and these were selected based upon their ability to signal through sIgM (Table 5). Whilst each sample demonstrated increased intracellular Ca^{2+} mobilisation in at least 5% of cells following anti-IgM treatment, this response varied greatly between the samples selected (ranging from 5-89%, Table 5). This differential signalling capacity between samples is likely to impact on the results seen in my experiments. Thus, although induction of mRNA translation by anti-IgM and its inhibition by eIF4Ai/eIF4Ei appears to be a general feature of signal competent CLL samples, it is likely that differences exist between individual samples (sections 3.3.1, 5.3.1). Although my selected cohort was compromised of signalling competent samples of both U and M-CLL subsets, it is possible that differing B cell-of-origin of these samples (i.e. pre- and post-GC) might also influence the response. My study focused on detailed profiling of underlying molecular mechanisms and future studies could be performed using much larger numbers of samples whether any differences in the responses of CLL cells could relate to differing cell-of-origin, signalling capacity and/or other BCR features (such as VH-gene usage).

Genetic alterations also have a significant impact on the behaviour of CLL, and contribute to the heterogeneity of the disease. Particularly of significance for this study, are mutations in *XPO1* and *RPS15*, which are likely to influence the nuclear export and translation of mRNA. Although relatively infrequent in CLL, the presence of these, and other, mutations has not been determined in the

samples used here, and may influences responses. To fully investigate these responses the inclusion of samples with and without known mutations could be utilised in larger studies to investigate the impact on responses, such as *XPO1*/*RPS15* mutations and the effect of anti-IgM on the nuclear export of mRNAs.

6.3 The consequences of inhibition of eIF4A and eIF4E in CLL

The differential regulation of components of the eIF4F complex between CLL and normal B cells (Yeomans et al., 2015) implies that targeting these factors could allow for specificity of inhibition of mRNA translation in malignant cells. Particularly, sIgM stimulation of CLL cells results in induction of eIF4A, whilst no change is seen in normal B cells (Yeomans et al., 2015). Less is known about the effect of stimulation on eIF4E in CLL, although in normal B cells sIgM stimulation has no effect on eIF4E expression (Steinhardt et al., 2014) and in CLL cells, eIF4E is highly expressed compared to normal B cells (Martinez-Marignac et al., 2013, Urtishak et al., 2019). Here, chemical inhibition of translation initiation factors eIF4A and eIF4E had differential consequences on mRNA translation and regulation of MYC/MCL1 expression (summarised in Table 16).

Table 16. Comparing the consequences of eIF4A and eIF4E inhibition

	eIF4Ai	**eIF4Ei**
OPP-LABELLING – CLL	Basal: Small reduction Anti-IgM-induced: strong inhibition	Basal: No effect Anti-IgM-induced: Partial inhibition
OPP-LABELLING – HEALTHY DONOR B CELLS	Inhibition	No effect
MYC	Reduces protein expression, drives mRNA expression	Reduces protein expression with no effect on mRNA
MCL1	Reduces protein expression, slight increase in mRNA expression	No effect
CELL VIABILITY	Small reduction in viability	No effect
ERK PHOSPHORYLATION	No effect	No effect

Both eIF4Ai and eIF4Ei reduced anti-IgM-induced mRNA translation in CLL cells (albeit eIF4Ai to a greater extent). The extent to which eIF4Ei inhibited anti-IgM-induced mRNA translation in CLL cells was partial (Figure 5-1), implying that certain mRNAs are particularly dependent upon eIF4E for their translation. mRNAs with complex 5' UTR have a greater dependency on eIF4A for their translation, as the RNA helicase of eIF4A is needed to unwind the secondary structures within the 5' UTR for ribosome scanning to begin. Thus, inhibition of eIF4A will inhibit translation of mRNAs with complex 5' UTR that are dependent upon eIF4A. For example, the G-quadruplex in the 5' UTR of *MYC* mRNA (Table 15) makes *MYC* translation particularly dependent upon eIF4A (Wolfe et al., 2014), hence the inhibition of MYC protein expression by eIF4Ai (Figure 3-7). *MCL1* was shown to have a less complex 5' UTR (Table 15) and this may explain why it was less dramatically regulated compared to MYC (Figure 3-8).

In contrast to this, eIF4E has a role in both translation initiation and the nuclear export of RNA. The role of eIF4E in the regulation of translation is also mRNA specific, as some mRNAs are demonstrated to be less dependent upon eIF4E for their translation, such as *CCND1*. mRNAs which are particularly dependent upon eIF4E for their translation typically have a long and complex 5' UTR, but those that utilise eIF4E for nuclear export additionally require a 4E-SE in their 3' UTR. Thus, the differential regulation of transcripts for translation by eIF4E and eIF4A occurs through multiple mechanisms, and only targets specific mRNAs.

eIF4Ai did inhibit mRNA translation regardless of sIgM stimulation, as basal OPP-labelling was (modestly) reduced by eIF4Ai (Figure 3-1,Figure 3-2) and so mRNAs dependent upon eIF4A are still translated without induced eIF4A expression by anti-IgM treatment (Figure 3-6). In contrast to this, whilst sIgM stimulation has no effect on eIF4E expression, and eIF4E is highly expressed in unstimulated CLL cells, ribavirin did not inhibit basal mRNA translation (Figure 5-1). Thus, the function of eIF4E is key in its role in translation of mRNA, rather than its expression. This may link to the induction of eIF4E-phosphorylation following sIgM stimulation increasing eIF4E's function in translation initiation. Although, eIF4Es roles in mRNA translation and nuclear export (and the consequences on this of ribavirin treatment) are not revealed by the OPP-incorporation assay. It may be that stimulation of the BCR is required for export of eIF4E-target mRNAs from the nucleus, and inhibition of this by ribavirin results in partial reductions of global mRNA translation as seen in Figure 5-1 (due to the reduced presence of mRNA in the cytoplasm).

In B cells from healthy donors, inhibition of eIF4A following sIgM stimulation (although its expression is not induced) resulted in reduced mRNA translation (Figure 3-11). This response did not occur following inhibition of eIF4E (Figure 5-1). Clearly, anti-IgM-induced mRNA translation in normal B cells is much more reliant upon eIF4A than eIF4E even without induction of these factors.

Inhibition of eIF4A in anti-IgM-treated cells also inhibited MYC expression to a greater extent than eIF4Ei. The differences in the extent of inhibition may be due to the role of eIF4E in the nuclear export of *MYC* mRNA. Particularly, as I demonstrated that nuclear export of *MYC* mRNA is induced by anti-IgM and reduced by ribavirin pre-treatment (Figure 5-16), and given the different time-points required to inhibit MYC expression (Figure 3-7, Figure 5-3), it is likely that longer time-points may be required to see further reductions in MYC expression. I suspect that ribavirin appears to inhibit mRNA translation due to its ability to inhibit nuclear export of certain mRNAs, resulting in less mRNA available for the translation machinery in the cytoplasm. This process is likely to take longer than inhibition of mRNA translation alone, hence the differential regulation of MYC expression by these two sets of inhibitors. Urtishak and colleagues demonstrated that ribavirin does not reduce global mRNA translation, using polysome profiling, in an acute leukaemia cell line (Urtishak et al., 2019). Clearly, the effects of ribavirin on global mRNA translation are unclear due to the interplay of nuclear export and translation initiation by eIF4E. Moreover, inhibition of individual translation initiation factors can have differential consequences, despite eIF4E and eIF4A both being components of the eIF4F complex.

Inhibition of eIF4A by silvestrol also resulted in the accumulation of *MYC* mRNA due to an increase in its stability (Figure 4-5, Figure 4-10), which may be in part due to the fact that translation of *MYC* is coupled to its degradation (Lemm and Ross, 2002). The increase in *MCL1* mRNA in cells treated with eIF4Ai and anti-IgM was much less clear (Figure 4-6), likely due to a reduced requirement for eIF4A for its translation. As ribavirin only modestly reduced anti-IgM-induced MYC protein expression (Figure 5-4), with no clear effect on mRNA expression (Figure 5-6), I did not investigate the effect of eIF4E inhibition on stability of *MYC* mRNA. This lack of accumulation of *MYC* by eIF4Ei (considering coupling of translation and degradation) further suggests that eIF4Ei inhibits the nuclear export of *MYC* mRNA rather than its translation *per se*.

Another important consideration with regards to the use of inhibitors *in vitro* is that there is a difficulty in distinguishing between target and off-target effects, which could skew our understanding of the mechanisms by which certain proteins or processes are regulated. To confirm these findings, it may be useful to utilise genetic approaches. For example, utilising small interfering RNA (siRNA) to perform RNA interference (RNAi) assays to understand the impact of silencing genes such as those encoding initiation factors. An issue with utilising genetic approaches for CLL is the difficulty in using primary cells, due to the limited genetic material available and complications in transfection.

6.3.1 The efficacy of inhibitors of translation initiation factors *in vivo*

Studies have demonstrated the potential utility of silvestrol in the Eμ-*TCL1* transgenic mouse model with a significantly increased survival rate (Lucas et al., 2009). In my studies, treatment with eIF4Ai reduced expression of MYC and MCL1 (Figure 3-7, Figure 3-8). Notably, MCL1 expression is associated with resistance to fludarabine treatment in CLL (Johnston et al., 2004) and so targeting MCL1 expression by eIF4Ai may be useful in treatments for relapsed/refractory CLL. Silvestrol treatment may be useful in combination for these cases, to target MYC and MCL1 to prevent resistance to fludarabine treatments and so combination of fludarabine with silvestrol may overcome mechanisms of resistance.

Previous studies utilised a PDX model of DLBCL and demonstrated that ribavirin reduced tumour growth, but not complete ablation of tumour (Culjkovic-Kraljacic et al., 2016). Here, I utilised an adoptive transfer model using Eμ-*TCL1* leukaemic cells to determine the efficacy of ribavirin treatment, as inhibition of eIF4E had no effect on mRNA translation in B cells from healthy donors (in contrast to eIF4Ai). At well tolerated doses, ribavirin reduced total leukaemic cell counts compared to the vehicle control (Figure 5-20). Towards the end of the study, in the ribavirin-treated group the leukaemic cell counts began to increase, which requires further study to understand this progression and measure whether counts would ultimately equal that of PBS-treated mice. At the end of the study, the spleens of ribavirin treated mice were generally smaller and weighed less (Figure 5-21). There was also a clear reduction in tumour burden with ribavirin between all sites investigated (being the peritoneal cavity/PC, spleen and peripheral blood) (Figure 5-22). A repeat of this study correlated the findings by demonstrating that ribavirin treatment reduced leukaemic cell counts compared to vehicle control (Figure 5-23). Overall, the data suggests that ribavirin treatment is cytostatic, consistent with the *in vitro* data demonstrating no induction of apoptosis and no inhibition of anti-IgM-induced MCL1 expression (Figure 5-13, Figure 5-14, Figure 5-5).

Further studies require longer duration of treatment and potentially combination therapy with a pro-apoptotic agent, such as a BH3-mimetic to have greater effects in reduction of disease burden. An interesting potential combination therapy for ribavirin would be venetoclax, to inhibit pro-survival protein BCL2. BCL2 is over-expressed in CLL (Robertson et al., 1996) and so its inhibition could exacerbate the cytostatic effects of ribavirin, reducing leukaemic cell count and preventing the slow increase in leukaemic cell counts towards the end of the study that were demonstrated here (Figure 5-20). An interesting alternative model would a PDX. This would recapitulate the complexity of CLL to a greater extent, which is a key factor when understanding the efficacy of therapies in a heterogeneous disease such as CLL. Particularly, studies utilising PDX models of different subtypes of CLL (i.e U versus M-CLL), could demonstrate the potential of these treatments for different disease subsets.

6.4 The clinical significance of selective inhibitors of mRNA translation

Ultimately, the greatest consideration when acknowledging this data is the potential clinical significance of inhibitors of mRNA translation initiation factors for use as treatments in CLL. Whilst kinase inhibitors are rapidly increasing in use as first-line treatments in CLL, cases of resistance are becoming more common. Inhibition of translation in relapsed/refractory CLL may provide a strategy to overcome resistance mechanisms, such as by reducing expression of anti-apoptotic protein MCL1, commonly associated with resistance to some current treatments (Johnston et al., 2004). Of course, treatments cannot be utilised without extensive clinical trials. Promising evidence to support the use of translation inhibitors for the treatment of B-cell malignancies was described where a patient diagnosed with hepatitis C and follicular lymphoma underwent ribavirin treatment for anti-viral therapy and experienced full remission from lymphoma (Maciocia et al., 2016). Similar to this, another patient with hepatitis C virus undertook therapy with ribavirin (in combination with another anti-viral treatment) and achieved complete remission of marginal zone lymphoma (Lim et al., 2015). As ribavirin is already well profiled clinically it is a strong choice for early clinical trials as a treatment for B cell malignancies. A focus for drug development is to develop inhibitors of eIFs, for example new inhibitors of eIF4A, which are specific to tumour cells with less off-target effects than previous inhibitors like silvestrol, such as eFT226. eEFT226 is a small molecule compound developed to selectively inhibit eIF4A, developed by eFFECTOR therapeutics (California, USA), which is currently in the pre-clinical stages of testing and soon to be used in a phase I trial for solid tumours. Clearly, inhibitors of eIFs show promise in B cell malignancies, and the potential of them particularly in CLL remain to be explored. Further *in vivo* studies and initiation of clinical trials are next key in developing their use in treatment regimens for CLL.

6.5 Future work to understand the consequences of inhibition of translation initiation factors in CLL

Whilst my results suggest many interesting areas of research to pursue, I would consider the following experiments to be of the highest priority;

- Understand the effects of ribavirin on the proliferation of CLL cells
- Unpick the role of nuclear export versus translation of *MYC* and *MCL1* regulation
- Comparison of the expression (and phosphorylation) of eIFs and levels of mRNA translation in B cell subsets
- Combination treatments *in vivo* utilising translation inhibitors

A consequence of ribavirin treatment described in other models is a reduction in proliferation (Urtishak et al., 2019). Given that here ribavirin reduced the expression of cell cycle-associated proteins, MYC and cyclin D1 (Figure 5-15) with little effect on apoptosis and MCL1 expression, I hypothesise that the principle effect of ribavirin will be to inhibit the proliferation of CLL cells. Whilst CLL cells do not typically proliferate *in vitro*, this can be induced with a cocktail of anti-IgM, CD40L, IL-4 and IL-21 (Schleiss et al., 2019). Induction of proliferation can then be measured via flow cytometry analysis of carboxyfluorescein diacetate succinimidyl ester (CFSE) staining intensity. Intensity of CFSE decreases as cells divide and thus allows calculation of the percentage of dividing cells in a sample, and number of cell generations. Calculating the effect of ribavirin on proliferation *in vitro* would allow us to understand the role of eIF4E (and any consequent inhibition) on proliferation of CLL cells, whilst also providing further information for any practical use of ribavirin *in vivo*.

To fully unpick the role of eIF4E and its inhibition by ribavirin in the regulation of *MYC* and *MCL1,* it is necessary to determine the impact of both nuclear export and the translation of their mRNAs. Having demonstrated that ribavirin reduces the nuclear export of *MYC* and *MCL1* mRNA (and *CCND1)*, it would next be interesting to undertake polysome profiling to distinguish any effects by ribavirin on the translation of these mRNAs. As the translation of *CCND1* is not influenced by ribavirin (Volpon et al., 2017), this could be measured in polysome profiling to confirm the results of this experiment. This would give understanding of ribavirin as an inhibitor of eIF4E and the role of eIF4E in both nuclear export and translation of mRNAs.

To investigate the differences in regulation of eIF4E and its phosphorylation, it would also be important to study eIF4E expression (and other eIFs) and its phosphorylation in subsets of normal B cells. Particularly, studying anergic B cells, as this would be a good comparator for M-CLL cells and provide an insight into the role of signalling capacity (via sIgM) on mRNA translation and other associated responses.

Finally, having demonstrated the efficacy of ribavirin alone in initial studies utilising adoptive transfer of Eμ-*TCL1* leukaemic cells in chapter 5, I would next consider performing *in vivo* combination studies utilising ribavirin and a BH3-mimetic such as venetoclax, to boost the responses seen and add a potential pro-apoptotic effect on the leukaemic cells. With this, I would also recommend parallel analysis of the normal lymphocyte population in these studies to further understand any non-tumour cell toxicity.

List of References

ABDUL RAZAK, A. R., MAU-SOERENSEN, M., GABRAIL, N. Y., GERECITANO, J. F., SHIELDS, A. F., UNGER, T. J., SAINT-MARTIN, J. R., CARLSON, R., LANDESMAN, Y., MCCAULEY, D., RASHAL, T., LASSEN, U., KIM, R., STAYNER, L. A., MIRZA, M. R., KAUFFMAN, M., SHACHAM, S. & MAHIPAL, A. 2016. First-in-Class, First-in-Human Phase I Study of Selinexor, a Selective Inhibitor of Nuclear Export, in Patients With Advanced Solid Tumors. *J Clin Oncol,* 34**,** 4142-4150.

ADEM, J., HAMALAINEN, A., ROPPONEN, A., EEVA, J., ERAY, M., NUUTINEN, U. & PELKONEN, J. 2015. ERK1/2 has an essential role in B cell receptor- and CD40-induced signaling in an in vitro model of germinal center B cell selection. *Mol Immunol,* 67**,** 240-7.

ADIMOOLAM, S. & FORD, J. M. 2003. p53 and regulation of DNA damage recognition during nucleotide excision repair. *DNA Repair (Amst),* 2**,** 947-54.

ALT, F. W. 1986. Antibody diversity. New mechanism revealed. *Nature,* 322**,** 772-3.

AMAN, M. J., LAMKIN, T. D., OKADA, H., KUROSAKI, T. & RAVICHANDRAN, K. S. 1998. The inositol phosphatase SHIP inhibits Akt/PKB activation in B cells. *J Biol Chem,* 273**,** 33922-8.

AMATI, B., FRANK, S. R., DONJERKOVIC, D. & TAUBERT, S. 2001. Function of the c-Myc oncoprotein in chromatin remodeling and transcription. *Biochim Biophys Acta,* 1471**,** M135-45.

ANDERSON, M. A., DENG, J., SEYMOUR, J. F., TAM, C., KIM, S. Y., FEIN, J., YU, L., BROWN, J. R., WESTERMAN, D., SI, E. G., MAJEWSKI, I. J., SEGAL, D., HEITNER ENSCHEDE, S. L., HUANG, D. C., DAVIDS, M. S., LETAI, A. & ROBERTS, A. W. 2016. The BCL2 selective inhibitor venetoclax induces rapid onset apoptosis of CLL cells in patients via a TP53-independent mechanism. *Blood,* 127**,** 3215-24.

ANDERSON, P. & KEDERSHA, N. 2002. Visibly stressed: the role of eIF2, TIA-1, and stress granules in protein translation. *Cell Stress Chaperones,* 7**,** 213-21.

ASSOULINE, S., CULJKOVIC-KRALJACIC, B., BERGERON, J., CAPLAN, S., COCOLAKIS, E., LAMBERT, C., LAU, C. J., ZAHREDDINE, H. A., MILLER, W. H., JR. & BORDEN, K. L. 2015. A phase I trial of ribavirin and low-dose cytarabine for the treatment of relapsed and refractory acute myeloid leukemia with elevated eIF4E. *Haematologica,* 100**,** e7-9.

ASSOULINE, S., CULJKOVIC, B., COCOLAKIS, E., ROUSSEAU, C., BESLU, N., AMRI, A., CAPLAN, S., LEBER, B., ROY, D. C., MILLER, W. H., JR. & BORDEN, K. L. 2009. Molecular targeting of the oncogene eIF4E in acute myeloid leukemia (AML): a proof-of-principle clinical trial with ribavirin. *Blood,* 114**,** 257-60.

ATHANASIADOU, A., STAMATOPOULOS, K., TSOMPANAKOU, A., GAITATZI, M., KALOGIANNIDIS, P., ANAGNOSTOPOULOS, A., FASSAS, A. & TSEZOU, A. 2006. Clinical, immunophenotypic, and molecular profiling of trisomy 12 in chronic lymphocytic leukemia and comparison with other karyotypic subgroups defined by cytogenetic analysis. *Cancer Genet Cytogenet,* 168**,** 109-19.

BAGNARA, D., KAUFMAN, M. S., CALISSANO, C., MARSILIO, S., PATTEN, P. E., SIMONE, R., CHUM, P., YAN, X. J., ALLEN, S. L., KOLITZ, J. E., BASKAR, S., RADER, C., MELLSTEDT, H., RABBANI, H., LEE, A., GREGERSEN, P. K., RAI, K. R. & CHIORAZZI, N. 2011. A novel adoptive transfer

model of chronic lymphocytic leukemia suggests a key role for T lymphocytes in the disease. *Blood,* 117**,** 5463-72.

BAKER, K. E. & COLLER, J. 2006. The many routes to regulating mRNA translation. *Genome Biol,* 7**,** 332.

BALATTI, V., BOTTONI, A., PALAMARCHUK, A., ALDER, H., RASSENTI, L. Z., KIPPS, T. J., PEKARSKY, Y. & CROCE, C. M. 2012. NOTCH1 mutations in CLL associated with trisomy 12. *Blood,* 119**,** 329-31.

BALATTI, V., PEKARKY, Y. & CROCE, C. M. 2015. Role of microRNA in chronic lymphocytic leukemia onset and progression. *J Hematol Oncol,* 8**,** 12.

BANCHEREAU, J., DUBOIS, B., FAYETTE, J., BURDIN, N., BRIERE, F., MIOSSEC, P., RISSOAN, M. C., VAN KOOTEN, C. & CAUX, C. 1995. Functional CD40 antigen on B cells, dendritic cells and fibroblasts. *Adv Exp Med Biol,* 378**,** 79-83.

BARRANS, S. L., FENTON, J. A., BANHAM, A., OWEN, R. G. & JACK, A. S. 2004. Strong expression of FOXP1 identifies a distinct subset of diffuse large B-cell lymphoma (DLBCL) patients with poor outcome. *Blood,* 104**,** 2933-5.

BEELMAN, C. A. & PARKER, R. 1994. Differential effects of translational inhibition in cis and in trans on the decay of the unstable yeast MFA2 mRNA. *J Biol Chem,* 269**,** 9687-92.

BERNDT, S. I., SKIBOLA, C. F., JOSEPH, V., CAMP, N. J., NIETERS, A., WANG, Z., COZEN, W., MONNEREAU, A., WANG, S. S., KELLY, R. S., LAN, Q., TERAS, L. R., CHATTERJEE, N., CHUNG, C. C., YEAGER, M., BROOKS-WILSON, A. R., HARTGE, P., PURDUE, M. P., BIRMANN, B. M., ARMSTRONG, B. K., COCCO, P., ZHANG, Y., SEVERI, G., ZELENIUCH-JACQUOTTE, A., LAWRENCE, C., BURDETTE, L., YUENGER, J., HUTCHINSON, A., JACOBS, K. B., CALL, T. G., SHANAFELT, T. D., NOVAK, A. J., KAY, N. E., LIEBOW, M., WANG, A. H., SMEDBY, K. E., ADAMI, H. O., MELBYE, M., GLIMELIUS, B., CHANG, E. T., GLENN, M., CURTIN, K., CANNON-ALBRIGHT, L. A., JONES, B., DIVER, W. R., LINK, B. K., WEINER, G. J., CONDE, L., BRACCI, P. M., RIBY, J., HOLLY, E. A., SMITH, M. T., JACKSON, R. D., TINKER, L. F., BENAVENTE, Y., BECKER, N., BOFFETTA, P., BRENNAN, P., FORETOVA, L., MAYNADIE, M., MCKAY, J., STAINES, A., RABE, K. G., ACHENBACH, S. J., VACHON, C. M., GOLDIN, L. R., STROM, S. S., LANASA, M. C., SPECTOR, L. G., LEIS, J. F., CUNNINGHAM, J. M., WEINBERG, J. B., MORRISON, V. A., CAPORASO, N. E., NORMAN, A. D., LINET, M. S., DE ROOS, A. J., MORTON, L. M., SEVERSON, R. K., RIBOLI, E., VINEIS, P., KAAKS, R., TRICHOPOULOS, D., MASALA, G., WEIDERPASS, E., CHIRLAQUE, M. D., VERMEULEN, R. C., TRAVIS, R. C., GILES, G. G., ALBANES, D., VIRTAMO, J., WEINSTEIN, S., CLAVEL, J., ZHENG, T., HOLFORD, T. R., OFFIT, K., ZELENETZ, A., KLEIN, R. J., SPINELLI, J. J., BERTRAND, K. A., et al. 2013. Genome-wide association study identifies multiple risk loci for chronic lymphocytic leukemia. *Nat Genet,* 45**,** 868-76.

BI, X. & GOSS, D. J. 2000. Kinetic proofreading scanning models for eukaryotic translational initiation: the cap and poly(A) tail dependency of translation. *J Theor Biol,* 207**,** 145-57.

BICHI, R., SHINTON, S. A., MARTIN, E. S., KOVAL, A., CALIN, G. A., CESARI, R., RUSSO, G., HARDY, R. R. & CROCE, C. M. 2002. Human chronic lymphocytic leukemia modeled in mouse by targeted TCL1 expression. *Proc Natl Acad Sci U S A,* 99**,** 6955-60.

BINET, J. L., AUQUIER, A., DIGHIERO, G., CHASTANG, C., PIGUET, H., GOASGUEN, J., VAUGIER, G., POTRON, G., COLONA, P., OBERLING, F., THOMAS, M., TCHERNIA, G., JACQUILLAT, C., BOIVIN, P., LESTY, C., DUAULT, M. T., MONCONDUIT, M., BELABBES, S. & GREMY, F. 1981. A new prognostic classification of chronic lymphocytic leukemia derived from a multivariate survival analysis. *Cancer,* 48**,** 198-206.

BLUM, J. H., STEVENS, T. L. & DEFRANCO, A. L. 1993. Role of the mu immunoglobulin heavy chain transmembrane and cytoplasmic domains in B cell antigen receptor expression and signal transduction. *J Biol Chem,* 268**,** 27236-45.

BLUNT, M. D., CARTER, M. J., LARRAYOZ, M., SMITH, L. D., AGUILAR-HERNANDEZ, M., COX, K. L., TIPTON, T., REYNOLDS, M., MURPHY, S., LEMM, E., DIAS, S., DUNCOMBE, A., STREFFORD, J. C., JOHNSON, P. W., FORCONI, F., STEVENSON, F. K., PACKHAM, G., CRAGG, M. S. & STEELE, A. J. 2015. The PI3K/mTOR inhibitor PF-04691502 induces apoptosis and inhibits microenvironmental signaling in CLL and the Emicro-TCL1 mouse model. *Blood,* 125**,** 4032-41.

BORDELEAU, M. E., MORI, A., OBERER, M., LINDQVIST, L., CHARD, L. S., HIGA, T., BELSHAM, G. J., WAGNER, G., TANAKA, J. & PELLETIER, J. 2006. Functional characterization of IRESes by an inhibitor of the RNA helicase eIF4A. *Nat Chem Biol,* 2**,** 213-20.

BORDELEAU, M. E., ROBERT, F., GERARD, B., LINDQVIST, L., CHEN, S. M., WENDEL, H. G., BREM, B., GREGER, H., LOWE, S. W., PORCO, J. A., JR. & PELLETIER, J. 2008. Therapeutic suppression of translation initiation modulates chemosensitivity in a mouse lymphoma model. *J Clin Invest,* 118**,** 2651-60.

BORDEN, K. L. 2016. The eukaryotic translation initiation factor eIF4E wears a "cap" for many occasions. *Translation (Austin),* 4**,** e1220899.

BRACK, C., HIRAMA, M., LENHARD-SCHULLER, R. & TONEGAWA, S. 1978. A complete immunoglobulin gene is created by somatic recombination. *Cell,* 15**,** 1-14.

BRESIN, A., D'ABUNDO, L., NARDUCCI, M. G., FIORENZA, M. T., CROCE, C. M., NEGRINI, M. & RUSSO, G. 2016. TCL1 transgenic mouse model as a tool for the study of therapeutic targets and microenvironment in human B-cell chronic lymphocytic leukemia. *Cell Death Dis,* 7**,** e2071.

BUCHAN, J. R. & PARKER, R. 2009. Eukaryotic stress granules: the ins and outs of translation. *Mol Cell,* 36**,** 932-41.

BURGER, J. A., TEDESCHI, A., BARR, P. M., ROBAK, T., OWEN, C., GHIA, P., BAIREY, O., HILLMEN, P., BARTLETT, N. L., LI, J., SIMPSON, D., GROSICKI, S., DEVEREUX, S., MCCARTHY, H., COUTRE, S., QUACH, H., GAIDANO, G., MASLYAK, Z., STEVENS, D. A., JANSSENS, A., OFFNER, F., MAYER, J., O'DWYER, M., HELLMANN, A., SCHUH, A., SIDDIQI, T., POLLIACK, A., TAM, C. S., SURI, D., CHENG, M., CLOW, F., STYLES, L., JAMES, D. F., KIPPS, T. J. & INVESTIGATORS, R.-. 2015a. Ibrutinib as Initial Therapy for Patients with Chronic Lymphocytic Leukemia. *N Engl J Med,* 373**,** 2425-37.

BURGER, J. A., TEDESCHI, A., BARR, P. M., ROBAK, T., OWEN, C., GHIA, P., BAIREY, O., HILLMEN, P., BARTLETT, N. L., LI, J., SIMPSON, D., GROSICKI, S., DEVEREUX, S., MCCARTHY, H., COUTRE, S., QUACH, H., GAIDANO, G., MASLYAK, Z., STEVENS, D. A., JANSSENS, A., OFFNER, F., MAYER, J., O'DWYER, M., HELLMANN, A., SCHUH, A., SIDDIQI, T., POLLIACK, A., TAM, C. S., SURI, D., CHENG, M., CLOW, F., STYLES, L., JAMES, D. F., KIPPS, T. J., KEATING, M., JEN, J., JINDRA, P., SIMKOVIC, M., BRAESTER, A., RUCHLEMER, R., FOA, R., SEMENZATO, G., HAWKINS, T., ATANASIO, C. M., DEMIRKAN, F., KAYNAR, L., PYLYPENKO, H., FOX, C., THIRMAN, M., CAMPBELL, P., COUGHLIN, P., HARRUP, R., KUSS, B., TURNER, P., WU, K. L., LARRATT, L., FINEMAN, R., MARASCA, R., ZINZANI, P. L., CORBETT, G., ABRISQUETA, P., DELGADO, J., GONZALEZ-BARCA, E., DE OTEYZA, J. P., ARSLAND, O., KAPLAN, P., OLIYNYK, H., HAMBLIN, M., ATKINS, J., BARRIENTOS, J., GASIC, S., HOU, J. Z., KINGSLEY, E., SHADMAN, M., BADOUX, X., GILL, D., OPAT, S., BRON, D., VAN DEN NESTE, E., JING, H. M., ZHU, J., VANDENBERGHE, E., TADMOR, T., CORTELEZZI, A., GANLY, P., WEINKOVE, R., PLUTA, A., PRISTUPA, A., MARCO, J. A. G., VURAL, F., YAGCI, M., KASYCH, M., DUNCOMBE,

A., FEGAN, C., QUACKENBUSH, R., TIRUMALI, N. & INVESTIGATORS, R.-. 2015b. Ibrutinib as Initial Therapy for Patients with Chronic Lymphocytic Leukemia. *New England Journal of Medicine,* 373**,** 2425-2437.

BUTTGEREIT, F. & BRAND, M. D. 1995. A hierarchy of ATP-consuming processes in mammalian cells. *Biochem J,* 312 (Pt 1)**,** 163-7.

BYRD, J. C., FURMAN, R. R., COUTRE, S. E., BURGER, J. A., BLUM, K. A., COLEMAN, M., WIERDA, W. G., JONES, J. A., ZHAO, W., HEEREMA, N. A., JOHNSON, A. J., SHAW, Y., BILOTTI, E., ZHOU, C., JAMES, D. F. & O'BRIEN, S. 2015. Three-year follow-up of treatment-naive and previously treated patients with CLL and SLL receiving single-agent ibrutinib. *Blood,* 125**,** 2497-506.

BYRD, J. C., FURMAN, R. R., COUTRE, S. E., FLINN, I. W., BURGER, J. A., BLUM, K. A., GRANT, B., SHARMAN, J. P., COLEMAN, M., WIERDA, W. G., JONES, J. A., ZHAO, W., HEEREMA, N. A., JOHNSON, A. J., SUKBUNTHERNG, J., CHANG, B. Y., CLOW, F., HEDRICK, E., BUGGY, J. J., JAMES, D. F. & O'BRIEN, S. 2013. Targeting BTK with ibrutinib in relapsed chronic lymphocytic leukemia. *N Engl J Med,* 369**,** 32-42.

CAHILL, N., BERGH, A. C., KANDURI, M., GORANSSON-KULTIMA, H., MANSOURI, L., ISAKSSON, A., RYAN, F., SMEDBY, K. E., JULIUSSON, G., SUNDSTROM, C., ROSEN, A. & ROSENQUIST, R. 2013. 450K-array analysis of chronic lymphocytic leukemia cells reveals global DNA methylation to be relatively stable over time and similar in resting and proliferative compartments. *Leukemia,* 27**,** 150-8.

CALIN, G. A., CIMMINO, A., FABBRI, M., FERRACIN, M., WOJCIK, S. E., SHIMIZU, M., TACCIOLI, C., ZANESI, N., GARZON, R., AQEILAN, R. I., ALDER, H., VOLINIA, S., RASSENTI, L., LIU, X., LIU, C. G., KIPPS, T. J., NEGRINI, M. & CROCE, C. M. 2008. MiR-15a and miR-16-1 cluster functions in human leukemia. *Proc Natl Acad Sci U S A,* 105**,** 5166-71.

CALIN, G. A., DUMITRU, C. D., SHIMIZU, M., BICHI, R., ZUPO, S., NOCH, E., ALDLER, H., RATTAN, S., KEATING, M., RAI, K., RASSENTI, L., KIPPS, T., NEGRINI, M., BULLRICH, F. & CROCE, C. M. 2002. Frequent deletions and down-regulation of micro- RNA genes miR15 and miR16 at 13q14 in chronic lymphocytic leukemia. *Proc Natl Acad Sci U S A,* 99**,** 15524-9.

CALLAHAN, K. P., MINHAJUDDIN, M., CORBETT, C., LAGADINOU, E. D., ROSSI, R. M., GROSE, V., BALYS, M. M., PAN, L., JACOB, S., FRONTIER, A., GREVER, M. R., LUCAS, D. M., KINGHORN, A. D., LIESVELD, J. L., BECKER, M. W. & JORDAN, C. T. 2014. Flavaglines target primitive leukemia cells and enhance anti-leukemia drug activity. *Leukemia,* 28**,** 1960-8.

CAMUS, V., MILOUDI, H., TALY, A., SOLA, B. & JARDIN, F. 2017. XPO1 in B cell hematological malignancies: from recurrent somatic mutations to targeted therapy. *J Hematol Oncol,* 10**,** 47.

CARAYOL, N., KATSOULIDIS, E., SASSANO, A., ALTMAN, J. K., DRUKER, B. J. & PLATANIAS, L. C. 2008. Suppression of programmed cell death 4 (PDCD4) protein expression by BCR-ABL-regulated engagement of the mTOR/p70 S6 kinase pathway. *J Biol Chem,* 283**,** 8601-10.

CENCIC, R., CARRIER, M., GALICIA-VAZQUEZ, G., BORDELEAU, M. E., SUKARIEH, R., BOURDEAU, A., BREM, B., TEODORO, J. G., GREGER, H., TREMBLAY, M. L., PORCO, J. A., JR. & PELLETIER, J. 2009. Antitumor activity and mechanism of action of the cyclopenta[b]benzofuran, silvestrol. *PLoS One,* 4**,** e5223.

CENCIC, R. & PELLETIER, J. 2016. Hippuristanol - A potent steroid inhibitor of eukaryotic initiation factor 4A. *Translation (Austin),* 4**,** e1137381.

CHAN, L. Y., MUGLER, C. F., HEINRICH, S., VALLOTTON, P. & WEIS, K. 2018. Non-invasive measurement of mRNA decay reveals translation initiation as the major determinant of mRNA stability. *Elife,* 7.

CHEN, R., GUO, L., CHEN, Y., JIANG, Y., WIERDA, W. G. & PLUNKETT, W. 2011. Homoharringtonine reduced Mcl-1 expression and induced apoptosis in chronic lymphocytic leukemia. *Blood,* 117**,** 156-64.

CHESON, B. D., HEITNER ENSCHEDE, S., CERRI, E., DESAI, M., POTLURI, J., LAMANNA, N. & TAM, C. 2017. Tumor Lysis Syndrome in Chronic Lymphocytic Leukemia with Novel Targeted Agents. *Oncologist,* 22**,** 1283-1291.

CHU, J. & PELLETIER, J. 2015. Targeting the eIF4A RNA helicase as an anti-neoplastic approach. *Biochim Biophys Acta,* 1849**,** 781-91.

CIMMINO, A., CALIN, G. A., FABBRI, M., IORIO, M. V., FERRACIN, M., SHIMIZU, M., WOJCIK, S. E., AQEILAN, R. I., ZUPO, S., DONO, M., RASSENTI, L., ALDER, H., VOLINIA, S., LIU, C. G., KIPPS, T. J., NEGRINI, M. & CROCE, C. M. 2005. miR-15 and miR-16 induce apoptosis by targeting BCL2. *Proc Natl Acad Sci U S A,* 102**,** 13944-9.

COELHO, V., KRYSOV, S., STEELE, A., SANCHEZ HIDALGO, M., JOHNSON, P. W., CHANA, P. S., PACKHAM, G., STEVENSON, F. K. & FORCONI, F. 2013. Identification in CLL of circulating intraclonal subgroups with varying B-cell receptor expression and function. *Blood,* 122**,** 2664-72.

COFFMAN, R. L. & WEISSMAN, I. L. 1983. Immunoglobulin gene rearrangement during pre-B cell differentiation. *J Mol Cell Immunol,* 1**,** 31-41.

COLLINS, R. J., HARMON, B. V., SOUVLIS, T., POPE, J. H. & KERR, J. F. 1991. Effects of cycloheximide on B-chronic lymphocytic leukaemic and normal lymphocytes in vitro: induction of apoptosis. *Br J Cancer,* 64**,** 518-22.

COMPAGNO, M., WANG, Q., PIGHI, C., CHEONG, T. C., MENG, F. L., POGGIO, T., YEAP, L. S., KARACA, E., BLASCO, R. B., LANGELLOTTO, F., AMBROGIO, C., VOENA, C., WIESTNER, A., KASAR, S. N., BROWN, J. R., SUN, J., WU, C. J., GOSTISSA, M., ALT, F. W. & CHIARLE, R. 2017. Phosphatidylinositol 3-kinase delta blockade increases genomic instability in B cells. *Nature,* 542**,** 489-493.

CORFE, S. A. & PAIGE, C. J. 2012. The many roles of IL-7 in B cell development; mediator of survival, proliferation and differentiation. *Semin Immunol,* 24**,** 198-208.

COSTE, I., LE CORF, K., KFOURY, A., HMITOU, I., DRUILLENNEC, S., HAINAUT, P., EYCHENE, A., LEBECQUE, S. & RENNO, T. 2010. Dual function of MyD88 in RAS signaling and inflammation, leading to mouse and human cell transformation. *J Clin Invest,* 120**,** 3663-7.

COSTINEAN, S., ZANESI, N., PEKARSKY, Y., TILI, E., VOLINIA, S., HEEREMA, N. & CROCE, C. M. 2006. Pre-B cell proliferation and lymphoblastic leukemia/high-grade lymphoma in E(mu)-miR155 transgenic mice. *Proc Natl Acad Sci U S A,* 103**,** 7024-9.

CRESSWELL, P. 1994. Assembly, transport, and function of MHC class II molecules. *Annu Rev Immunol,* 12**,** 259-93.

CUI, B., CHEN, L., ZHANG, S., MRAZ, M., FECTEAU, J. F., YU, J., GHIA, E. M., ZHANG, L., BAO, L., RASSENTI, L. Z., MESSER, K., CALIN, G. A., CROCE, C. M. & KIPPS, T. J. 2014. MicroRNA-155 influences B-cell receptor signaling and associates with aggressive disease in chronic lymphocytic leukemia. *Blood,* 124**,** 546-54.

CULJKOVIC-KRALJACIC, B., FERNANDO, T. M., MARULLO, R., CALVO-VIDAL, N., VERMA, A., YANG, S., TABBO, F., GAUDIANO, M., ZAHREDDINE, H., GOLDSTEIN, R. L., PATEL, J., TALDONE, T., CHIOSIS, G., LADETTO, M., GHIONE, P., MACHIORLATTI, R., ELEMENTO, O., INGHIRAMI, G., MELNICK, A., BORDEN, K. L. & CERCHIETTI, L. 2016. Combinatorial targeting of nuclear export and translation of RNA inhibits aggressive B-cell lymphomas. *Blood,* 127**,** 858-68.

CULJKOVIC, B., TOPISIROVIC, I., SKRABANEK, L., RUIZ-GUTIERREZ, M. & BORDEN, K. L. 2005. eIF4E promotes nuclear export of cyclin D1 mRNAs via an element in the 3'UTR. *J Cell Biol,* 169**,** 245-56.

CULJKOVIC, B., TOPISIROVIC, I., SKRABANEK, L., RUIZ-GUTIERREZ, M. & BORDEN, K. L. 2006. eIF4E is a central node of an RNA regulon that governs cellular proliferation. *J Cell Biol,* 175**,** 415-26.

CUTRONA, G., COLOMBO, M., MATIS, S., FABBI, M., SPRIANO, M., CALLEA, V., VIGNA, E., GENTILE, M., ZUPO, S., CHIORAZZI, N., MORABITO, F. & FERRARINI, M. 2008. Clonal heterogeneity in chronic lymphocytic leukemia cells: superior response to surface IgM cross-linking in CD38, ZAP-70-positive cells. *Haematologica,* 93**,** 413-22.

D'AVOLA, A., DRENNAN, S., TRACY, I., HENDERSON, I., CHIECCHIO, L., LARRAYOZ, M., ROSE-ZERILLI, M., STREFFORD, J., PLASS, C., JOHNSON, P. W., STEELE, A. J., PACKHAM, G., STEVENSON, F. K., OAKES, C. C. & FORCONI, F. 2016. Surface IgM expression and function are associated with clinical behavior, genetic abnormalities, and DNA methylation in CLL. *Blood,* 128**,** 816-26.

DAL BO, M., BULIAN, P., BOMBEN, R., ZUCCHETTO, A., ROSSI, F. M., POZZO, F., TISSINO, E., BENEDETTI, D., BITTOLO, T., NANNI, P., CATTAROSSI, I., ZAINA, E., CHIVILO, H., DEGAN, M., ZAJA, F., POZZATO, G., CHIARENZA, A., DI RAIMONDO, F., DEL PRINCIPE, M. I., DEL POETA, G., ROSSI, D., GAIDANO, G. & GATTEI, V. 2016. CD49d prevails over the novel recurrent mutations as independent prognosticator of overall survival in chronic lymphocytic leukemia. *Leukemia,* 30**,** 2011-2018.

DAMLE, R. N., WASIL, T., FAIS, F., GHIOTTO, F., VALETTO, A., ALLEN, S. L., BUCHBINDER, A., BUDMAN, D., DITTMAR, K., KOLITZ, J., LICHTMAN, S. M., SCHULMAN, P., VINCIGUERRA, V. P., RAI, K. R., FERRARINI, M. & CHIORAZZI, N. 1999. Ig V gene mutation status and CD38 expression as novel prognostic indicators in chronic lymphocytic leukemia. *Blood,* 94**,** 1840-7.

DE BENEDETTI, A. & GRAFF, J. R. 2004. eIF-4E expression and its role in malignancies and metastases. *Oncogene,* 23**,** 3189-99.

DE CLARO, R. A., MCGINN, K. M., VERDUN, N., LEE, S. L., CHIU, H. J., SABER, H., BROWER, M. E., CHANG, C. J., PFUMA, E., HABTEMARIAM, B., BULLOCK, J., WANG, Y., NIE, L., CHEN, X. H., LU, D. R., AL-HAKIM, A., KANE, R. C., KAMINSKAS, E., JUSTICE, R., FARRELL, A. T. & PAZDUR, R. 2015. FDA Approval: Ibrutinib for Patients with Previously Treated Mantle Cell Lymphoma and Previously Treated Chronic Lymphocytic Leukemia. *Clin Cancer Res,* 21**,** 3586-90.

DE FALCO, F., SABATINI, R., DEL PAPA, B., FALZETTI, F., DI IANNI, M., SPORTOLETTI, P., BALDONI, S., SCREPANTI, I., MARCONI, P. & ROSATI, E. 2015. Notch signaling sustains the expression of Mcl-1 and the activity of eIF4E to promote cell survival in CLL. *Oncotarget,* 6**,** 16559-72.

DEAGLIO, S., VAISITTI, T., ZUCCHETTO, A., GATTEI, V. & MALAVASI, F. 2010. CD38 as a molecular compass guiding topographical decisions of chronic lymphocytic leukemia cells. *Semin Cancer Biol,* 20**,** 416-23.

DENNIS, M. D., JEFFERSON, L. S. & KIMBALL, S. R. 2012. Role of p70S6K1-mediated phosphorylation of eIF4B and PDCD4 proteins in the regulation of protein synthesis. *J Biol Chem,* 287**,** 42890-9.

DI BERNARDO, M. C., CROWTHER-SWANEPOEL, D., BRODERICK, P., WEBB, E., SELLICK, G., WILD, R., SULLIVAN, K., VIJAYAKRISHNAN, J., WANG, Y., PITTMAN, A. M., SUNTER, N. J., HALL, A. G., DYER, M. J., MATUTES, E., DEARDEN, C., MAINOU-FOWLER, T., JACKSON, G. H., SUMMERFIELD, G., HARRIS, R. J., PETTITT, A. R., HILLMEN, P., ALLSUP, D. J., BAILEY, J. R., PRATT, G., PEPPER, C., FEGAN, C., ALLAN, J. M., CATOVSKY, D. & HOULSTON, R. S. 2008. A genome-wide association study identifies six susceptibility loci for chronic lymphocytic leukemia. *Nat Genet,* 40**,** 1204-10.

DOHNER, H., STILGENBAUER, S., BENNER, A., LEUPOLT, E., KROBER, A., BULLINGER, L., DOHNER, K., BENTZ, M. & LICHTER, P. 2000. Genomic aberrations and survival in chronic lymphocytic leukemia. *N Engl J Med,* 343**,** 1910-6.

DOHNER, H., STILGENBAUER, S., JAMES, M. R., BENNER, A., WEILGUNI, T., BENTZ, M., FISCHER, K., HUNSTEIN, W. & LICHTER, P. 1997. 11q deletions identify a new subset of B-cell chronic lymphocytic leukemia characterized by extensive nodal involvement and inferior prognosis. *Blood,* 89**,** 2516-22.

DOLMETSCH, R. E., LEWIS, R. S., GOODNOW, C. C. & HEALY, J. I. 1997. Differential activation of transcription factors induced by Ca2+ response amplitude and duration. *Nature,* 386**,** 855-8.

DONAHUE, A. C. & FRUMAN, D. A. 2007. Distinct signaling mechanisms activate the target of rapamycin in response to different B-cell stimuli. *Eur J Immunol,* 37**,** 2923-36.

DUBREZ-DALOZ, L., DUPOUX, A. & CARTIER, J. 2008. IAPs: more than just inhibitors of apoptosis proteins. *Cell Cycle,* 7**,** 1036-46.

DUHREN-VON MINDEN, M., UBELHART, R., SCHNEIDER, D., WOSSNING, T., BACH, M. P., BUCHNER, M., HOFMANN, D., SUROVA, E., FOLLO, M., KOHLER, F., WARDEMANN, H., ZIRLIK, K., VEELKEN, H. & JUMAA, H. 2012. Chronic lymphocytic leukaemia is driven by antigen-independent cell-autonomous signalling. *Nature,* 489**,** 309-12.

DUNNICK, W. A., COLLINS, J. T., SHI, J., WESTFIELD, G., FONTAINE, C., HAKIMPOUR, P. & PAPAVASILIOU, F. N. 2009. Switch recombination and somatic hypermutation are controlled by the heavy chain 3' enhancer region. *J Exp Med,* 206**,** 2613-23.

DURIG, J., EBELING, P., GRABELLUS, F., SORG, U. R., MOLLMANN, M., SCHUTT, P., GOTHERT, J., SELLMANN, L., SEEBER, S., FLASSHOVE, M., DUHRSEN, U. & MORITZ, T. 2007. A novel nonobese diabetic/severe combined immunodeficient xenograft model for chronic lymphocytic leukemia reflects important clinical characteristics of the disease. *Cancer Res,* 67**,** 8653-61.

DURIG, J., NUCKEL, H., CREMER, M., FUHRER, A., HALFMEYER, K., FANDREY, J., MOROY, T., KLEIN-HITPASS, L. & DUHRSEN, U. 2003. ZAP-70 expression is a prognostic factor in chronic lymphocytic leukemia. *Leukemia,* 17**,** 2426-34.

EFREMOV, D. G., IVANOVSKI, M., BATISTA, F. D., POZZATO, G. & BURRONE, O. R. 1996. IgM-producing chronic lymphocytic leukemia cells undergo immunoglobulin isotype-switching without acquiring somatic mutations. *J Clin Invest,* 98**,** 290-8.

EHLICH, A., MARTIN, V., MULLER, W. & RAJEWSKY, K. 1994. Analysis of the B-cell progenitor compartment at the level of single cells. *Curr Biol,* 4**,** 573-83.

ETCHIN, J., SANDA, T., MANSOUR, M. R., KENTSIS, A., MONTERO, J., LE, B. T., CHRISTIE, A. L., MCCAULEY, D., RODIG, S. J., KAUFFMAN, M., SHACHAM, S., STONE, R., LETAI, A., KUNG, A. L. & THOMAS LOOK, A. 2013. KPT-330 inhibitor of CRM1 (XPO1)-mediated nuclear export has selective anti-leukaemic activity in preclinical models of T-cell acute lymphoblastic leukaemia and acute myeloid leukaemia. *Br J Haematol,* 161**,** 117-27.

EZINE, S., WEISSMAN, I. L. & ROUSE, R. V. 1984. Bone marrow cells give rise to distinct cell clones within the thymus. *Nature,* 309**,** 629-31.

FABBRI, G., RASI, S., ROSSI, D., TRIFONOV, V., KHIABANIAN, H., MA, J., GRUNN, A., FANGAZIO, M., CAPELLO, D., MONTI, S., CRESTA, S., GARGIULO, E., FORCONI, F., GUARINI, A., ARCAINI, L., PAULLI, M., LAURENTI, L., LAROCCA, L. M., MARASCA, R., GATTEI, V., OSCIER, D., BERTONI, F., MULLIGHAN, C. G., FOA, R., PASQUALUCCI, L., RABADAN, R., DALLA-FAVERA, R. & GAIDANO, G. 2011. Analysis of the chronic lymphocytic leukemia coding genome: role of NOTCH1 mutational activation. *J Exp Med,* 208**,** 1389-401.

FAIS, F., GHIOTTO, F., HASHIMOTO, S., SELLARS, B., VALETTO, A., ALLEN, S. L., SCHULMAN, P., VINCIGUERRA, V. P., RAI, K., RASSENTI, L. Z., KIPPS, T. J., DIGHIERO, G., SCHROEDER, H. W., JR., FERRARINI, M. & CHIORAZZI, N. 1998. Chronic lymphocytic leukemia B cells express restricted sets of mutated and unmutated antigen receptors. *J Clin Invest,* 102**,** 1515-25.

FERRER, A., OLLILA, J., TOBIN, G., NAGY, B., THUNBERG, U., AALTO, Y., VIHINEN, M., VILPO, J., ROSENQUIST, R. & KNUUTILA, S. 2004. Different gene expression in immunoglobulin-mutated and immunoglobulin-unmutated forms of chronic lymphocytic leukemia. *Cancer Genet Cytogenet,* 153**,** 69-72.

FISHER, W. G., YANG, P. C., MEDIKONDURI, R. K. & JAFRI, M. S. 2006. NFAT and NFkappaB activation in T lymphocytes: a model of differential activation of gene expression. *Ann Biomed Eng,* 34**,** 1712-28.

FORCONI, F., POTTER, K. N., WHEATLEY, I., DARZENTAS, N., SOZZI, E., STAMATOPOULOS, K., MOCKRIDGE, C. I., PACKHAM, G. & STEVENSON, F. K. 2010. The normal IGHV1-69-derived B-cell repertoire contains stereotypic patterns characteristic of unmutated CLL. *Blood,* 115**,** 71-7.

FORNEROD, M., OHNO, M., YOSHIDA, M. & MATTAJ, I. W. 1997. CRM1 is an export receptor for leucine-rich nuclear export signals. *Cell,* 90**,** 1051-60.

FORQUET, F., BAROIS, N., MACHY, P., TRUCY, J., ZIMMERMANN, V. S., LESERMAN, L. & DAVOUST, J. 1999. Presentation of antigens internalized through the B cell receptor requires newly synthesized MHC class II molecules. *J Immunol,* 162**,** 3408-16.

FRESNO, M., JIMENEZ, A. & VAZQUEZ, D. 1977. Inhibition of translation in eukaryotic systems by harringtonine. *Eur J Biochem,* 72**,** 323-30.

FU, C., TURCK, C. W., KUROSAKI, T. & CHAN, A. C. 1998. BLNK: a central linker protein in B cell activation. *Immunity,* 9**,** 93-103.

FUGMANN, S. D., LEE, A. I., SHOCKETT, P. E., VILLEY, I. J. & SCHATZ, D. G. 2000. The RAG proteins and V(D)J recombination: complexes, ends, and transposition. *Annu Rev Immunol,* 18**,** 495-527.

FUJIMOTO, M., KUWANO, Y., WATANABE, R., ASASHIMA, N., NAKASHIMA, H., YOSHITAKE, S., OKOCHI, H., TAMAKI, K., POE, J. C., TEDDER, T. F. & SATO, S. 2006. B cell antigen receptor and CD40 differentially regulate CD22 tyrosine phosphorylation. *J Immunol,* 176**,** 873-9.

FUKAO, A., MISHIMA, Y., TAKIZAWA, N., OKA, S., IMATAKA, H., PELLETIER, J., SONENBERG, N., THOMA, C. & FUJIWARA, T. 2014. MicroRNAs trigger dissociation of eIF4AI and eIF4AII from target mRNAs in humans. *Mol Cell,* 56**,** 79-89.

FULCHER, D. A., LYONS, A. B., KORN, S. L., COOK, M. C., KOLEDA, C., PARISH, C., FAZEKAS DE ST GROTH, B. & BASTEN, A. 1996. The fate of self-reactive B cells depends primarily on the degree of antigen receptor engagement and availability of T cell help. *J Exp Med,* 183**,** 2313-28.

FULDA, S. & DEBATIN, K. M. 2006. Targeting inhibitor of apoptosis proteins (IAPs) for diagnosis and treatment of human diseases. *Recent Pat Anticancer Drug Discov,* 1**,** 81-9.

FUNARO, A. & MALAVASI, F. 1999. Human CD38, a surface receptor, an enzyme, an adhesion molecule and not a simple marker. *J Biol Regul Homeost Agents,* 13**,** 54-61.

FURMAN, R. R., SHARMAN, J. P., COUTRE, S. E., CHESON, B. D., PAGEL, J. M., HILLMEN, P., BARRIENTOS, J. C., ZELENETZ, A. D., KIPPS, T. J., FLINN, I., GHIA, P., ERADAT, H., ERVIN, T., LAMANNA, N., COIFFIER, B., PETTITT, A. R., MA, S., STILGENBAUER, S., CRAMER, P., AIELLO, M., JOHNSON, D. M., MILLER, L. L., LI, D., JAHN, T. M., DANSEY, R. D., HALLEK, M. & O'BRIEN, S. M. 2014. Idelalisib and rituximab in relapsed chronic lymphocytic leukemia. *N Engl J Med,* 370**,** 997-1007.

GATTO, D. & BRINK, R. 2010. The germinal center reaction. *J Allergy Clin Immunol,* 126**,** 898-907; quiz 908-9.

GHIA, P., CHIORAZZI, N. & STAMATOPOULOS, K. 2008. Microenvironmental influences in chronic lymphocytic leukaemia: the role of antigen stimulation. *J Intern Med,* 264**,** 549-62.

GHIA, P., STAMATOPOULOS, K., BELESSI, C., MORENO, C., STELLA, S., GUIDA, G., MICHEL, A., CRESPO, M., LAOUTARIS, N., MONTSERRAT, E., ANAGNOSTOPOULOS, A., DIGHIERO, G., FASSAS, A., CALIGARIS-CAPPIO, F. & DAVI, F. 2005. Geographic patterns and pathogenetic implications of IGHV gene usage in chronic lymphocytic leukemia: the lesson of the IGHV3-21 gene. *Blood,* 105**,** 1678-85.

GINGRAS, A. C., GYGI, S. P., RAUGHT, B., POLAKIEWICZ, R. D., ABRAHAM, R. T., HOEKSTRA, M. F., AEBERSOLD, R. & SONENBERG, N. 1999a. Regulation of 4E-BP1 phosphorylation: a novel two-step mechanism. *Genes Dev,* 13**,** 1422-37.

GINGRAS, A. C., RAUGHT, B. & SONENBERG, N. 1999b. eIF4 initiation factors: effectors of mRNA recruitment to ribosomes and regulators of translation. *Annu Rev Biochem,* 68**,** 913-63.

GINGRAS, A. C., RAUGHT, B. & SONENBERG, N. 2001. Control of translation by the target of rapamycin proteins. *Prog Mol Subcell Biol,* 27**,** 143-74.

GLADSTONE, D. E., SWINNEN, L., KASAMON, Y., BLACKFORD, A., GOCKE, C. D., GRIFFIN, C. A., MEADE, J. B. & JONES, R. J. 2011. Importance of immunoglobulin heavy chain variable region mutational status in del(13q) chronic lymphocytic leukemia. *Leuk Lymphoma,* 52**,** 1873-81.

GOBESSI, S., LAURENTI, L., LONGO, P. G., SICA, S., LEONE, G. & EFREMOV, D. G. 2007. ZAP-70 enhances B-cell-receptor signaling despite absent or inefficient tyrosine kinase activation in chronic lymphocytic leukemia and lymphoma B cells. *Blood,* 109**,** 2032-9.

GOLDIN, L. R., BJORKHOLM, M., KRISTINSSON, S. Y., TURESSON, I. & LANDGREN, O. 2009. Elevated risk of chronic lymphocytic leukemia and other indolent non-Hodgkin's lymphomas among relatives of patients with chronic lymphocytic leukemia. *Haematologica,* 94**,** 647-53.

GOODNOW, C. C. & BASTEN, A. 1989. Self-tolerance in B lymphocytes. *Semin Immunol,* 1**,** 125-35.

GRAVINA, G. L., SENAPEDIS, W., MCCAULEY, D., BALOGLU, E., SHACHAM, S. & FESTUCCIA, C. 2014. Nucleo-cytoplasmic transport as a therapeutic target of cancer. *J Hematol Oncol,* 7**,** 85.

GREGORY, R. I., CHENDRIMADA, T. P., COOCH, N. & SHIEKHATTAR, R. 2005. Human RISC couples microRNA biogenesis and posttranscriptional gene silencing. *Cell,* 123**,** 631-40.

GREWAL, I. S. & FLAVELL, R. A. 1996. The role of CD40 ligand in costimulation and T-cell activation. *Immunol Rev,* 153**,** 85-106.

GUINN, D., RUPPERT, A. S., MADDOCKS, K., JAGLOWSKI, S., GORDON, A., LIN, T. S., LARSON, R., MARCUCCI, G., HERTLEIN, E., WOYACH, J., JOHNSON, A. J. & BYRD, J. C. 2015. miR-155 expression is associated with chemoimmunotherapy outcome and is modulated by Bruton's tyrosine kinase inhibition with Ibrutinib. *Leukemia,* 29**,** 1210-3.

HALLEK, M. 2010. Therapy of chronic lymphocytic leukaemia. *Best Pract Res Clin Haematol,* 23**,** 85-96.

HALLEK, M. 2015. Chronic lymphocytic leukemia: 2015 Update on diagnosis, risk stratification, and treatment. *Am J Hematol,* 90**,** 446-60.

HALLEK, M. 2017. Chronic lymphocytic leukemia: 2017 update on diagnosis, risk stratification, and treatment. *Am J Hematol,* 92**,** 946-965.

HALLEK, M., CHESON, B. D., CATOVSKY, D., CALIGARIS-CAPPIO, F., DIGHIERO, G., DOHNER, H., HILLMEN, P., KEATING, M., MONTSERRAT, E., CHIORAZZI, N., STILGENBAUER, S., RAI, K. R., BYRD, J. C., EICHHORST, B., O'BRIEN, S., ROBAK, T., SEYMOUR, J. F. & KIPPS, T. J. 2018. iwCLL guidelines for diagnosis, indications for treatment, response assessment, and supportive management of CLL. *Blood,* 131**,** 2745-2760.

HALLEK, M., CHESON, B. D., CATOVSKY, D., CALIGARIS-CAPPIO, F., DIGHIERO, G., DOHNER, H., HILLMEN, P., KEATING, M. J., MONTSERRAT, E., RAI, K. R., KIPPS, T. J. & INTERNATIONAL WORKSHOP ON CHRONIC LYMPHOCYTIC, L. 2008. Guidelines for the diagnosis and treatment of chronic lymphocytic leukemia: a report from the International Workshop on Chronic Lymphocytic Leukemia updating the National Cancer Institute-Working Group 1996 guidelines. *Blood,* 111**,** 5446-56.

HAMBLIN, T. J., DAVIS, Z., GARDINER, A., OSCIER, D. G. & STEVENSON, F. K. 1999. Unmutated Ig V(H) genes are associated with a more aggressive form of chronic lymphocytic leukemia. *Blood,* 94**,** 1848-54.

HARWOOD, N. E. & BATISTA, F. D. 2010a. Antigen presentation to B cells. *F1000 Biol Rep,* 2**,** 87.

HARWOOD, N. E. & BATISTA, F. D. 2010b. Early Events in B Cell Activation. *Annual Review of Immunology, Vol 28,* 28**,** 185-210.

HASHIMOTO, A., OKADA, H., JIANG, A., KUROSAKI, M., GREENBERG, S., CLARK, E. A. & KUROSAKI, T. 1998. Involvement of guanosine triphosphatases and phospholipase C-gamma2 in extracellular signal-regulated kinase, c-Jun NH2-terminal kinase, and p38 mitogen-activated protein kinase activation by the B cell antigen receptor. *J Exp Med,* 188**,** 1287-95.

HERISHANU, Y., PEREZ-GALAN, P., LIU, D., BIANCOTTO, A., PITTALUGA, S., VIRE, B., GIBELLINI, F., NJUGUNA, N., LEE, E., STENNETT, L., RAGHAVACHARI, N., LIU, P., MCCOY, J. P., RAFFELD, M., STETLER-STEVENSON, M., YUAN, C., SHERRY, R., ARTHUR, D. C., MARIC, I., WHITE, T., MARTI, G. E., MUNSON, P., WILSON, W. H. & WIESTNER, A. 2011. The lymph node

microenvironment promotes B-cell receptor signaling, NF-kappaB activation, and tumor proliferation in chronic lymphocytic leukemia. *Blood,* 117**,** 563-74.

HERRICK, D. J. & ROSS, J. 1994. The half-life of c-myc mRNA in growing and serum-stimulated cells: influence of the coding and 3' untranslated regions and role of ribosome translocation. *Mol Cell Biol,* 14**,** 2119-28.

HILLIARD, A., HILLIARD, B., ZHENG, S. J., SUN, H., MIWA, T., SONG, W., GOKE, R. & CHEN, Y. H. 2006. Translational regulation of autoimmune inflammation and lymphoma genesis by programmed cell death 4. *J Immunol,* 177**,** 8095-102.

HINNEBUSCH, A. G. 2011. Molecular mechanism of scanning and start codon selection in eukaryotes. *Microbiol Mol Biol Rev,* 75**,** 434-67, first page of table of contents.

HOLCIK, M., LEFEBVRE, C., YEH, C., CHOW, T. & KORNELUK, R. G. 1999. A new internal-ribosome-entry-site motif potentiates XIAP-mediated cytoprotection. *Nat Cell Biol,* 1**,** 190-2.

HOLZ, M. K. & BLENIS, J. 2005. Identification of S6 kinase 1 as a novel mammalian target of rapamycin (mTOR)-phosphorylating kinase. *J Biol Chem,* 280**,** 26089-93.

HOMIG-HOLZEL, C., HOJER, C., RASTELLI, J., CASOLA, S., STROBL, L. J., MULLER, W., QUINTANILLA-MARTINEZ, L., GEWIES, A., RULAND, J., RAJEWSKY, K. & ZIMBER-STROBL, U. 2008. Constitutive CD40 signaling in B cells selectively activates the noncanonical NF-kappaB pathway and promotes lymphomagenesis. *J Exp Med,* 205**,** 1317-29.

HOOGEBOOM, R., VAN KESSEL, K. P., HOCHSTENBACH, F., WORMHOUDT, T. A., REINTEN, R. J., WAGNER, K., KATER, A. P., GUIKEMA, J. E., BENDE, R. J. & VAN NOESEL, C. J. 2013. A mutated B cell chronic lymphocytic leukemia subset that recognizes and responds to fungi. *J Exp Med,* 210**,** 59-70.

HORVILLEUR, E., SBARRATO, T., HILL, K., SPRIGGS, R. V., SCREEN, M., GOODREM, P. J., SAWICKA, K., CHAPLIN, L. C., TOURIOL, C., PACKHAM, G., POTTER, K. N., DIRNHOFER, S., TZANKOV, A., DYER, M. J., BUSHELL, M., MACFARLANE, M. & WILLIS, A. E. 2014. A role for eukaryotic initiation factor 4B overexpression in the pathogenesis of diffuse large B-cell lymphoma. *Leukemia,* 28**,** 1092-102.

HUANG, Y. & CARMICHAEL, G. G. 1996. Role of polyadenylation in nucleocytoplasmic transport of mRNA. *Mol Cell Biol,* 16**,** 1534-42.

IBORRA, F. J., JACKSON, D. A. & COOK, P. R. 2001. Coupled transcription and translation within nuclei of mammalian cells. *Science,* 293**,** 1139-42.

IIKURA, M., FURIHATA, T., MIZUGUCHI, M., NAGAI, M., IKEDA, M., KATO, N., TSUBOTA, A. & CHIBA, K. 2012. ENT1, a ribavirin transporter, plays a pivotal role in antiviral efficacy of ribavirin in a hepatitis C virus replication cell system. *Antimicrob Agents Chemother,* 56**,** 1407-13.

IWASAKI, S., FLOOR, S. N. & INGOLIA, N. T. 2016. Rocaglates convert DEAD-box protein eIF4A into a sequence-selective translational repressor. *Nature,* 534**,** 558-61.

JACOB, A., COONEY, D., PRADHAN, M. & COGGESHALL, K. M. 2002. Convergence of signaling pathways on the activation of ERK in B cells. *J Biol Chem,* 277**,** 23420-6.

JAIN, P., KANAGAL-SHAMANNA, R., WIERDA, W., KEATING, M., SARWARI, N., ROZOVSKI, U., THOMPSON, P., BURGER, J., KANTARJIAN, H., PATEL, K. P., MEDEIROS, L. J., LUTHRA, R. & ESTROV, Z. 2016. Clinical and molecular characteristics of XPO1 mutations in patients with chronic lymphocytic leukemia. *Am J Hematol,* 91**,** E478-E479.

JARVIS, L. J., MAGUIRE, J. E. & LEBIEN, T. W. 1997. Contact between human bone marrow stromal cells and B lymphocytes enhances very late antigen-4/vascular cell adhesion molecule-1-independent tyrosine phosphorylation of focal adhesion kinase, paxillin, and ERK2 in stromal cells. *Blood,* 90**,** 1626-35.

JIA, L. & GRIBBEN, J. G. 2014. Dangerous power: mitochondria in CLL cells. *Blood,* 123**,** 2596-7.

JOHNSEN, H. E., BERGKVIST, K. S., SCHMITZ, A., KJELDSEN, M. K., HANSEN, S. M., GAIHEDE, M., NORGAARD, M. A., BAECH, J., GRONHOLDT, M. L., JENSEN, F. S., JOHANSEN, P., BODKER, J. S., BOGSTED, M., DYBKAER, K. & MYELOMA STEM CELL, N. 2014. Cell of origin associated classification of B-cell malignancies by gene signatures of the normal B-cell hierarchy. *Leuk Lymphoma,* 55**,** 1251-60.

JOHNSON, K., SHAPIRO-SHELEF, M., TUNYAPLIN, C. & CALAME, K. 2005. Regulatory events in early and late B-cell differentiation. *Mol Immunol,* 42**,** 749-61.

JOHNSTON, J. B., PAUL, J. T., NEUFELD, N. J., HANEY, N., KROPP, D. M., HU, X., CHEANG, M. & GIBSON, S. B. 2004. Role of myeloid cell factor-1 (Mcl-1) in chronic lymphocytic leukemia. *Leuk Lymphoma,* 45**,** 2017-27.

JONES, R. M., BRANDA, J., JOHNSTON, K. A., POLYMENIS, M., GADD, M., RUSTGI, A., CALLANAN, L. & SCHMIDT, E. V. 1996. An essential E box in the promoter of the gene encoding the mRNA cap-binding protein (eukaryotic initiation factor 4E) is a target for activation by c-myc. *Mol Cell Biol,* 16**,** 4754-64.

KAIDA, D., MOTOYOSHI, H., TASHIRO, E., NOJIMA, T., HAGIWARA, M., ISHIGAMI, K., WATANABE, H., KITAHARA, T., YOSHIDA, T., NAKAJIMA, H., TANI, T., HORINOUCHI, S. & YOSHIDA, M. 2007. Spliceostatin A targets SF3b and inhibits both splicing and nuclear retention of pre-mRNA. *Nat Chem Biol,* 3**,** 576-83.

KANAREK, N., LONDON, N., SCHUELER-FURMAN, O. & BEN-NERIAH, Y. 2010. Ubiquitination and degradation of the inhibitors of NF-kappaB. *Cold Spring Harb Perspect Biol,* 2**,** a000166.

KANDURI, M., CAHILL, N., GORANSSON, H., ENSTROM, C., RYAN, F., ISAKSSON, A. & ROSENQUIST, R. 2010. Differential genome-wide array-based methylation profiles in prognostic subsets of chronic lymphocytic leukemia. *Blood,* 115**,** 296-305.

KATAGIRI, T., OGIMOTO, M., HASEGAWA, K., ARIMURA, Y., MITOMO, K., OKADA, M., CLARK, M. R., MIZUNO, K. & YAKURA, H. 1999. CD45 negatively regulates lyn activity by dephosphorylating both positive and negative regulatory tyrosine residues in immature B cells. *J Immunol,* 163**,** 1321-6.

KENTSIS, A., TOPISIROVIC, I., CULJKOVIC, B., SHAO, L. & BORDEN, K. L. 2004. Ribavirin suppresses eIF4E-mediated oncogenic transformation by physical mimicry of the 7-methyl guanosine mRNA cap. *Proc Natl Acad Sci U S A,* 101**,** 18105-10.

KEREKATTE, V., SMILEY, K., HU, B., SMITH, A., GELDER, F. & DE BENEDETTI, A. 1995. The proto-oncogene/translation factor eIF4E: a survey of its expression in breast carcinomas. *Int J Cancer,* 64**,** 27-31.

KHOSRAVI, S., TAM, K. J., ARDEKANI, G. S., MARTINKA, M., MCELWEE, K. J. & ONG, C. J. 2015. eIF4E is an adverse prognostic marker of melanoma patient survival by increasing melanoma cell invasion. *J Invest Dermatol,* 135**,** 1358-1367.

KIEFT, J. S. 2008. Viral IRES RNA structures and ribosome interactions. *Trends Biochem Sci,* 33**,** 274-83.

KIMBALL, S. R. 2002. Regulation of global and specific mRNA translation by amino acids. *J Nutr,* 132**,** 883-6.

KINDT, J. T., GOLDSBY, R.A., OSBORNE, B.A. 2007. *Kuby Immunology* Basingstoke, UK, W.H. Freeman and Company

KING, M. L., CHIANG, C. C., LING, H. C., FUJITA, E., OCHIAI, M. & MCPHAIL, A. T. 1982. X-Ray Crystal-Structure of Rocaglamide, a Novel Antileukemic 1h-Cyclopenta[B]Benzofuran from Aglaia-Elliptifolia. *Journal of the Chemical Society-Chemical Communications***,** 1150-1151.

KISSELEV, L. L. & FROLOVA, L. 1995. Termination of translation in eukaryotes. *Biochem Cell Biol,* 73**,** 1079-86.

KLEIN, U., LIA, M., CRESPO, M., SIEGEL, R., SHEN, Q., MO, T., AMBESI-IMPIOMBATO, A., CALIFANO, A., MIGLIAZZA, A., BHAGAT, G. & DALLA-FAVERA, R. 2010. The DLEU2/miR-15a/16-1 cluster controls B cell proliferation and its deletion leads to chronic lymphocytic leukemia. *Cancer Cell,* 17**,** 28-40.

KOGURE, T., KINGHORN, A. D., YAN, I., BOLON, B., LUCAS, D. M., GREVER, M. R. & PATEL, T. 2013. Therapeutic potential of the translation inhibitor silvestrol in hepatocellular cancer. *PLoS One,* 8**,** e76136.

KOJIMA, K., KORNBLAU, S. M., RUVOLO, V., DILIP, A., DUVVURI, S., DAVIS, R. E., ZHANG, M., WANG, Z., COOMBES, K. R., ZHANG, N., QIU, Y. H., BURKS, J. K., KANTARJIAN, H., SHACHAM, S., KAUFFMAN, M. & ANDREEFF, M. 2013. Prognostic impact and targeting of CRM1 in acute myeloid leukemia. *Blood,* 121**,** 4166-74.

KOROMILAS, A. E., LAZARIS-KARATZAS, A. & SONENBERG, N. 1992. mRNAs containing extensive secondary structure in their 5' non-coding region translate efficiently in cells overexpressing initiation factor eIF-4E. *EMBO J,* 11**,** 4153-8.

KOZAK, M. 1987. At least six nucleotides preceding the AUG initiator codon enhance translation in mammalian cells. *J Mol Biol,* 196**,** 947-50.

KRALJACIC, B. C., ARGUELLO, M., AMRI, A., CORMACK, G. & BORDEN, K. 2011. Inhibition of eIF4E with ribavirin cooperates with common chemotherapies in primary acute myeloid leukemia specimens. *Leukemia,* 25**,** 1197-200.

KRYSOV, S., DIAS, S., PATERSON, A., MOCKRIDGE, C. I., POTTER, K. N., SMITH, K. A., ASHTON-KEY, M., STEVENSON, F. K. & PACKHAM, G. 2012. Surface IgM stimulation induces MEK1/2-dependent MYC expression in chronic lymphocytic leukemia cells. *Blood,* 119**,** 170-9.

KRYSOV, S., STEELE, A. J., COELHO, V., LINLEY, A., SANCHEZ HIDALGO, M., CARTER, M., POTTER, K. N., KENNEDY, B., DUNCOMBE, A. S., ASHTON-KEY, M., FORCONI, F., STEVENSON, F. K. & PACKHAM, G. 2014. Stimulation of surface IgM of chronic lymphocytic leukemia cells induces an unfolded protein response dependent on BTK and SYK. *Blood,* 124**,** 3101-9.

KUROSAKI, T. 2002. Regulation of B-cell signal transduction by adaptor proteins. *Nat Rev Immunol,* 2**,** 354-63.

KUROSAKI, T., MAEDA, A., ISHIAI, M., HASHIMOTO, A., INABE, K. & TAKATA, M. 2000. Regulation of the phospholipase C-gamma2 pathway in B cells. *Immunol Rev,* 176**,** 19-29.

KUROSAKI, T., TAKATA, M., YAMANASHI, Y., INAZU, T., TANIGUCHI, T., YAMAMOTO, T. & YAMAMURA, H. 1994. Syk activation by the Src-family tyrosine kinase in the B cell receptor signaling. *J Exp Med,* 179**,** 1725-9.

KUROSAKI, T. & TSUKADA, S. 2000. BLNK: connecting Syk and Btk to calcium signals. *Immunity,* 12**,** 1-5.

KURUVILLA, J., SAVONA, M., BAZ, R., MAU-SORENSEN, P. M., GABRAIL, N., GARZON, R., STONE, R., WANG, M., SAVOIE, L., MARTIN, P., FLINN, I., JACOBY, M., UNGER, T. J., SAINT-MARTIN, J. R., RASHAL, T., FRIEDLANDER, S., CARLSON, R., KAUFFMAN, M., SHACHAM, S. & GUTIERREZ, M. 2017. Selective inhibition of nuclear export with selinexor in patients with non-Hodgkin lymphoma. *Blood,* 129**,** 3175-3183.

LAINE, J., KUNSTLE, G., OBATA, T., SHA, M. & NOGUCHI, M. 2000. The protooncogene TCL1 is an Akt kinase coactivator. *Mol Cell,* 6**,** 395-407.

LAM, K. P., KUHN, R. & RAJEWSKY, K. 1997. In vivo ablation of surface immunoglobulin on mature B cells by inducible gene targeting results in rapid cell death. *Cell,* 90**,** 1073-83.

LAMPSON, B. L., KASAR, S. N., MATOS, T. R., MORGAN, E. A., RASSENTI, L., DAVIDS, M. S., FISHER, D. C., FREEDMAN, A. S., JACOBSON, C. A., ARMAND, P., ABRAMSON, J. S., ARNASON, J. E., KIPPS, T. J., FEIN, J., FERNANDES, S., HANNA, J., RITZ, J., KIM, H. T. & BROWN, J. R. 2016. Idelalisib given front-line for treatment of chronic lymphocytic leukemia causes frequent immune-mediated hepatotoxicity. *Blood,* 128**,** 195-203.

LANDAU, D. A., TAUSCH, E., TAYLOR-WEINER, A. N., STEWART, C., REITER, J. G., BAHLO, J., KLUTH, S., BOZIC, I., LAWRENCE, M., BOTTCHER, S., CARTER, S. L., CIBULSKIS, K., MERTENS, D., SOUGNEZ, C. L., ROSENBERG, M., HESS, J. M., EDELMANN, J., KLESS, S., KNEBA, M., RITGEN, M., FINK, A., FISCHER, K., GABRIEL, S., LANDER, E. S., NOWAK, M. A., DOHNER, H., HALLEK, M., NEUBERG, D., GETZ, G., STILGENBAUER, S. & WU, C. J. 2015. Mutations driving CLL and their evolution in progression and relapse. *Nature,* 526**,** 525-30.

LANDGREN, O., ALBITAR, M., MA, W., ABBASI, F., HAYES, R. B., GHIA, P., MARTI, G. E. & CAPORASO, N. E. 2009. B-cell clones as early markers for chronic lymphocytic leukemia. *N Engl J Med,* 360**,** 659-67.

LANEMO MYHRINDER, A., HELLQVIST, E., SIDOROVA, E., SODERBERG, A., BAXENDALE, H., DAHLE, C., WILLANDER, K., TOBIN, G., BACKMAN, E., SODERBERG, O., ROSENQUIST, R., HORKKO, S. & ROSEN, A. 2008. A new perspective: molecular motifs on oxidized LDL, apoptotic cells, and bacteria are targets for chronic lymphocytic leukemia antibodies. *Blood,* 111**,** 3838-48.

LANHAM, S., HAMBLIN, T., OSCIER, D., IBBOTSON, R., STEVENSON, F. & PACKHAM, G. 2003. Differential signaling via surface IgM is associated with VH gene mutational status and CD38 expression in chronic lymphocytic leukemia. *Blood,* 101**,** 1087-93.

LAPALOMBELLA, R., SUN, Q., WILLIAMS, K., TANGEMAN, L., JHA, S., ZHONG, Y., GOETTL, V., MAHONEY, E., BERGLUND, C., GUPTA, S., FARMER, A., MANI, R., JOHNSON, A. J., LUCAS, D., MO, X., DAELEMANS, D., SANDANAYAKA, V., SHECHTER, S., MCCAULEY, D., SHACHAM, S., KAUFFMAN, M., CHOOK, Y. M. & BYRD, J. C. 2012. Selective inhibitors of nuclear export show that CRM1/XPO1 is a target in chronic lymphocytic leukemia. *Blood,* 120**,** 4621-34.

LAPLANTE, M. & SABATINI, D. M. 2012. mTOR signaling in growth control and disease. *Cell,* 149**,** 274-93.

LAZARIS-KARATZAS, A., MONTINE, K. S. & SONENBERG, N. 1990. Malignant transformation by a eukaryotic initiation factor subunit that binds to mRNA 5' cap. *Nature,* 345**,** 544-7.

LE GARFF-TAVERNIER, M., BLONS, H., NGUYEN-KHAC, F., PANNETIER, M., BRISSARD, M., GUEGUEN, S., JACOB, F., YSEBAERT, L., SUSIN, S. A. & MERLE-BERAL, H. 2011. Functional assessment of p53 in chronic lymphocytic leukemia. *Blood Cancer J,* 1**,** e5.

LEBIEN, T. W. & TEDDER, T. F. 2008. B lymphocytes: how they develop and function. *Blood,* 112**,** 1570-80.

LEMM, I. & ROSS, J. 2002. Regulation of c-myc mRNA decay by translational pausing in a coding region instability determinant. *Mol Cell Biol,* 22**,** 3959-69.

LIM, L. Y., LA, D., CSERTI-GAZDEWICH, C. M. & SHAH, H. 2015. Lymphoma Remission by Interferon-Free HCV Eradication Without Chemotherapy. *ACG Case Rep J,* 3**,** 69-70.

LIMON, J. J. & FRUMAN, D. A. 2012. Akt and mTOR in B Cell Activation and Differentiation. *Front Immunol,* 3**,** 228.

LIN, C. J., CENCIC, R., MILLS, J. R., ROBERT, F. & PELLETIER, J. 2008. c-Myc and eIF4F are components of a feedforward loop that links transcription and translation. *Cancer Res,* 68**,** 5326-34.

LINDER, P. & JANKOWSKY, E. 2011. From unwinding to clamping - the DEAD box RNA helicase family. *Nat Rev Mol Cell Biol,* 12**,** 505-16.

LORTHOLARY, P., BOIRON, M., RIPAULT, P., LEVY, J. P., MANUS, A. & BERNARD, J. 1964. [Chronic Lymphoid Leukemia Secondarily Associated with a Malignant Reticulopathy: Richter's Syndrome]. *Nouv Rev Fr Hematol,* 4**,** 621-44.

LUCAS, D. M., EDWARDS, R. B., LOZANSKI, G., WEST, D. A., SHIN, J. D., VARGO, M. A., DAVIS, M. E., ROZEWSKI, D. M., JOHNSON, A. J., SU, B. N., GOETTL, V. M., HEEREMA, N. A., LIN, T. S., LEHMAN, A., ZHANG, X., JARJOURA, D., NEWMAN, D. J., BYRD, J. C., KINGHORN, A. D. & GREVER, M. R. 2009. The novel plant-derived agent silvestrol has B-cell selective activity in chronic lymphocytic leukemia and acute lymphoblastic leukemia in vitro and in vivo. *Blood,* 113**,** 4656-66.

LUND, F. E., YU, N., KIM, K. M., RETH, M. & HOWARD, M. C. 1996. Signaling through CD38 augments B cell antigen receptor (BCR) responses and is dependent on BCR expression. *J Immunol,* 157**,** 1455-67.

MA, L., CHEN, Z., ERDJUMENT-BROMAGE, H., TEMPST, P. & PANDOLFI, P. P. 2005. Phosphorylation and functional inactivation of TSC2 by Erk implications for tuberous sclerosis and cancer pathogenesis. *Cell,* 121**,** 179-93.

MA, Y., PANNICKE, U., SCHWARZ, K. & LIEBER, M. R. 2002. Hairpin opening and overhang processing by an Artemis/DNA-dependent protein kinase complex in nonhomologous end joining and V(D)J recombination. *Cell,* 108**,** 781-94.

MACIOCIA, N., O'BRIEN, A. & ARDESHNA, K. 2016. Remission of Follicular Lymphoma after Treatment for Hepatitis C Virus Infection. *N Engl J Med,* 375**,** 1699-1701.

MAGNUSON, B., EKIM, B. & FINGAR, D. C. 2012. Regulation and function of ribosomal protein S6 kinase (S6K) within mTOR signalling networks. *Biochem J,* 441**,** 1-21.

MAJID, A., TSOULAKIS, O., WALEWSKA, R., GESK, S., SIEBERT, R., KENNEDY, D. B. & DYER, M. J. 2008. BCL2 expression in chronic lymphocytic leukemia: lack of association with the BCL2 938A>C promoter single nucleotide polymorphism. *Blood,* 111**,** 874-7.

MALAVASI, F., FUNARO, A., ROGGERO, S., HORENSTEIN, A., CALOSSO, L. & MEHTA, K. 1994. Human CD38: a glycoprotein in search of a function. *Immunol Today,* 15**,** 95-7.

MALCIKOVA, J., SMARDOVA, J., ROCNOVA, L., TICHY, B., KUGLIK, P., VRANOVA, V., CEJKOVA, S., SVITAKOVA, M., SKUHROVA FRANCOVA, H., BRYCHTOVA, Y., DOUBEK, M., BREJCHA, M.,

KLABUSAY, M., MAYER, J., POSPISILOVA, S. & TRBUSEK, M. 2009. Monoallelic and biallelic inactivation of TP53 gene in chronic lymphocytic leukemia: selection, impact on survival, and response to DNA damage. *Blood,* 114**,** 5307-14.

MANSOURI, M. R., SEVOV, M., ALESKOG, A., JONDAL, M., MERUP, M., SUNDSTROM, C., OSORIO, L. & ROSENQUIST, R. 2010. IGHV3-21 gene usage is associated with high TCL1 expression in chronic lymphocytic leukemia. *Eur J Haematol,* 84**,** 109-16.

MARAMPON, F., CICCARELLI, C. & ZANI, B. M. 2006. Down-regulation of c-Myc following MEK/ERK inhibition halts the expression of malignant phenotype in rhabdomyosarcoma and in non muscle-derived human tumors. *Mol Cancer,* 5**,** 31.

MARECHAL, A. & ZOU, L. 2013. DNA damage sensing by the ATM and ATR kinases. *Cold Spring Harb Perspect Biol,* 5.

MARSHALL, A. J., FLEMING, H. E., WU, G. E. & PAIGE, C. J. 1998. Modulation of the IL-7 dose-response threshold during pro-B cell differentiation is dependent on pre-B cell receptor expression. *J Immunol,* 161**,** 6038-45.

MARTENSSON, I. L., ROLINK, A., MELCHERS, F., MUNDT, C., LICENCE, S. & SHIMIZU, T. 2002. The pre-B cell receptor and its role in proliferation and Ig heavy chain allelic exclusion. *Semin Immunol,* 14**,** 335-42.

MARTINEZ-MARIGNAC, V., SHAWI, M., PINEDO-CARPIO, E., WANG, X., PANASCI, L., MILLER, W., PETTERSSON, F. & ALOYZ, R. 2013. Pharmacological targeting of eIF4E in primary CLL lymphocytes. *Blood Cancer J,* 3**,** e146.

MARTINEZ-SALAS, E., PINEIRO, D. & FERNANDEZ, N. 2012. Alternative Mechanisms to Initiate Translation in Eukaryotic mRNAs. *Comp Funct Genomics,* 2012**,** 391546.

MATUTES, E. 1996. Trisomy 12 in chronic lymphocytic leukaemia. *Leuk Res,* 20**,** 375-7.

MAUL, R. W. & GEARHART, P. J. 2010. AID and somatic hypermutation. *Adv Immunol,* 105**,** 159-91.

MCMAHON, H. T. & BOUCROT, E. 2011. Molecular mechanism and physiological functions of clathrin-mediated endocytosis. *Nat Rev Mol Cell Biol,* 12**,** 517-33.

MELAMED, D., BENSCHOP, R. J., CAMBIER, J. C. & NEMAZEE, D. 1998. Developmental regulation of B lymphocyte immune tolerance compartmentalizes clonal selection from receptor selection. *Cell,* 92**,** 173-82.

MELCHERS, F. 2005. The pre-B-cell receptor: selector of fitting immunoglobulin heavy chains for the B-cell repertoire. *Nat Rev Immunol,* 5**,** 578-84.

MERTENS, D., WOLF, S., TSCHUCH, C., MUND, C., KIENLE, D., OHL, S., SCHROETER, P., LYKO, F., DOHNER, H., STILGENBAUER, S. & LICHTER, P. 2006. Allelic silencing at the tumor-suppressor locus 13q14.3 suggests an epigenetic tumor-suppressor mechanism. *Proc Natl Acad Sci U S A,* 103**,** 7741-6.

MICHELIS, F. V., KOURTI, G., SKERTSOU, M., KARMIRIS, T., RONTOGIANNI, D. P. & HARHALAKIS, N. 2012. Richter transformation of chronic lymphocytic leukemia into composite diffuse large B-cell and Hodgkin lymphoma. *Leuk Lymphoma,* 53**,** 2302-3.

MIGNONE, F., GISSI, C., LIUNI, S. & PESOLE, G. 2002. Untranslated regions of mRNAs. *Genome Biol,* 3**,** REVIEWS0004.

MIKOSHIBA, K. 2007. The IP3 receptor/Ca2+ channel and its cellular function. *Biochem Soc Symp***,** 9-22.

MIYAKE, K., HASUNUMA, Y., YAGITA, H. & KIMOTO, M. 1992. Requirement for VLA-4 and VLA-5 integrins in lymphoma cells binding to and migration beneath stromal cells in culture. *J Cell Biol,* 119**,** 653-62.

MIZUNO, T. & ROTHSTEIN, T. L. 2005. B cell receptor (BCR) cross-talk: CD40 engagement enhances BCR-induced ERK activation. *J Immunol,* 174**,** 3369-76.

MOCKRIDGE, C. I., POTTER, K. N., WHEATLEY, I., NEVILLE, L. A., PACKHAM, G. & STEVENSON, F. K. 2007. Reversible anergy of sIgM-mediated signaling in the two subsets of CLL defined by VH-gene mutational status. *Blood,* 109**,** 4424-31.

MONTICELLI, S. & RAO, A. 2002. NFAT1 and NFAT2 are positive regulators of IL-4 gene transcription. *Eur J Immunol,* 32**,** 2971-8.

MOORE, K. W., ROGERS, J., HUNKAPILLER, T., EARLY, P., NOTTENBURG, C., WEISSMAN, I., BAZIN, H., WALL, R. & HOOD, L. E. 1981. Expression of IgD may use both DNA rearrangement and RNA splicing mechanisms. *Proc Natl Acad Sci U S A,* 78**,** 1800-4.

MRAZ, M., MALINOVA, K., KOTASKOVA, J., PAVLOVA, S., TICHY, B., MALCIKOVA, J., STANO KOZUBIK, K., SMARDOVA, J., BRYCHTOVA, Y., DOUBEK, M., TRBUSEK, M., MAYER, J. & POSPISILOVA, S. 2009. miR-34a, miR-29c and miR-17-5p are downregulated in CLL patients with TP53 abnormalities. *Leukemia,* 23**,** 1159-63.

MURPHY, L. O., MACKEIGAN, J. P. & BLENIS, J. 2004. A network of immediate early gene products propagates subtle differences in mitogen-activated protein kinase signal amplitude and duration. *Mol Cell Biol,* 24**,** 144-53.

MURRAY, F., DARZENTAS, N., HADZIDIMITRIOU, A., TOBIN, G., BOUDJOGRA, M., SCIELZO, C., LAOUTARIS, N., KARLSSON, K., BARAN-MARZSAK, F., TSAFTARIS, A., MORENO, C., ANAGNOSTOPOULOS, A., CALIGARIS-CAPPIO, F., VAUR, D., OUZOUNIS, C., BELESSI, C., GHIA, P., DAVI, F., ROSENQUIST, R. & STAMATOPOULOS, K. 2008. Stereotyped patterns of somatic hypermutation in subsets of patients with chronic lymphocytic leukemia: implications for the role of antigen selection in leukemogenesis. *Blood,* 111**,** 1524-33.

NGO, V. N., YOUNG, R. M., SCHMITZ, R., JHAVAR, S., XIAO, W., LIM, K. H., KOHLHAMMER, H., XU, W., YANG, Y., ZHAO, H., SHAFFER, A. L., ROMESSER, P., WRIGHT, G., POWELL, J., ROSENWALD, A., MULLER-HERMELINK, H. K., OTT, G., GASCOYNE, R. D., CONNORS, J. M., RIMSZA, L. M., CAMPO, E., JAFFE, E. S., DELABIE, J., SMELAND, E. B., FISHER, R. I., BRAZIEL, R. M., TUBBS, R. R., COOK, J. R., WEISENBURGER, D. D., CHAN, W. C. & STAUDT, L. M. 2011. Oncogenically active MYD88 mutations in human lymphoma. *Nature,* 470**,** 115-9.

NUTT, S. L., ROLINK, A. G. & BUSSLINGER, M. 1999. The molecular basis of B-cell lineage commitment. *Cold Spring Harb Symp Quant Biol,* 64**,** 51-9.

O'NEILL, L. A. & BOWIE, A. G. 2007. The family of five: TIR-domain-containing adaptors in Toll-like receptor signalling. *Nat Rev Immunol,* 7**,** 353-64.

O'ROURKE, L. M., TOOZE, R., TURNER, M., SANDOVAL, D. M., CARTER, R. H., TYBULEWICZ, V. L. & FEARON, D. T. 1998. CD19 as a membrane-anchored adaptor protein of B lymphocytes: costimulation of lipid and protein kinases by recruitment of Vav. *Immunity,* 8**,** 635-45.

OERTEL, J., OERTEL, B., SCHLEICHER, J. & HUHN, D. 1996. Immunotyping of blasts in human bone marrow. *Ann Hematol,* 72**,** 125-9.

OKKENHAUG, K. 2013. Signaling by the phosphoinositide 3-kinase family in immune cells. *Annu Rev Immunol,* 31**,** 675-704.

ONO, M., OKADA, H., BOLLAND, S., YANAGI, S., KUROSAKI, T. & RAVETCH, J. V. 1997. Deletion of SHIP or SHP-1 reveals two distinct pathways for inhibitory signaling. *Cell,* 90**,** 293-301.

OSBORNE, M. J. & BORDEN, K. L. 2015. The eukaryotic translation initiation factor eIF4E in the nucleus: taking the road less traveled. *Immunol Rev,* 263**,** 210-23.

PACKHAM, G., KRYSOV, S., ALLEN, A., SAVELYEVA, N., STEELE, A. J., FORCONI, F. & STEVENSON, F. K. 2014. The outcome of B-cell receptor signaling in chronic lymphocytic leukemia: proliferation or anergy. *Haematologica,* 99**,** 1138-48.

PALOMERO, T., LIM, W. K., ODOM, D. T., SULIS, M. L., REAL, P. J., MARGOLIN, A., BARNES, K. C., O'NEIL, J., NEUBERG, D., WENG, A. P., ASTER, J. C., SIGAUX, F., SOULIER, J., LOOK, A. T., YOUNG, R. A., CALIFANO, A. & FERRANDO, A. A. 2006. NOTCH1 directly regulates c-MYC and activates a feed-forward-loop transcriptional network promoting leukemic cell growth. *Proc Natl Acad Sci U S A,* 103**,** 18261-6.

PAPAKONSTANTINOU, N., NTOUFA, S., CHARTOMATSIDOU, E., PAPADOPOULOS, G., HATZIGEORGIOU, A., ANAGNOSTOPOULOS, A., CHLICHLIA, K., GHIA, P., MUZIO, M., BELESSI, C. & STAMATOPOULOS, K. 2013. Differential microRNA profiles and their functional implications in different immunogenetic subsets of chronic lymphocytic leukemia. *Mol Med,* 19**,** 115-23.

PAREKH, A. B. & PUTNEY, J. W., JR. 2005. Store-operated calcium channels. *Physiol Rev,* 85**,** 757-810.

PARIKH, S. A., RABE, K. G., KAY, N. E., CALL, T. G., DING, W., SCHWAGER, S. M., BOWEN, D. A., CONTE, M., JELINEK, D. F., SLAGER, S. L. & SHANAFELT, T. D. 2014. Chronic lymphocytic leukemia in young (</= 55 years) patients: a comprehensive analysis of prognostic factors and outcomes. *Haematologica,* 99**,** 140-7.

PARKER, H., ROSE-ZERILLI, M. J., PARKER, A., CHAPLIN, T., WADE, R., GARDINER, A., GRIFFITHS, M., COLLINS, A., YOUNG, B. D., OSCIER, D. G. & STREFFORD, J. C. 2011. 13q deletion anatomy and disease progression in patients with chronic lymphocytic leukemia. *Leukemia,* 25**,** 489-97.

PEPPER, C., HOY, T. & BENTLEY, D. P. 1997. Bcl-2/Bax ratios in chronic lymphocytic leukaemia and their correlation with in vitro apoptosis and clinical resistance. *Br J Cancer,* 76**,** 935-8.

PEPPER, C., LIN, T. T., PRATT, G., HEWAMANA, S., BRENNAN, P., HILLER, L., HILLS, R., WARD, R., STARCZYNSKI, J., AUSTEN, B., HOOPER, L., STANKOVIC, T. & FEGAN, C. 2008. Mcl-1 expression has in vitro and in vivo significance in chronic lymphocytic leukemia and is associated with other poor prognostic markers. *Blood,* 112**,** 3807-17.

PEPPER, C., WARD, R., LIN, T. T., BRENNAN, P., STARCZYNSKI, J., MUSSON, M., ROWNTREE, C., BENTLEY, P., MILLS, K., PRATT, G. & FEGAN, C. 2007. Highly purified CD38+ and CD38- sub-clones derived from the same chronic lymphocytic leukemia patient have distinct gene expression signatures despite their monoclonal origin. *Leukemia,* 21**,** 687-96.

PETLICKOVSKI, A., LAURENTI, L., LI, X., MARIETTI, S., CHIUSOLO, P., SICA, S., LEONE, G. & EFREMOV, D. G. 2005. Sustained signaling through the B-cell receptor induces Mcl-1 and promotes survival of chronic lymphocytic leukemia B cells. *Blood,* 105**,** 4820-7.

PFLUG, N., BAHLO, J., SHANAFELT, T. D., EICHHORST, B. F., BERGMANN, M. A., ELTER, T., BAUER, K., MALCHAU, G., RABE, K. G., STILGENBAUER, S., DOHNER, H., JAGER, U., ECKART, M. J., HOPFINGER, G., BUSCH, R., FINK, A. M., WENDTNER, C. M., FISCHER, K., KAY, N. E. & HALLEK, M. 2014. Development of a comprehensive prognostic index for patients with chronic lymphocytic leukemia. *Blood,* 124**,** 49-62.

PLEIMAN, C. M., D'AMBROSIO, D. & CAMBIER, J. C. 1994. The B-cell antigen receptor complex: structure and signal transduction. *Immunol Today,* 15**,** 393-9.

POGUE, S. L., KUROSAKI, T., BOLEN, J. & HERBST, R. 2000. B cell antigen receptor-induced activation of Akt promotes B cell survival and is dependent on Syk kinase. *J Immunol,* 165**,** 1300-6.

PONADER, S., CHEN, S. S., BUGGY, J. J., BALAKRISHNAN, K., GANDHI, V., WIERDA, W. G., KEATING, M. J., O'BRIEN, S., CHIORAZZI, N. & BURGER, J. A. 2012. The Bruton tyrosine kinase inhibitor PCI-32765 thwarts chronic lymphocytic leukemia cell survival and tissue homing in vitro and in vivo. *Blood,* 119**,** 1182-9.

POTTER, K. N., ORCHARD, J., CRITCHLEY, E., MOCKRIDGE, C. I., JOSE, A. & STEVENSON, F. K. 2003. Features of the overexpressed V1-69 genes in the unmutated subset of chronic lymphocytic leukemia are distinct from those in the healthy elderly repertoire. *Blood,* 101**,** 3082-4.

PRESNYAK, V., ALHUSAINI, N., CHEN, Y. H., MARTIN, S., MORRIS, N., KLINE, N., OLSON, S., WEINBERG, D., BAKER, K. E., GRAVELEY, B. R. & COLLER, J. 2015. Codon optimality is a major determinant of mRNA stability. *Cell,* 160**,** 1111-24.

PSATHAS, J. N., DOONAN, P. J., RAMAN, P., FREEDMAN, B. D., MINN, A. J. & THOMAS-TIKHONENKO, A. 2013. The Myc-miR-17-92 axis amplifies B-cell receptor signaling via inhibition of ITIM proteins: a novel lymphomagenic feed-forward loop. *Blood,* 122**,** 4220-9.

PUENTE, X. S., BEA, S., VALDES-MAS, R., VILLAMOR, N., GUTIERREZ-ABRIL, J., MARTIN-SUBERO, J. I., MUNAR, M., RUBIO-PEREZ, C., JARES, P., AYMERICH, M., BAUMANN, T., BEEKMAN, R., BELVER, L., CARRIO, A., CASTELLANO, G., CLOT, G., COLADO, E., COLOMER, D., COSTA, D., DELGADO, J., ENJUANES, A., ESTIVILL, X., FERRANDO, A. A., GELPI, J. L., GONZALEZ, B., GONZALEZ, S., GONZALEZ, M., GUT, M., HERNANDEZ-RIVAS, J. M., LOPEZ-GUERRA, M., MARTIN-GARCIA, D., NAVARRO, A., NICOLAS, P., OROZCO, M., PAYER, A. R., PINYOL, M., PISANO, D. G., PUENTE, D. A., QUEIROS, A. C., QUESADA, V., ROMEO-CASABONA, C. M., ROYO, C., ROYO, R., ROZMAN, M., RUSSINOL, N., SALAVERRIA, I., STAMATOPOULOS, K., STUNNENBERG, H. G., TAMBORERO, D., TEROL, M. J., VALENCIA, A., LOPEZ-BIGAS, N., TORRENTS, D., GUT, I., LOPEZ-GUILLERMO, A., LOPEZ-OTIN, C. & CAMPO, E. 2015. Non-coding recurrent mutations in chronic lymphocytic leukaemia. *Nature,* 526**,** 519-24.

PUENTE, X. S., PINYOL, M., QUESADA, V., CONDE, L., ORDONEZ, G. R., VILLAMOR, N., ESCARAMIS, G., JARES, P., BEA, S., GONZALEZ-DIAZ, M., BASSAGANYAS, L., BAUMANN, T., JUAN, M., LOPEZ-GUERRA, M., COLOMER, D., TUBIO, J. M., LOPEZ, C., NAVARRO, A., TORNADOR, C., AYMERICH, M., ROZMAN, M., HERNANDEZ, J. M., PUENTE, D. A., FREIJE, J. M., VELASCO, G., GUTIERREZ-FERNANDEZ, A., COSTA, D., CARRIO, A., GUIJARRO, S., ENJUANES, A., HERNANDEZ, L., YAGUE, J., NICOLAS, P., ROMEO-CASABONA, C. M., HIMMELBAUER, H., CASTILLO, E., DOHM, J. C., DE SANJOSE, S., PIRIS, M. A., DE ALAVA, E., SAN MIGUEL, J., ROYO, R., GELPI, J. L., TORRENTS, D., OROZCO, M., PISANO, D. G., VALENCIA, A., GUIGO, R., BAYES, M., HEATH, S., GUT, M., KLATT, P., MARSHALL, J., RAINE, K., STEBBINGS, L. A., FUTREAL, P. A., STRATTON, M. R., CAMPBELL, P. J., GUT, I., LOPEZ-GUILLERMO, A., ESTIVILL, X., MONTSERRAT, E., LOPEZ-OTIN, C. & CAMPO, E. 2011. Whole-genome sequencing identifies recurrent mutations in chronic lymphocytic leukaemia. *Nature,* 475**,** 101-5.

QUESADA, V., CONDE, L., VILLAMOR, N., ORDONEZ, G. R., JARES, P., BASSAGANYAS, L., RAMSAY, A. J., BEA, S., PINYOL, M., MARTINEZ-TRILLOS, A., LOPEZ-GUERRA, M., COLOMER, D., NAVARRO, A., BAUMANN, T., AYMERICH, M., ROZMAN, M., DELGADO, J., GINE, E., HERNANDEZ, J. M., GONZALEZ-DIAZ, M., PUENTE, D. A., VELASCO, G., FREIJE, J. M., TUBIO,

J. M., ROYO, R., GELPI, J. L., OROZCO, M., PISANO, D. G., ZAMORA, J., VAZQUEZ, M., VALENCIA, A., HIMMELBAUER, H., BAYES, M., HEATH, S., GUT, M., GUT, I., ESTIVILL, X., LOPEZ-GUILLERMO, A., PUENTE, X. S., CAMPO, E. & LOPEZ-OTIN, C. 2011. Exome sequencing identifies recurrent mutations of the splicing factor SF3B1 gene in chronic lymphocytic leukemia. *Nat Genet,* 44**,** 47-52.

RADHAKRISHNAN, A. & GREEN, R. 2016. Connections Underlying Translation and mRNA Stability. *J Mol Biol,* 428**,** 3558-64.

RAI, K. R., SAWITSKY, A., CRONKITE, E. P., CHANANA, A. D., LEVY, R. N. & PASTERNACK, B. S. 1975. Clinical staging of chronic lymphocytic leukemia. *Blood,* 46**,** 219-34.

RASSENTI, L. Z., HUYNH, L., TOY, T. L., CHEN, L., KEATING, M. J., GRIBBEN, J. G., NEUBERG, D. S., FLINN, I. W., RAI, K. R., BYRD, J. C., KAY, N. E., GREAVES, A., WEISS, A. & KIPPS, T. J. 2004. ZAP-70 compared with immunoglobulin heavy-chain gene mutation status as a predictor of disease progression in chronic lymphocytic leukemia. *N Engl J Med,* 351**,** 893-901.

RAUGHT, B. & GINGRAS, A. C. 1999. eIF4E activity is regulated at multiple levels. *Int J Biochem Cell Biol,* 31**,** 43-57.

RAZA, F., WALDRON, J. A. & QUESNE, J. L. 2015. Translational dysregulation in cancer: eIF4A isoforms and sequence determinants of eIF4A dependence. *Biochem Soc Trans,* 43**,** 1227-33.

RICCI, F., TEDESCHI, A., MORRA, E. & MONTILLO, M. 2009. Fludarabine in the treatment of chronic lymphocytic leukemia: a review. *Ther Clin Risk Manag,* 5**,** 187-207.

RICHES, J. C., O'DONOVAN, C. J., KINGDON, S. J., MCCLANAHAN, F., CLEAR, A. J., NEUBERG, D. S., WERNER, L., CROCE, C. M., RAMSAY, A. G., RASSENTI, L. Z., KIPPS, T. J. & GRIBBEN, J. G. 2014. Trisomy 12 chronic lymphocytic leukemia cells exhibit upregulation of integrin signaling that is modulated by NOTCH1 mutations. *Blood,* 123**,** 4101-10.

ROBERTS, A. W., DAVIDS, M. S., PAGEL, J. M., KAHL, B. S., PUVVADA, S. D., GERECITANO, J. F., KIPPS, T. J., ANDERSON, M. A., BROWN, J. R., GRESSICK, L., WONG, S., DUNBAR, M., ZHU, M., DESAI, M. B., CERRI, E., HEITNER ENSCHEDE, S., HUMERICKHOUSE, R. A., WIERDA, W. G. & SEYMOUR, J. F. 2016. Targeting BCL2 with Venetoclax in Relapsed Chronic Lymphocytic Leukemia. *N Engl J Med,* 374**,** 311-22.

ROBERTSON, L. E., PLUNKETT, W., MCCONNELL, K., KEATING, M. J. & MCDONNELL, T. J. 1996. Bcl-2 expression in chronic lymphocytic leukemia and its correlation with the induction of apoptosis and clinical outcome. *Leukemia,* 10**,** 456-9.

ROSATI, E., SABATINI, R., RAMPINO, G., TABILIO, A., DI IANNI, M., FETTUCCIARI, K., BARTOLI, A., COACCIOLI, S., SCREPANTI, I. & MARCONI, P. 2009. Constitutively activated Notch signaling is involved in survival and apoptosis resistance of B-CLL cells. *Blood,* 113**,** 856-65.

ROSENWALD, A., ALIZADEH, A. A., WIDHOPF, G., SIMON, R., DAVIS, R. E., YU, X., YANG, L., PICKERAL, O. K., RASSENTI, L. Z., POWELL, J., BOTSTEIN, D., BYRD, J. C., GREVER, M. R., CHESON, B. D., CHIORAZZI, N., WILSON, W. H., KIPPS, T. J., BROWN, P. O. & STAUDT, L. M. 2001. Relation of gene expression phenotype to immunoglobulin mutation genotype in B cell chronic lymphocytic leukemia. *J Exp Med,* 194**,** 1639-47.

ROSSI, D., BRUSCAGGIN, A., SPINA, V., RASI, S., KHIABANIAN, H., MESSINA, M., FANGAZIO, M., VAISITTI, T., MONTI, S., CHIARETTI, S., GUARINI, A., DEL GIUDICE, I., CERRI, M., CRESTA, S., DEAMBROGI, C., GARGIULO, E., GATTEI, V., FORCONI, F., BERTONI, F., DEAGLIO, S., RABADAN, R., PASQUALUCCI, L., FOA, R., DALLA-FAVERA, R. & GAIDANO, G. 2011.

Mutations of the SF3B1 splicing factor in chronic lymphocytic leukemia: association with progression and fludarabine-refractoriness. *Blood,* 118**,** 6904-8.

ROSSI, D., CERRI, M., CAPELLO, D., DEAMBROGI, C., ROSSI, F. M., ZUCCHETTO, A., DE PAOLI, L., CRESTA, S., RASI, S., SPINA, V., FRANCESCHETTI, S., LUNGHI, M., VENDRAMIN, C., BOMBEN, R., RAMPONI, A., MONGA, G., CONCONI, A., MAGNANI, C., GATTEI, V. & GAIDANO, G. 2008. Biological and clinical risk factors of chronic lymphocytic leukaemia transformation to Richter syndrome. *Br J Haematol,* 142**,** 202-15.

ROSSI, D., FANGAZIO, M., RASI, S., VAISITTI, T., MONTI, S., CRESTA, S., CHIARETTI, S., DEL GIUDICE, I., FABBRI, G., BRUSCAGGIN, A., SPINA, V., DEAMBROGI, C., MARINELLI, M., FAMA, R., GRECO, M., DANIELE, G., FORCONI, F., GATTEI, V., BERTONI, F., DEAGLIO, S., PASQUALUCCI, L., GUARINI, A., DALLA-FAVERA, R., FOA, R. & GAIDANO, G. 2012. Disruption of BIRC3 associates with fludarabine chemorefractoriness in TP53 wild-type chronic lymphocytic leukemia. *Blood,* 119**,** 2854-62.

ROSSI, D., KHIABANIAN, H., SPINA, V., CIARDULLO, C., BRUSCAGGIN, A., FAMA, R., RASI, S., MONTI, S., DEAMBROGI, C., DE PAOLI, L., WANG, J., GATTEI, V., GUARINI, A., FOA, R., RABADAN, R. & GAIDANO, G. 2014. Clinical impact of small TP53 mutated subclones in chronic lymphocytic leukemia. *Blood,* 123**,** 2139-47.

ROTH, D. B. 2014. V(D)J Recombination: Mechanism, Errors, and Fidelity. *Microbiol Spectr,* 2.

ROUX, P. P., SHAHBAZIAN, D., VU, H., HOLZ, M. K., COHEN, M. S., TAUNTON, J., SONENBERG, N. & BLENIS, J. 2007. RAS/ERK signaling promotes site-specific ribosomal protein S6 phosphorylation via RSK and stimulates cap-dependent translation. *J Biol Chem,* 282**,** 14056-64.

ROWE, D. S., HUG, K., FORNI, L. & PERNIS, B. 1973. Immunoglobulin D as a lymphocyte receptor. *J Exp Med,* 138**,** 965-72.

RUBIO, C. A., WEISBURD, B., HOLDERFIELD, M., ARIAS, C., FANG, E., DERISI, J. L. & FANIDI, A. 2014. Transcriptome-wide characterization of the eIF4A signature highlights plasticity in translation regulation. *Genome Biol,* 15**,** 476.

RUGGERO, D. 2009. The role of Myc-induced protein synthesis in cancer. *Cancer Res,* 69**,** 8839-43.

RUGGERO, D., MONTANARO, L., MA, L., XU, W., LONDEI, P., CORDON-CARDO, C. & PANDOLFI, P. P. 2004. The translation factor eIF-4E promotes tumor formation and cooperates with c-Myc in lymphomagenesis. *Nat Med,* 10**,** 484-6.

RUSH, L. J., RAVAL, A., FUNCHAIN, P., JOHNSON, A. J., SMITH, L., LUCAS, D. M., BEMBEA, M., LIU, T. H., HEEREMA, N. A., RASSENTI, L., LIYANARACHCHI, S., DAVULURI, R., BYRD, J. C. & PLASS, C. 2004. Epigenetic profiling in chronic lymphocytic leukemia reveals novel methylation targets. *Cancer Res,* 64**,** 2424-33.

SANDEL, P. C. & MONROE, J. G. 1999. Negative selection of immature B cells by receptor editing or deletion is determined by site of antigen encounter. *Immunity,* 10**,** 289-99.

SBARRATO, T., HORVILLEUR, E., POYRY, T., HILL, K., CHAPLIN, L. C., SPRIGGS, R. V., STONELEY, M., WILSON, L., JAYNE, S., VULLIAMY, T., BECK, D., DOKAL, I., DYER, M. J., YEOMANS, A. M., PACKHAM, G., BUSHELL, M., WAGNER, S. D. & WILLIS, A. E. 2016. A ribosome-related signature in peripheral blood CLL B cells is linked to reduced survival following treatment. *Cell Death Dis,* 7**,** e2249.

SCHEPER, G. C. & PROUD, C. G. 2002. Does phosphorylation of the cap-binding protein eIF4E play a role in translation initiation? *Eur J Biochem,* 269**,** 5350-9.

SCHLEISS, C., ILIAS, W., TAHAR, O., GULER, Y., MIGUET, L., MAYEUR-ROUSSE, C., MAUVIEUX, L., FORNECKER, L. M., TOUSSAINT, E., HERBRECHT, R., BERTRAND, F., MAUMY-BERTRAND, M., MARTIN, T., FOURNEL, S., GEORGEL, P., BAHRAM, S. & VALLAT, L. 2019. BCR-associated factors driving chronic lymphocytic leukemia cells proliferation ex vivo. *Sci Rep,* 9**,** 701.

SCHMIDT-ZACHMANN, M. S., DARGEMONT, C., KUHN, L. C. & NIGG, E. A. 1993. Nuclear export of proteins: the role of nuclear retention. *Cell,* 74**,** 493-504.

SCHNEIDER-POETSCH, T., JU, J., EYLER, D. E., DANG, Y., BHAT, S., MERRICK, W. C., GREEN, R., SHEN, B. & LIU, J. O. 2010. Inhibition of eukaryotic translation elongation by cycloheximide and lactimidomycin. *Nat Chem Biol,* 6**,** 209-217.

SCHWANHAUSSER, B., BUSSE, D., LI, N., DITTMAR, G., SCHUCHHARDT, J., WOLF, J., CHEN, W. & SELBACH, M. 2011. Global quantification of mammalian gene expression control. *Nature,* 473**,** 337-42.

SCHWARTZ, D. C. & PARKER, R. 1999. Mutations in translation initiation factors lead to increased rates of deadenylation and decapping of mRNAs in Saccharomyces cerevisiae. *Mol Cell Biol,* 19**,** 5247-56.

SEARS, R., NUCKOLLS, F., HAURA, E., TAYA, Y., TAMAI, K. & NEVINS, J. R. 2000. Multiple Ras-dependent phosphorylation pathways regulate Myc protein stability. *Genes Dev,* 14**,** 2501-14.

SEIFERT, M., SCHOLTYSIK, R. & KUPPERS, R. 2013. Origin and pathogenesis of B cell lymphomas. *Methods Mol Biol,* 971**,** 1-25.

SHANAFELT, T. D., GEYER, S. M., BONE, N. D., TSCHUMPER, R. C., WITZIG, T. E., NOWAKOWSKI, G. S., ZENT, C. S., CALL, T. G., LAPLANT, B., DEWALD, G. W., JELINEK, D. F. & KAY, N. E. 2008. CD49d expression is an independent predictor of overall survival in patients with chronic lymphocytic leukaemia: a prognostic parameter with therapeutic potential. *Br J Haematol,* 140**,** 537-46.

SHANAFELT, T. D., WITZIG, T. E., FINK, S. R., JENKINS, R. B., PATERNOSTER, S. F., SMOLEY, S. A., STOCKERO, K. J., NAST, D. M., FLYNN, H. C., TSCHUMPER, R. C., GEYER, S., ZENT, C. S., CALL, T. G., JELINEK, D. F., KAY, N. E. & DEWALD, G. W. 2006. Prospective evaluation of clonal evolution during long-term follow-up of patients with untreated early-stage chronic lymphocytic leukemia. *J Clin Oncol,* 24**,** 4634-41.

SHANMUGAM, A., SHI, M. J., YAUCH, L., STAVNEZER, J. & KENTER, A. L. 2000. Evidence for class-specific factors in immunoglobulin isotype switching. *J Exp Med,* 191**,** 1365-80.

SHETH, U. & PARKER, R. 2003. Decapping and decay of messenger RNA occur in cytoplasmic processing bodies. *Science,* 300**,** 805-8.

SHIMIZU, A. & HONJO, T. 1984. Immunoglobulin class switching. *Cell,* 36**,** 801-3.

SHRINER, A. K., LIU, H., SUN, G., GUIMOND, M. & ALUGUPALLI, K. R. 2010. IL-7-dependent B lymphocytes are essential for the anti-polysaccharide response and protective immunity to Streptococcus pneumoniae. *J Immunol,* 185**,** 525-31.

SHVEYGERT, M., KAISER, C., BRADRICK, S. S. & GROMEIER, M. 2010. Regulation of eukaryotic initiation factor 4E (eIF4E) phosphorylation by mitogen-activated protein kinase occurs through modulation of Mnk1-eIF4G interaction. *Mol Cell Biol,* 30**,** 5160-7.

SIDDIQUI-JAIN, A., GRAND, C. L., BEARSS, D. J. & HURLEY, L. H. 2002. Direct evidence for a G-quadruplex in a promoter region and its targeting with a small molecule to repress c-MYC transcription. *Proc Natl Acad Sci U S A,* 99**,** 11593-8.

SILVERA, D., FORMENTI, S. C. & SCHNEIDER, R. J. 2010. Translational control in cancer. *Nat Rev Cancer,* 10**,** 254-66.

SIMONETTI, G., BERTILACCIO, M. T., GHIA, P. & KLEIN, U. 2014. Mouse models in the study of chronic lymphocytic leukemia pathogenesis and therapy. *Blood,* 124**,** 1010-9.

SLAGER, S. L., RABE, K. G., ACHENBACH, S. J., VACHON, C. M., GOLDIN, L. R., STROM, S. S., LANASA, M. C., SPECTOR, L. G., RASSENTI, L. Z., LEIS, J. F., CAMP, N. J., GLENN, M., KAY, N. E., CUNNINGHAM, J. M., HANSON, C. A., MARTI, G. E., WEINBERG, J. B., MORRISON, V. A., LINK, B. K., CALL, T. G., CAPORASO, N. E. & CERHAN, J. R. 2011. Genome-wide association study identifies a novel susceptibility locus at 6p21.3 among familial CLL. *Blood,* 117**,** 1911-6.

SLAINE, P. D., KLEER, M., SMITH, N. K., KHAPERSKYY, D. A. & MCCORMICK, C. 2017. Stress Granule-Inducing Eukaryotic Translation Initiation Factor 4A Inhibitors Block Influenza A Virus Replication. *Viruses,* 9.

SMIT, L. A., HALLAERT, D. Y., SPIJKER, R., DE GOEIJ, B., JASPERS, A., KATER, A. P., VAN OERS, M. H., VAN NOESEL, C. J. & ELDERING, E. 2007. Differential Noxa/Mcl-1 balance in peripheral versus lymph node chronic lymphocytic leukemia cells correlates with survival capacity. *Blood,* 109**,** 1660-8.

SONENBERG, N. & HINNEBUSCH, A. G. 2009. Regulation of translation initiation in eukaryotes: mechanisms and biological targets. *Cell,* 136**,** 731-45.

SPRIGGS, K. A., COBBOLD, L. C., JOPLING, C. L., COOPER, R. E., WILSON, L. A., STONELEY, M., COLDWELL, M. J., PONCET, D., SHEN, Y. C., MORLEY, S. J., BUSHELL, M. & WILLIS, A. E. 2009. Canonical initiation factor requirements of the Myc family of internal ribosome entry segments. *Mol Cell Biol,* 29**,** 1565-74.

STAVNEZER, J., GUIKEMA, J. E. & SCHRADER, C. E. 2008. Mechanism and regulation of class switch recombination. *Annu Rev Immunol,* 26**,** 261-92.

STEINHARDT, J. J., PEROUTKA, R. J., MAZAN-MAMCZARZ, K., CHEN, Q., HOUNG, S., ROBLES, C., BARTH, R. N., DUBOSE, J., BRUNS, B., TESORIERO, R., STEIN, D., FANG, R., HANNA, N., PASLEY, J., RODRIGUEZ, C., KLIGMAN, M. D., BRADLEY, M., RABIN, J., SHACKELFORD, S., DAI, B., LANDON, A. L., SCALEA, T., LIVAK, F. & GARTENHAUS, R. B. 2014. Inhibiting CARD11 translation during BCR activation by targeting the eIF4A RNA helicase. *Blood,* 124**,** 3758-67.

STEININGER, C., WIDHOPF, G. F., 2ND, GHIA, E. M., MORELLO, C. S., VANURA, K., SANDERS, R., SPECTOR, D., GUINEY, D., JAGER, U. & KIPPS, T. J. 2012. Recombinant antibodies encoded by IGHV1-69 react with pUL32, a phosphoprotein of cytomegalovirus and B-cell superantigen. *Blood,* 119**,** 2293-301.

STILGENBAUER, S., EICHHORST, B., SCHETELIG, J., COUTRE, S., SEYMOUR, J. F., MUNIR, T., PUVVADA, S. D., WENDTNER, C. M., ROBERTS, A. W., JURCZAK, W., MULLIGAN, S. P., BOTTCHER, S., MOBASHER, M., ZHU, M., DESAI, M., CHYLA, B., VERDUGO, M., ENSCHEDE, S. H., CERRI, E., HUMERICKHOUSE, R., GORDON, G., HALLEK, M. & WIERDA, W. G. 2016. Venetoclax in relapsed or refractory chronic lymphocytic leukaemia with 17p deletion: a multicentre, open-label, phase 2 study. *Lancet Oncol,* 17**,** 768-778.

STONELEY, M., PAULIN, F. E., LE QUESNE, J. P., CHAPPELL, S. A. & WILLIS, A. E. 1998. C-Myc 5' untranslated region contains an internal ribosome entry segment. *Oncogene,* 16**,** 423-8.

STRATI, P. & SHANAFELT, T. D. 2015. Monoclonal B-cell lymphocytosis and early-stage chronic lymphocytic leukemia: diagnosis, natural history, and risk stratification. *Blood,* 126**,** 454-62.

SUN, M., SCHWALB, B., SCHULZ, D., PIRKL, N., ETZOLD, S., LARIVIERE, L., MAIER, K. C., SEIZL, M., TRESCH, A. & CRAMER, P. 2012. Comparative dynamic transcriptome analysis (cDTA) reveals mutual feedback between mRNA synthesis and degradation. *Genome Res,* 22**,** 1350-9.

SWERDLOW, S. H., KUZU, I., DOGAN, A., DIRNHOFER, S., CHAN, J. K., SANDER, B., OTT, G., XERRI, L., QUINTANILLA-MARTINEZ, L. & CAMPO, E. 2016. The many faces of small B cell lymphomas with plasmacytic differentiation and the contribution of MYD88 testing. *Virchows Arch,* 468**,** 259-75.

TABE, Y., KOJIMA, K., YAMAMOTO, S., SEKIHARA, K., MATSUSHITA, H., DAVIS, R. E., WANG, Z., MA, W., ISHIZAWA, J., KAZUNO, S., KAUFFMAN, M., SHACHAM, S., FUJIMURA, T., UENO, T., MIIDA, T. & ANDREEFF, M. 2015. Ribosomal Biogenesis and Translational Flux Inhibition by the Selective Inhibitor of Nuclear Export (SINE) XPO1 Antagonist KPT-185. *PLoS One,* 10**,** e0137210.

TAGAWA, H., IKEDA, S. & SAWADA, K. 2013. Role of microRNA in the pathogenesis of malignant lymphoma. *Cancer Sci,* 104**,** 801-9.

TAMURA, Y., SIMIZU, S. & OSADA, H. 2004. The phosphorylation status and anti-apoptotic activity of Bcl-2 are regulated by ERK and protein phosphatase 2A on the mitochondria. *FEBS Lett,* 569**,** 249-55.

TEITELL, M. A. 2005. The TCL1 family of oncoproteins: co-activators of transformation. *Nat Rev Cancer,* 5**,** 640-8.

TEN HACKEN, E. & BURGER, J. A. 2016. Microenvironment interactions and B-cell receptor signaling in Chronic Lymphocytic Leukemia: Implications for disease pathogenesis and treatment. *Biochim Biophys Acta,* 1863**,** 401-13.

TEN HACKEN, E., SIVINA, M., KIM, E., O'BRIEN, S., WIERDA, W. G., FERRAJOLI, A., ESTROV, Z., KEATING, M. J., OELLERICH, T., SCIELZO, C., GHIA, P., CALIGARIS-CAPPIO, F. & BURGER, J. A. 2016. Functional Differences between IgM and IgD Signaling in Chronic Lymphocytic Leukemia. *J Immunol,* 197**,** 2522-31.

THOMPSON, P. A., TAM, C. S., O'BRIEN, S. M., WIERDA, W. G., STINGO, F., PLUNKETT, W., SMITH, S. C., KANTARJIAN, H. M., FREIREICH, E. J. & KEATING, M. J. 2016. Fludarabine, cyclophosphamide, and rituximab treatment achieves long-term disease-free survival in IGHV-mutated chronic lymphocytic leukemia. *Blood,* 127**,** 303-9.

TOBIN, G. 2005. The immunoglobulin genes and chronic lymphocytic leukemia (CLL). *Ups J Med Sci,* 110**,** 97-113.

TONEGAWA, S. 1983. Somatic generation of antibody diversity. *Nature,* 302**,** 575-81.

TOPISIROVIC, I., RUIZ-GUTIERREZ, M. & BORDEN, K. L. 2004. Phosphorylation of the eukaryotic translation initiation factor eIF4E contributes to its transformation and mRNA transport activities. *Cancer Res,* 64**,** 8639-42.

TOPISIROVIC, I., SIDDIQUI, N., LAPOINTE, V. L., TROST, M., THIBAULT, P., BANGERANYE, C., PINOL-ROMA, S. & BORDEN, K. L. 2009. Molecular dissection of the eukaryotic initiation factor 4E (eIF4E) export-competent RNP. *EMBO J,* 28**,** 1087-98.

TORRES, R. M., FLASWINKEL, H., RETH, M. & RAJEWSKY, K. 1996. Aberrant B cell development and immune response in mice with a compromised BCR complex. *Science,* 272**,** 1804-8.

TRUITT, M. L., CONN, C. S., SHI, Z., PANG, X., TOKUYASU, T., COADY, A. M., SEO, Y., BARNA, M. & RUGGERO, D. 2015. Differential Requirements for eIF4E Dose in Normal Development and Cancer. *Cell,* 162**,** 59-71.

TZE, L. E., HIPPEN, K. L. & BEHRENS, T. W. 2003. Late immature B cells (IgMhighIgDneg) undergo a light chain receptor editing response to soluble self-antigen. *J Immunol,* 171**,** 678-82.

ULLMAN, K. S., POWERS, M. A. & FORBES, D. J. 1997. Nuclear export receptors: from importin to exportin. *Cell,* 90**,** 967-70.

URTISHAK, K. A., WANG, L. S., CULJKOVIC-KRALJACIC, B., DAVENPORT, J. W., PORAZZI, P., VINCENT, T. L., TEACHEY, D. T., TASIAN, S. K., MOORE, J. S., SEIF, A. E., JIN, S., BARRETT, J. S., ROBINSON, B. W., CHEN, I. L., HARVEY, R. C., CARROLL, M. P., CARROLL, A. J., HEEREMA, N. A., DEVIDAS, M., DREYER, Z. E., HILDEN, J. M., HUNGER, S. P., WILLMAN, C. L., BORDEN, K. L. B. & FELIX, C. A. 2019. Targeting EIF4E signaling with ribavirin in infant acute lymphoblastic leukemia. *Oncogene,* 38**,** 2241-2262.

VAN DER BURG, M., TUMKAYA, T., BOERMA, M., DE BRUIN-VERSTEEG, S., LANGERAK, A. W. & VAN DONGEN, J. J. 2001. Ordered recombination of immunoglobulin light chain genes occurs at the IGK locus but seems less strict at the IGL locus. *Blood,* 97**,** 1001-8.

VAN GENT, D. C., RAMSDEN, D. A. & GELLERT, M. 1996. The RAG1 and RAG2 proteins establish the 12/23 rule in V(D)J recombination. *Cell,* 85**,** 107-13.

VOLPON, L., CULJKOVIC-KRALJACIC, B., OSBORNE, M. J., RAMTEKE, A., SUN, Q., NIESMAN, A., CHOOK, Y. M. & BORDEN, K. L. 2016. Importin 8 mediates m7G cap-sensitive nuclear import of the eukaryotic translation initiation factor eIF4E. *Proc Natl Acad Sci U S A,* 113**,** 5263-8.

VOLPON, L., CULJKOVIC-KRALJACIC, B., SOHN, H. S., BLANCHET-COHEN, A., OSBORNE, M. J. & BORDEN, K. L. B. 2017. A biochemical framework for eIF4E-dependent mRNA export and nuclear recycling of the export machinery. *RNA,* 23**,** 927-937.

VOLPON, L., OSBORNE, M. J., ZAHREDDINE, H., ROMEO, A. A. & BORDEN, K. L. 2013. Conformational changes induced in the eukaryotic translation initiation factor eIF4E by a clinically relevant inhibitor, ribavirin triphosphate. *Biochem Biophys Res Commun,* 434**,** 614-9.

WAKABAYASHI, C., ADACHI, T., WIENANDS, J. & TSUBATA, T. 2002. A distinct signaling pathway used by the IgG-containing B cell antigen receptor. *Science,* 298**,** 2392-5.

WALKER, M. A., VOLPI, S., SIMS, K. B., WALTER, J. E. & TRAGGIAI, E. 2014. Powering the immune system: mitochondria in immune function and deficiency. *J Immunol Res,* 2014**,** 164309.

WANG, H., KADLECEK, T. A., AU-YEUNG, B. B., GOODFELLOW, H. E., HSU, L. Y., FREEDMAN, T. S. & WEISS, A. 2010. ZAP-70: an essential kinase in T-cell signaling. *Cold Spring Harb Perspect Biol,* 2**,** a002279.

WANG, H., LEE, C. H., QI, C., TAILOR, P., FENG, J., ABBASI, S., ATSUMI, T. & MORSE, H. C., 3RD 2008. IRF8 regulates B-cell lineage specification, commitment, and differentiation. *Blood,* 112**,** 4028-38.

WANG, L. & PROUD, C. G. 2002. Ras/Erk signaling is essential for activation of protein synthesis by Gq protein-coupled receptor agonists in adult cardiomyocytes. *Circ Res,* 91**,** 821-9.

WANG, S., ROSENWALD, I. B., HUTZLER, M. J., PIHAN, G. A., SAVAS, L., CHEN, J. J. & WODA, B. A. 1999. Expression of the eukaryotic translation initiation factors 4E and 2alpha in non-Hodgkin's lymphomas. *Am J Pathol,* 155**,** 247-55.

WASKIEWICZ, A. J., FLYNN, A., PROUD, C. G. & COOPER, J. A. 1997. Mitogen-activated protein kinases activate the serine/threonine kinases Mnk1 and Mnk2. *EMBO J,* 16**,** 1909-20.

WEBER, M., TREANOR, B., DEPOIL, D., SHINOHARA, H., HARWOOD, N. E., HIKIDA, M., KUROSAKI, T. & BATISTA, F. D. 2008. Phospholipase C-gamma2 and Vav cooperate within signaling microclusters to propagate B cell spreading in response to membrane-bound antigen. *J Exp Med,* 205**,** 853-68.

WEISSMAN, I. L. 2000. Stem cells: units of development, units of regeneration, and units in evolution. *Cell,* 100**,** 157-68.

WENDEL, H. G., SILVA, R. L., MALINA, A., MILLS, J. R., ZHU, H., UEDA, T., WATANABE-FUKUNAGA, R., FUKUNAGA, R., TERUYA-FELDSTEIN, J., PELLETIER, J. & LOWE, S. W. 2007. Dissecting eIF4E action in tumorigenesis. *Genes Dev,* 21**,** 3232-7.

WENSVEEN, F. M., DERKS, I. A., VAN GISBERGEN, K. P., DE BRUIN, A. M., MEIJERS, J. C., YIGITTOP, H., NOLTE, M. A., ELDERING, E. & VAN LIER, R. A. 2012. BH3-only protein Noxa regulates apoptosis in activated B cells and controls high-affinity antibody formation. *Blood,* 119**,** 1440-9.

WESTPHAL, C. H., ROWAN, S., SCHMALTZ, C., ELSON, A., FISHER, D. E. & LEDER, P. 1997. atm and p53 cooperate in apoptosis and suppression of tumorigenesis, but not in resistance to acute radiation toxicity. *Nat Genet,* 16**,** 397-401.

WIEGERING, A., UTHE, F. W., JAMIESON, T., RUOSS, Y., HUTTENRAUCH, M., KUSPERT, M., PFANN, C., NIXON, C., HEROLD, S., WALZ, S., TARANETS, L., GERMER, C. T., ROSENWALD, A., SANSOM, O. J. & EILERS, M. 2015. Targeting Translation Initiation Bypasses Signaling Crosstalk Mechanisms That Maintain High MYC Levels in Colorectal Cancer. *Cancer Discov,* 5**,** 768-81.

WILLIS, R. C., CARSON, D. A. & SEEGMILLER, J. E. 1978. Adenosine kinase initiates the major route of ribavirin activation in a cultured human cell line. *Proc Natl Acad Sci U S A,* 75**,** 3042-4.

WILSON, A. & TRUMPP, A. 2006. Bone-marrow haematopoietic-stem-cell niches. *Nat Rev Immunol,* 6**,** 93-106.

WISDOM, R. & LEE, W. 1991. The protein-coding region of c-myc mRNA contains a sequence that specifies rapid mRNA turnover and induction by protein synthesis inhibitors. *Genes Dev,* 5**,** 232-43.

WOLFE, A. L., SINGH, K., ZHONG, Y., DREWE, P., RAJASEKHAR, V. K., SANGHVI, V. R., MAVRAKIS, K. J., JIANG, M., RODERICK, J. E., VAN DER MEULEN, J., SCHATZ, J. H., RODRIGO, C. M., ZHAO, C., RONDOU, P., DE STANCHINA, E., TERUYA-FELDSTEIN, J., KELLIHER, M. A., SPELEMAN, F., PORCO, J. A., JR., PELLETIER, J., RATSCH, G. & WENDEL, H. G. 2014. RNA G-quadruplexes cause eIF4A-dependent oncogene translation in cancer. *Nature,* 513**,** 65-70.

WOYACH, J. A., FURMAN, R. R., LIU, T. M., OZER, H. G., ZAPATKA, M., RUPPERT, A. S., XUE, L., LI, D. H., STEGGERDA, S. M., VERSELE, M., DAVE, S. S., ZHANG, J., YILMAZ, A. S., JAGLOWSKI, S. M., BLUM, K. A., LOZANSKI, A., LOZANSKI, G., JAMES, D. F., BARRIENTOS, J. C., LICHTER, P., STILGENBAUER, S., BUGGY, J. J., CHANG, B. Y., JOHNSON, A. J. & BYRD, J. C. 2014. Resistance mechanisms for the Bruton's tyrosine kinase inhibitor ibrutinib. *N Engl J Med,* 370**,** 2286-94.

XIAO, C., SRINIVASAN, L., CALADO, D. P., PATTERSON, H. C., ZHANG, B., WANG, J., HENDERSON, J. M., KUTOK, J. L. & RAJEWSKY, K. 2008. Lymphoproliferative disease and autoimmunity in mice with increased miR-17-92 expression in lymphocytes. *Nat Immunol,* 9**,** 405-14.

XU, D., GRISHIN, N. V. & CHOOK, Y. M. 2012. NESdb: a database of NES-containing CRM1 cargoes. *Mol Biol Cell,* 23**,** 3673-6.

YAN, Y., SVITKIN, Y., LEE, J. M., BISAILLON, M. & PELLETIER, J. 2005. Ribavirin is not a functional mimic of the 7-methyl guanosine mRNA cap. *RNA,* 11**,** 1238-44.

YEOMANS, A., THIRDBOROUGH, S. M., VALLE-ARGOS, B., LINLEY, A., KRYSOV, S., SANCHEZ HIDALGO, M., LEONARD, E., ISHFAQ, M., WAGNER, S. D., WILLIS, A. E., STEELE, A. J., STEVENSON, F. K., FORCONI, F., COLDWELL, M. J. & PACKHAM, G. 2015. Engagement of the B-cell receptor of chronic lymphocytic leukemia cells drives global and MYC-specific mRNA translation. *Blood*.

ZENZ, T., HABE, S., DENZEL, T., WINKLER, D., DOHNER, H. & STILGENBAUER, S. 2008a. How little is too much? p53 inactivation: from laboratory cutoff to biological basis of chemotherapy resistance. *Leukemia,* 22**,** 2257-8.

ZENZ, T., MERTENS, D., DOHNER, H. & STILGENBAUER, S. 2008b. Molecular diagnostics in chronic lymphocytic leukemia - pathogenetic and clinical implications. *Leuk Lymphoma,* 49**,** 864-73.

ZENZ, T., MOHR, J., ELDERING, E., KATER, A. P., BUHLER, A., KIENLE, D., WINKLER, D., DURIG, J., VAN OERS, M. H., MERTENS, D., DOHNER, H. & STILGENBAUER, S. 2009. miR-34a as part of the resistance network in chronic lymphocytic leukemia. *Blood,* 113**,** 3801-8.

ZHANG, K., WANG, M., TAMAYO, A. T., SHACHAM, S., KAUFFMAN, M., LEE, J., ZHANG, L., OU, Z., LI, C., SUN, L., FORD, R. J. & PHAM, L. V. 2013. Novel selective inhibitors of nuclear export CRM1 antagonists for therapy in mantle cell lymphoma. *Exp Hematol,* 41**,** 67-78 e4.

ZHOU, S., WANG, G. P., LIU, C. & ZHOU, M. 2006. Eukaryotic initiation factor 4E (eIF4E) and angiogenesis: prognostic markers for breast cancer. *BMC Cancer,* 6**,** 231.

ZOU, X., PIPER, T. A., SMITH, J. A., ALLEN, N. D., XIAN, J. & BRUGGEMANN, M. 2003. Block in development at the pre-B-II to immature B cell stage in mice without Ig kappa and Ig lambda light chain. *J Immunol,* 170**,** 1354-61.

ZUCCHETTO, A., CALDANA, C., BENEDETTI, D., TISSINO, E., ROSSI, F. M., HUTTERER, E., POZZO, F., BOMBEN, R., DAL BO, M., D'ARENA, G., ZAJA, F., POZZATO, G., DI RAIMONDO, F., HARTMANN, T. N., ROSSI, D., GAIDANO, G., DEL POETA, G. & GATTEI, V. 2013. CD49d is overexpressed by trisomy 12 chronic lymphocytic leukemia cells: evidence for a methylation-dependent regulation mechanism. *Blood,* 122**,** 3317-21.

Appendix A Data related to chapters 3 and 4

Overlay of APC expression as a measure of OPP-incorporation after anti-IgM-induced mRNA translational inhibition in CLL cells by rocaglamide

Representative FACS histogram overlays shown for OPP staining assay, using sample M-604G, performed on the BD FACSCanto™ and data analysed using FlowJo® software v10.3. Gating was performed by initially selecting lymphocytes based upon their forward scatter (FSC-A) and side-scatter (SSC-A) profiles, removing debris and dead cells from analysis. These cells were then further gated for positive CD19 (Pacific Blue-A) and CD5 (PerCP-Cy5-5-A) expression to identify CLL cells. These CLL cells were then measured for OPP incorporation (APC). Overlays demonstrated to show unstained, isotype treated, untreated, anti-IgM treated and anti-IgM DMSO treated cells. Below graph shows anti-IgM DMSO treated cells overlayed with anti-IgM and Rocaglamide treatment. Expression of APC measured as OPP incorporation, to represent global mRNA translation.

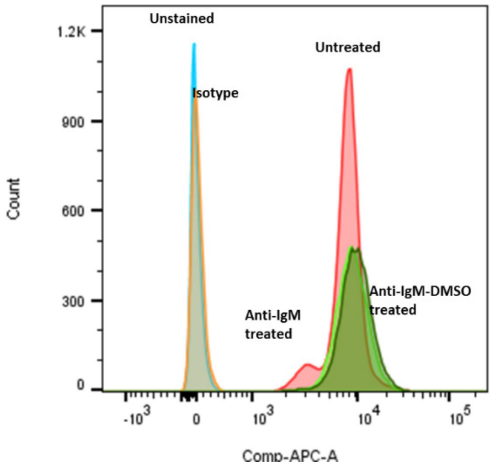

	Sample Name	Subset Name	Count
	604G_IgM DMSO.fcs	Q2: Comp-PerCP-Cy5-5-A+ , Comp-Pacific Blue-A	12569
	604G_IgM.fcs	Q2: Comp-PerCP-Cy5-5-A+ , Comp-Pacific Blue-A	12325
	604G_Iso.fcs	Q2: Comp-PerCP-Cy5-5-A+ , Comp-Pacific Blue-A	8826
	604G_US.fcs	Q2: Comp-PerCP-Cy5-5-A+ , Comp-Pacific Blue-A	8019
	604G_Untreated.fcs	Q2: Comp-PerCP-Cy5-5-A+ , Comp-Pacific Blue-A	19444

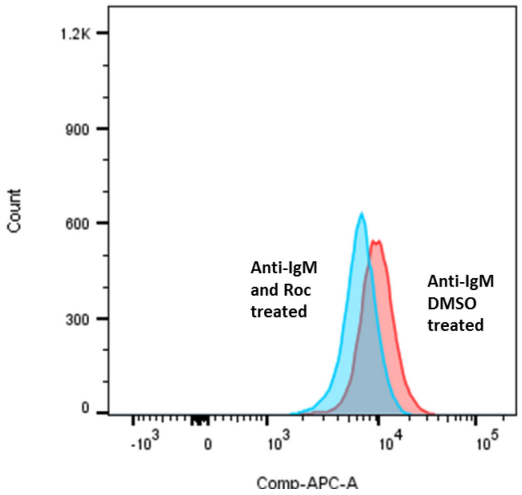

	Sample Name	Subset Name	Count
	604G_IgM R20.fcs	Q2: Comp-PerCP-Cy5-5-A+ , Comp-Pacific Blue-A	13008
	604G_IgM DMSO.fcs	Q2: Comp-PerCP-Cy5-5-A+ , Comp-Pacific Blue-A	12569

Polysome profiling following sIgM-engagement and silvestrol treatment (10 and 20 nM)

CLL cells were pre-treated with silvestrol (10 or 20 nM), DMSO or left untreated for one hour. Cells were then incubated with control antibody or anti-IgM for 24 hours as indicated. Polysome lysate samples were then collected and analysed by polysome profiling, as described in sections 2.5.1 and 2.5.2. Note that some profiles are missing due to software issues at the time of collection. However, this did not affect fraction collection for subsequent qPCR analysis.

M-654B:

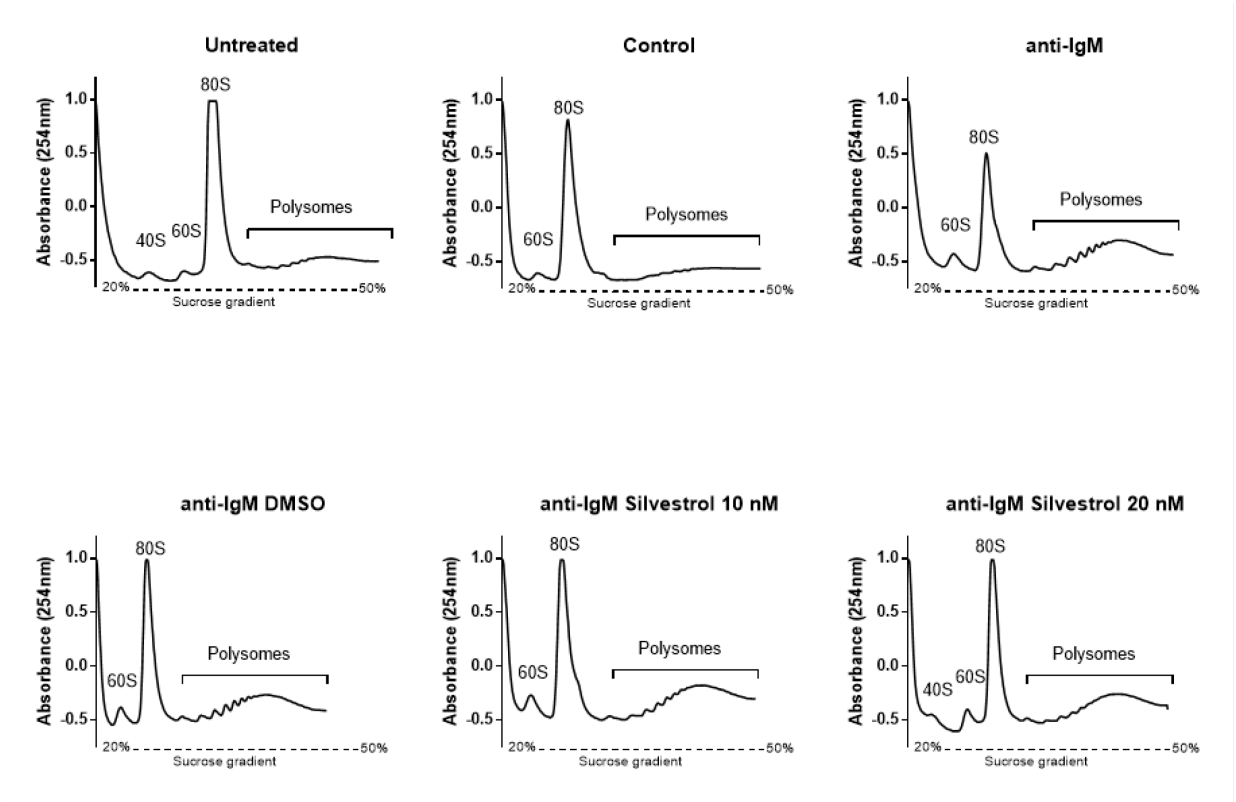

Appendix A

M-604F:

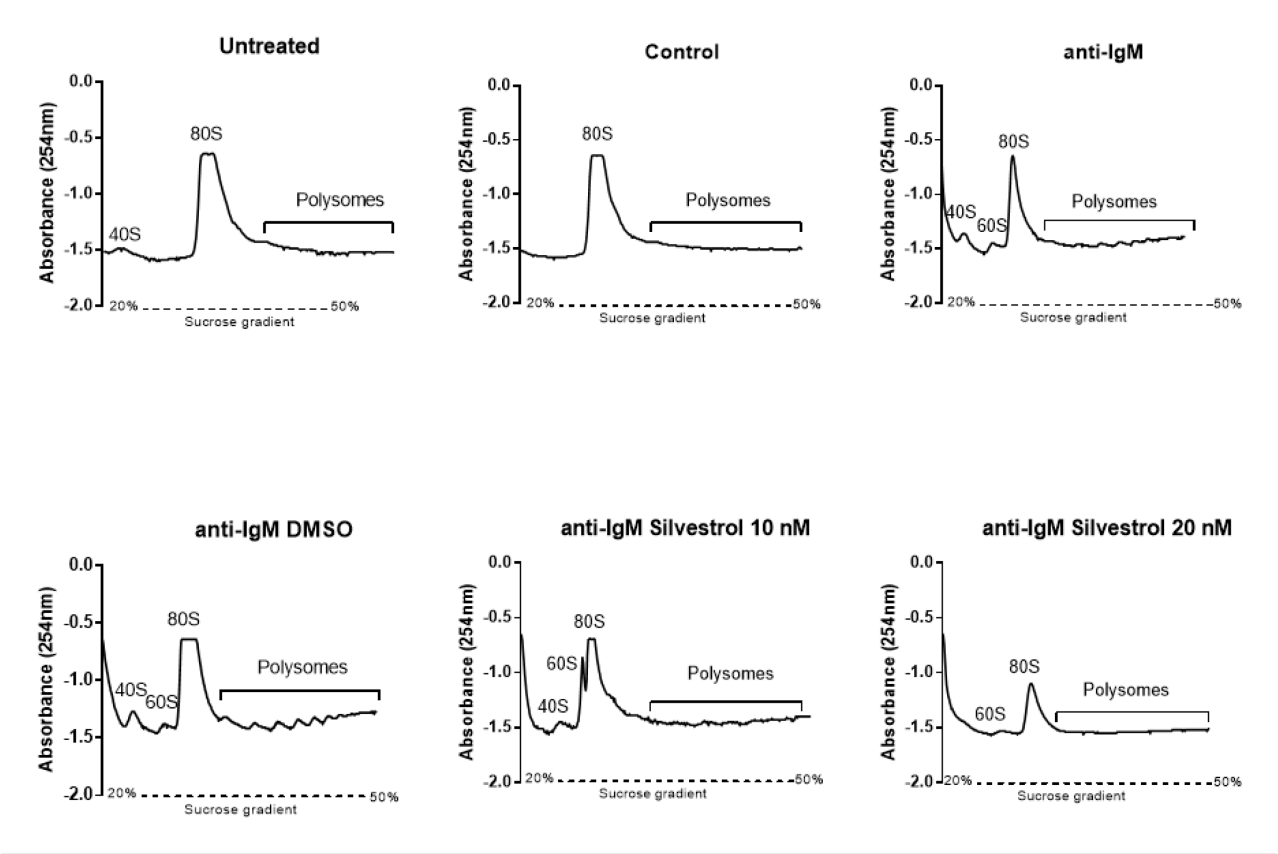

M-684D:

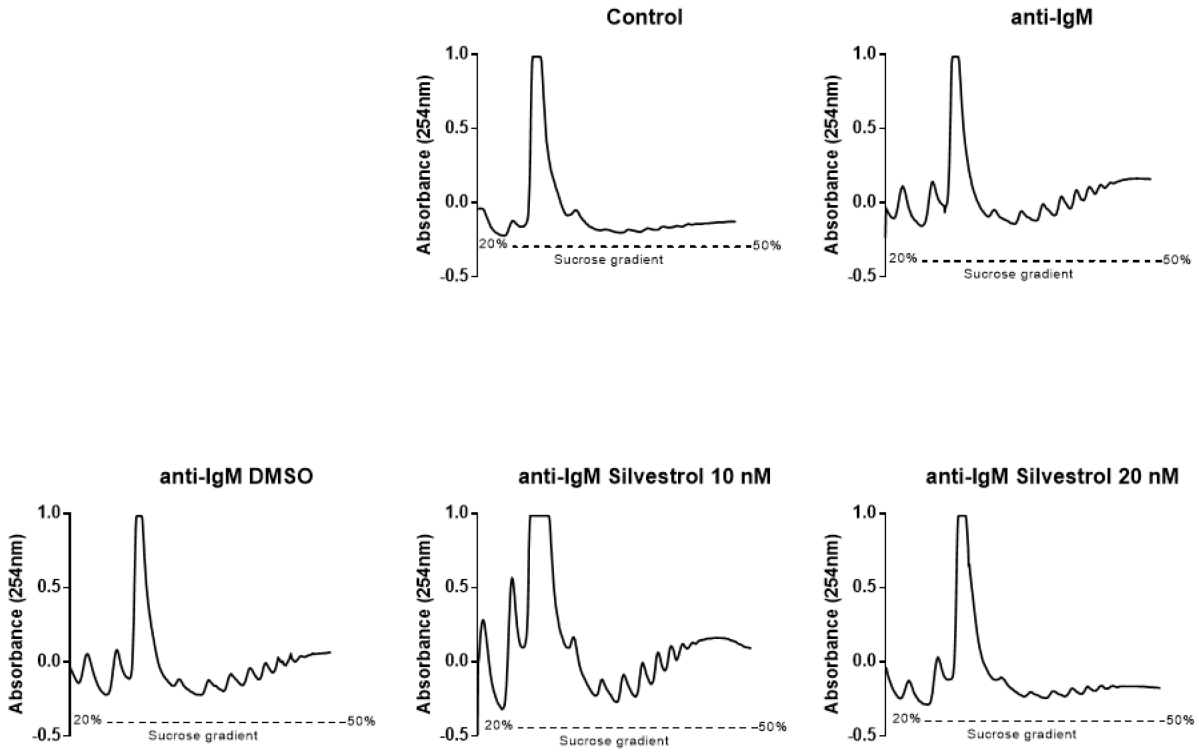
Control
anti-IgM
anti-IgM DMSO
anti-IgM Silvestrol 10 nM
anti-IgM Silvestrol 20 nM
Absorbance (254nm)
1.0
0.5
0.0
-0.5
20%
50%
Sucrose gradient

Appendix A

M-575E:

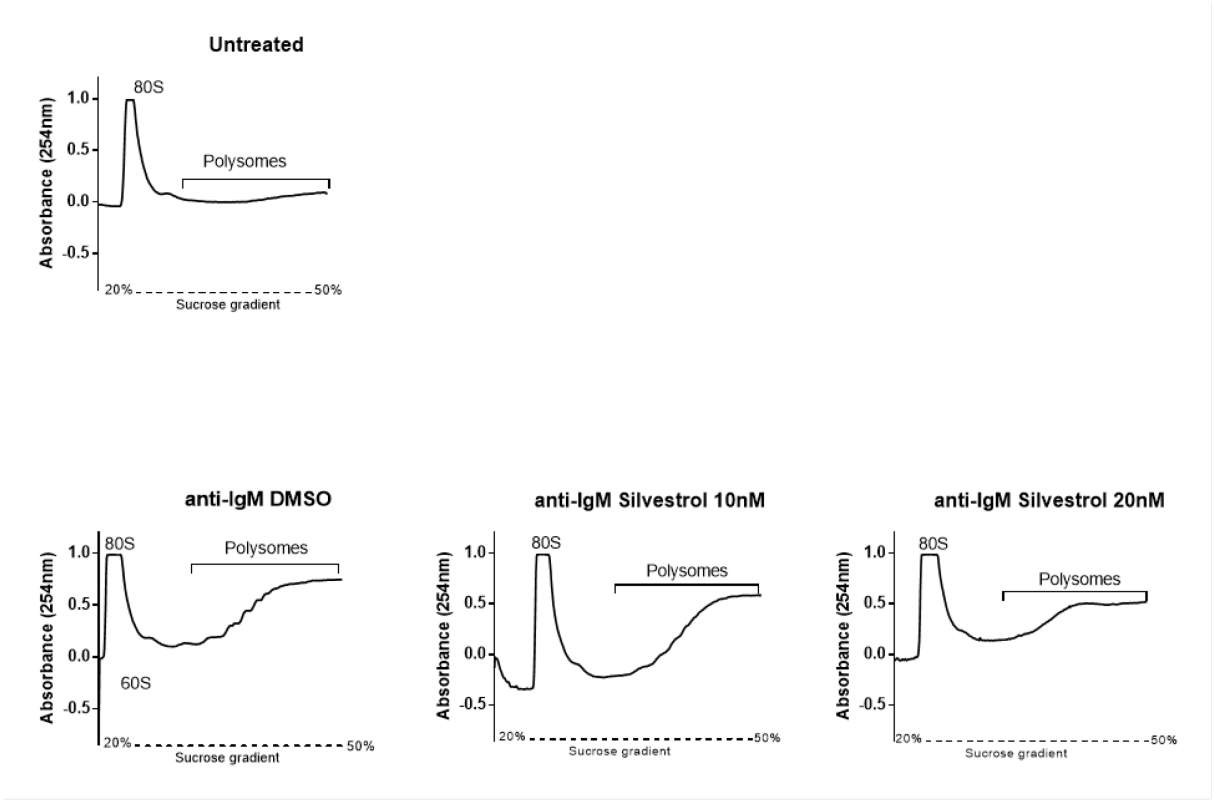

Relative polysome-associated *B2M* RNA expression after sIgM-stimulation and silvestrol treatment

CLL samples (n=5) were pre-treated with silvestrol or DMSO for one hour, followed by an additional 24 hours of control antibody or anti-IgM treatment. Cells were then lysed and used in polysome profiling as described. Polysome profiling fractions (1-10) were collected and RNA extracted. RNA was used in cDNA synthesis and qPCR using Taqman primers for *B2M*. Polysome-associated *B2M* RNA was determined by making polysome-associated (fractions 5-10) *B2M* RNA relative to monosome-associated *B2M* RNA (fractions 1-4). Values for anti-IgM/DMSO treated cells were set to 1. Error bars show SEM and the statistical significance of the indicated differences were determined using a paired T-test.

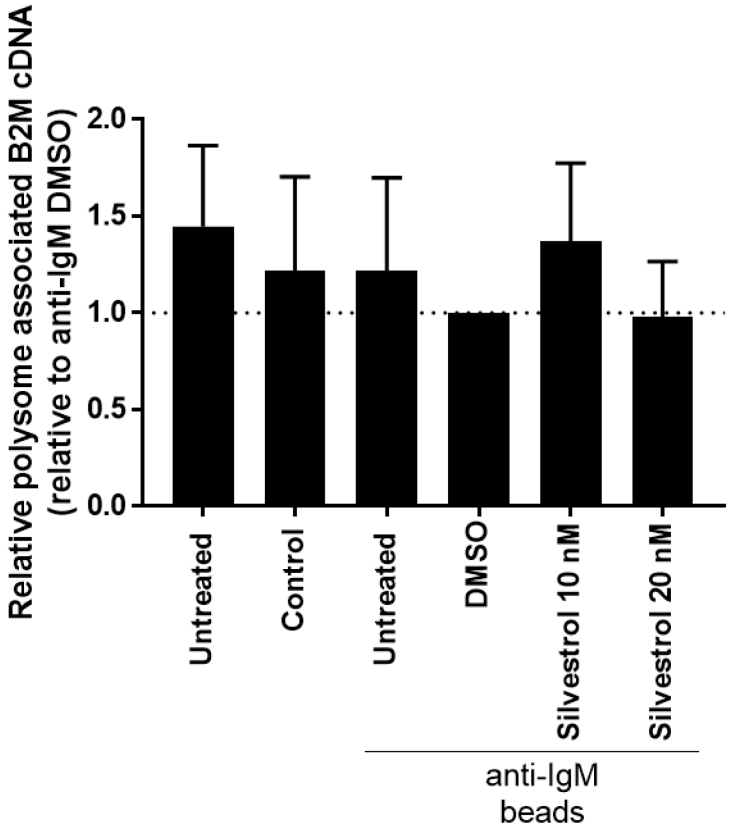

Combined polysome profiling fractions/total *B2M* RNA expression after sIgM-stimulation and silvestrol treatment

CLL samples (n=5) were pre-treated with silvestrol or DMSO for one hour, followed by an additional 24 hours of control antibody or anti-IgM treatment. Cells were then lysed and used in polysome profiling as described. Polysome profiling fractions (1-10) were collected and RNA extracted. RNA was used in cDNA synthesis and qPCR using Taqman primers for *B2M*. Total *B2M* expression (RNA per fraction of each condition was combined). Values for anti-IgM/DMSO treated cells were set to 1. Error bars show SEM and the statistical significance of the indicated differences was determined using a paired T test.

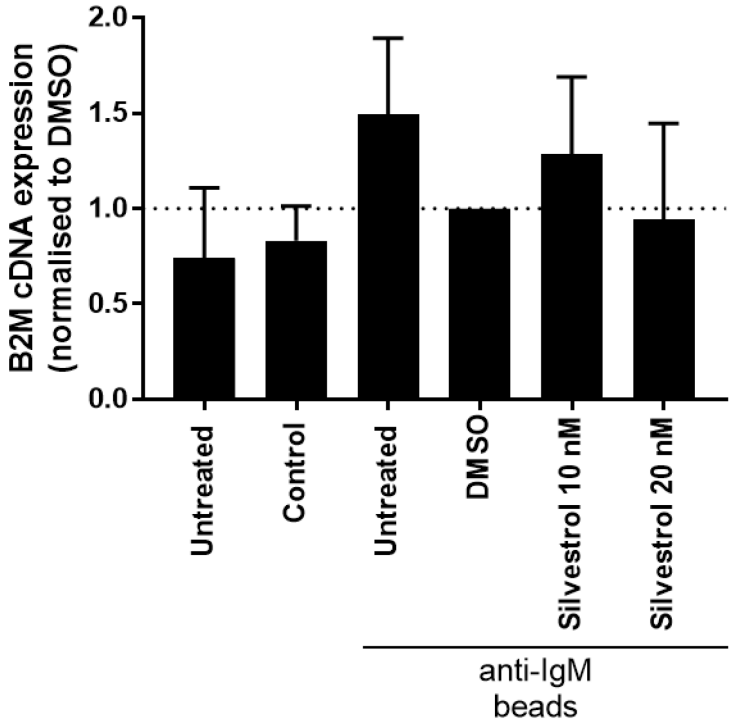

B2M mRNA expression following anti-IgM and silvestrol or rocaglamide treatment

CLL samples (n=10) were pre-treated for one hour with silvestrol or rocaglamide (10 or 20 nM) then treated with control antibody or anti-IgM for an additional 24 hours. *B2M* mRNA expression measured by Taqman qPCR. Error bars show SEM and the statistical significance of the indicated differences was determined using a paired T test.

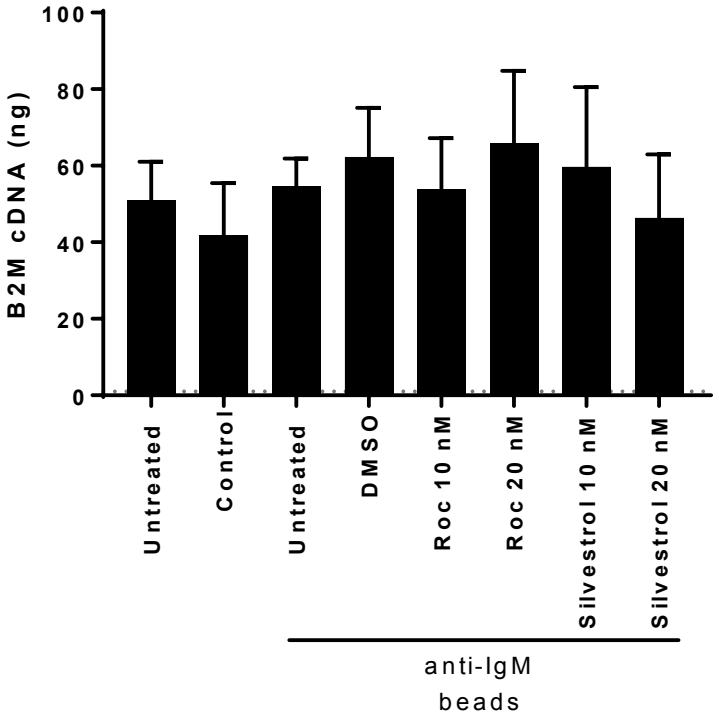

MYC mRNA expression following silvestrol or rocaglamide treatment

CLL samples (n=4) were treated for one hour with silvestrol or rocaglamide (20 nM) followed by treatment with control antibody for an additional 24 hours. *MYC* and *B2M* mRNA expression measured by Taqman qPCR. Data normalised to *B2M* expression with values for control antibody treated cells set to 1. Error bars show SEM and the statistical significance of the indicated differences was determined using a paired T test.

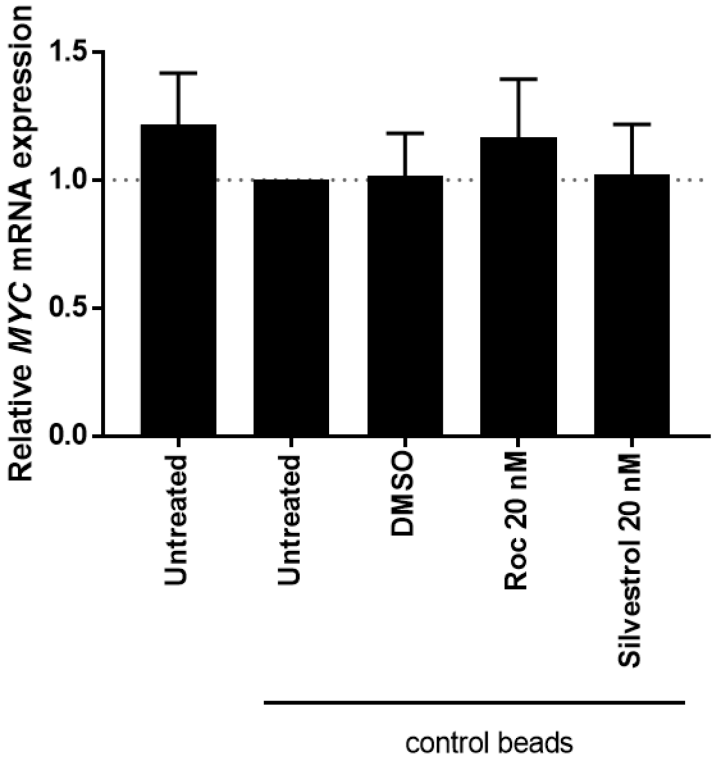

MCL1 mRNA expression following silvestrol or rocaglamide treatment

CLL samples (n=4) were treated for one hour with silvestrol or rocaglamide (20 nM) followed by treatment with control antibody for an additional 24 hours. *MCL1* and *B2M* mRNA expression measured by Taqman qPCR. Data normalised to *B2M* expression with values for control antibody treated cells set to 1. Error bars show SEM and the statistical significance of the indicated differences was determined using a paired T test.

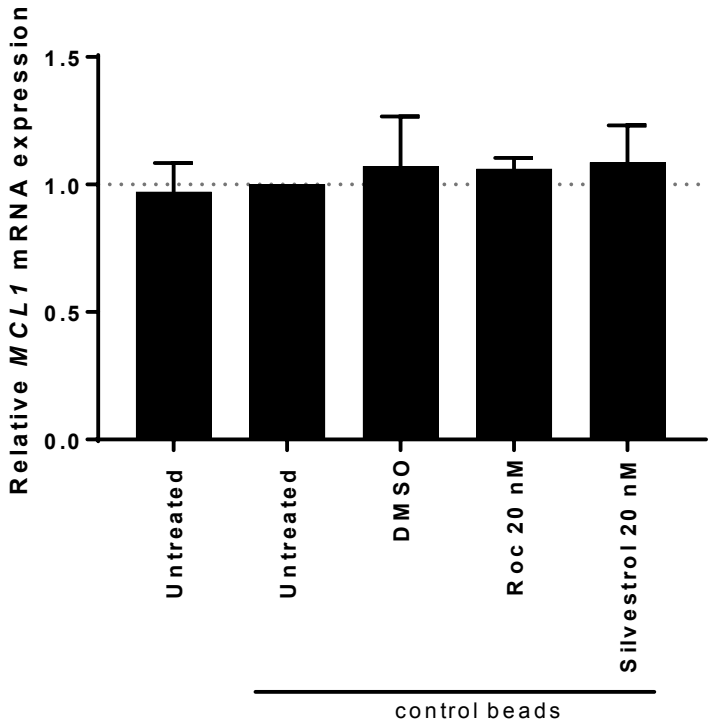

Cell viability (%) following Actinomycin D treatment over a time-course.

A representative CLL sample was treated for 1,3 or 6 hours with the indicated concentration of actinomycin D (5 µg/ml), or left untreated. Cells were collected and cell survival was analysed via Annexin V-PI incorporation in the $CD5^+$ $CD19^+$ cell population. Data shown is relative to untreated control of each time-point set to 100.

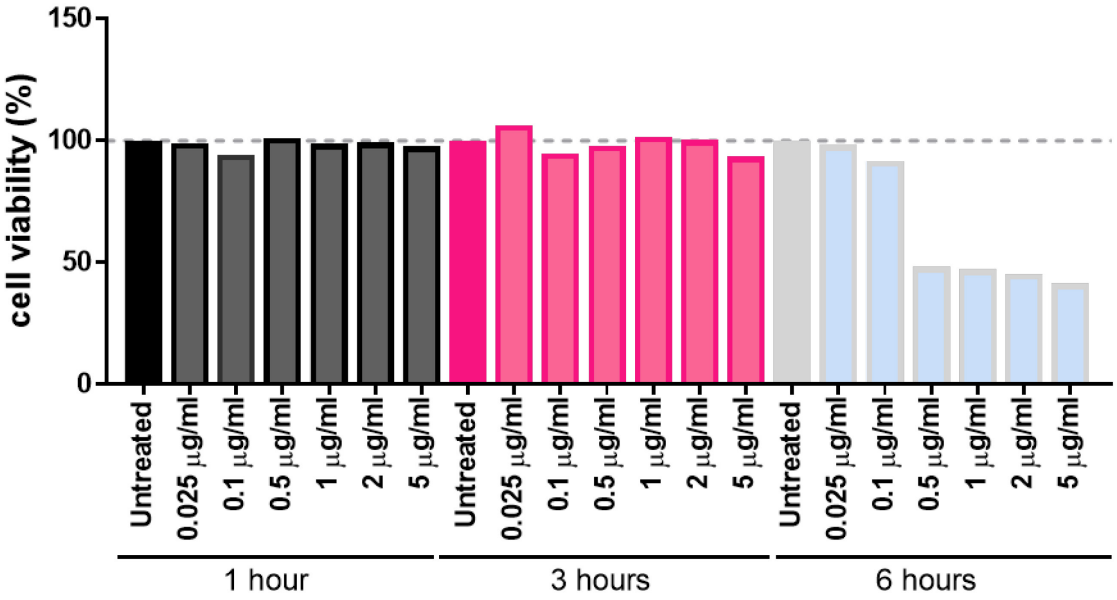

Appendix B Data related to chapter 5

B2M expression following sIgM-stimulation and ribavirin or selinexor treatment

CLL samples (n=4) were pre-treated with ribavirin, selinexor (XPO1i) or DMSO for one hour and then treated with control antibody or anti-IgM for an additional 24 hours. *B2M* mRNA quantified by Taqman qPCR. Error bars show SEM and the statistical significance of the indicated differences was determined using paired T tests.

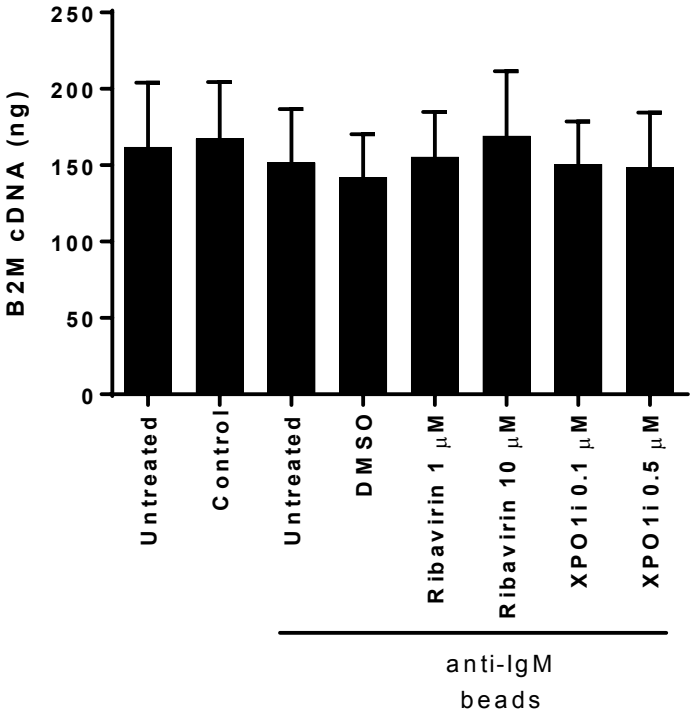

PARP cleavage following BCR engagement and ribavirin treatment

Samples were treated for one hour with ribavirin or DMSO, and incubated for 24, 48 or 72-hours with control antibody or anti-IgM. Cells were then lysed and proteins extracted, then immunoblotting was undertaken and blots probed for PARP and HSC70 as a loading control.

M-523H:

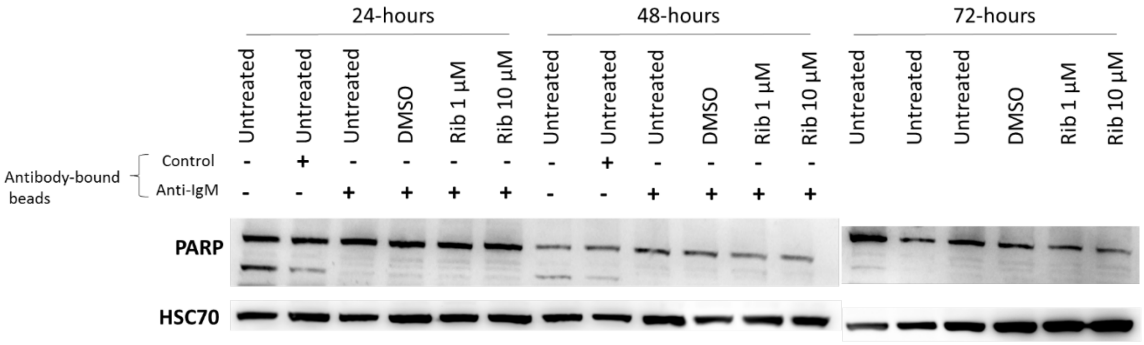

M-681:

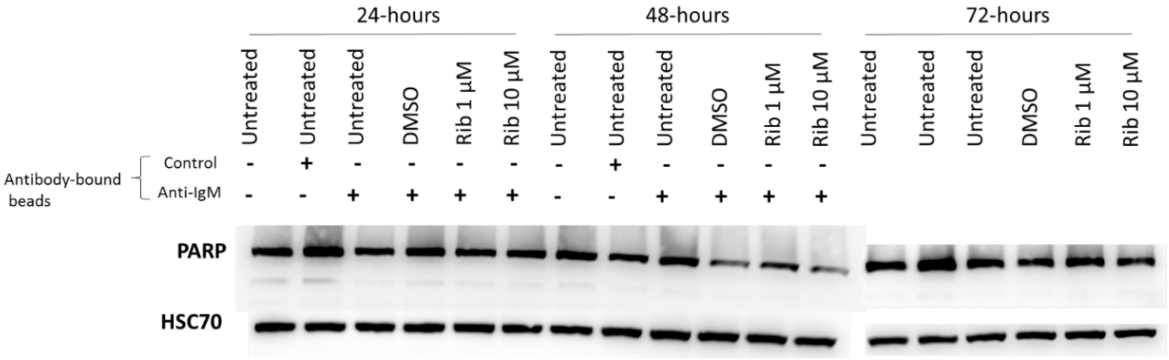
24-hours
48-hours
72-hours
Untreated
Untreated
Untreated
DMSO
Rib 1 µM
Rib 10 µM
Untreated
Untreated
Untreated
DMSO
Rib 1 µM
Rib 10 µM
Untreated
Untreated
Untreated
DMSO
Rib 1 µM
Rib 10 µM
Antibody-bound beads
Control
Anti-IgM
PARP
HSC70

The effect of selinexor on basal CLL cell viability with and without Q-VD-OPh

CLL samples (n=4) were treated with or without selinexor (XPO1i) or DMSO, and Q-VD-OPh caspase inhibitor added where stated, and incubated for 24 hours before analysis. Cells were collected and cell survival was analysed via Annexin V-PI incorporation in the $CD5^{+}CD19^{+}$ cell population. Data shown is relative to Q-VD-OPh/DMSO control set to 100. Error bars show SEM and the statistical significance of the indicated differences determined using paired T tests.